EDGEWOOD ARSENAL
SPECIAL PUBLICATION

EASP 100-108

AN ANALYSIS OF THE DYNAMIC AND AERODYNAMIC PERFORMANCE OF A SELF-DEPLOYING ARTICULATED AUTOROTOR DECELERATOR

by

Miles C. Miller

October 1971

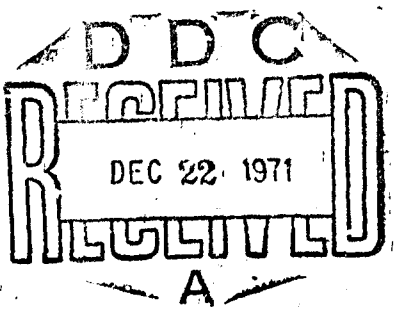

DEPARTMENT OF THE ARMY
EDGEWOOD ARSENAL
Research Laboratories
Office of the Director
Edgewood Arsenal, Maryland 21010

UNCLASSIFIED

Security Classification

DOCUMENT CONTROL DATA - R & D

(Security classification of title, body of abstract and indexing annotation must be entered when the overall report is classified)

1. ORIGINATING ACTIVITY (Corporate author)	2a. REPORT SECURITY CLASSIFICATION
CO, Edgewood Arsenal ATTN: SMUEA-R-A Edgewood Arsenal, Maryland 21010	UNCLASSIFIED
	2b. GROUP NA

3. REPORT TITLE

AN ANALYSIS OF THE DYNAMIC AND AERODYNAMIC PERFORMANCE OF A SELF-DEPLOYING ARTICULATED AUTOROTOR DECELERATOR

4. DESCRIPTIVE NOTES (Type of report and inclusive dates)

5. AUTHOR(S) (First name, middle initial, last name)

Miles C. Miller

6. REPORT DATE	7a. TOTAL NO. OF PAGES	7b. NO OF REFS
October 1971	200	7

8a. CONTRACT OR GRANT NO.	9a. ORIGINATOR'S REPORT NUMBER(S)
b. PROJECT NO. None	EASP 100-108
c.	9b. OTHER REPORT NO(S) (Any other numbers that may be assigned this report)
d.	

10 DISTRIBUTION STATEMENT

Approved for public release; distribution unlimited.

11. SUPPLEMENTARY NOTES	12. SPONSORING MILITARY ACTIVITY
	NA

13. ABSTRACT

The articulated autorotor decelerator is a device intended to provide retardation and stability to air delivered stores. This unique device, combining aerodynamics, dynamics, and gyroscopics, shows promise of having a significant potential in the decelerator field. Limited wind tunnel tests using small models indicate that this device gives the largest drag coefficient, based on solidity factor and tip speed ratio considerations, of any known decelerator, including parachutes. The system is composed of a number of blades attached to a hub at the rear of the store body. Each blade is free to spin about its long axis by means of a bearing at the point where the blade is attached to the hub. The hub, in turn, is free to spin about an axis through the store center line. As the store falls through the air, the air flow over the blades will cause them to spin (or autorotate) about their long axes. The autorotation is accomplished by proper shaping of the blade cross section. The aerodynamic lift and drag forces acting on the autorotating blades result in a torque about the store center line, thus imparting a spin rate to the hub (and attached blades). The aerodynamic forces acting on the blades, because of the blade spin and hub spin, result in a large force opposite to the direction of the store flight (parallel to the store center line), which is the system drag. The blades are also free to travel through a fore and aft flap angle. This third degree of freedom eliminates large bending loads on the blade and also results in a self correcting action for stability. The method considered for initial blade deployment is to utilize small turbine vanes mounted on the hub which will initiate hub rotation. The blades, which are initially lying back parallel to the store center line, are thrown out and forward (deployed) by the centrifugal force due to hub rotation. As the blades pivot out, they will spin and, in turn, will sustain the hub spin. The blades will finally deploy to an equilibrium position at a near right angle to the store center line. This method of deployment has the added feature of providing a positive means of initiating blade autorotation during deployment. The study includes the derivation of the equations describing the dynamic motion of the decelerator system. These equations involve the inertial, gyroscopic, and aerodynamic effects. The aerodynamic terms are written so that

DD FORM 1 NOV 68 1473 REPLACES DD FORM 1473, 1 JAN 64, WHICH IS OBSOLETE FOR ARMY USE.

UNCLASSIFIED

Security Classification

Distribution Statement

Approved for public release; distribution unlimited.

Disclaimer

The findings in this report are not to be construed as an official Department of the Army position unless so designated by other authorized documents.

Disposition

Destroy this report when no longer needed. Do not return it to the originator.

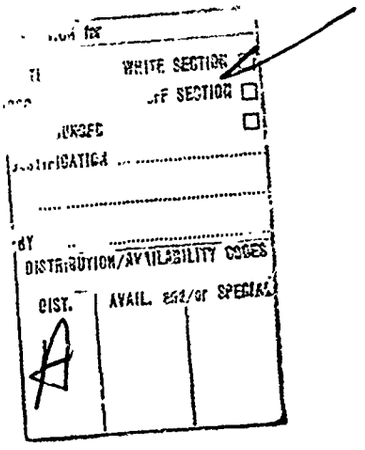

14. KEY WORDS	LINK A		LINK B		LINK C	
	ROLE	WT	ROLE	WT	ROLE	WT

13. ABSTRACT (Continued)

the aerodynamic sectional characteristics of the autorotating blades, obtained from wind tunnel tests, can be utilized directly. These equations are programmed to be solved on a digital computer so that deployment transients and steady state performance characteristics can be investigated. Experimental data obtained from wind tunnel tests with a representative full scale rotor system are presented. These results are used to determine a blade interference factor, which, when incorporated in the basic theory, gives excellent correlation between analytical and experimental results. The qualitative and quantitative effects of various system parameters on the steady state and deployment transient performance of the system are investigated. The results of this study afford an understanding in the mechanics of the overall system by investigating the relative effects of the various physical terms on the system performance. This study als provides an insight into the performance potential of the basic configuration and represents a basic analytical approach for future applications of the device.

14. KEYWORDS

Autorotors
Aerodynamic decelerators
Retardation devices
Aerodynamics
Air-delivered store

EDGEWOOD ARSENAL SPECIAL PUBLICATION

EASP 100-108

AN ANALYSIS OF THE DYNAMIC AND AERODYNAMIC PERFORMANCE OF A SELF-DEPLOYING ARTICULATED AUTOROTOR DECELERATOR

by

Miles C. Miller

Aerodynamics Research Group

October 1971

DEPARTMENT OF THE ARMY
EDGEWOOD ARSENAL
Research Laboratories
Office of the Director
Edgewood Arsenal, Maryland 21010

FOREWORD

The work described in this report represents an extension of the project effort undertaken in support of DA Project 1X728012D628, Defense Communications Planning Group. This report is based on a thesis originally submitted to the Faculty of the Graduate School of the University of Maryland in partial fulfillment of the requirements for the degree of Master of Science.

Acknowledgments

This report represents the analysis of a relatively complex dynamic and aerodynamic system; consequently, the participation of a number of individuals was vital to achieving the results of this study. Without their combined contributions, this effort would not have been possible. I should like to thank each of them and to acknowledge the general areas of their efforts.

Particularly important to the accomplishment of this analysis were large amounts of diversified experimental data. I wish to thank Richard Raup, Norman Singleton, Owen Smith, Dell Crouch, Frank Wrede, and Jack Molnar, all members of the Aerodynamics Research Group, Edgewood Arsenal, Maryland, for their efforts in obtaining the wind tunnel data in this report.

I should also like to thank Donald Olson for his advice and consultation on many of the technical aspects of the analysis and especially his contributions toward the design of the full-scale autorotor decelerator, which provided the key experimental data toward the analytical results.

To Miss Elaine Westervelt, Systems Analysis Division, Edgewood Arsenal, goes special thanks. Not only did Miss Westervelt do the computer programming so vital to the analysis, but her assistance in making the many runs involved and working with the author to solve the many problems during the formulation of the analytical effort is very much appreciated.

The technical knowledge and confidence to attempt this report were provided, in great part, by the excellent Advanced Dynamics course presented by Dr. Patrick Cuniff, University of Maryland.

Dr. Colin Marks, University of Maryland, acted as my report adviser, and his technical advice and suggestions as to the content of the report were pertinent and kept the author heading in the proper direction.

I wish to especially thank Abraham Flatau, who is responsible for the basic autorotor decelerator concept itself, and at whose suggestion I selected this report subject. His technical advice on autorotors and his encouragement were essential to realization of the final results.

Finally, I should like to thank Mrs. Mary Wroten and Mrs. Frances Revis for typing the original draft and final report.

DIGEST

The articulated autorotor decelerator is a device intended to provide retardation and stability to air-delivered stores. This unique device, combining aerodynamics, dynamics, and gyroscopics, shows promise of having a significant potential in the decelerator field. Limited wind tunnel tests using small models indicate that this device gives the largest drag coefficient, based on solidity factor and tip speed ratio considerations, of any known decelerator, including parachutes.

The system is composed of a number of blades attached to a hub at the rear of the store body. Each blade is free to spin about its long axis by means of a bearing at the point where the blade is attached to the hub. The hub, in turn, is free to spin about an axis through the store center line. As the store falls through the air, the air flow over the blades will cause them to spin (or autorotate) about their long axes. This autorotation is accomplished by proper shaping of the blade cross section. The aerodynamic lift and drag forces acting on the autorotating blades result in a torque about the store center line, thus imparting a spin rate to the hub (and attached blades). The aerodynamic forces acting on the blades, because of the blade spin and hub spin, result in a large force opposite to the direction of the store flight (parallel to the store center line), which is the system drag. The blades are also free to travel through a fore and aft flap angle. This third degree of freedom eliminates large bending loads on the blade and also results in a self-correcting action for stability.

The method considered for initial blade deployment is to utilize small turbine vanes mounted on the hub, which will initiate hub rotation. The blades, which are initially lying back parallel to the store center line, are thrown out and forward (deployed) by the centrifugal force due to hub rotation. As the blades pivot out, they will spin and, in turn, will sustain the hub spin. The blades will finally deploy to an equilibrium position at a near right angle to the store center line. This method of deployment has the added feature of providing a positive means of initiating blade autorotation during deployment.

The study includes the derivation of the equations describing the dynamic motion of the decelerator system. These equations involve the inertial, gyroscopic, and aerodynamic effects. The aerodynamic terms are written so that the aerodynamic sectional characteristics of the autorotating blades, obtained from wind tunnel tests, can be utilized directly. These equations are programmed to be solved on a digital computer so that deployment transients and steady state performance characteristics can be investigated.

Experimental data obtained from wind tunnel tests with a representative full scale rotor system are presented. These results are used to determine a blade interference factor, which, when incorporated in the basic theory, gives excellent correlation between analytical and experimental results.

The qualitative and quantitative effects of various system parameters on the steady state and deployment transient performance of the system are investigated. The results of this study afford an understanding of the mechanics of the overall system by investigating the relative effects of the various physical terms on the system performance. This study also provides an insight into the performance potential of the basic configuration and represents a basic analytical approach for future applications of the device.

CONTENTS

CONTENTS (Continued)

LIST OF FIGURES

LIST OF FIGURES (Continued)

LIST OF FIGURES (Continued)

LIST OF FIGURES (Continued)

AN ANALYSIS OF THE DYNAMIC AND AERODYNAMIC PERFORMANCE OF A SELF-DEPLOYING ARTICULATED AUTOROTOR DECELERATOR

I. INTRODUCTION.

The articulated autorotor decelerator is the invention of James Brunk and Abraham Flatau.[1] Limited wind tunnel tests at Edgewood Arsenal using small models indicated an extremely large drag coefficient for a relatively low value of solidity factor and tip speed ratio when compared with other decelerator devices which utilize some form of autorotation motion in their mode of operation. These devices would include: vortex ring parachute, rotochute, flexirotor, and rotafoil parachute.

Limited wind tunnel data have indicated the basic potential of this device and verify the original reasoning that led to the articulated autorotor decelerator concept in that a large system drag coefficient would result because of the combination of both a large lift and a large drag coefficient characteristic of the basic autorotor blade.

This report presents the first known attempt to analyze the qualitative and quantitative performance characteristics of the articulated autorotor from a detailed dynamic and aerodynamic viewpoint.

The articulated autorotor decelerator, which appears in figure 1, is particularly applicable for retardation of air-delivered stores because of the stability it would provide in addition to the basic decelerator function. This analysis is concerned mainly with utilizing the device for the air-delivered store application. Thus, the selection of the general analytical model configuration and associated dimensions is swayed in this direction. The physical system analyzed is intended to include all the terms basic to the mechanics of the system, yet be as simple as possible to facilitate an understanding of the fundamental aspects of the device.

This analysis involves the dynamic motion and aerodynamic performance of the articulated autorotor decelerator system in a constant and axisymmetric free stream velocity; it does not include trajectory aspects nor consider an accelerating body system. Nonetheless, the performance analysis is illustrative of the behavior of the system, and the general approach and the equations thus derived are valid for future analyses of other applications of the basic system.

II. GENERAL DESCRIPTION OF THE SYSTEM.

The articulated autorotor decelerator system as applied to an air-delivered store application is illustrated in figure 1 and functions in the following manner. The system is composed of a number of blades (four are shown in the illustration), which are attached to a hub at the rear end of the store body. Each blade is free to spin about its long axis by means of a bearing at the point where the blade is attached to the hub. The hub, with the blades attached, is free to spin about an axis coincident with the store center line by means of a bearing between the hub and the store body.

As the store falls through the air, the air flow over the blades will cause them to spin or autorotate about their long axes. This spin rate is shown as ω in figure 1. This autorotation is accomplished by proper shaping of the blade cross section. The aerodynamic lift and drag acting on

[1] Flatau, A., and Brunk, J. E. Free Spinning Articulated Rotor. US Patent 3,291,418. 13 December 1966.

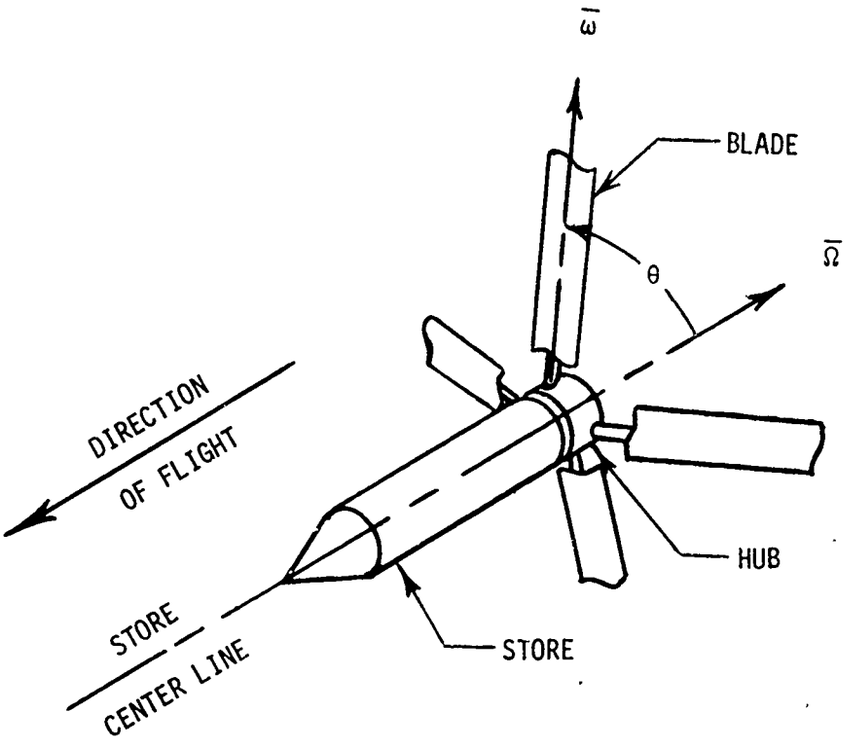

Figure 1. General Configuration of Articulated Autorotor Decelerator System

the blades caused by their autorotation will result in a torque about the store center line, thus imparting a spin rate to the hub (and the attached blades). This hub spin rate is shown as Ω in figure 1. The aerodynamic forces acting on the blades caused by the combination of blade spin and hub spin result in a large force in the direction opposite to the store flight direction (parallel to the store center line), which is the system drag.

The blades are also free to pivot through a flap angle, shown as θ in figure 1. This third degree of freedom eliminates large bending loads on the blade and also results in a self-correcting action for stability. The autorotor blade used in this analysis is rectangular in plan form and has a cross-sectional shape similar to a flattened S. This shape is usually referred to as an S-section autorotor.

A method for initial deployment of the blades is shown in figure 2. Prior to deployment, the blades are lying back parallel to the store center line. A hub spin rate is achieved by some means such as small external turbine vanes mounted to the hub. When released, the blades are thrown out and forward by the centrifugal force resulting from the hub spin rate. As the blades pivot out to larger values of θ, they will spin about their long axes; the resulting aerodynamic forces on the blades will sustain the hub spin rate. The blades will finally deploy to an equilibrium position at a near right angle to the store center line. Thus, the flap angle θ will hereafter be referred to as the deployment angle.

This aft-to-forward deployment method not only minimizes blade bending loads that would occur in a forward-to-aft deployment when the blades impacted the necessary stop, but it also has the added feature of providing a positive means of initiating blade autorotation during

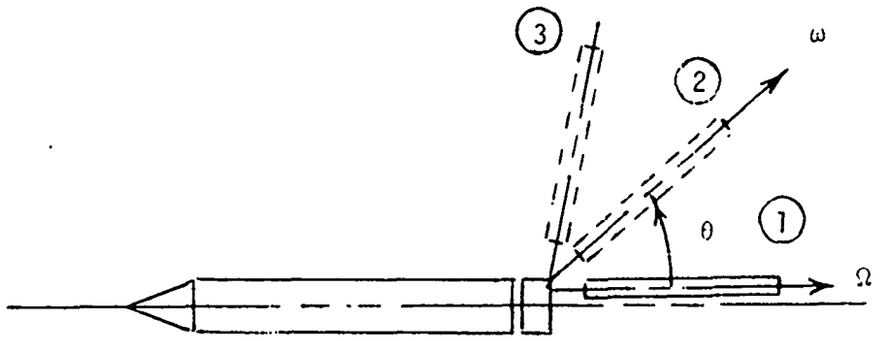

Figure 2. Deployment Methodology

1. Blade position prior to deployment:

$$\theta = \dot{\theta} = \ddot{\theta} = 0 \qquad \omega = \dot{\omega} = 0 \qquad \dot{\Omega} = 0, \quad \Omega = \Omega_0$$

2. Blade position during deployment transient: all terms and their derivatives have values

3. Blade position at steady state condition:

$$\dot{\theta} = \ddot{\theta} = 0 \qquad \dot{\omega} = 0 \qquad \dot{\Omega} = 0$$

$$\theta = \theta_{ss} \qquad \omega = \omega_{ss} \qquad \Omega = \Omega_{ss}$$

deployment. It is this automatic initiation of blade autorotation along with the unassisted deployment motion of the blades when released (assuming a sufficient hub spin rate) that are the reasons behind the term "self-deploying" in the system description.

III. GENERAL METHOD OF ANALYSIS.

The equations describing the motion of the system are developed (section IV) for the case of an inertially fixed (i.e., nonaccelerating) body. The aerodynamic effects are treated for the case of constant and axisymmetric flow (i.e., parallel to the store center line). These conditions represent the physical situation of the system when installed in a wind tunnel (fixed mount), and therefore the results are for a condition that can be experimentally verified.

The basic blade element approach, used in propeller theory, is utilized to determine the aerodynamic load distribution over the blade, covered in section V. This approach allows the experimentally determined aerodynamic sectional characteristics of the autorotor blades to be used directly and also permits a detailed understanding of the aerodynamic effects over the blade.

These equations were programmed to be solved on a digital computer, as described in section VI, not only to facilitate the solution of the several complex equations, but also to allow a detailed insight into the results because a large number of terms could be computed and investigated.

Steady state system performance (for a constant free stream velocity) was computed and compared with experimental results obtained in a wind tunnel test using a full scale system

described in section VII. Comparison between the initial analytical predictions and experimental results showed fair correlation, but the differences were unsatisfactorily large.

A parametric study was conducted in which each physical property and condition were varied about a nominal condition to determine if the sensitivity of certain terms would explain the poor correlation between the theoretical and experimental results (section VIII). None of the parameters studied influenced the performance either qualitatively or quantitatively toward the experimental results. Attention was then centered on the aerodynamic load distribution over the blades. From an initial inspection of local flow directional effects and an empirical analysis using various degrees of this effect, it was determined that mutual blade interference effects on the air flow direction over the blades (i.e., local angle of attack) would bring all the analytically predicted terms more in agreement with their experimental values. Differences between the analytical and experimental results were effectively eliminated in all terms by adding a blade interference effect to the theoretical analysis.

With the theoretical approach verified, a parameter study was conducted to indicate the effects of the various terms on the system performance. Also presented is a detailed examination of the steady state values of specific terms of interest. These results are included in section IX.

Finally, the transient behavior of the system during deployment is presented in section X.

IV. DERIVATION OF THE EQUATIONS OF MOTION.

A. Formulation of the Basic Equations.

The basic physical model representing the articulated autorotor decelerator system is shown in figure 3. The equations describing the motion of this system will be developed using the modified Euler's equations approach.[2]

Referring to figure 3, X, Y, Z^* is an inertial axes system fixed to the store body with the origin (O) at the intersection of the blade spin axis and hub spin axis, where X is directed along the store center line, and Z is directed downward. The body axes system x, y, z is fixed to the blade and oriented along the principal axes of the blade, with the x-axis oriented along the blade.

Let ω' be the absolute angular velocity of the blade with respect to the X, Y, Z system. Let ω be the absolute angular velocity of the x-, y-, z-axes system (fixed to the blade) with respect to the X, Y, Z system. The x-axis is oriented along the blade as shown, and the x-, y-, z-axes system could be rotating about the x-axis.

$$\text{Angular momentum} = \bar{H} = I\bar{\omega}' \tag{4-1}$$

Expanding (4-1):

$$\begin{aligned} H_x &= I_x \omega'_x \\ H_y &= I_y \omega'_y \\ H_z &= I_z \omega'_z \end{aligned} \tag{4-2}$$

[2]Greenwood, D. F. Principals of Dynamics. Prentice-Hall Inc., Englewood Cliffs, New Jersey.

*The mathematical terms are defined in glossary at the end of the text.

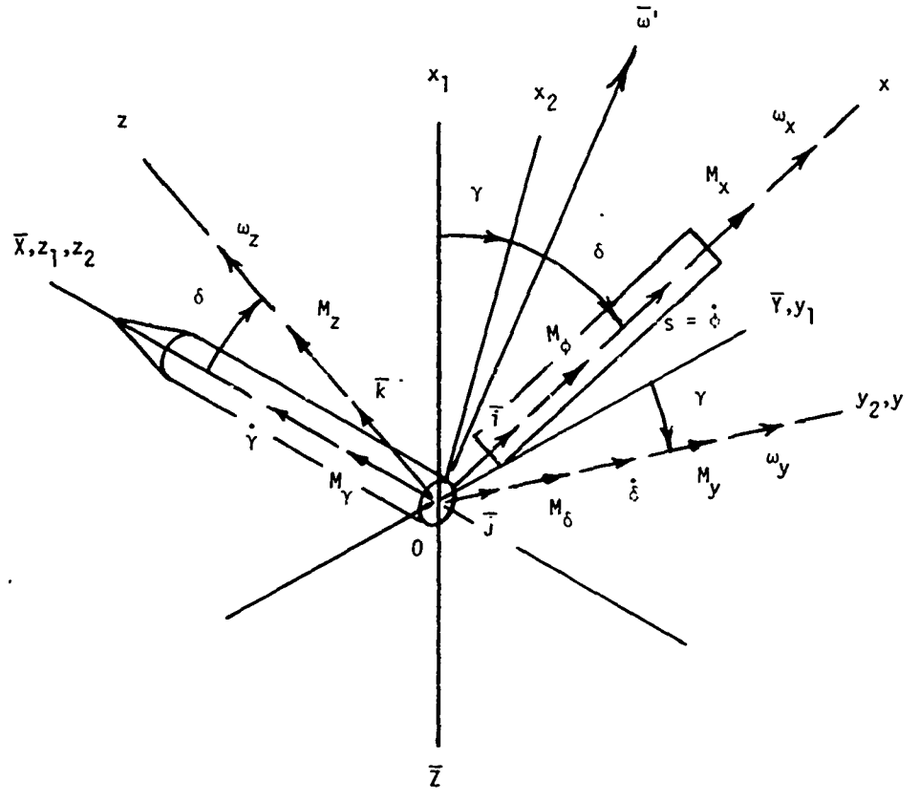

Figure 3. Basic System Physical Model

Let:

$$I_x = I_1$$
$$I_y = I_z = I_0$$

Although the instantaneous moment of inertia of the blade about the point O would depend on whether the blade were oriented with the flat face or edge on relative to the axis considered, the fact that the blade has a high spin rate allows a mean value for the moment of inertia to be used. This value, which is between the two extreme values mentioned, is still close enough to these in magnitude to allow the blade to be considered as a symmetrical body.

Substituting these into (4-2) through (4-4):

$$H_x = I_1 \omega'_x$$
$$H_y = I_0 \omega'_y \qquad (4\text{-}3)$$
$$H_z = I_0 \omega'_z$$

Let the blade rotate about its axis of symmetry (x) with angular velocity s (with respect to the x-, y-, z-axes system).

$$\begin{aligned} \omega'_x &= \omega_x + s \\ \omega'_y &= \omega_y \\ \omega'_z &= \omega_z \end{aligned} \tag{4-4}$$

Substituting these results into the angular momentum expression (4-3),

$$\begin{aligned} H_x &= I_1 (\omega_x + s) \\ H_y &= I_0 \omega_y \\ H_z &= I_0 \omega_z \end{aligned} \tag{4-5}$$

Differentiating equations (4-5) with respect to time:

$$\begin{aligned} \dot{H}_x &= I_1 (\dot{\omega}_x + \dot{s}) \\ \dot{H}_y &= I_0 \dot{\omega}_y \\ \dot{H}_z &= I_0 \dot{\omega}_z \end{aligned} \tag{4-6}$$

where the dot over the term indicates differentiation with respect to time:

$$\dot{(\ )} = \frac{d(\ )}{dt} \quad \text{and} \quad \ddot{(\ )} = \frac{d^2(\ )}{dt^2}$$

The time rate of change of angular momentum referred to an inertial coordinate system in terms of a rotating coordinate system expressed in vector notation is

$$\dot{\overline{H}} = (\dot{\overline{H}})_r + \overline{\omega} \times \overline{H} \tag{4-7}$$

where $(\dot{\overline{H}})_r$ is the time rate of change of the absolute angular momentum referred to the rotating coordinate system, $\overline{H}$ is the absolute angular momentum referred to the rotating coordinate system, and $\overline{\omega}$ is the angular velocity of the rotating coordinate system relative to the inertial coordinate system.

Expanding the terms of (4-7),

$$(\dot{\overline{H}})_r = \dot{H}_x \overline{i} + \dot{H}_y \overline{j} + \dot{H}_z \overline{k} \tag{4-8}$$

$$\overline{\omega} = \omega_x \overline{i} + \omega_y \overline{j} + \omega_z \overline{k} \tag{4-9}$$

$$\overline{H} = H_x \overline{i} + H_y \overline{j} + H_z \overline{k} \tag{4-10}$$

where $\overline{i}, \overline{j}, \overline{k}$ are unit vectors for the x, y, z system.

Evaluating the first term on the right-hand side of (4-7), and substituting (4-6) into (4-8),

$$(\dot{\overline{H}})_r = I_1 (\dot{\omega}_x + \dot{s}) \overline{i} + I_0 \dot{\omega}_y \overline{j} + I_0 \dot{\omega}_z \overline{k} \tag{4-11}$$

Evaluating the second term on the right-hand side of (4-7),

$$\overline{\omega} \times \overline{H} = \begin{vmatrix} \overline{i} & \overline{j} & \overline{k} \\ \omega_x & \omega_y & \omega_z \\ H_x & H_y & H_z \end{vmatrix}$$

$$\overline{\omega} \times \overline{H} = (\omega_y H_z - \omega_z H_y) \overline{i} + (\omega_z H_x - \omega_x H_z) \overline{j} + (\omega_x H_y - \omega_y H_x) \overline{k} \tag{4-12}$$

Substituting the expressions from (4-11) and (4-12) into (4-7) gives:

$$\bar{H} = [I_1(\dot{\omega}_x + \dot{s}) + \omega_y H_z - \omega_z H_y]\bar{i} + (I_0\dot{\omega}_y + \omega_z H_y - \omega_x H_z)\bar{j} + (I_0\dot{\omega}_z + \omega_x H_y - \omega_y H_z)\bar{k} \quad (4\text{-}13)$$

Expanding (4-13) gives:

$$\begin{aligned}\dot{\bar{H}} = {} & (I_1\dot{\omega}_x + I_1\dot{s} + \omega_y I_0\omega_z - \omega_z I_0\omega_y)\bar{i} \\ & + [I_0\dot{\omega}_y + \omega_z I_1(\omega_x + s) - \omega_x I_0\omega_z]\bar{j} \\ & + [I_0\dot{\omega}_z + \omega_x I_0\omega_y - \omega_y I_1(\omega_x + s)]\bar{k}\end{aligned} \quad (4\text{-}14)$$

The time rate of change of angular momentum is equal to the net external moment; in vector notation,

$$\bar{M} = \dot{\bar{H}} \quad (4\text{-}15)$$

Expanding (4-15) and substituting in the expressions from (4-14):

$$\begin{aligned}M_x &= I_1\dot{\omega}_x + I_1\dot{s} \\ M_y &= I_0\dot{\omega}_y - (I_0 - I_1)\omega_x\omega_z + I_1\omega_z s \\ M_z &= I_0\dot{\omega}_z + (I_0 - I_1)\omega_x\omega_y - I_1\omega_y s\end{aligned} \quad (4\text{-}16)$$

B. Conversion of Euler Angles.

The Euler angles (γ, δ, ϕ), which describe the orientation of the blade with respect to the $\bar{X}$-, $\bar{Y}$-, $\bar{Z}$-axes system, are chosen so that the Y-axis always remains in the $\bar{Y}\bar{Z}$ plane (i.e., γ is measured in the $\bar{Y}\bar{Z}$ plane), as shown in figure 3.

Expressing the angular rates in terms of these Euler angles,

$$s = \dot{\phi} \quad (4\text{-}17)$$

$$\begin{aligned}\omega_x &= -\dot{\gamma}\sin\delta \\ \omega_y &= \dot{\delta} \\ \omega_z &= \dot{\gamma}\cos\delta\end{aligned} \quad (4\text{-}18)$$

Differentiating (4-18) with respect to time:

$$\begin{aligned}\dot{\omega}_x &= \dot{\gamma}\dot{\delta}\cos\delta - \ddot{\gamma}\sin\delta \\ \dot{\omega}_y &= \ddot{\delta} \\ \dot{\omega}_z &= \dot{\gamma}\dot{\delta}\sin\delta + \ddot{\gamma}\cos\delta\end{aligned} \quad (4\text{-}19)$$

Substituting (4-17), (4-18), and (4-19) into (4-16):

$$\begin{aligned}M_x &= -I_1\dot{\gamma}\dot{\delta}\cos\delta - I_1\ddot{\gamma}\sin\delta + I_1\ddot{\phi} \\ M_y &= I_0\ddot{\delta} + (I_0 - I_1)\dot{\gamma}^2\sin\delta\cos\delta + I_1\dot{\gamma}\dot{\phi}\cos\delta \\ M_z &= -I_0\dot{\gamma}\dot{\delta}\sin\delta + I_0\ddot{\gamma}\cos\delta - (I_0 - I_1)\dot{\gamma}\dot{\delta}\sin\delta - I_1\dot{\phi}\dot{\delta}\end{aligned} \quad (4\text{-}20)$$

Expressing the moment terms about the Euler axes system as defined in figure 3:

$$\begin{aligned}M_\gamma &= -M_x\sin\delta + M_z\cos\delta \\ M_\delta &= M_y \\ M_\phi &= M_x\end{aligned} \quad (4\text{-}21)$$

Substituting (4-20) into (4-21) results in:

$$\begin{aligned} M_\gamma &= \ddot{\gamma}(I_0 \cos^2\delta + I_1 \sin^2\delta) - 2(I_0 - I_1)\dot{\gamma}\dot{\delta}\sin\delta\cos\delta - I_1\ddot{\phi}\dot{\delta}\cos\delta - I_1\ddot{\phi}\sin\delta \\ M_\delta &= I_0\ddot{\delta} + (I_0 - I_1)\dot{\gamma}^2\sin\delta\cos\delta + I_1\dot{\gamma}\dot{\phi}\cos\delta \\ M_\phi &= I_1\dot{\gamma}\dot{\delta}\cos\delta - I_1\ddot{\gamma}\sin\delta + I_1\ddot{\phi} \end{aligned} \qquad (4\text{-}22)$$

Note that the equations do not contain the terms γ or ϕ, nor any functions of them, but include only the first and second derivatives (rates and accelerations) of these terms.

C. Changing Descriptive Terminology Symbols.

The basic symbols used thus far to evolve these equations are now changed to different symbols, which have more meaning to the physical system being analyzed. These changes are shown in figure 4.

The symbol denoting rotational rate of the blade about the store center line $\dot{\gamma}$ is replaced by the symbol Ω, which is common terminology for hub rotation rate. All other terms are altered accordingly:

$$\dot{\gamma} = \Omega \qquad \ddot{\gamma} = \dot{\Omega} \qquad M_\gamma = M_\Omega$$

The symbol denoting rotational rate of the blade about its long axis $\dot{\phi}$ is replaced by the symbol ω, which is common terminology for autorotor spin rate, resulting in:

$$\dot{\phi} = \omega \qquad \ddot{\phi} = \dot{\omega} \qquad M_\phi = M_\omega$$

The angular symbol δ, which describes the angle of the blade measured from a plane perpendicular to the store center line (hub spin axis), is replaced by its complementary angle θ so that:

$$\sin\delta = \cos\theta \qquad \cos\delta = \sin\theta \qquad \delta = 90° - \theta$$

$$\dot{\delta} = -\dot{\theta} \qquad \ddot{\delta} = -\ddot{\theta} \qquad M_\delta = -M_\theta$$

The angle θ is then termed the "deployment angle," which has a more useful physical meaning in this application.

Substituting these new terms in equations (4-22) gives:

$$\begin{aligned} M_\Omega &= \dot{\Omega}(I_0 \sin^2\theta + I_1 \cos^2\theta) + 2(I_0 - I_1)\Omega\dot{\theta}\sin\theta\cos\theta + I_1\omega\dot{\theta}\sin\theta - I_1\dot{\omega}\cos\theta \\ -M_\theta &= -I_0\ddot{\theta} + (I_0 - I_1)\Omega^2\sin\theta\cos\theta + I_1\Omega\omega\sin\theta \\ M\omega &= I_1\Omega\dot{\theta}\sin\theta - I_1\dot{\Omega}\cos\theta + I_1\dot{\omega} \end{aligned} \qquad (4\text{-}23)$$

Solving for the angular accelerations:

$$\begin{aligned} \dot{\omega} &= \frac{M_\omega}{I_1} - \Omega\dot{\theta}\sin\theta + \dot{\Omega}\cos\theta \\ \ddot{\theta} &= \frac{M_\theta}{I_0} + (I_0 - I_1)\Omega^2\sin\theta\cos\theta + I_1\Omega\omega\sin\theta \\ \dot{\Omega} &= \frac{1}{(I_0\sin^2\theta + I_1\cos^2\theta)}\left[M_\Omega - 2(I_0 - I_1)\Omega\dot{\theta}\sin\theta\cos\theta - I_1\omega\dot{\theta}\sin\theta + I_1\dot{\omega}\cos\theta\right] \end{aligned} \qquad (4\text{-}24)$$

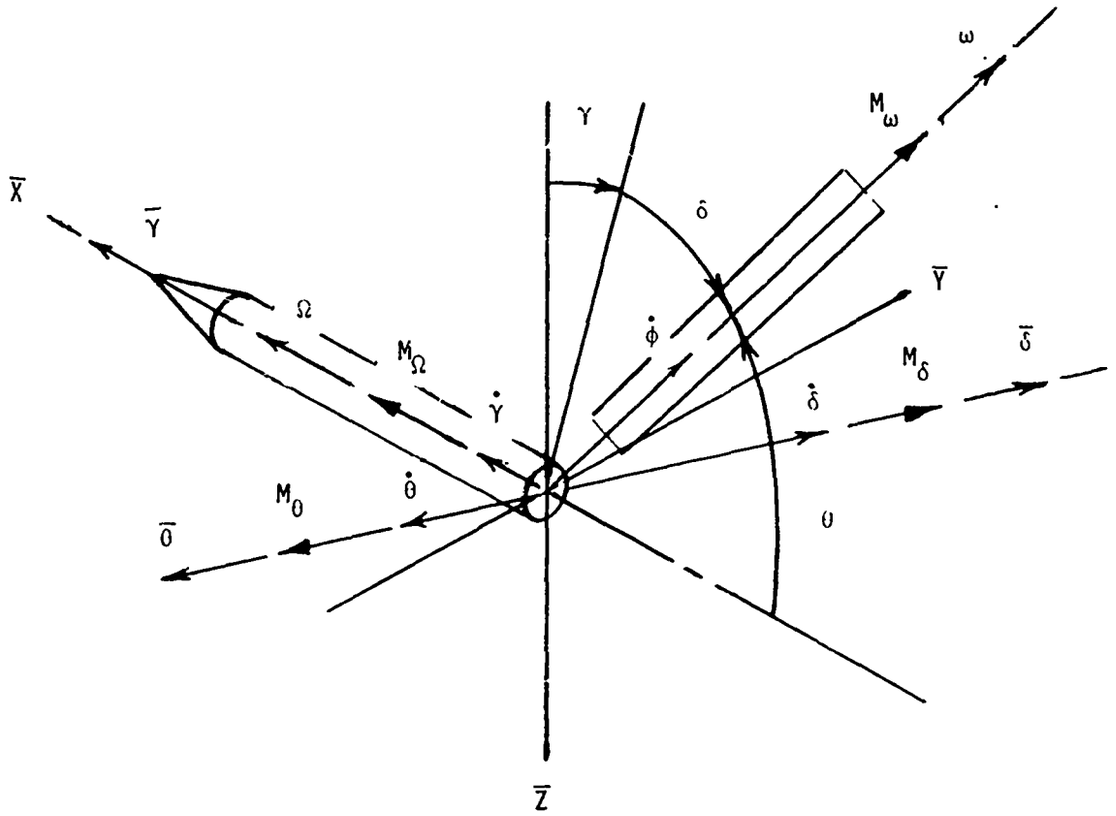

Figure 4. Basic System Terminology

D. Formulation of the Aerodynamic Moments.

The external moments M_ω, M_θ, and M_Ω in expressions (4-24) are assumed to result solely from aerodynamic forces. Blade weight and bearing friction for both the blade and hub are not considered.

The aerodynamic load distribution acting over the blade is evaluated by the standard blade element propeller theory method.[3] In this method, the magnitude and directional sense of the aerodynamic force is evaluated at distinct locations, these being the center of area elements located at incremental intervals along the blade. The forces are a function of the basic aerodynamic characteristics of the blade shape and the local flow conditions at each element.

In addition to the determination of the aerodynamic load distribution, the forces evaluated at each element are summed up, resulting in the net force and, consequently, the net moment acting on the blade.

In this analysis, axisymmetric flow relative to the store body is assumed where the free stream velocity V_∞ is parallel to the body center line ($\bar{X}$-axis, which is also the hub spin axis, Ω). Consider the aerodynamic forces acting on an element of the blade located at a distance r from the

[3]Von Mises, R. Theory of Flight. Dover Publications, Inc., New York, New York. 1959.

point where the blade intersects the body center line axis $\bar{X}$, as shown in figure 5. The equations describing the motion of the blade derived thus far do not depend on the angular position of the blade as it rotates about the store center line, indicated as γ in figure 4. Thus, to simplify the geometry in the following analysis, the blade is considered to be oriented in the $\bar{X}\bar{Z}$ plane.

The relative velocity at this element is $\bar{V}$, which is the vector sum of the free stream velocity and the tangential velocity of the element caused by the hub spin.

$$V = \sqrt{V_\infty{}^2 + (r\Omega \sin\theta)^2} \tag{4-25}$$

The relative angle of attack $\bar{\alpha}$, which is defined here as the angle between the resultant local velocity $\bar{V}$ and the free stream velocity V_∞, is as follows:

$$\bar{\alpha} = \tan^{-1}\left(\frac{r\,|\Omega|\sin\theta}{V_\infty}\right) \tag{4-26}$$

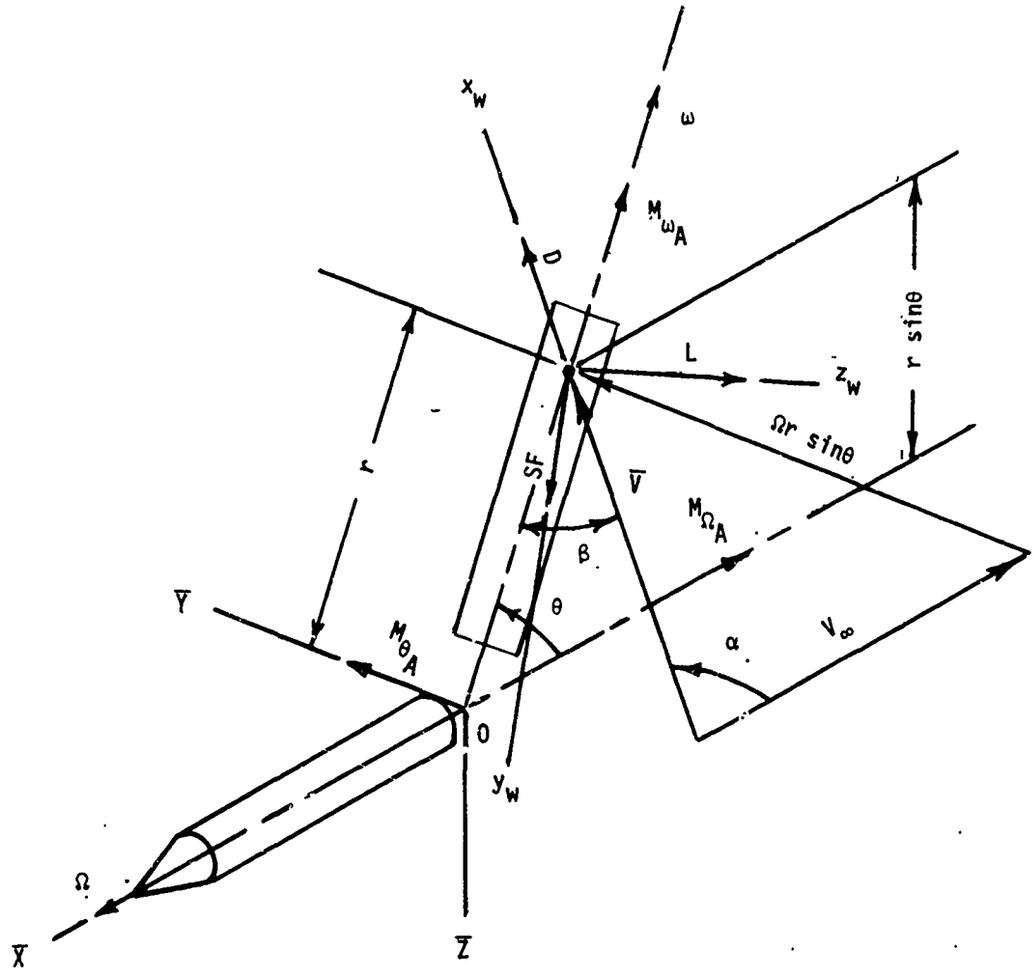

Figure 5. Aerodynamic Conditions at a Typical Blade Element

The velocity component at the element resulting from the blade deployment rate, $r\dot{\theta}$, is not included in the computation of the relative velocity because it is small, relative to the other velocity terms; its inclusion is not warranted in light of the increased complexity that would be added to the already complicated terms.

Let x_w, y_w, z_w be a wind axes coordinate system centered at the blade element considered (r), where x_w is parallel to $\overline{V}$, z_w is perpendicular to both $\overline{V}$ and $\overline{\omega}$, and y_w is perpendicular to the plane defined by $x_w z_w$. The aerodynamic force acting at this element can be expressed as a drag force component (D), acting along x_w, a lift force component (L) acting along z_w, and a side force component (SF) acting along y_w. The directional sense of the aerodynamic forces are indicated in figure 5. It should be noted that the wind axes system used is a "left-hand" system, as opposed to the commonly used "right-hand rule" concerning the positive direction of orthogonal vectors. This was done to facilitate the derivation of the angular relations for the physical system considered.

The aerodynamic forces acting on the blade in the autorotor decelerator system will be expressed in such a way that the autorotor blade sectional aerodynamic coefficients can be utilized directly in the same form in which they have been determined from wind tunnel tests of the particular autorotor blade sectional configuration.

The aerodynamic forces are expressed in the standard coefficient form where:

$$\begin{aligned} D &= C_D \overline{q} S \\ L &= C_L \overline{q} S \\ SF &= C_Y \overline{q} S \end{aligned} \tag{4-27}$$

$$\overline{q} = \text{dynamic pressure} = \frac{\rho \overline{V}^2}{2} \tag{4-28}$$

$$S = \text{planform area} = C\Delta l \tag{4-29}$$

The dynamic pressure used is the local value, evaluated at the center of the element; the area of the element $C\Delta r$ is used as the reference area, as shown in figure 6.

The aerodynamic coefficients C_L, C_D, and C_Y are obtained from wind tunnel tests on a rotor blade of identical cross-sectional shape.[4]

It should be noted that once the blade spin ω has been initiated, the aerodynamics are not a function of the angle of the air flow relative to the blade in a plane normal to the blade spin axis. The aerodynamic coefficient values, however, are a function of the blade tip speed ratio $\frac{\omega C}{2V}$ at the element, and the yaw angle ψ of the blade to the local velocity vector $\overline{V}$, as shown in figure 6.

A more detailed description of the form of these coefficients, as well as the method by which they are obtained, is included in section V.

The aerodynamic characteristics of the autorotor blade, as determined from wind tunnel tests, are expressed as a function of the yaw angle ψ, as illustrated in figure 6.

[4]Flatau, A. CRDL Technical Memorandum 15-49. Preliminary Investigation of Modified Autorotating Finned Cylinders. 17 August 1961. UNCLASSIFIED Memorandum.

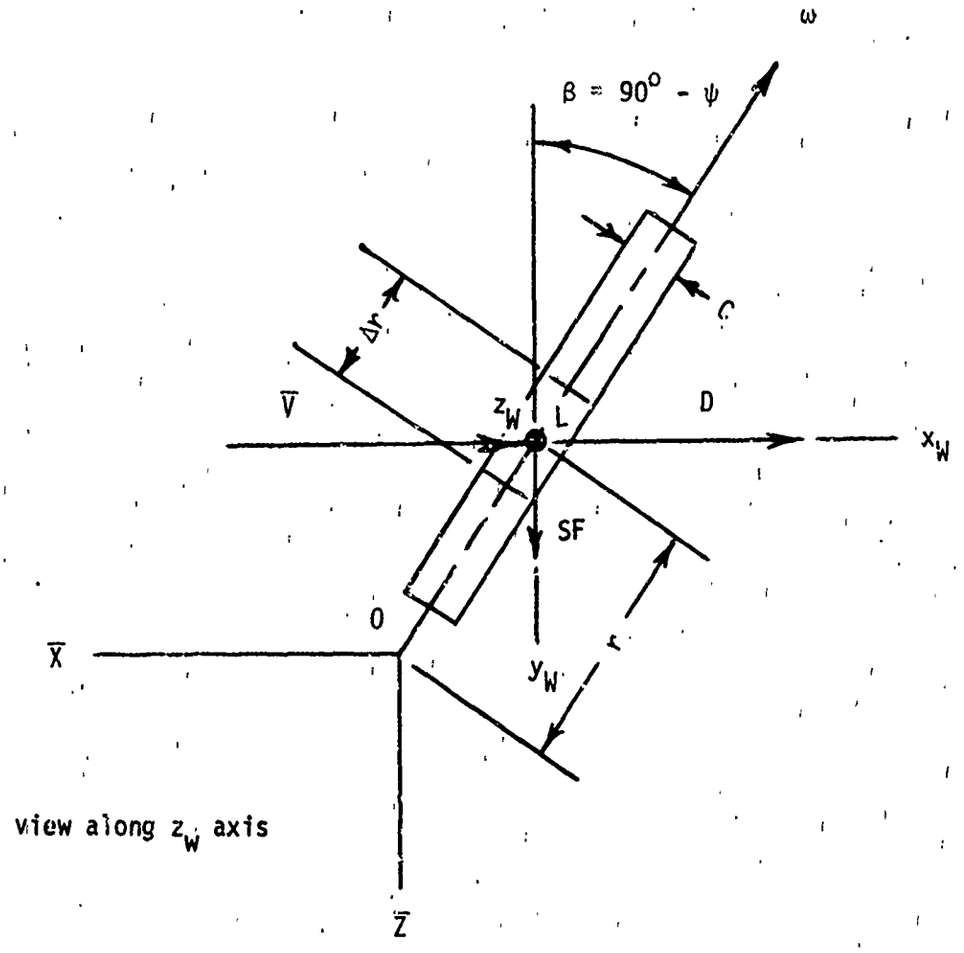

Figure 6. Details of Blade Element Terminology

For the autorotor decelerator system, the true yaw angle between the relative velocity vector $\bar{V}$ and the blade spin axis $\bar{\omega}$ is termed β, as shown in figure 6. The angle β is the complement of the angle ψ,

$$\beta = 90° - \psi \tag{4-30}$$

From figure 7 it can be seen that the angle β is a function of both θ and $\bar{\alpha}$:

$$\beta = \cos^{-1}(\cos\theta \cos\bar{\alpha}) \tag{4-31}$$

Figure 7 also illustrates the details of the derivation of the angular relations between the wind axes and the body axes systems that are required to resolve the aerodynamic forces in the proper form for inclusion into the equations of motion of the system. Let the wind axes system X_w, Y_w, Z_w be initially oriented to coincide with the $\bar{X}$-, $\bar{Y}$-, $\bar{Z}$-axes, with X_w directed along $\bar{Y}$, Y_w

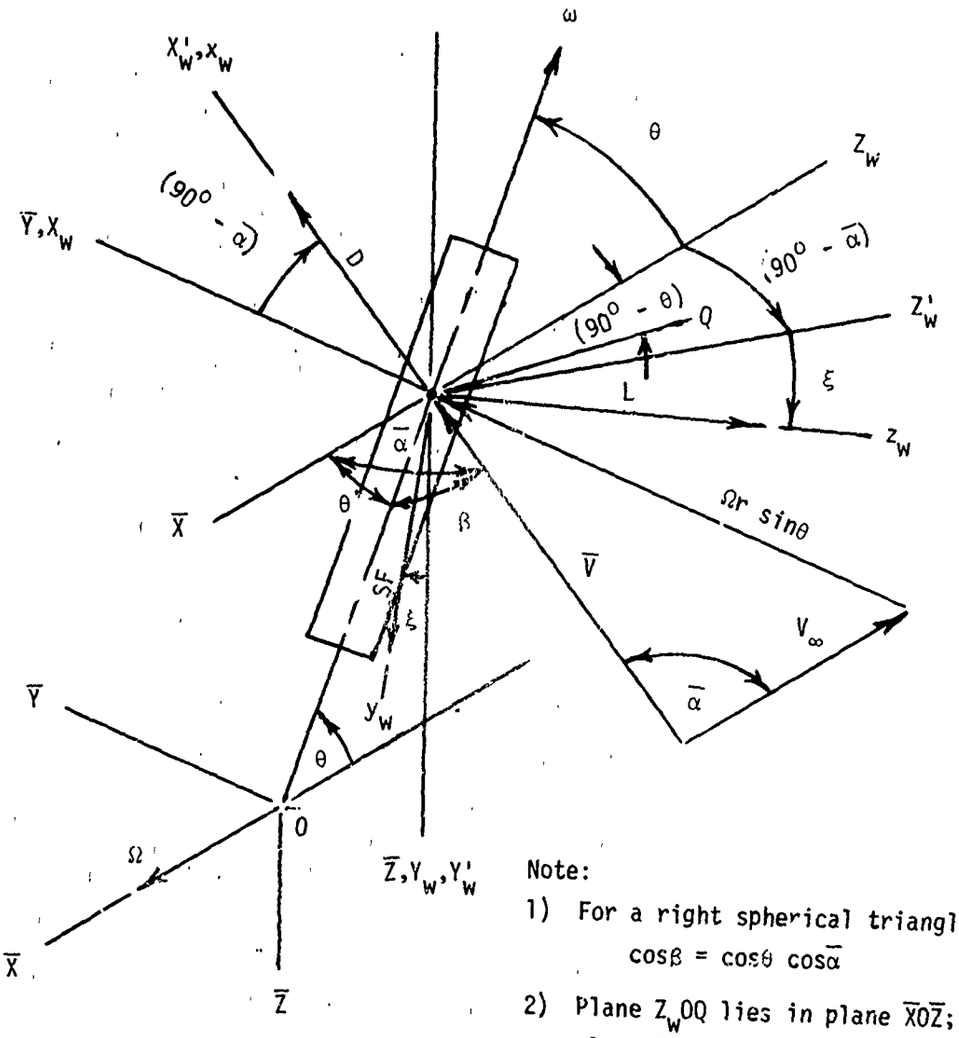

Note:

1) For a right spherical triangle:

$$\cos\beta = \cos\theta \cos\bar{\alpha}$$

2) Plane $Z_w OQ$ lies in plane $\bar{X}O\bar{Z}$;
plane QOz_w is perpendicular to $\bar{\omega}$;
plane $Z'_w Oz_w$ is perpendicular to $\bar{V}$;
$\therefore$ intersection of planes QOz_w and $Z'_w Oz_w$ define a line z_w which is perpendicular to both $\bar{\omega}$ and $\bar{V}$

where:

$$\tan\xi = \tan(90^o - \theta)\cos(90^o - \bar{\alpha})$$

or: $$\tan\xi = \mathrm{ctn}\theta \sin\bar{\alpha}$$

Figure 7. Derivation of True Blade Yaw Angle and Wind Axes Angular Relations

directed along $\bar{Z}$, and Z_w directed along the negative $\bar{X}$-axis. Rotate the X_w, Y_w, Z_w system about the Y_w-axis through the angle $(90° - \bar{\alpha})$. Now X_w is parallel to $\bar{V}$, and Z'_w is perpendicular to $\bar{V}$. Next, rotate the axes X'_w, Y'_w, Z'_w about the axis X'_w through the angle ξ, where:

$$\tan \xi = \tan(90° - \theta) \cos(90° - \bar{\alpha})$$

or:

$$\xi = \tan^{-1}(ctn\theta \sin \bar{\alpha}) \tag{4-32}$$

Now z_w is perpendicular to both $\bar{V}$ and $\bar{\omega}$ (i.e., the long axis of the blade). The y_w-axis is likewise perpendicular to $\bar{V}$, but lies in the plane of $\bar{V}$ and $\bar{\omega}$. The drag force (D) is directed along x_w, which is parallel to $\bar{V}$; the lift force (L) is directed along z_w, which is perpendicular to the plane of β. The side force (SF) is directed along y_w, which is perpendicular to $\bar{V}$ and lies in the plane of β. The aerodynamic forces relative to the blade and to the relative velocity are now identical in form to the wind tunnel data; the relations between these forces and the autorotor decelerator system body axes are defined.

The aerodynamic forces acting along the x_w-, y_w-, z_w-axes will not be resolved along the $\bar{X}$-, $\bar{Y}$-, $\bar{Z}$-axes, figures 5 and 7.

Considering figure 8, which contains a view at the blade element looking along the $\bar{Z}$-axis toward the inertial axes origin, and figure 9, which contains a view looking along the $\bar{Y}$-axis toward the origin, it can be seen that:

$$\begin{aligned} F_{\bar{X}} &= L \cos \xi \sin \bar{\alpha} + D \cos \bar{\alpha} - SF \sin \xi \sin \bar{\alpha} \\ F_{\bar{Y}} &= L \cos \xi \cos \bar{\alpha} - D \sin \bar{\alpha} - SF \sin \xi \cos \bar{\alpha} \\ F_{\bar{Z}} &= L \sin \xi + SF \cos \xi \end{aligned} \tag{4-33}$$

Now consider figure 9, which contains a view of the blade element looking along the Y-axis toward the element. The forces of (4-33) can be resolved into a force component that is normal to the blade spin axis in the $\bar{X}$-, $\bar{Z}$-plane.

$$F_N = F_{\bar{X}} \sin \theta + F_{\bar{Z}} \cos \theta \tag{4-34}$$

Substituting the expressions from (4-33) into (4-34) results in:

$$F_N = (L \cos \xi \sin \bar{\alpha} + D \cos \bar{\alpha} - SF \sin \xi \sin \bar{\alpha}) \sin \theta + (L \sin \xi + SF \cos \xi) \cos \theta \tag{4-35}$$

Thus, the component of the aerodynamic force acting normal to the blade in the θ-plane (i.e., the $\bar{X}$-, $\bar{Z}$-plane) for a particular blade element is:

$$F_\theta = F_N = L(\cos \xi \sin \bar{\alpha} \sin \theta + \sin \xi \cos \theta) + D \cos \bar{\alpha} \sin \theta + SF(\cos \xi \cos \theta - \sin \xi \sin \bar{\alpha} \sin \theta) \tag{4-36}$$

The net normal force acting on the blade in the θ-plane is the summation of the normal forces evaluated at all the elements along the entire length of the blade. Using the aerodynamic expressions of (4-27) through (4-29) in (4-36), and integrating over the length of the blade results in the following expression for the net normal force:

$$\begin{aligned} F_\theta = \int_{r_0}^{r_f} \Big| & C_L \frac{\rho V^2}{2} C(\cos \xi \sin \bar{\alpha} \sin \theta + \sin \xi \cos \theta) + C_D \frac{\rho V^2}{2} C \cos \bar{\alpha} \sin \theta \\ & + C_Y \frac{\rho V^2}{2} C (\cos \xi \cos \theta - \sin \xi \sin \bar{\alpha} \sin \theta) \Big| \, dr \end{aligned} \tag{4-37}$$

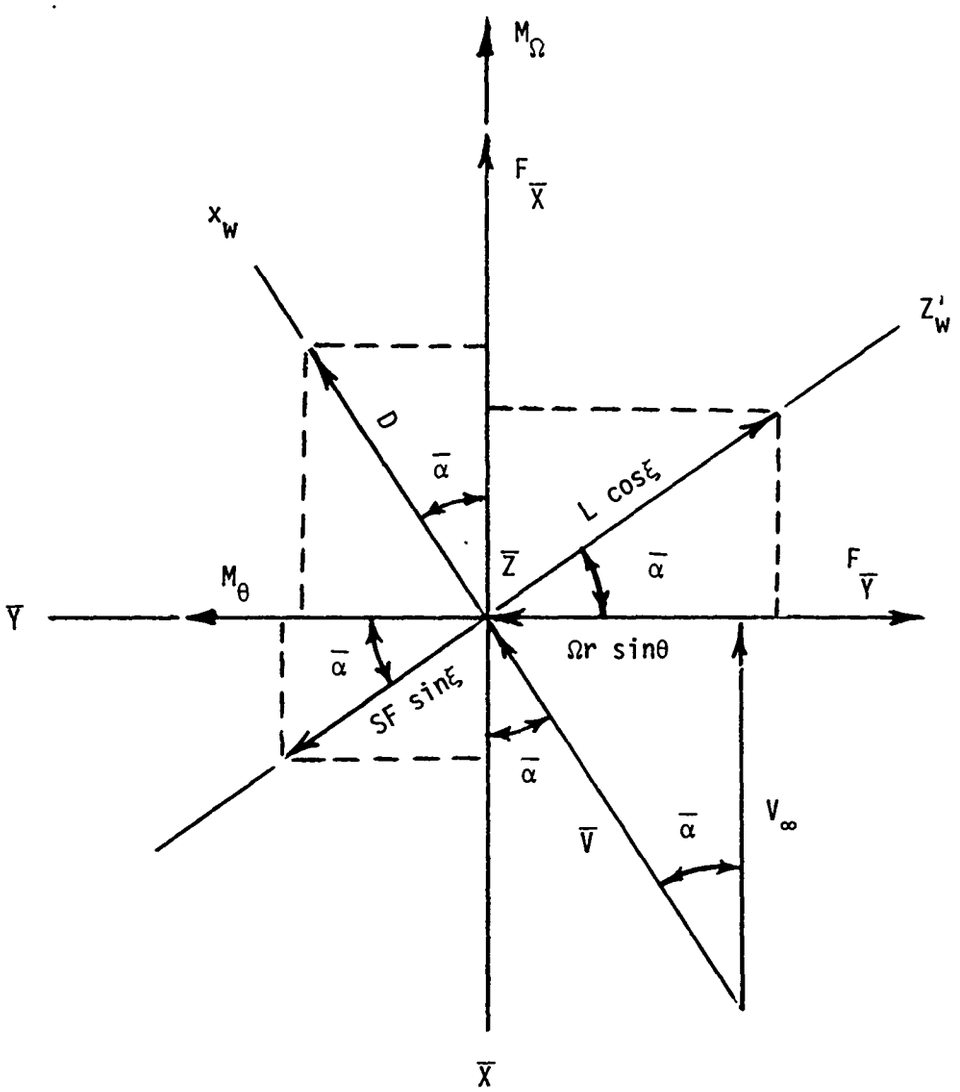

Note: View along $\bar{Z}$ axis toward $\bar{X},\bar{Y},\bar{Z}$ origin

Figure 8. Aerodynamic Forces Contributing to Hub Spin Moment and System Drag

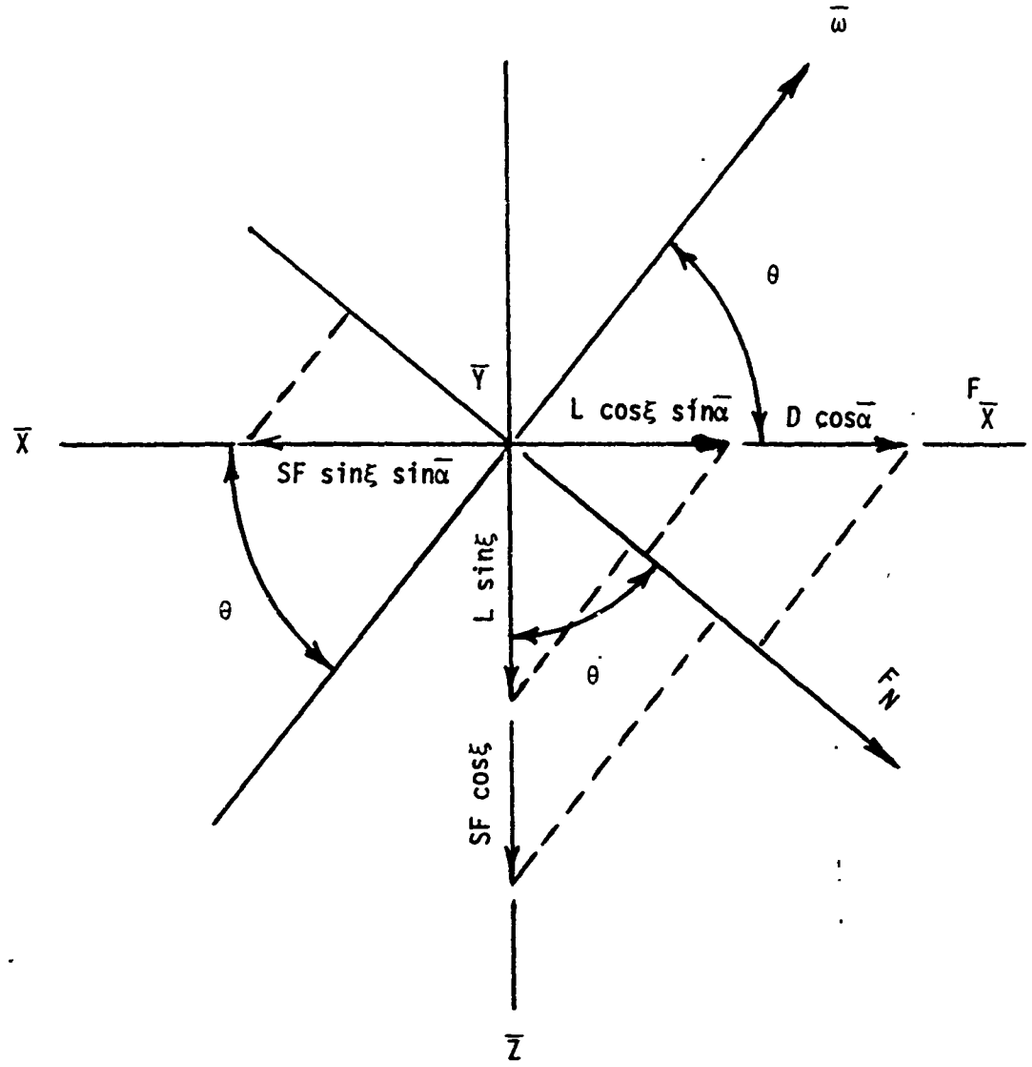

Note: View along $\bar{Y}$ axis toward $\bar{X},\bar{Y},\bar{Z}$ origin

Figure 9. Aerodynamic Forces Contributing to Blade Deployment Moment

Where r_0 indicates the location of the initial blade element, nearest the root of the blade, and r_f indicates the final outermost element, near the blade tip.

Thus, the net aerodynamic moment acting on the blade, about the blade/hub pivot point, in the θ-plane is:

$$M_\theta = \int_{r_0}^{r_f} \left\{ C_L \frac{\rho V^2}{2} C(\cos\xi \sin\bar{\alpha} \sin\theta + \sin\xi \cos\theta) + C_D \frac{\rho V^2}{2} C \cos\bar{\alpha} \sin\theta \right.$$

$$\left. + C_Y \frac{\rho V^2}{2} C (\cos\xi \cos\theta - \sin\xi \sin\bar{\alpha} \sin\theta) \right\} rdr \qquad (4\text{-}38)$$

The component of the aerodynamic force at each blade element acting normal to the blade spin axis and in the Ω-plane (i.e., the plane normal to the M_Ω vector in figure 4) is shown from figure 8 to be:

$$F_\Omega = F_{\bar{Y}} = L \cos\xi \cos\bar{\alpha} - D \sin\bar{\alpha} - SF \sin\xi \cos\bar{\alpha} \qquad (4\text{-}39)$$

The net force acting to give a "torque" to the blade, about the hub spin axis, is obtained by the summation of these load forces evaluated at all the elements along the entire length of the blade. Substituting the aerodynamic terms of (4-27) through (4-29) into the expression (4-39), and integrating over the length of the blade, results in the following expression for the net hub "torque" force:

$$F_\Omega = \int_{r_0}^{r_f} \left\{ C_L \frac{\rho V^2}{2} C \cos\xi \cos\bar{\alpha} - C_D \frac{\rho V^2}{2} C \sin\bar{\alpha} - C_Y \frac{\rho V^2}{2} C \sin\xi \cos\bar{\alpha} \right\} dr \qquad (4\text{-}40)$$

Thus, the aerodynamic moment acting on the blade about the blade/hub pivot point, in the Ω-plane is:

$$M_\Omega = \int_{r_0}^{r_f} \left\{ C_L \frac{\rho V^2}{2} C \cos\xi \cos\bar{\alpha} - C_D \frac{\rho V^2}{2} C \sin\bar{\alpha} - C_Y \frac{\rho V^2}{2} C \sin\xi \cos\bar{\alpha} \right\} rdr \qquad (4\text{-}41)$$

The aerodynamic moment acting to spin the blade about its long axis at a particular blade element is:

$$M_\omega = C_m \frac{\rho V^2}{2} SC \qquad (4\text{-}42)$$

where, as before, the dynamic pressure and reference area are for the local conditions at the element. The spin moment coefficient C_m, like the force coefficients, is a function of the blade tip speed ratio and yaw angle.

The total moment acting to spin the blade about its long axis is the summation of the moments at all elements (i.e., the integral of the moment distribution over the blade).

$$M_\omega = \int_{r_0}^{r_f} C_m \frac{\rho V^2}{2} C^2 dr \qquad (4\text{-}43)$$

Substitution of the moment expressions (4-38), (4-41), and (4-43) into the equations of motion (4-24) results in the general equations of motion for the articulated autorotor decelerator. These equations are shown summarized in figure 10. along with a simplified sketch of the decelerator system and the main variables.

The equations of (4-24) represent the equations of motion for *one* blade. The analysis to this point assumes that all the blades act as independent entities, with no mutual effect on each other. Further, it is assumed that all blades act in unison in that the motion of one blade is identical to all others.

The first equation of (4-33) represents the component of the aerodynamic force at the blade element, which contributes to the system drag (i.e., the force opposite in direction to the free stream velocity V_∞). The total drag force D_s resulting from one blade is the integral of this force component over the length of the blade:

$$D_s = \int_{r_0}^{r_f} \{C_L \frac{\rho V^2}{2} C \cos \xi \sin \bar{\alpha} + C_D \frac{\rho V^2}{2} C \cos \bar{\alpha} - C_Y \frac{\rho V^2}{2} C \sin \xi \sin \bar{\alpha}\} dr \qquad (4\text{-}44)$$

The total system drag is obtained by multiplying the drag determined for a single blade by tne number of blades included in the system. The autorotor decelerator system considered here has four blades; therefore:

$$\text{Total system drag} = D = 4D_s \qquad (4\text{-}45)$$

E. Additional Considerations.

It should be noted that in an actual physical system, the blade spin axis might not intersect directly with the hub spin axis because the blade pivot point would probably be located on the hub at some radial distance from the store center line. This factor has not been included in this analysis because it would incorporate an additional term into an already complicated system. The purpose of this analysis is to obtain a general understanding of the system from as simplified a view as possible. Future effort could include this feature without altering the general results of this study.

Inspection of the equations of (4-24) reveals that the equation describing the deployment angle is a second-order differential equation and, as such, could have an oscillatory form of solution. For this type of equation, a term containing $\dot{\theta}$, usually referred to as a damping term, is required. Even if the system described is basically stable, the creation of spurious, positive damping effects in the solution process could result in an invalid buildup of the basic terms and eventual "blowing-up" of the solution. This was seen to be the case in this instance, and an aerodynamic damping term was therefore added to the moment expression. The damping term was assumed to result from the action of the blade deployment rate θ relative to the free stream velocity expressed in the following form:

$$M_{\dot{\theta}} = C_{m_{\dot{\theta}}} \left(\frac{\dot{\theta} b}{V_\infty}\right) \frac{\rho V^2}{2} Sb \sin^2 \theta \qquad (4\text{-}46)$$

where $\frac{\dot{\theta} b}{V_\infty}$ is the nondimensional deployment rate of the blade referred to the free stream velocity. $C_{m_{\dot{\theta}}}$ is the damping moment derivative with respect to the nondimensional deployment rate. The

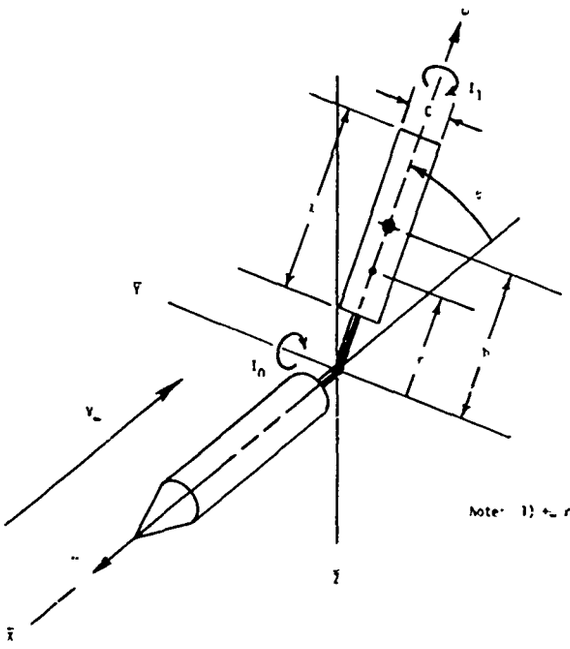

Note: $\dot{\psi}$ results in -

Differential Equations of Motion:

$$\dot{\omega}_x = \dot{\omega}_z \cos\psi - \omega_x \omega_z \sin\psi + \frac{M_x}{I_1}$$

$$\dot{\omega}_z = \frac{1}{(I_H/4 + I_1 \cos^2\phi + I_0 \sin^2\phi)} \{ I_1 \dot{\omega}_z \cos\psi - 2\omega_x \omega_z (I_0 - I_1) \sin\psi \cos\psi - \dot{\omega}_x I_1 \sin\psi + M_z \}$$

$$\dot{\omega}_\phi = \frac{1}{I_0} \{ \omega_x \omega_z I_1 \sin\psi + \omega_z^2 (I_0 - I_1) \sin\psi \cos\psi + M_\phi + M_{\phi_f} \}$$

Net Aerodynamic Moments:

$$M_x = \int_{r_0}^{r_f} C_n \frac{\rho V^2}{2} C^2 dr$$

$$M_z = \int_{r_0}^{r_f} \left(C_L \frac{\rho V^2}{2} C \cos\xi \cos\bar{\alpha} - C_D \frac{\rho V^2}{2} C \sin\bar{\alpha} - C_Y \frac{\rho V^2}{2} C \sin\xi \cos\bar{\alpha} \right) r dr$$

$$M_\xi = \int_{r_0}^{r_f} \left(C_L \frac{\rho V^2}{2} C (\cos\xi \sin\bar{\alpha} \sin\psi + \sin\xi \cos\phi) + C_D \frac{\rho V^2}{2} C \cos\bar{\alpha} \sin\psi + C_Y \frac{\rho V^2}{2} C (\cos\xi \cos\psi - \sin\xi \sin\alpha \sin\psi) \right) r dr$$

$$M_\phi = C_{m_{\dot{\phi}}} \left(\frac{\dot{\phi} b}{V_\infty} \right) \frac{\rho V_\infty^2}{2} S b \sin^2\phi$$

Figure 10. Summary of the Equations Describing the Motion of the Articulated Autorotor Decelerator System

Where:

$$\xi = \tan^{-1}(\text{ctn}\theta \sin\bar{\alpha})$$

$$\bar{\alpha} = \tan^{-1}\left(\frac{r\,|\Omega|\sin\theta}{V_\infty}\right)$$

$$C_L = C_L(\beta, \hat{\omega})$$

$$C_D = C_D(\beta, \hat{\omega})$$

$$C_Y = C_Y(\beta, \hat{\omega})$$

$$C_m = C_m(\beta, \hat{\omega})$$

$$\beta = \cos^{-1}(\cos\theta \cos\bar{\alpha})$$

$$\hat{\omega} = \frac{\omega C}{2\bar{V}}$$

$$\bar{V} = \sqrt{V_\infty^2 + (\Omega r \sin\theta)^2}$$

$$S = \ell C$$

Figure 10. Continued

term b is the distance from the store center line to the blade midpoint, measured along the blade span. The term $\sin^2\theta$ introduces the effect of the blade angle relative to the free stream velocity (normal component of b is $b \sin \theta$).

In addition to the moments of inertia of the blade, the moment of inertia of the hub I_H must also be considered in the Ω equation (4-24). Therefore, a factor of $I_H/4$ (for a four-bladed system) is added to the basic moment of inertia term for the blade.

V. AUTOROTOR SECTIONAL AERODYNAMIC CHARACTERISTICS.

A. S-Blade Autorotor Configuration.

Figure 11 illustrates the type of autorotor utilized in this analysis. The shaping of the blade cross section in an S-shape causes the blade to autorotate. This cross-sectional shape offers excellent lift and drag coefficients, and its geometry allows good stowage potential (prior to deployment) along with good structural qualities resulting from the corregated effect.

B. Testing Methodology.

In using the blade element propeller theory method outlined in section IV, the sectional aerodynamic characteristics of the autorotor blade are used directly. No satisfactory method has been developed to analytically predict the characteristics for autorotating shapes; thus, these characteristics must be determined experimentally from wind tunnel tests of the autorotor blade. Although somewhat different in testing procedure, because of the unique spinning properties of the autorotor, the general method and results are analogous to the approach used for airfoil sectional characteristics and their use in standard propeller analysis.

The aerodynamic characteristics of the autorotor blade cross section are determined experimentally in the wind tunnel using the testing arrangement shown in figure 12. The rotor is mounted on a yoke type mount, which is attached to the tunnel balance system. Each end of the rotor spin axis shaft is attached to the upright yoke arms with high-speed precision bearings. This allows the rotor to spin about its long axis with a minimum amount of friction. The rotor can be tested at various yaw angles to the air flow by rotating the yoke about its single center support. Figure 13 shows an S-section rotor blade model installed in the wind tunnel. The yoke is mounted to a pyramidal type strain gage balance located beneath the test section floor. This balance measures the three forces and the three moments directed along and about the three wind axes directions. The strain gage deflections are read out as microvolts and are calibrated to determine the actual

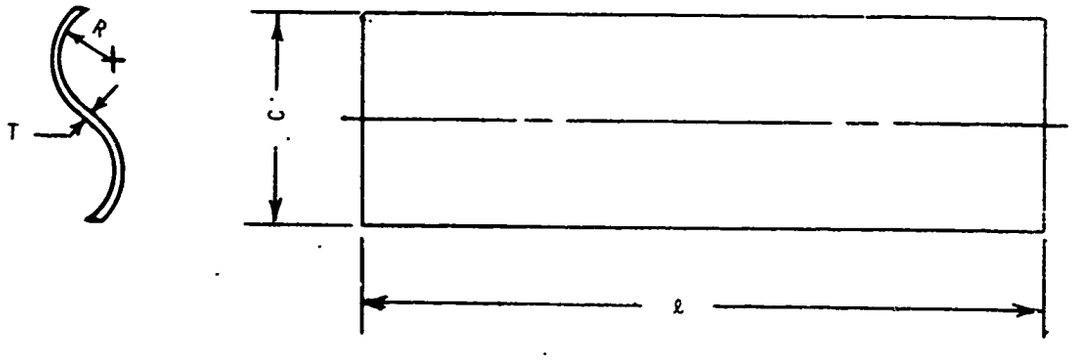

Figure 11. S-Section Autorotor Configuration

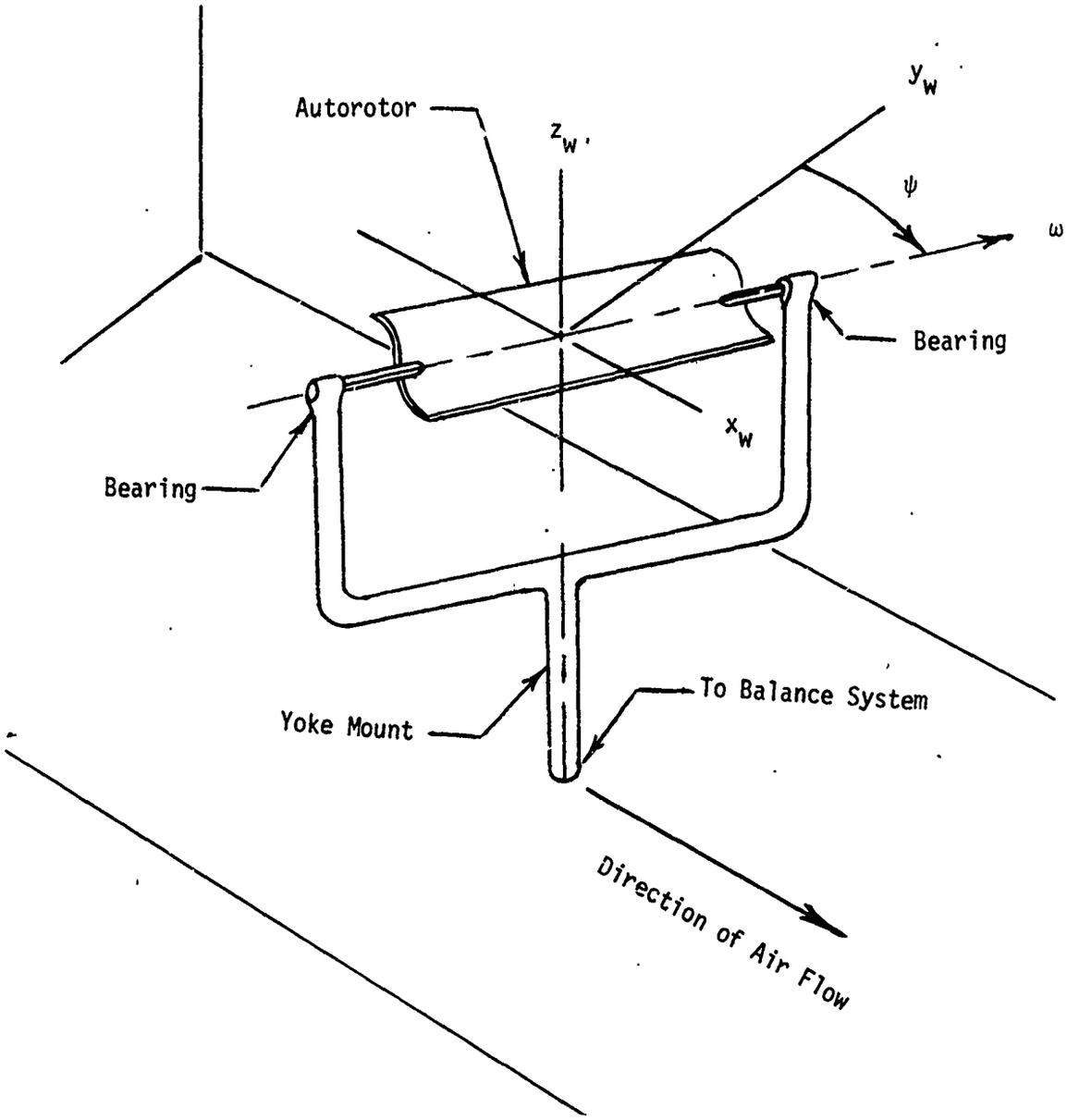

Figure 12. Autorotor Wind Tunnel Testing Technique

loads acting on the autorotor. A strip chart recorder is used so that all six load components can be recorded simultaneously during the run and so that the transient effects can be determined.

Autorotation spin rates were obtained by means of an optical tachometer. This basically consists of a light source that projects a light beam on the autorotor normal to the autorotor spin axis. The light beam is positioned so that the beam is interrupted by the surface of the autorotor. A light pick up senses the reflection of the beam over one-half cycle. Then the periodic reflection of the light beam is counted by the counter part of the device, and the spin rate of the autorotor is recorded on the strip chart along with the balance loads.

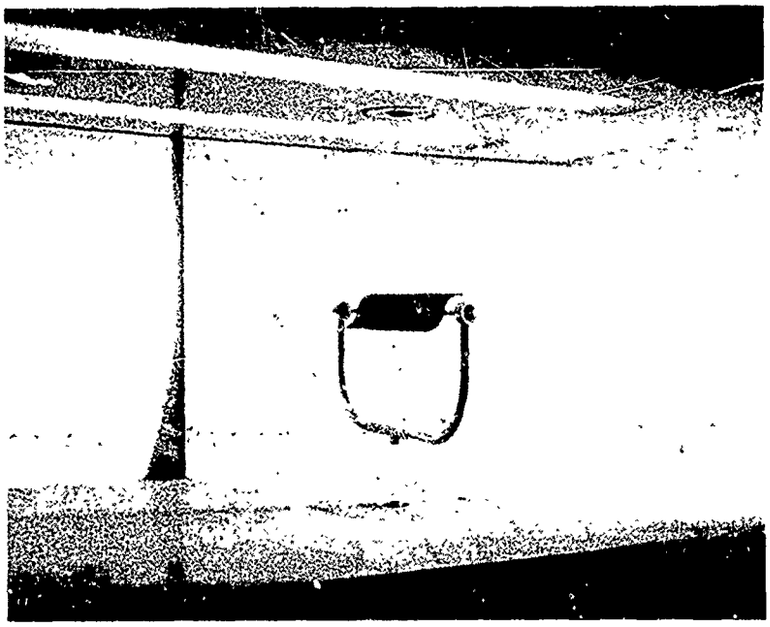

Figure 13. Autorotor Blade Installed in Aerodynamics Research Group 14- by 20-Inch Subsonic Wind Tunnel

The procedure of only testing the autorotor over a range of yaw angles in the plane defined by the rotor spin axis and the free stream velocity will provide the complete relationships between the aerodynamic characteristics and the angle of the free stream velocity to the autorotor for all combinations of pitch and yaw angles. This happens because once spin is initiated, the aerodynamic characteristics are not a function of the angle between the autorotor spin axis and the free stream velocity, measured in the plane perpendicular to the spin axis. Thus, the autorotor can be considered to be a purely symmetrical body, aerodynamically, thereby permitting this simplified testing method.

C. Aerodynamic Characteristics Nomenclature.

The axes system and the associated terms and symbols used in the wind tunnel data are illustrated in figure 14.

D. Aerodynamic Characteristics at Steady State Spin Rate.

If the autorotor is set at a fixed yaw angle ψ in a constant velocity air stream V_∞, it will assume a constant spin rate ω. The "steady state" spin characteristics of the rotor can be expressed in nondimensional form as the steady state tip speed ratio $\hat{\omega}_{ss}$ where:

$$\hat{\omega}_{ss} = \frac{\omega_{ss} C}{2V_\infty} \tag{5-1}$$

The subscript *ss* refers to the terms evaluated at the steady state condition. When discussing the aerodynamics of the basic autorotor, the tip referred to is the leading edge of the autorotor shape as viewed along the spin axis of the autorotor. Thus, the tip speed ratio is the ratio of the tangential velocity of the rotor tip, caused by spin, to the free stream velocity. The steady state tip speed ratio is a constant for the particular rotor cross-sectional shape and the particular yaw angle.

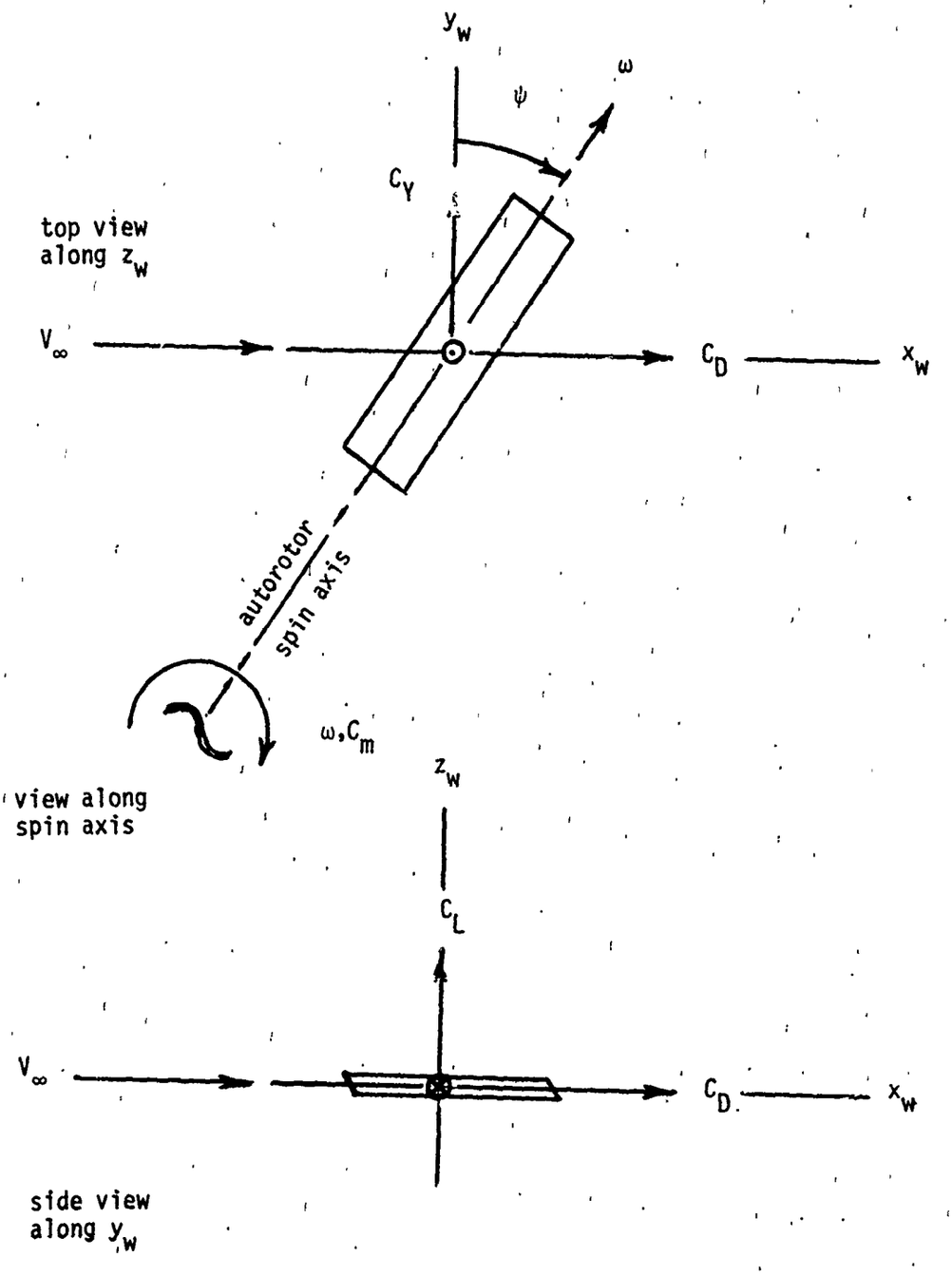

Figure 14. Definitions of Wind Tunnel Axes Systems and Aerodynamic Nomenclature

Another parameter that influences the steady state tip speed ratio and the other aerodynamic characteristics is the rotor aspect ratio (ℓ/C). In this sense, the assumption that the aerodynamic characteristics obtained in the wind tunnel on a rotor with an arbitrary aspect ratio can be utilized in the blade element method for the analysis of the autorotor decelerator has the same rationale as using general airfoil section data in evolving propeller performance using the same method. In addition, for the case of the autorotor, the combination of yaw angle with the consequent span wise flow would seem to be affected by aspect ratio. However, other than using autorotors of relatively high aspect ratios in the wind tunnel tests to determine the sectional characteristics, no aspect ratio corrections have been utilized in this analysis.

It might also be mentioned that the aerodynamic characteristics of autorotors are also a function of Mach number. However, this analysis does not involve situations outside of subsonic velocities, and compressibility effects are not considered.

At a steady state spin condition, the autorotor has an aerodynamic lift, drag, and side force that can be expressed in standard coefficient form ($C_{L_{ss}}$, $C_{D_{ss}}$, $C_{Y_{ss}}$) where the subscript ss denotes terms evaluated at a steady state spin condition. The autorotor also experiences a yawing moment and rolling moment. But in the case of the S-blade with no end plates, considered here, the yawing and rolling moments are extremely small and have no meaning because they are a result of side flow and end effects for the blade aspect ratio and constant test conditions of the tunnel that cannot be applied to the variable conditions along the blade for the autorotor deceleration system. Thus, they are not utilized in this analysis.

At steady state spin rate, the moment about the spin axis, or spin moment, is zero (otherwise, the rotor would experience spin acceleration, and the steady state condition would not exist). During the condition when the autorotor is spinning up to the steady state spin rate, the spin moment does have a value, and this will be treated in detail in the section on spinup transient.

The steady state values for the force coefficients and tip speed ratio are shown as functions of yaw angle in figure 15. These parts of this figure contain actual wind tunnel data for an S-section autorotor. As can be seen, the steady state characteristics can be expressed as a function of yaw angle as:

$$\hat{\omega}_{ss} = \hat{\omega}_{ss_0} \cos^2 \psi \tag{5-2}$$

$$C_{L_{ss}} = C_{L_{ss_0}} \cos^2 \psi \tag{5-3}$$

$$C_{D_{ss}} = C_{D_{ss_0}} \cos^2 \psi \tag{5-4}$$

$$C_{Y_{ss}} = C_{Y_{ss_0}} \sin^2 2\psi \tag{5-5}$$

where the subscript (0) refers to the terms maximum value (i.e., $C_{L_{ss_0}}$ and $C_{D_{ss_0}}$ are evaluated at $\psi = 0°$, and $C_{Y_{ss_0}}$ is evaluated at $\psi = 45°$). Because the aerodynamic characteristics of the autorotor can be expressed in standard coefficient form, wind tunnel tests at one velocity are sufficient to determine these coefficients. Actually, all wind tunnel tests were conducted at several free stream velocities to evaluate such effects as Reynolds' number, bearing friction, etc. In the case of the general autorotor shape, inertial properties, Reynolds' numbers, etc., used in this analysis, the constant coefficient properties assumed in

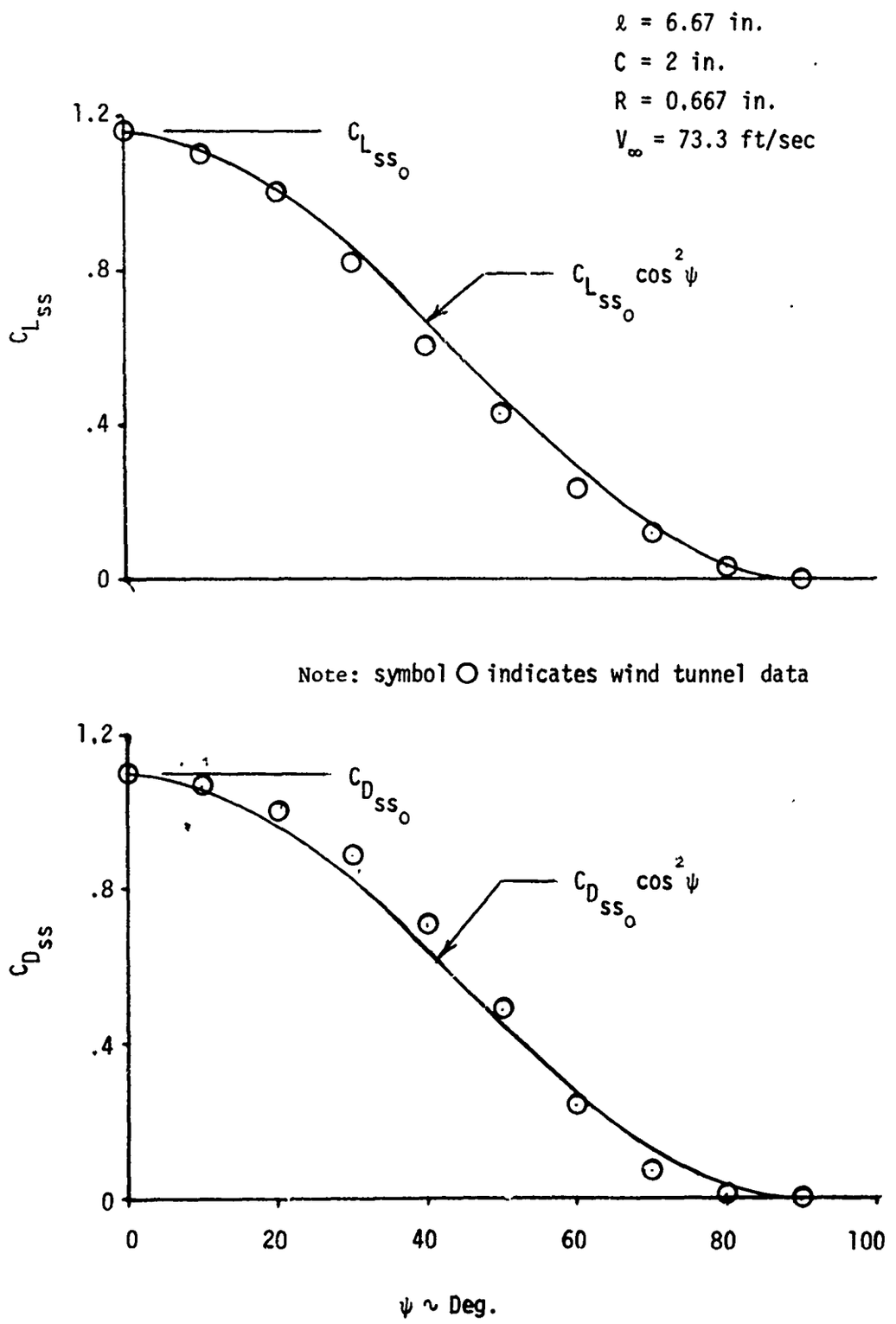

Figure 15. Aerodynamic Characteristics as a Function of Angle of Attack for an S-Section Autorotor at Steady State Spin

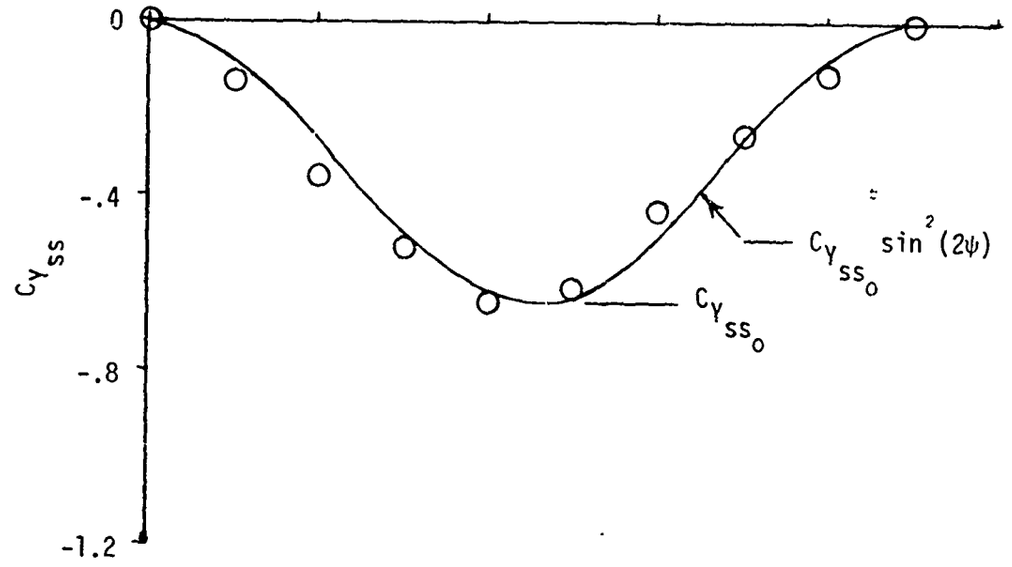

Note: symbol O indicates wind tunnel data

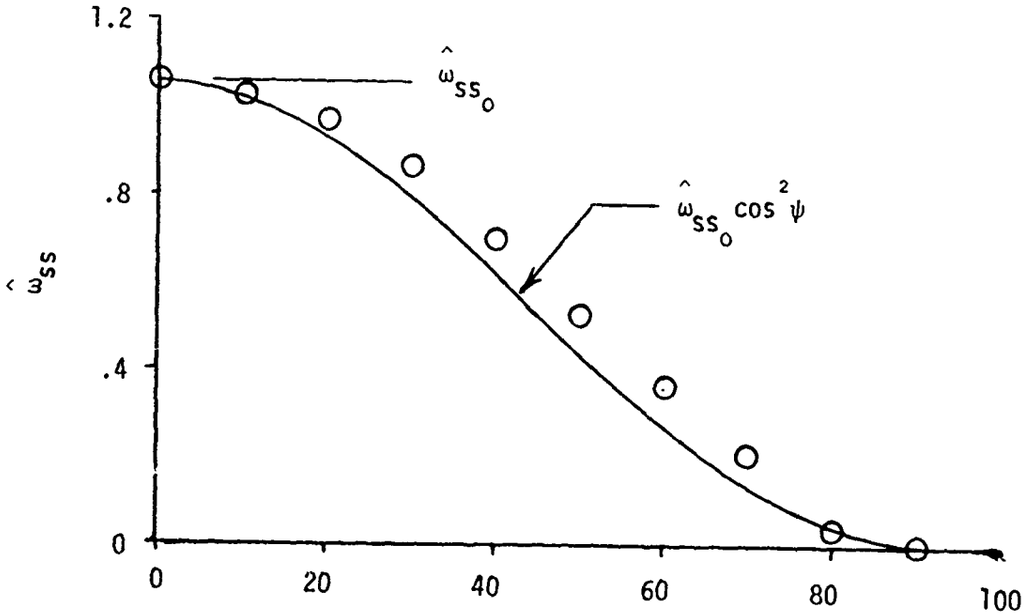

Figure 15. Continued

the analysis were verified by wind tunnel tests. Thus, the wind tunnel data are presented for a single set of wind tunnel conditions merely to illustrate a typical case or to evaluate a general expression.

E. Aerodynamic Characteristics During Spinup (Transient).

If the autorotor is set as a fixed angle of yaw in a constant free stream velocity and released, it will spinup to the particular steady state spin rate corresponding to the steady state tip speed ratio as described in the previous section. Figure 16 indicates how the various terms vary during a typical spinup in the wind tunnel. As can be seen, the drag coefficient and side force coefficient remain fairly constant during spinup; however, the lift coefficient and spin moment coefficient (indicated by the relative slope of the tip speed ratio versus time curve) vary with the spin rate in the transient condition.

If the ratio of the lift coefficient to its steady state value is plotted versus the ratio of the tip speed ratio to its steady state value, as shown in figure 17, it can be seen that the generalized lift coefficient can be expressed as a second-order function of the generalized tip speed ratio as follows:

$$\frac{C_L}{C_{L_{ss}}} = C_{L_1}\left(\frac{\hat{\omega}}{\hat{\omega}_{ss}}\right) + C_{L_2}\left(\frac{\hat{\omega}}{\hat{\omega}_{ss}}\right)^2 \tag{5-6}$$

where C_{L_1} and C_{L_2} are constants for the general autorotor configuration, and $C_{L_{ss}}$ and $\hat{\omega}_{ss}$ are steady values for the particular autorotor shape and for a specific yaw angle. The data curve (solid line) in figure 17 was formed using a second-order curve fit of the wind tunnel data.

Substituting expressions (5-2) and (5-3) into (5-6) results in:

$$C_L = C_{L_{ss_0}}\left(C_{L_1}\frac{\hat{\omega}}{\hat{\omega}_{ss_0}} + C_{L_2}\frac{\hat{\omega}^2}{\hat{\omega}_{ss_0}^2\cos^2\psi}\right) \tag{5-7}$$

Therefore, the lift coefficient during the transient spinup condition can be expressed as a function of the tip speed ratio, yaw angle, and the maximum steady state values of the lift coefficient and tip speed ratio. The specific lift characteristics of the S-section autorotor, utilized for the blade in the autorotor decelerator system and presented in the form of expression (5-7), are shown in figure 18. These data, which were obtained in wind tunnel tests, show the maximum steady state tip speed ratio $\hat{\omega}_{ss_0}$ to be 1.0, and the maximum steady state lift coefficient $C_{L_{ss_0}}$ to be 1.55.

Equation (5-7), which describes the transient behavior of the lift coefficient for any yaw angle and tip speed ratio, is based on the assumption that the transient coefficients C_{L_1} and C_{L_2}—which were determined from spinup tests at a 0° yaw angle—are valid for all yaw angles. This assumption was verified by wind tunnel tests in which the autorotor was allowed to spinup while being held at various fixed yaw angles. Figure 18, in addition to containing the lift coefficient values versus tip speed ratio for several yaw angles using expression (5-7), also shows data points determined directly from a spinup test for the autorotor at a yaw angle of 30° as a means of illustrating the justification for expression (5-7).

All the aerodynamic forces and moments are measured directly during the wind tunnel test using the standard tunnel balance system, except for the spin moment. The spin moment is determined indirectly from spin rate versus time traces obtained during the spinup process. The slope of this curve at any instant of time is the spin acceleration at that time. The product of the

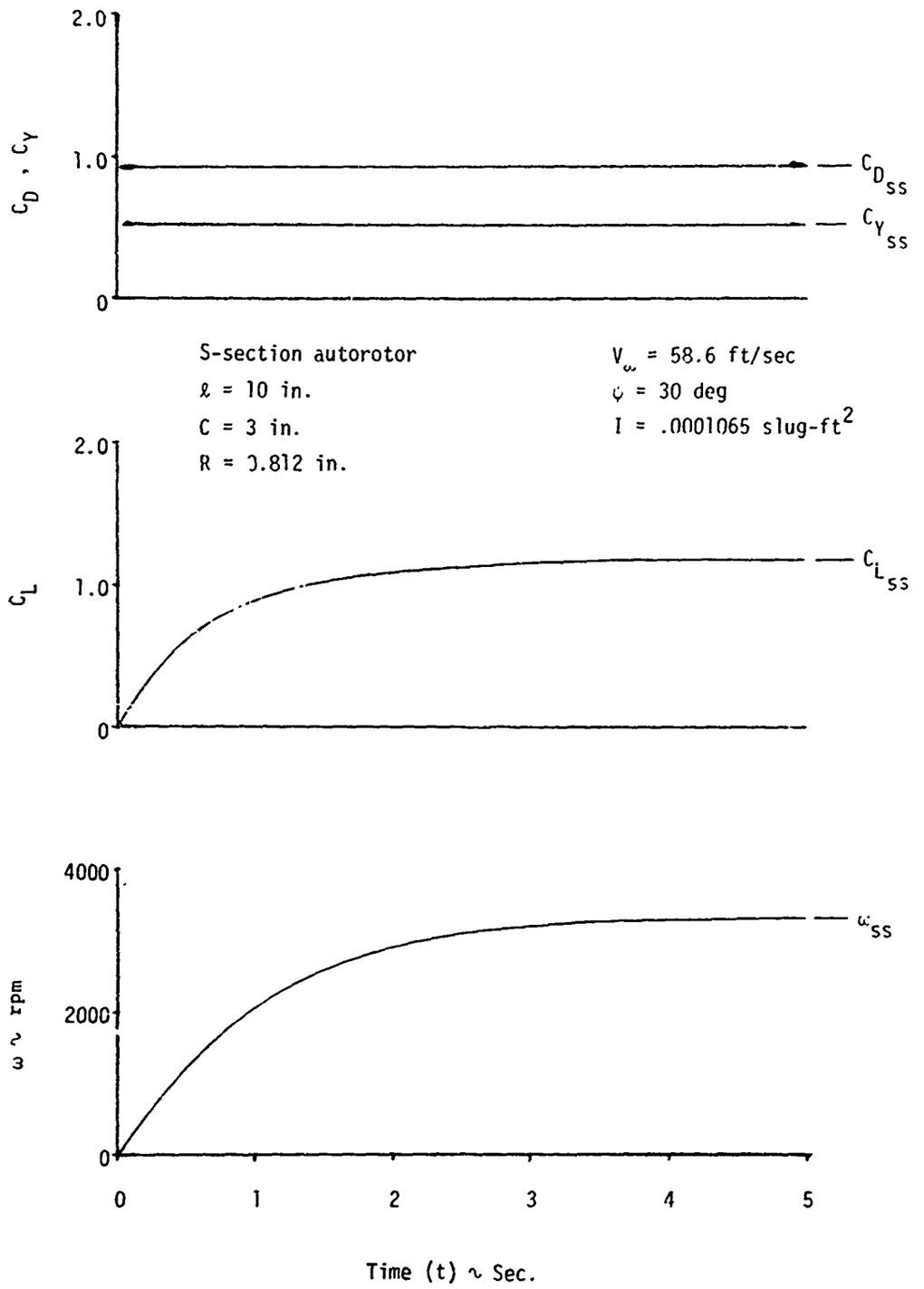

Figure 16. Typical Autorotor Aerodynamic Characteristics During Spinup Transient

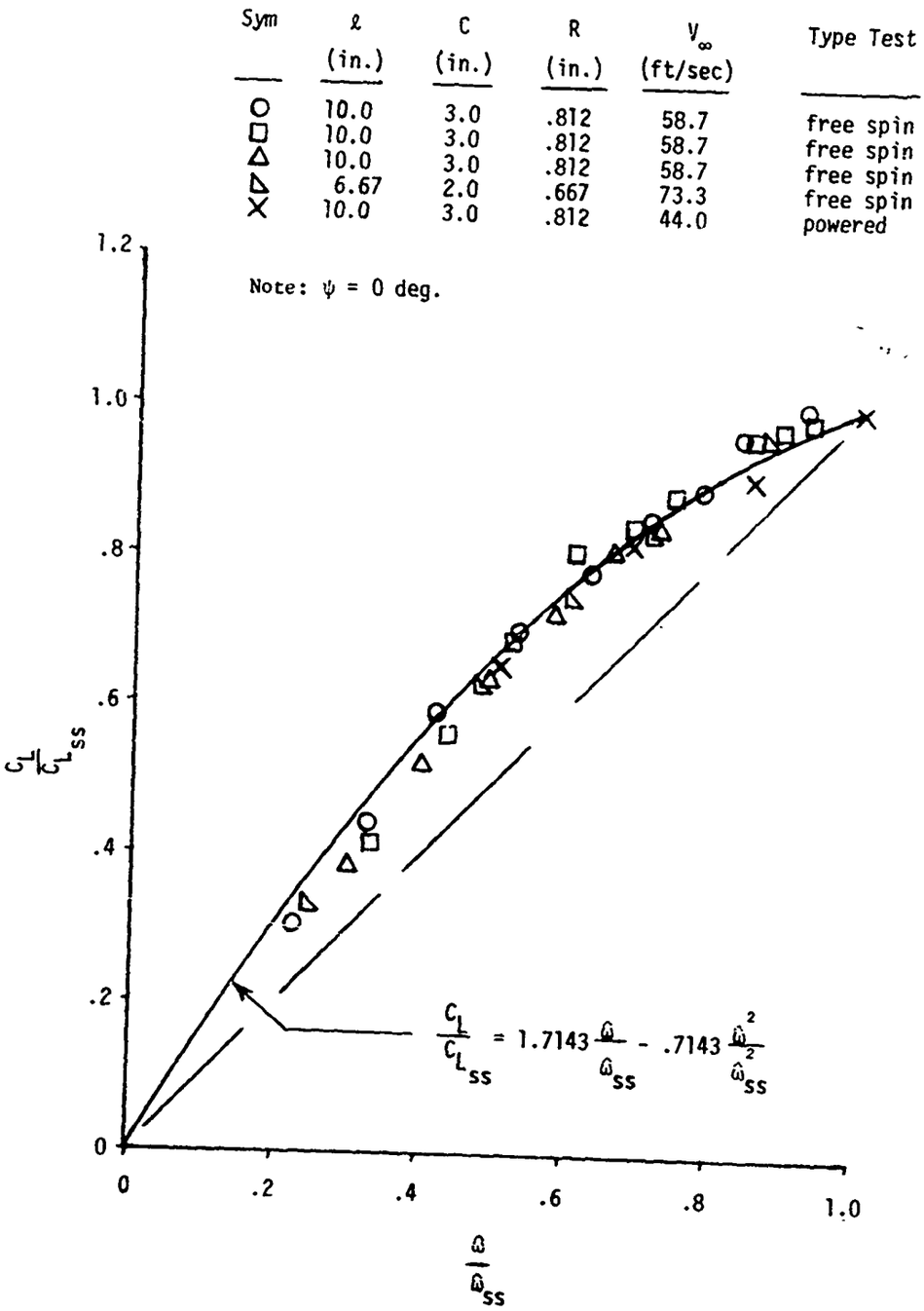

Figure 17. Generalized Lift Coefficient as a Function of Generalized Tip Speed Ratio for an S-Section Autorotor

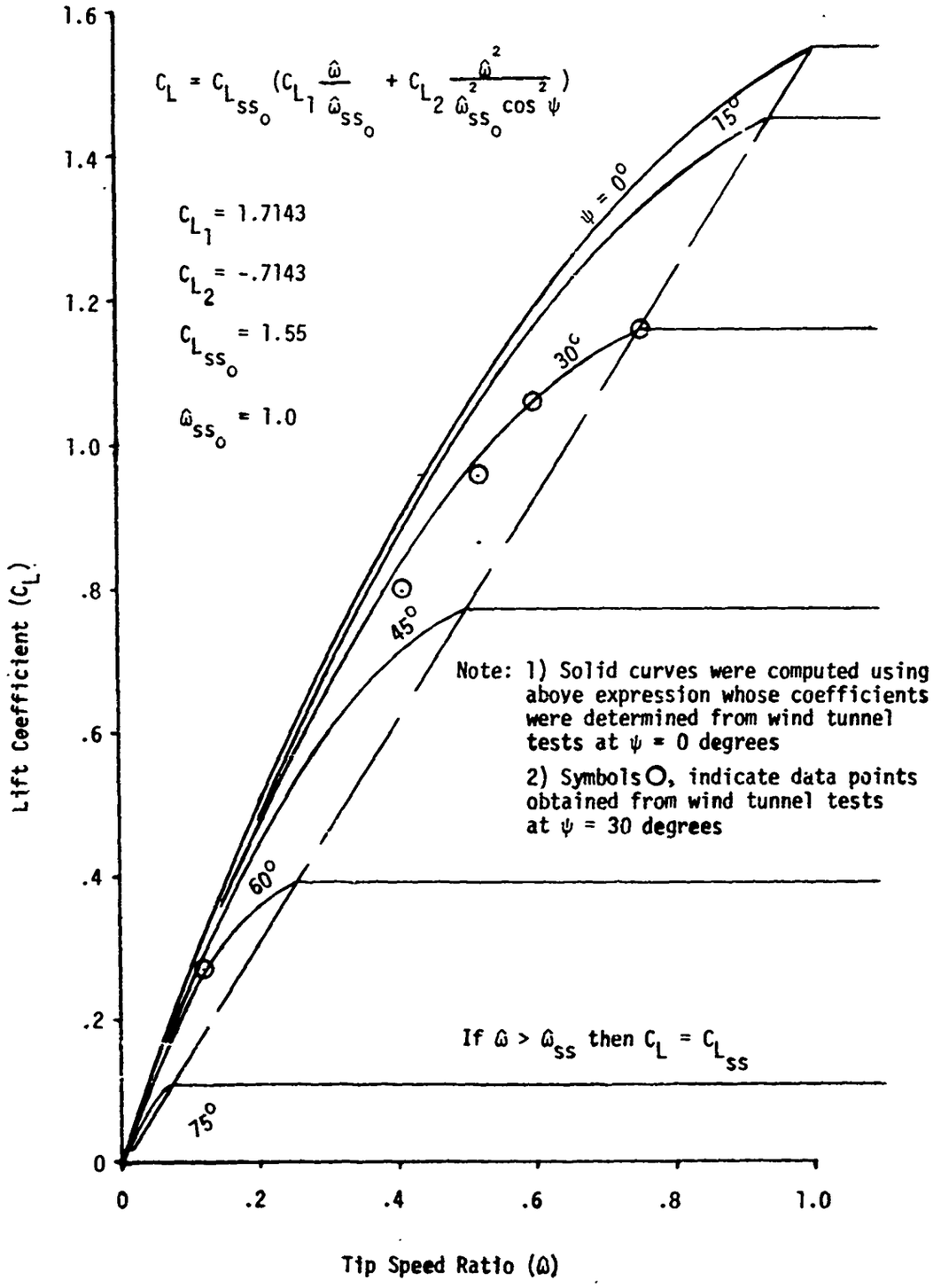

Figure 18. Lift Coefficient as a Function of Tip Speed Ratio and Yaw Angle for an S-Section Autorotor

spin acceleration and the autorotor moment of inertia about the spin axis at a particular instant of time is equal to the spin moment acting on the autorotor at that instant. The spin moment can then be reduced to a spin moment coefficient in the standard way:

$$C_m = \frac{I\dot{\omega}}{\rho V_\infty^2 SC}$$

where

I = moment of inertia about spin axis

$\dot{\omega} = \frac{d\omega}{dt}$ = spin acceleration

Thus, the plot of spin moment coefficient as a function of tip speed ratio can be determined by following this procedure for a large number of points from the spin rate versus time data.

The most common method, however, is to use a three-point curve fit from the spin rate versus time data to form a second-order equation of spin moment coefficient as a function of tip speed ratio. The three points chosen to evaluate the coefficients are the initial slope, the final steady state condition, and some intermediate point, usually the point where the spin rate is one-half its steady state value. The resulting expression is extremely accurate.[5]

The spin moment coefficient can be plotted versus the tip speed ratio (similar to the method used with the lift coefficient), as shown in figure 19, and can be expressed in the following form:

$$\frac{C_m}{C_{m\bar{0}}} = 1. + C_{m_1}\left(\frac{\hat{\omega}}{\hat{\omega}_{ss}}\right) + C_{m_2}\left(\frac{\hat{\omega}^2}{\hat{\omega}_{ss}^2}\right) \tag{5-8}$$

where C_{m_1} and C_{m_2} are constants for the general autorotor configuration and $\hat{\omega}_{ss}$ is the steady state value of the tip speed ratio for the particular autorotor shape and for a particular yaw angle. The data curve in figure 19 was determined from wind tunnel data using the second-order curve fit technique.

$C_{m\bar{0}}$ is the value of the spin moment coefficient at zero spin rate (the value at steady state is zero) and is a constant for the particular autorotor shape and angle of yaw.

$$C_{m\bar{0}} = C_{m_0} \cos^2\psi \tag{5-9}$$

where C_{m_0} is the value of the spin moment coefficient (evaluated at $\psi = 0°$).

Substituting (5-2) and (5-8) into (5-7) results in:

$$C_m = C_{m_0} \cos^2\psi + C_{m_1}\frac{\hat{\omega}}{\hat{\omega}_{ss_0}} + C_{m_2}\frac{\hat{\omega}^2}{\hat{\omega}_{ss_0}^2 \cos^2\psi} \tag{5-10}$$

[5]Brunk, J. E. Final Summary Report. Contract DA-18-108 AMC 236(A). Analytical and Aerodynamic Studies of Rotating Bomblet Motion. 31 January 1965. UNCLASSIFIED Report.

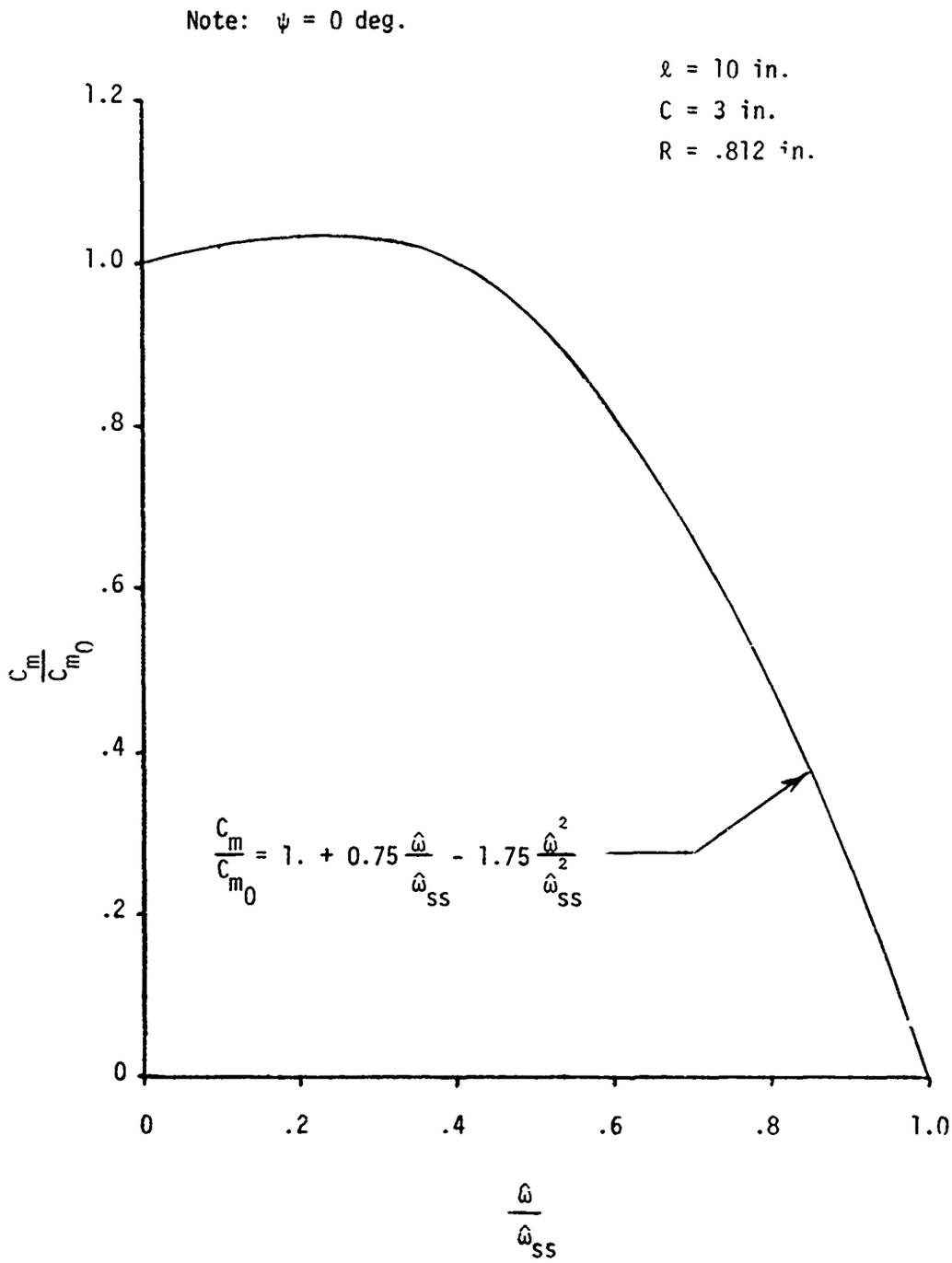

Figure 19. Generalized Spin Moment Coefficient as a Function of Generalized Tip Speed Ratio for an S-Section Autorotor

where the new constants are evaluated as:

$$C_{m_1} = C_{m_0} C_{m_1} \text{ and } C_{m_2} = C_{m_0} C_{m_2}$$

Therefore, the spin moment coefficient during transient spinup can be expressed as a function of the tip speed ratio, yaw angle, steady state tip speed ratio, and the maximum spin moment coefficient evaluated at zero spin.

The spin moment characteristics of the S-section autorotor, illustrated in figure 11, are presented in the form of expression (5-10) in figure 20. These data, which were obtained in wind tunnel tests, show the spin moment coefficient at zero spin and zero yaw angle C_{m_0} to be equal to 0.20.

As was the case with the lift coefficient, the transient coefficients C_{m_0}, C_{m_1}, and C_{m_2} for the spin moment coefficient, which were determined from tests with the autorotor set at 0° of yaw, are valid in equation (5-10) for all yaw angles as demonstrated by the wind tunnel data points included in figure 11 for the example case of a 30° yaw angle.

For the autorotor decelerator system mathematical model evolved in section IV, the relative angle between the velocity and the autorotor blade spin axis is β, where:

$$\beta = 90° - \psi \tag{4-30}$$

Hence:

$$\sin\psi = \cos\beta$$

$$\cos\psi = \sin\beta$$

Thus, in terms of the system angle β, the expressions for the steady state aerodynamic coefficients (5-2) through (5-5) become:

$$\hat{\omega}_{ss} = \hat{\omega}_{ss_0} \sin^2\beta \tag{5-10}$$

$$C_{L_{ss}} = C_{L_{ss_0}} \sin^2\beta \tag{5-11}$$

$$C_{D_{ss}} = C_{D_{ss_0}} \sin^2\beta \tag{5-12}$$

$$C_{Y_{ss}} = C_{Y_{ss_0}} \sin^2 2\beta \tag{5-13}$$

The expressions for the transient values of the aerodynamic coefficients (5-7) and (5-10) become:

$$C_L = C_{L_{ss_0}} \left(C_{L_1} \frac{\hat{\omega}}{\hat{\omega}_{ss_0}} + C_{L_2} \frac{\hat{\omega}^2}{\hat{\omega}^2_{ss_0}} \sin^2\beta \right) \tag{5-14}$$

$$C_m = C_{m_0} \sin^2\beta + C_{m_1} \frac{\hat{\omega}}{\hat{\omega}_{ss_0}} + C_{m_2} \frac{\hat{\omega}^2}{\hat{\omega}_{ss_0}} \sin^2\beta \tag{5-15}$$

F. Aerodynamic Characteristics for an Overspin Condition.

As described in the previous section, the autorotor aerodynamics can be basically expressed as a function of the tip speed ratio. Up to this point, only the spin regime between zero and steady state has been considered, i.e., $0 \leqq \hat{\omega} \leqq \hat{\omega}_{ss}$.

In using the blade element method in the analysis of the rotor decelerator system, if the tip speed ratio, yaw angle, local dynamic pressure, etc., are known at a particular element of the

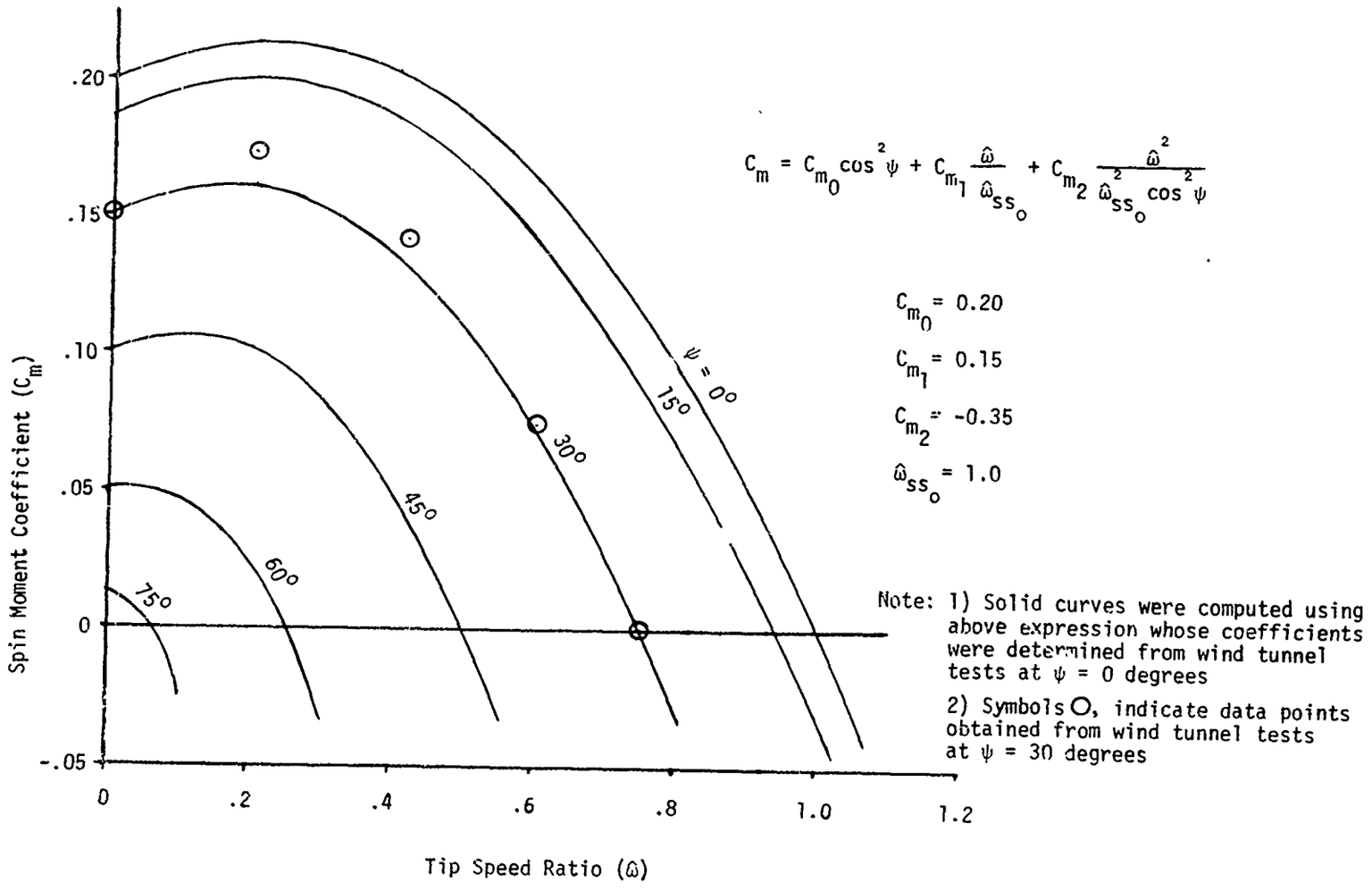

Figure 20. Spin Moment Coefficient as a Function of Tip Speed Ratio and Yaw Angle for an S-Section Autorotor

blade, the aerodynamic coefficient for that element can be determined by the functional relationships for the blade shape. For the case of the rotor retardation system, the blade, being a rigid body, has the same spin rate at any point along its length. However, the velocity varies along the length of the blade. The tip speed, therefore, varies along the blade, decreasing in value from root to tip. At some elements on the blade, a condition exists in which the tip speed ratio is greater than the steady state value corresponding to the conditions at the element; this condition is termed "overspin." Therefore, an understanding of the autorotor characteristics for an overspin condition (i.e., $\hat{\omega} > \hat{\omega}_{ss}$) is required.

A wind tunnel test was conducted in which the aerodynamic loads were measured on the S-section autorotor, which was forced to overspin by an electric motor. Figure 21 illustrates the rotor and mount used in the test. The results of this test are found in figure 22. As can be seen, the lift and drag remain at their respective steady state values, even when the rotor spin rate is 40% above the steady state value for the test conditions.

Therefore, if $\hat{\omega} > \hat{\omega}_{ss}$:

$$C_L = C_{L_{ss}},\ C_D = C_{D_{ss}},\ \text{and}\ C_Y = C_{Y_{ss}}$$

The lift and drag values were also measured with the motor holding the rotor spin rates at values less than steady state. The agreement of these data with data obtained from rotor transient tests using the free-spinning rotor method, as indicated in figure 17, demonstrates that the motor mounting installation did not introduce invalid or spurious conditions.

The overspin condition also affects the blade spin moment coefficient in that in an overspin condition, the blade will experience a negative spin moment coefficient tending to decrease the spin rate. A wind tunnel test was conducted to determine the nature of the spin moment acting on the autorotor in an overspin condition. The S-section autorotor and yoke mount arrangement shown in figure 21 was used. An external motorized friction wheel was utilized to give the

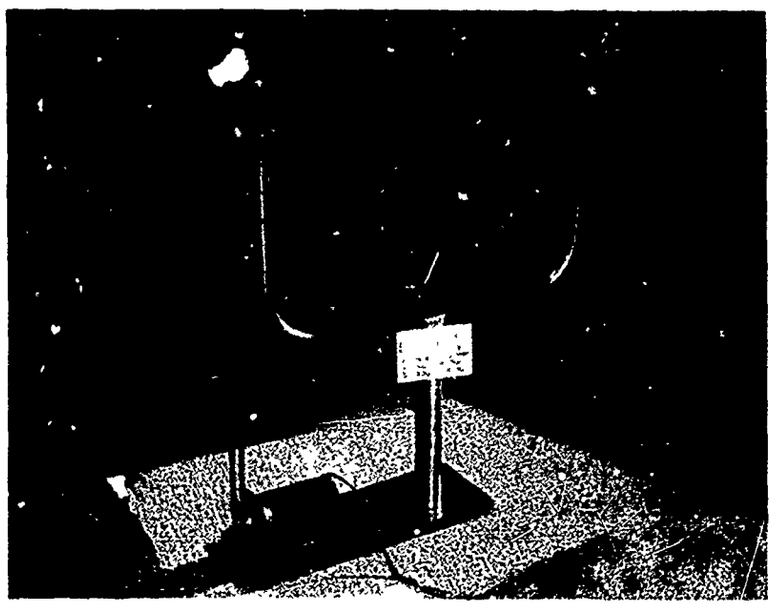

Figure 21. Autorotor Overspin Wind Tunnel Test Mounting Arrangment

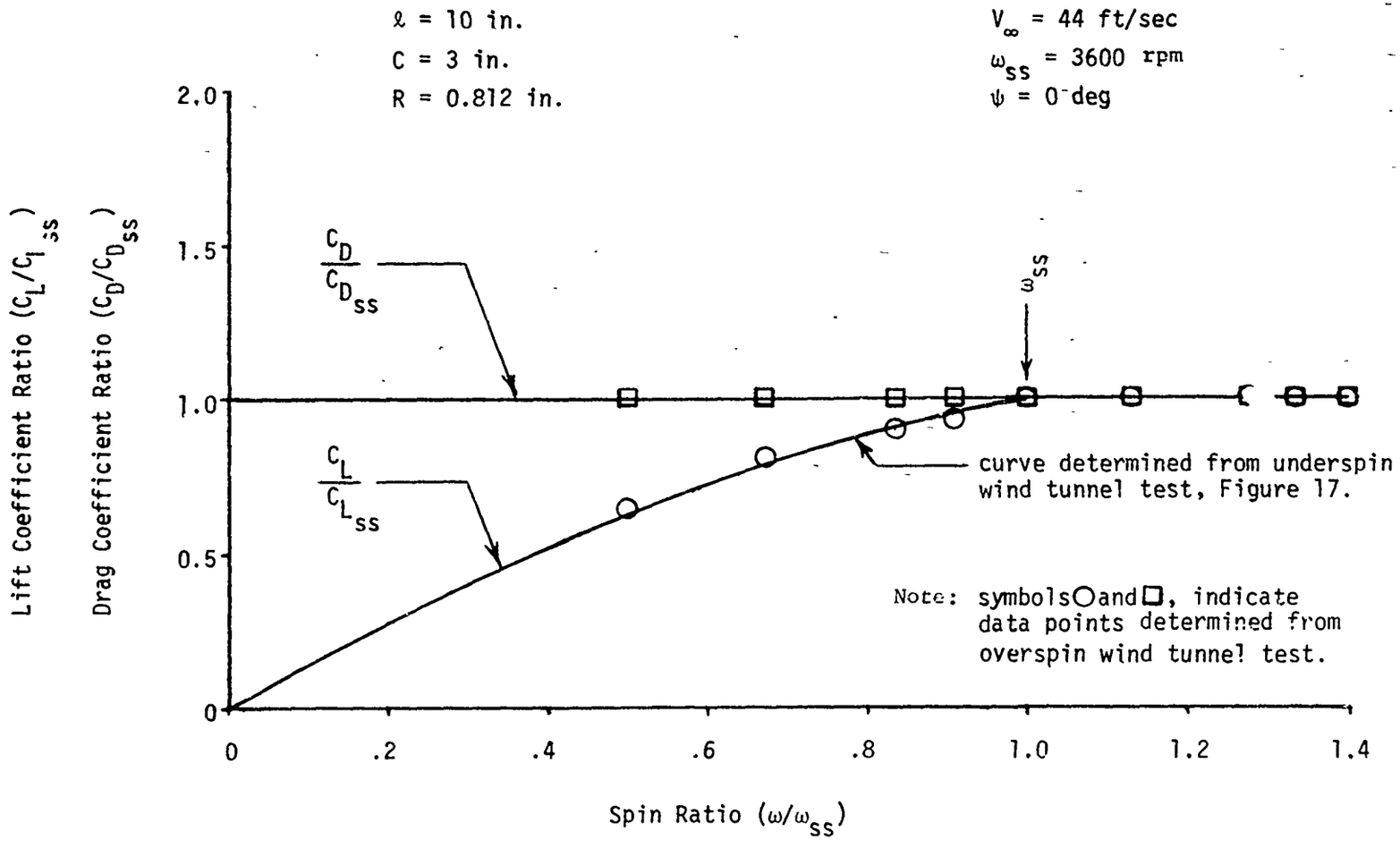

Figure 22. Results From Wind Tunnel Test to Determine Effect of Autorotor Overspin on the Lift and Drag Coefficients

autorotor a higher spin rate than the steady state value for the particular free stream velocity at which the test was conducted. When a sufficiently high spin rate had been achieved, the friction driving wheel was disengaged, thus allowing the autorotor blade to freely spin down to the steady state spin rate. The spin rate versus time data trace was analyzed in the same manner as for the underspin case. The results of this test revealed that the expression for the spin moment coefficient (5-10) previously determined for the underspin condition remained valid for the overspin condition, at least up to a blade tip speed ratio of 1.45, which was the highest value attained during the test. Thus, a very strong negative spin moment coefficient is present for the overspin condition, as indicated in figure 23.

G. Autorotor Spin Initiation.

Almost all autorotating shapes have the common characteristic that they will not automatically initiate spin for all attitudes of the rotor chord to the direction of the free stream velocity (which is actually the definition of the angle of attack in the commonly used sense). The angle of attack in this instance, as defined in figure 24, is important only to the action of the spin initiation. Once the autorotor is spinning, the angle of attack loses meaning in the description of the magnitude of the blade section aerodynamic characteristics. Actually, the aerodynamic forces act in a cyclic manner over a complete rotation. This periodic nature of the lift, drag, etc., can be observed at low spin rates or in water.[6] At the higher spin rates common to the rotors in air, the cyclic variances are too rapid to be measurable, and only an average value is indicated.

Wind tunnel tests of a nonspinning S-section rotor blade at various angles of attack indicate that there exists angle of attack ranges in which the rotor is statically stable in pitching moment (dead zone) and ranges where it is statically unstable (live zones). These conditions are apparent in figure 24, which shows the pitching moment coefficient as a function of angle of attack, where a live zone extends from $-105°$ to $-60°$, and a dead zone extends from $-60°$ to $+75°$, with a stable trim point at $-25°$. Thus, the S-blade autorotor considered has four alternating zones (two live and two dead) in a one complete 360° rotation.

This means that if the rotor were oriented at an angle of attack within the dead zone and released, it would assume a very stable trim altitude at an angle of attack of 25°. If oriented at an angle in the live zone and released, it would initiate spin and proceed to spin up to the corresponding steady state spin rate. In actuality, releasing the rotor in the outer fringes of the dead zones still might result in spin initiation because of overshoot of the blade past the trim point and into the live zone. This results in more realistic live and dead regions, each covering a 90° range as indicated in figure 25.

[6]Dupleich, P. NASA TM 1201. Rotation in Free Fall of Rectangular Wings of Elongated Shape. April 1949.

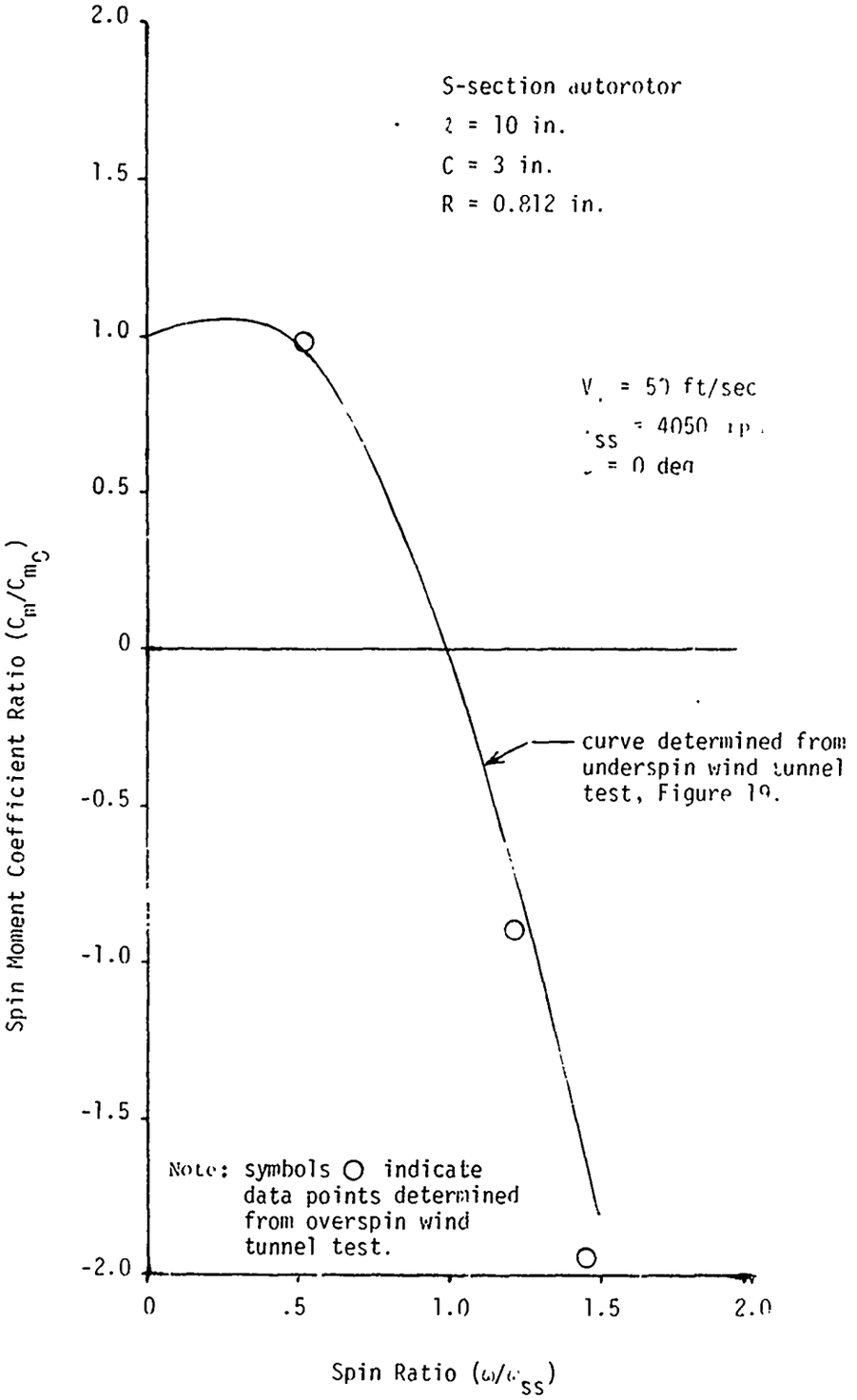

Figure 23. Results From Wind Tunnel Test To Determine Effect of Autorotor Overspin on the Spin Moment Coefficient

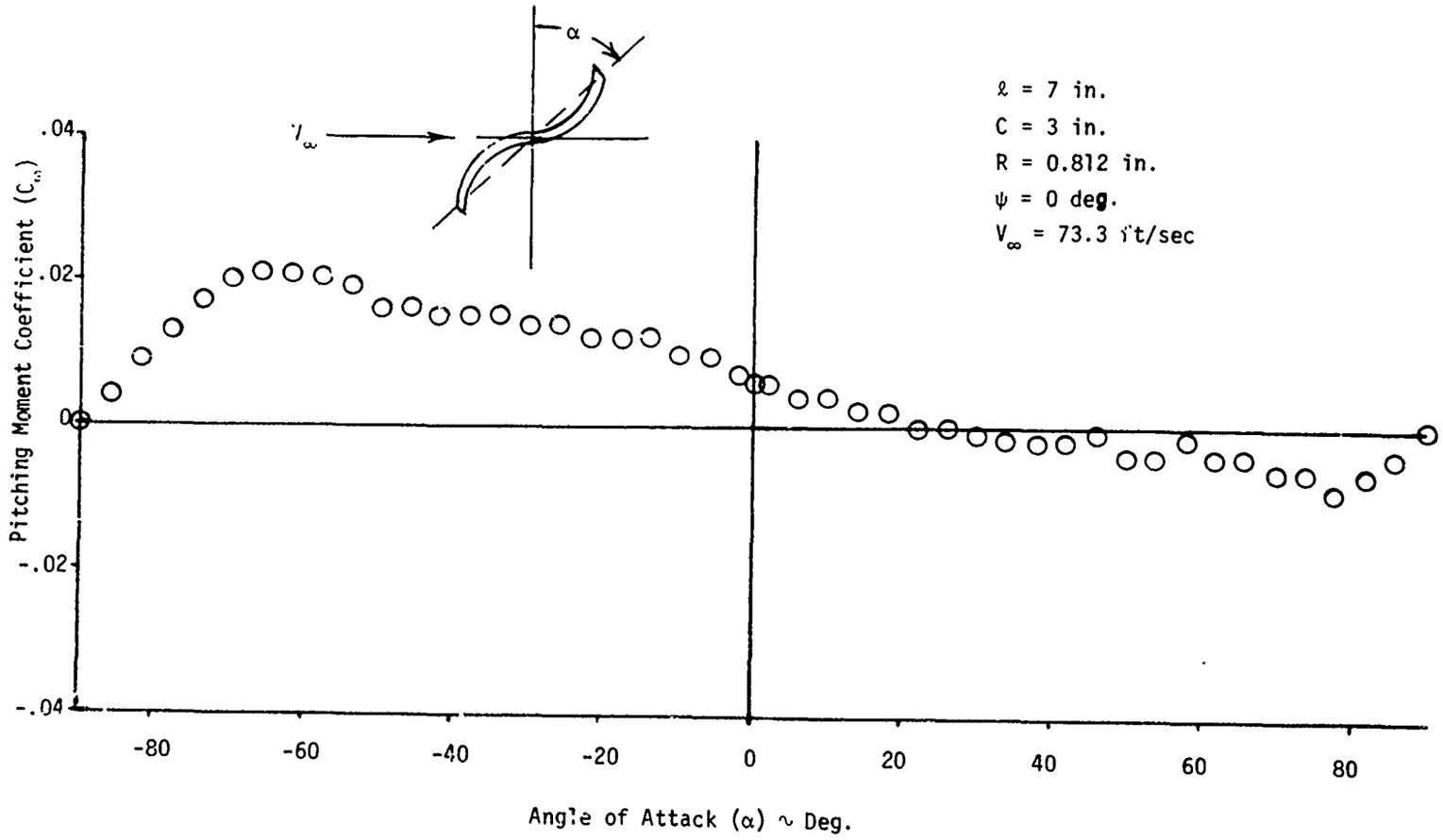

Figure 24. Pitching Moment Coefficient as a Function of Angle of Attack for a Nonspinning S-Section Autorotor

The inability of the autorotor shape to initiate spin at any altitude is of particular importance in the autorotor decelerator system application. Experience has shown that if the blades of the autorotor decelerator system are manually deployed (i.e., thrown out a near right angle to the body center line) without blade spin, the blades would assume a "stall" attitude or angle in which they would not autorotate about their long axes. Because this stall angle results in the blades being at a slight cant angle, they will initiate a steady state hub spin rate opposite in direction to that which would be obtained if the blades were autorotating. Although the resulting hub spin rate is greater for the stalled condition than the autorotating condition, the system drag of the former is less.

This stalled condition occurs whether the blades are deployed aft to forward or forward to aft. It is extremely difficult to get all the blades to autorotate; usually one or more are in the stalled condition with a resultant loss in system performance.

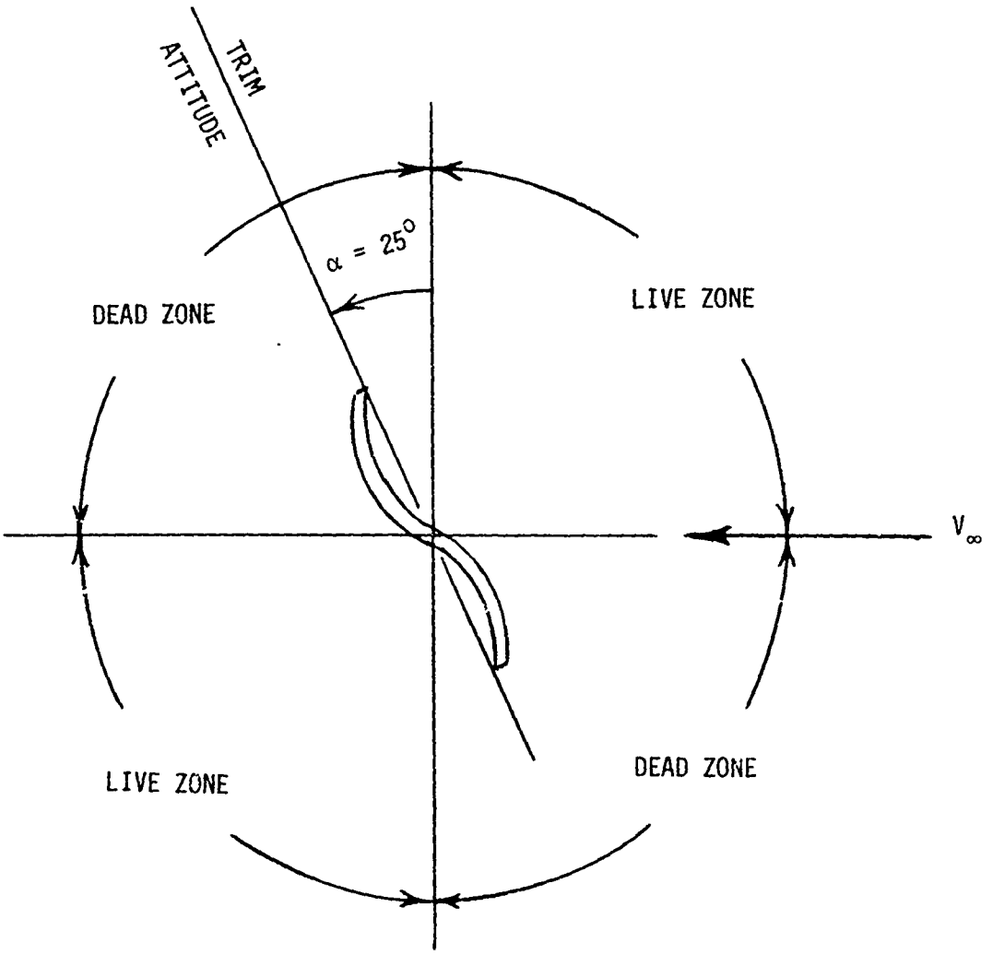

Figure 25. "Live" and "Dead" Angle of Attack Zones for Spin Initiation for S-Section Autorotor

The aft to forward blade deployment method (from an initial hub spin rate) considered here always results in all the blades achieving the proper autorotation. This is a result of several factors. Frist, the blades start out with an initial spin rate caused by the hub rotation; secondly, their angular movement during deployment from a deployment angle of 0° to an angle of near 60° causes portions of the blades to see angles of attack in the live zones. Most important, as will be shown in section X, a gyroscopic moment due to the hub spin rate and the blade deployment rate would seem to be the main cause of blade spin initiation for the autorotor decelerator system.

Figures 26 and 27 contain the lift coefficient and drag coefficient, respectively, that were obtained during the wind tunnel test on the nonspinning autorotor. These data are included for completeness and also to give an appreciation for the effects of the spin on the aerodynamic coefficients by comparing these nonspin values with the values at steady state spin (figure 15). It should be noted that the lift coefficient at steady state spin is about twice the value of the maximum lift coefficient for the nonspinning case. It is also interesting to note that the maximum spin moment coefficient, as determined from the spinup type tests, figure 20, is much larger than the maximum spin moment coefficient measured on the nonspinning autorotor. This also emphasizes the significance of the effects of the induced flow field created by the autorotation.

VI. METHOD OF SOLUTION.

A. General Approach.

The equations describing the motion of the autorotor decelerator system (figure 10) were programmed to be solved on a digital computer The physical characteristics of the system (blade weight, blade length, etc.), the free stream conditions (velocity, air density, etc.), and the autorotor aerodynamic sectional characteristics (lift coefficient, drag coefficient, etc.) are read into the program for each run. Starting from a set of initial conditions (blade deployment angle, hub spin rate, etc.), the program solves the equations and computes the system motion as a function of time.

The aerodynamic load distribution acting over the blade span and the resultant net moments are determined by computing the aerodynamic loads acting at several elements over the blade span and summing these to get the total load. Thus, all the local conditions at each blade element, as well as their distribution over the blade span, can be determined, in addition to the net effect, at each instant of time. The differential equations are solved using the improved Euler-Cauchy method of numerical solution.[7]

The steady state solution is obtained by initiating the program with arbitrary values for the initial conditions for each term. The program will then solve for the system motion as a function of time as the system experiences a transient motion converging toward a steady state condition. The steady state condition is achieved when the higher derivatives of θ, ω, and Ω are negligibly small, indicating the absence of nonsteady effects. The closeness of the initial condition values to the final steady state values determines the rapidity with which the steady state solution is achieved.

B. Description of the Computer Program.

The form, as well as the nomenclature, of some of the equations evolved in sections IV and V to describe the motion of the autorotor decelerator system have been altered to facilitate programming on the digital computer. Thus, where applicable in this section, the computer program expressions have been designated with the corresponding equation number from sections IV and V.

---

[7]Kreyszic, E. Advanced Engineering Mathematics. John Wiley and Sons Inc., New York, New York. 1962.

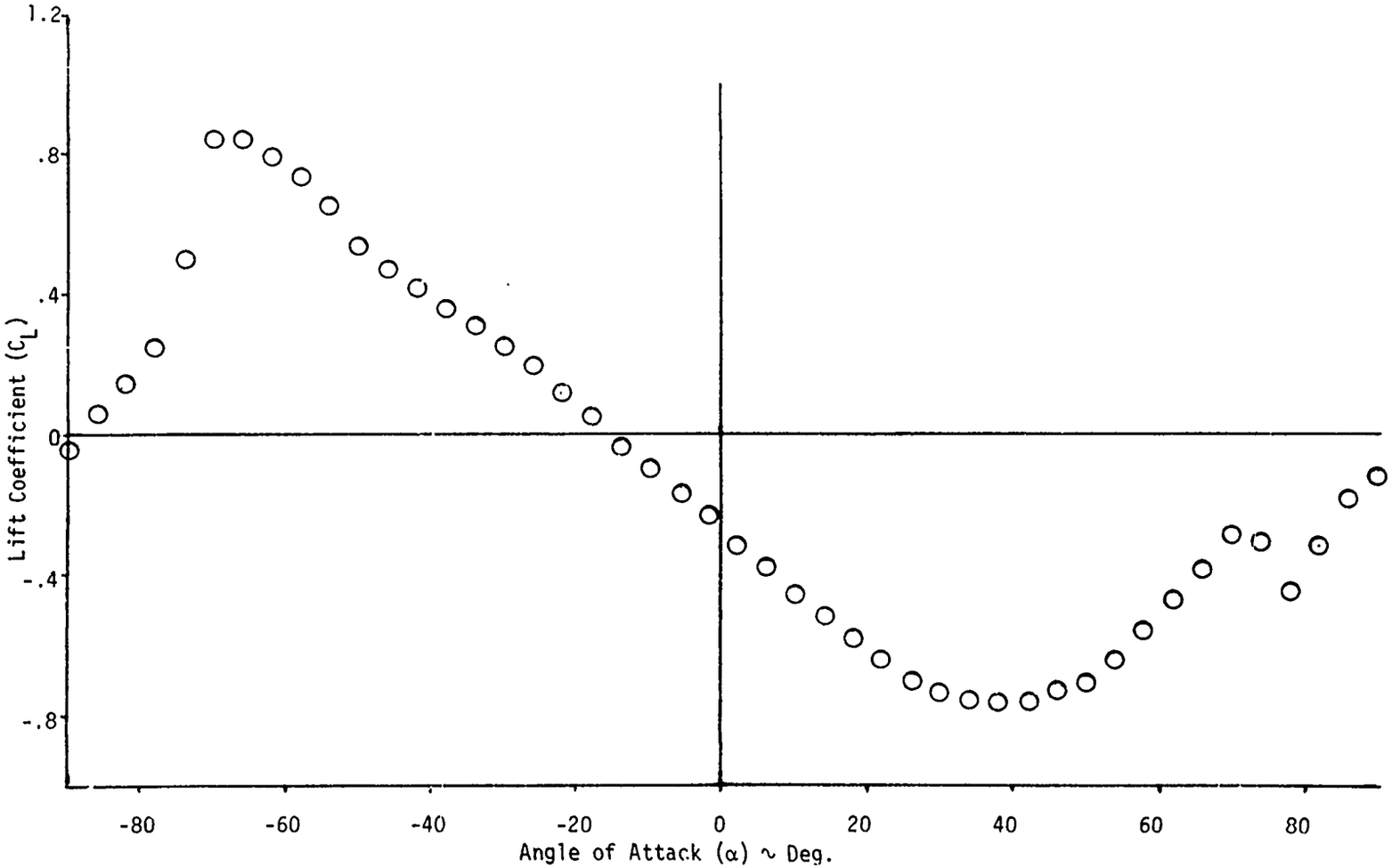

Figure 26. Lift Coefficient as a Function of Angle of Attack for a Nonspinning S-Section Autorotor

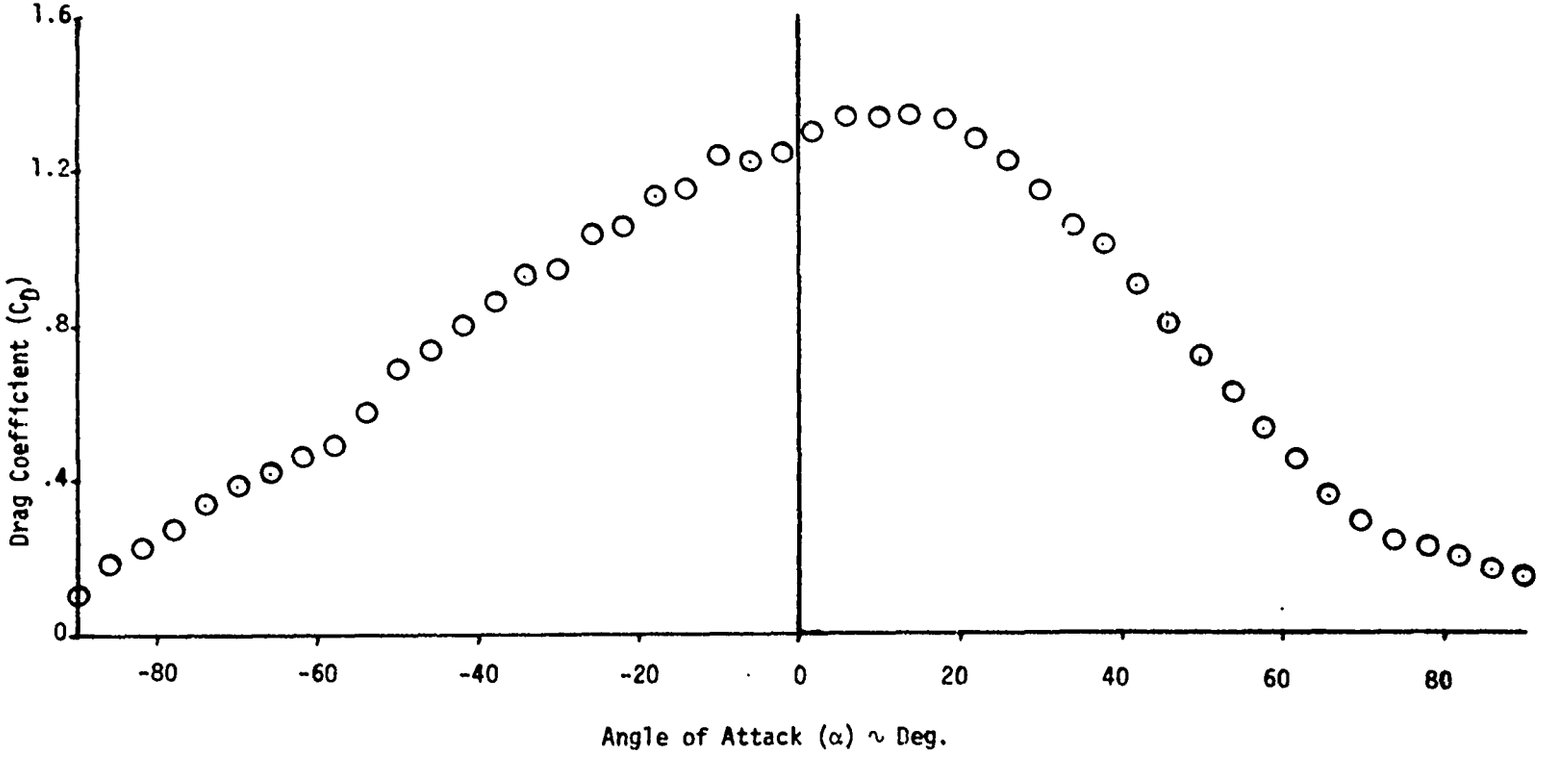

Figure 27. Drag Coefficient as a Function of Angle of Attack for a Nonspinning S-Section Autorotor

The digital computer program essentially solves the three basic differential equations that describe the motion of the system in terms of the angular accelerations of the three main system variables θ, Ω, and ω.

$$\dot{\omega} = \dot{\Omega}\cos\theta - \Omega\dot{\theta}\sin\theta + \frac{M_\omega}{I_1}$$

$$\dot{\Omega} = \frac{1}{(I_H/4 + I_1\cos^2\theta + I_0\sin^2\theta)}\left[I_1\dot{\omega}\cos\theta - 2\Omega\dot{\theta}(I_0 - I_1)\sin\theta\cos\theta - \dot{\theta}\omega I_1\sin\theta - M_\Omega\right]$$

$$\ddot{\theta} = \frac{1}{I_0}\left[\omega\Omega I_1\sin\theta + \Omega^2(I_0 - I_1)\sin\theta\cos\theta + M_{\dot{\theta}} + M_\theta\right] \qquad (4\text{-}24)$$

These equations are coupled and contain terms that are, themselves, functions of various time dependent system conditions.

The method by which the equations are solved is to start with a known or assumed value for each motion term corresponding to conditions at a given instant of time (t_0). Although the terms actually vary as a function of time, it is assumed that they remain constant over a small time increment, (Δt), providing the time increment is extremely small. Using this assumption, the values of the main system variables and their time derivatives can be determined at the end of the selected time increment ($t = t_0 + \Delta t$) by using the improved Euler-Cauchy numerical method as follows:

$$\dot{\theta} = \dot{\theta}_0 + \ddot{\theta}_0\Delta t$$

$$\Delta\theta = (\dot{\theta}_0 + \dot{\theta})\frac{\Delta t}{2}$$

$$\theta = \theta_0 + \Delta\theta$$

$$\Omega = \Omega_0 + \dot{\Omega}\,\Delta t$$

$$\omega = \omega_0 + \dot{\omega}\,\Delta t$$

where the subscript 0 indicates the term value at time t_0.

Using the values for the main system variables and their time derivatives computed for the new time (t), the other system terms can be computed, including the values of $\dot{\omega}$, $\dot{\Omega}$, and $\ddot{\theta}$, thus totally describing the system performance at time t. These term values then are used as the initial conditions for computing the values at the end of the next time increment. This procedure is repeated, thus providing a continual solution as a function of time. The small time element or integration time used in this analysis was $\Delta t = 0.001$ second. Check transient runs made with integration time elements of 0.0001 seconds did not indicate any appreciable change in the results.

C. Aerodynamic Load Distribution Over Blade Span.

The aerodynamic load distribution over the blade span is determined in the following manner. The blade span or length is divided into 10 equal spanwise area elements (Δr). The center of each element is termed a blade spanwise station and is identified by the distance (r) it is located from the hub spin axis (i.e., store center line) as measured along the blade, illustrated in figure 28.

The aerodynamic conditions and the associated aerodynamic coefficients are evaluated at each blade spanwise station as follows:

$$V = \sqrt{V_\infty^2 + (\Omega r\sin\theta)^2} \qquad (4\text{-}25)$$

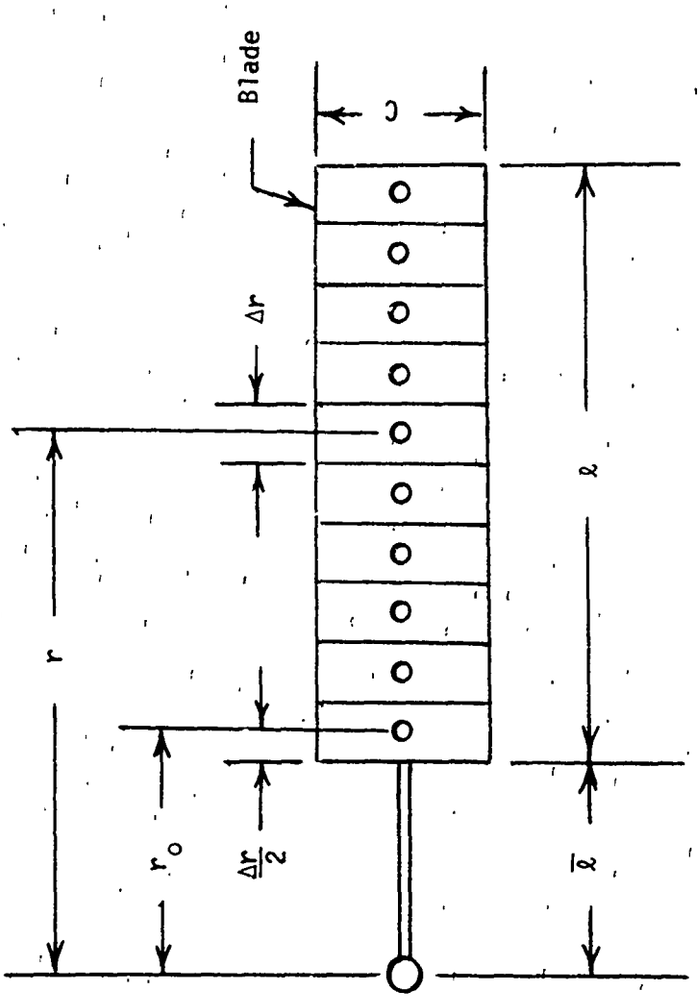

Figure 28. Definitions of Terms Used in Blade Element Method

$$\bar{\alpha} = \tan^{-1}\left(\frac{r\,|\Omega|\sin\theta}{V_\infty}\right) \tag{4-26}$$

$$\xi = \tan^{-1}(ctn\,\theta\,\sin\bar{\alpha})$$

$$\beta = \cos^{-1}(\cos\theta\,\cos\bar{\alpha}) = \tan^{-1}\left(\frac{1.-\cos^2\theta\,\cos^2\bar{\alpha}}{\cos\theta\,\cos\bar{\alpha}}\right) \tag{4-31}$$

$$\hat{\omega} = \frac{\omega C}{2\bar{V}}$$

$$\bar{q} = \frac{\rho\bar{V}^2}{2} \tag{4-28}$$

$$C_L = C_{L_{ss_0}}\left(C_{L_1}\frac{\hat{\omega}}{\hat{\omega}_{ss_0}} + C_{L_2}\frac{\hat{\omega}^2}{\hat{\omega}^2_{ss_0}\sin^2\beta}\right) \tag{5-14}$$

$$\hat{\omega}_{ss} = \hat{\omega}_{ss_0}\sin^2\beta \tag{5-10}$$

If $\hat{\omega} > \hat{\omega}_{ss}$, then

$$C_L = C_{L_{ss_0}}\sin^2\beta$$

$$C_D = C_{D_{ss_0}}\sin^2\beta \tag{5-12}$$

$$C_Y = C_{Y_{ss_0}}\sin^2(2\beta)$$

$$C_m = C_{m_0}\sin^2\beta + C_{m_1}\frac{\hat{\omega}}{\hat{\omega}_{ss_0}} + C_{m_2}\frac{\hat{\omega}^2}{\hat{\omega}^2_{ss_0}\sin^2\beta} \tag{5-15}$$

These conditions and the resulting aerodynamic loads are assumed to act over the area element ($C\Delta r$) at the particular spanwise station (r). The aerodynamic loads acting at a particular station (i) are determined as follows:

$$D_{B_i} = C_D\,\bar{q}\,C\Delta r \tag{4-27}$$

$$L_{B_i} = C_L\bar{q}C\Delta r \tag{4-27}$$

$$SF_{B_i} = C_Y\bar{q}C\Delta r \tag{4-27}$$

$$M_{B_i} = C_m\bar{q}C^2\Delta r \tag{4-12}$$

$$D_{S_i} = L_{B_i} \cos\xi \sin\bar{\alpha} + D_{B_i} \cos\bar{\alpha} - SF_{B_i} \sin\xi \sin\bar{\alpha}$$

$$T_{S_i} = L_{B_i} \cos\xi \cos\bar{\alpha} - D_{B_i} \sin\bar{\alpha} - SF_{B_i} \sin\xi \cos\bar{\alpha} \qquad (4\text{-}39)$$

$$F_{N_i} = L_{B_i}(\cos\xi \sin\bar{\alpha} \sin\theta + \sin\xi \cos\theta) + D_{B_i} \cos\bar{\alpha} \sin\theta$$
$$+ SF_{B_i}(\cos\xi \cos\theta - \sin\xi \sin\bar{\alpha} \sin\theta) \qquad (4\text{-}36)$$

The total or net loads acting on the blade in the various directional senses are determined by summing the loads of all the spanwise stations.

$$D_B = \sum_1^{10} D_{B_i}$$

$$L_B = \sum_1^{10} L_{B_i}$$

$$D_S = \sum_1^{10} D_{S_i} \qquad (4\text{-}44)$$

$$T_S = \sum_1^{10} T_{S_i} \qquad (4\text{-}40)$$

$$SF_B = \sum_1^{10} SF_{B_i}$$

$$F_N = \sum_1^{10} F_{N_i} \qquad (4\text{-}37)$$

The net aerodynamic moments acting on the blade are determined by summing the moments of all the spanwise stations.

$$M_{\omega_A} = \sum_1^{10} M_{B_i} \qquad (4\text{-}43)$$

$$M_{\theta_A} = \sum_1^{10} F_{N_i} r \qquad (4\text{-}38)$$

$$M_{\Omega_A} = \sum_1^{10} T_{S_i} r \qquad (4\text{-}41)$$

The remaining system performance terms are computed using the following expressions:

$$
\begin{aligned}
q_\infty &= \frac{\rho V_\infty^2}{2} \\
D &= qC_S \\
\hat{\Omega} &= \frac{\Omega(b + \ell/2)\sin\theta}{V_\infty} \\
M_\omega &= I_1 \dot{\omega} \\
M_\theta &= I_0 \ddot{\theta} \\
M_\Omega &= (I_H/4 + I_1 \cos^2\theta + I_0 \sin^2\theta)\dot{\Omega} \\
F_A &= m_b b(\Omega^2 \sin^2\theta + \dot{\theta}^2) \\
F_N &= F_N - m_b b\Omega^2 \sin\theta \cos\theta \\
F_X &= F_A \cos\theta + F_N \sin\theta \\
F_Z &= F_A \sin\theta - F_N \cos\theta \\
F &= \sqrt{F_X^2 + F_Z^2} \\
S_T &= \pi(b + \ell/2)^2 \sin^2\theta \\
C_{D_T} &= \frac{D}{q_\infty S_T} \\
r_{B_\theta} &= \frac{M_{\theta_A}}{F_N} \\
r_{B_\Omega} &= \frac{M_{\Omega_A}}{T_S} \\
m_b &= \frac{wgt}{g} \\
\hat{\omega}_r &= \frac{\hat{\omega}}{\omega_{ss_0} \sin^2\beta}
\end{aligned}
\qquad (4\text{-}45)
$$

Figure 29 contains a summary of these terms and illustrates their directional sense relative to the physical system.

Appendix A contains a listing of the actual computer program along with a listing of the definitions of the computer program terms. Also in appendix A is an example of a typical solution printout format. The first block of data for each run contains the physical and aerodynamic characteristics of the various elements of the autorotor decelerator system, the free stream conditions, and the initial conditions for the particular run or case to be solved.

The solution giving the various term values describing the system motion, and other conditions, are printed out at preselected time intervals. At each time, two blocks of data are printed out. The first data block describes the aerodynamic effects acting over the blade span. The values of the various terms at each blade element station, as well as the net effect of certain of these terms, are presented. The second block of data printed out at each time interval contains the various system motion and force terms.

It should be pointed out that the computer program includes terms for Mach number effects and trajectory determination; however, these areas are not included in this analysis.

VII. EXPERIMENTAL RESULTS.

A. General.

A large-scale autorotor decelerator system was tested in the University of Maryland 7- by 10-foot subsonic wind tunnel. The unit tested actually represented realistic full-scale dimensions and structuring for application to a typical air delivered store that was used as the forebody in these tests.

The hardware was fabricated, and the test was conducted under an Edgewood Arsenal project.[8] Although this test was not conducted specifically for the thesis purposes, it afforded an excellent opportunity to obtain performance data on a representative full-scale system, which could then be compared to the theoretical predictions based on the thesis material.

B. Model Configurational Details.

Figure 30 contains the structural details of the unit tested. The autorotor blades were of S-cross-sectional type and were 11 inches long by 3 inch chord, as shown in figure 11. The blades were made of aluminum of 0.0625-inch thickness.

The maximum forebody diameter (i.e., hub diameter) was 5 inches. The blades were sized to fit within this 5-inch diameter envelope when in the stowed (undeployed) condition (i.e., blades lying back parallel to the store center line).

C. Test Setup and Procedure.

Figure 31 shows the unit mounted in the wind tunnel test section. A single strut mount was used to attach the model to the beam balance system beneath the test section floor. The unit was tested in 0° angle of attack and sideslip. Steady state drag load measurements were made by means of the tunnel balance system. Transient and steady state spin rates of the blades and hub were obtained from a high speed camera. Blade deployment angles were measured from a low speed camera viewing the unit hub from the side.

---

[8] Autorotor Decelerator Retardation System. All American Engineering Company, Wilmington, Delaware. Contract DA 18-035 AMC-356(A). 1969.

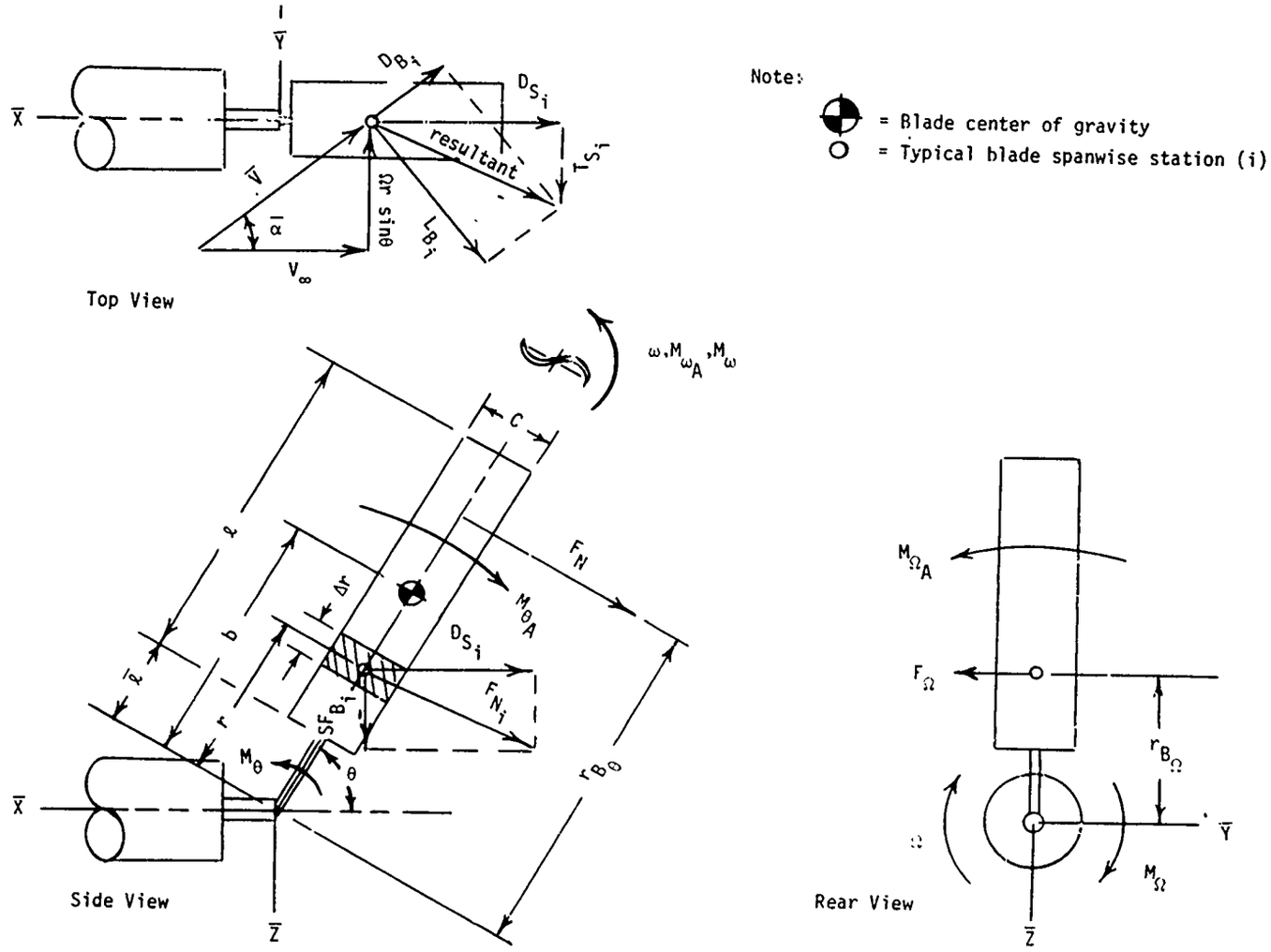

Figure 29. Summary of Computer Program Terms Describing System Performance

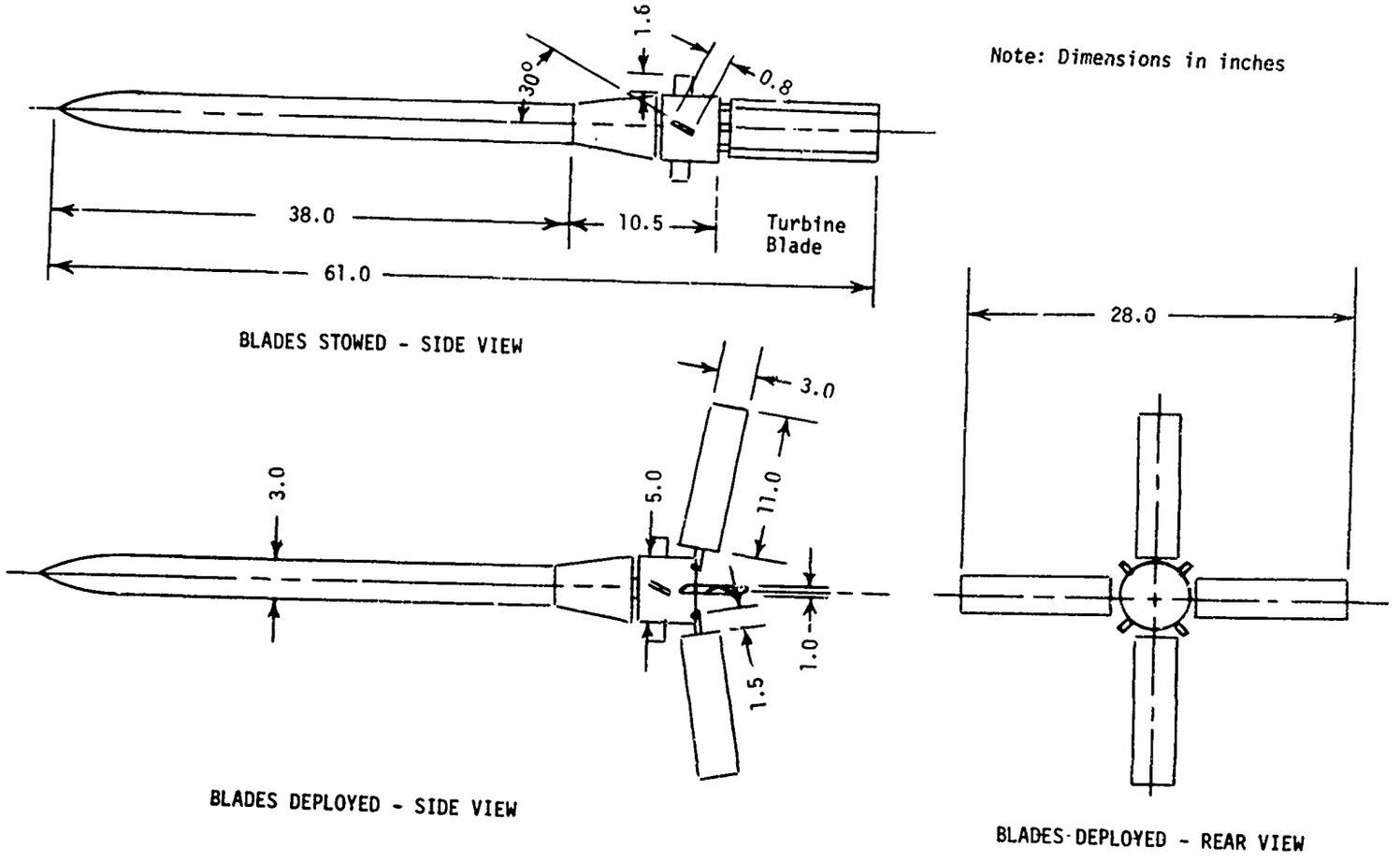

Figure 30. General Configuration of Full-Scale Autorotor Decelerator Tested in the University of Maryland 7- by 10-Foot Subsonic Wind Tunnel

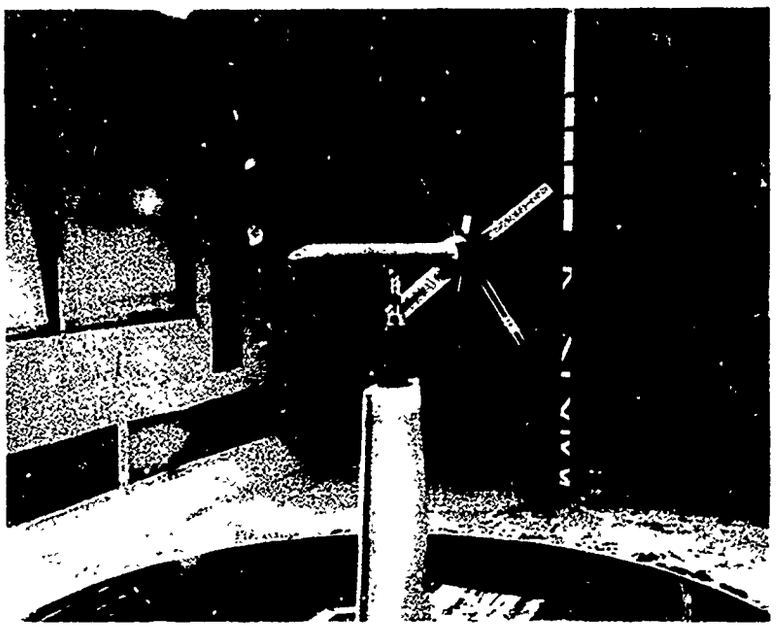

Figure 31. Full-Scale Autorotor Decelerator Mounted in University of Maryland 7- by 10-foot Subsonic Wind Tunnel

Tests were conducted at three velocities: 100, 141, and 173 ft/sec. The procedure for each test was as follows. The autorotor blades were initially pivoted back to lie parallel to the body center line. The blades were held in place by a single strand of break cord looped around the folded blades at their tips. The break cord was kept from slipping off the blades by a small notch in each blade edge located about an inch from the blade tip. The break cord was of 11-pound break strength and would break because of centrifugal force tending to deploy the blades at a hub spin rate of about 900 rpm. This initial hub spin rate was obtained by four small turbine vanes located on the hub.

The turbine vanes initially were folded down inside the hub structure and held there by a cord loop with a simple pull release knot, which could be released by pulling it outside the tunnel test section.

After the tunnel had been brought up to the desired velocity, the turbine vanes were deployed, thus initiating hub rotation. The hub spin rate would increase until the break cord holding down the autorotor blades would break. The blades would then deploy, and the system would undergo a deployment transient motion and finally achieve a steady state condition. Figure 32 shows details of the blades and turbine vanes.

D. Test Results.

Figures 33 through 35 contain the steady state performance results obtained from these tests. Two separate units of identical configurations were tested as indicated. The spin rate of the blade (ω) and the hub (Ω) are linear with velocity, as shown in figure 34. The deployment angle (θ), the ratio of blade spin rate to hub spin rate (ω/Ω), drag coefficient based on swept area (C_{D_T}), and consequently the effective drag area, seem to be constant with velocity.

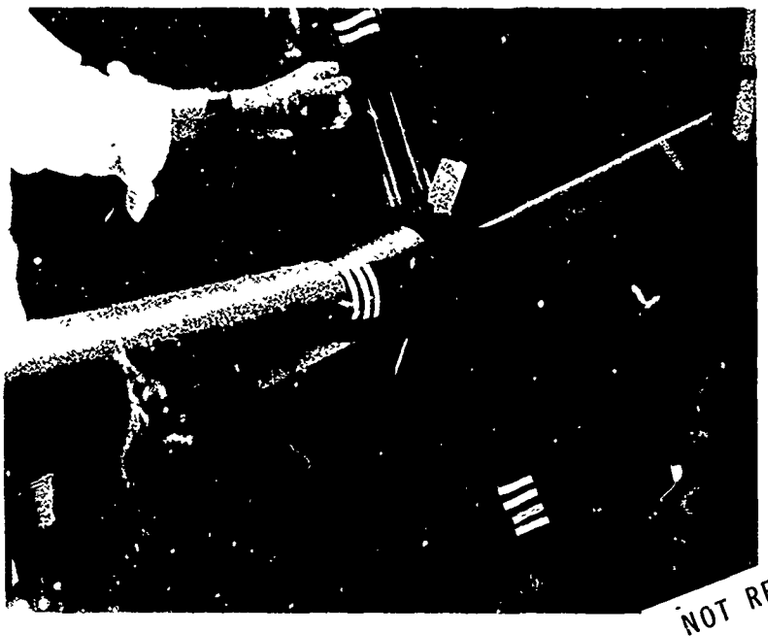

Figure 32. Blade and Hub Details of Full-Scale Autorotor Decelerator

A summary of these characteristic term values for the configuration tested as determined from the wind tunnel test is as follows:

Term	Steady state value
θ	76.5°
$\dot{\omega}/\Omega$	11.3
Ω	1.01
C_{D_T}	0.58
D/q	2.6 sq ft

In addition to the quantitative results, which could then be compared with the theoretical results, the test indicated other important factors concerning the design of this type of decelerator system. Comparison between the results obtained in the two separate but identical units indicates that consistent performance can be achieved with a large number of these items in spite of their seemingly complex nature.

The linear nature of the blade and hub spin rates with velocity indicates that no frictional or unbalance effects are present. Thus, initial fears that precision or advanced state-of-the-art bearings would be necessary are not substantiated. With regard to the bearing problem, it is realized that for actual application, the relatively short times of flight mean that the operational time is measured in seconds. Each run in the tunnel lasted an average 60 seconds. Yet at the end of the test, the bearings showed no indication of wear or degradation. Analysis of the test film record showed that all four blades had the same spin rates at any given time.

It should also be mentioned that the original concept of the deployment angle degree of freedom was to relieve the large bending moments on the blade/hub attachment point. Early

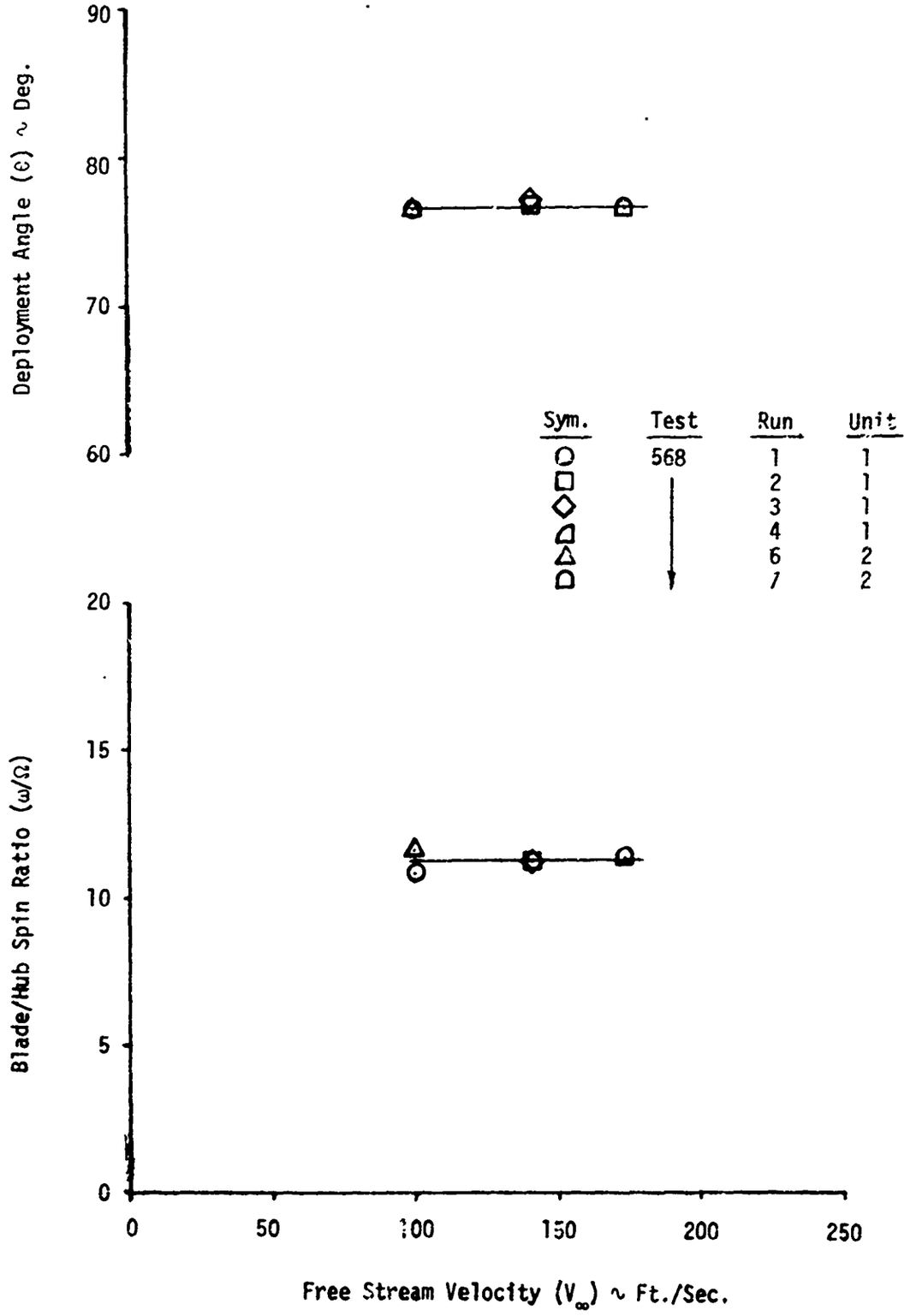

Figure 33. Steady State Deployment Angle and Blade/Hub Spin Ratio as Determined From Wind Tunnel Tests on a Full-Scale Autorotor Decelerator

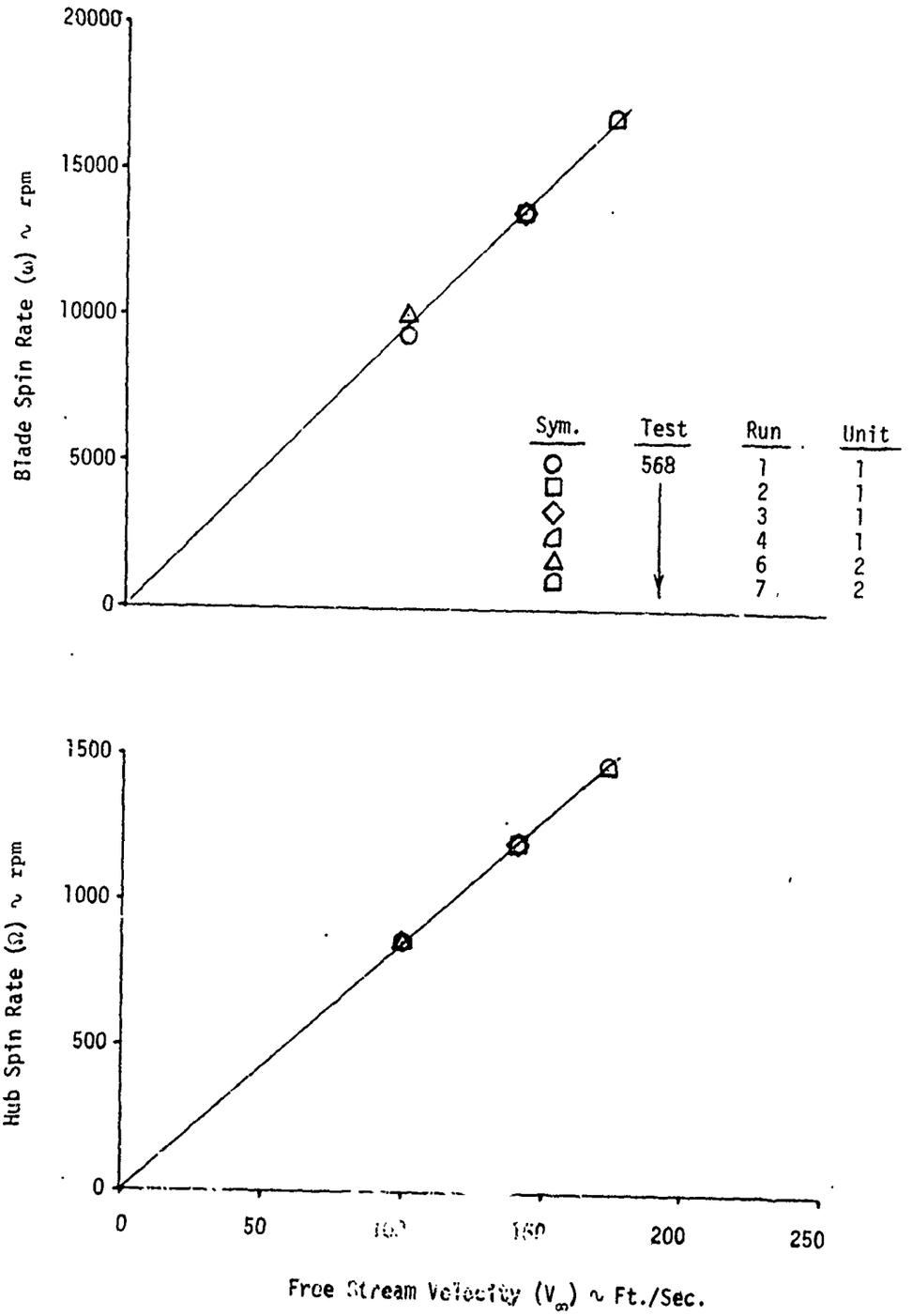

Figure 34. Steady State Blade and Hub Spin Rates as Determined From Wind Tunnel Tests on a Full-Scale Autorotor Decelerator

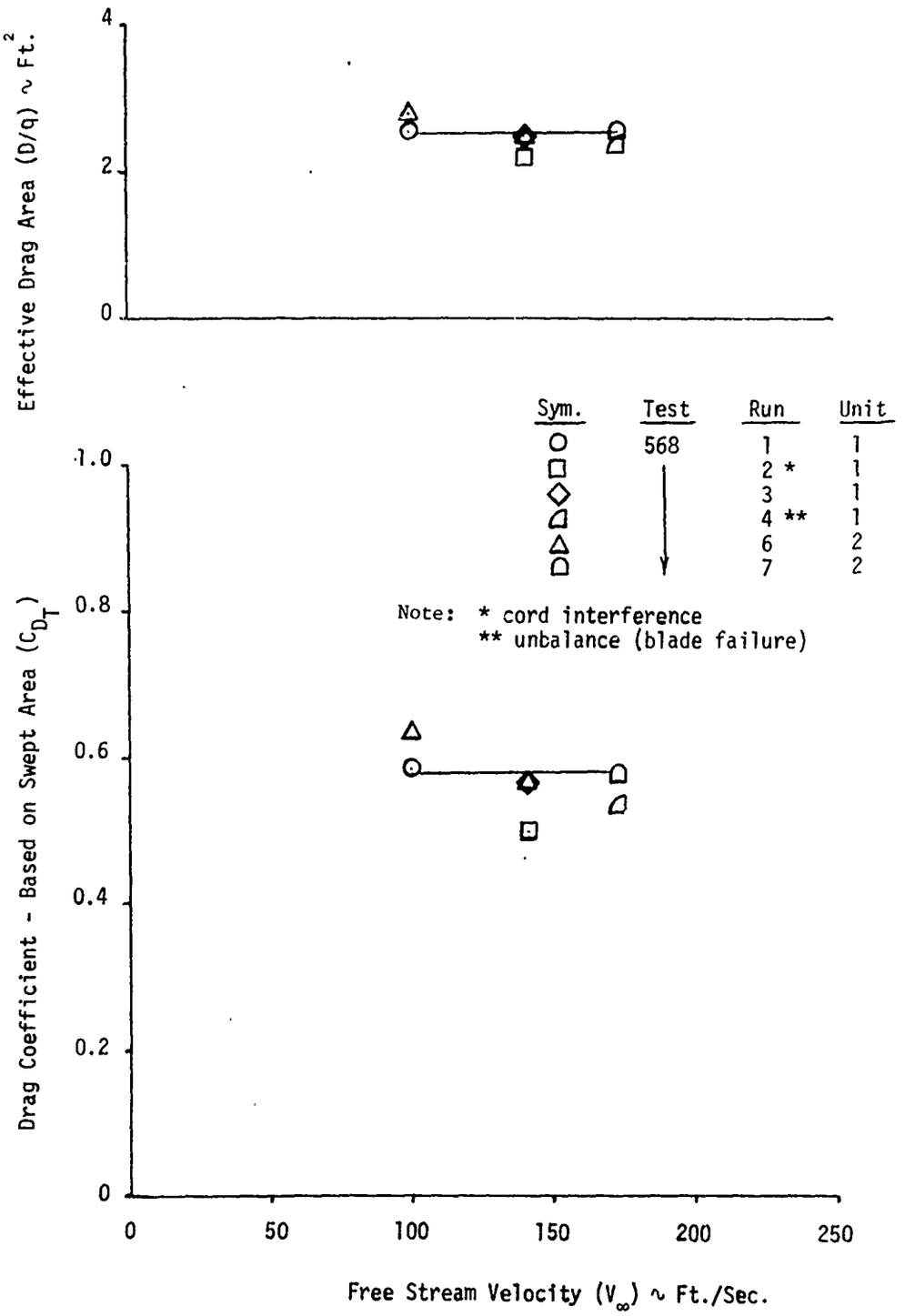

Figure 35. Steady State Drag Coefficient and Effective Drag Area as Determined From Wind Tunnel Tests on a Full-Scale Autorotor Decelerator

autorotor decelerator designs all had this "flapping" freedom, but rotation of the blade in a plane normal to the hub spin axis referred to as "lead-lag" was restricted. Tests with these early units resulted in the blade shafts fracturing completely. Analysis of the failure indicated that the shafts were experiencing large bending loads because of the restrictions of the movement in the lead-lag direction. Any unbalance or extraneous loads of the blade results in small precession about the blade spin axis. If this motion is restricted, the resultant moment is taken out by the blade shaft. In addition, these loads occurred at a high frequency (i.e., that of the blade spin rate), resulting in a fatigue effect on the blade shaft and consequent structural failure. The units used in the test described here were designed to give the blade a few degrees of angular motion freedom in the lead-lag direction. This relieved the high loads resulting from the small precession, but allowed the basic hub torque moment to be realized.

VIII. CORRELATION BETWEEN EXPERIMENTAL AND ANALYTICAL RESULTS.

The physical properties of the rotor system and the test conditions for the wind tunnel test were used in the computer program described in section VI, and the analytical steady state solution was obtained based on the equations derived in section V.

The conditions simulated and the resultant output are included in appendix B. A comparison between the computed theoretical results and the experimental results are shown below for a free stream velocity of 100 ft/sec. As can be seen, the agreement is not satisfactory.

Term	Experimental results	Analytical results
Ω	850 rpm	1330 rpm
ω	9650 rpm	11200 rpm
ω/Ω	11.3	8.4
θ	76.5°	80.8°
C_{D_T}	0.58	0.84
D/q	2.6 sq ft	3.8 sq ft
$\hat{\Omega}$	1.01	1.64

A general parameter study was instituted to determine if any term was so sensitive that a very accurate measurement was necessary and also to indicate any term or terms that could be altered to give better results. The procedure was to solve for the steady state results for conditions in which a single parameter was varied on incremental value above and below the nominal value. These parameters included: blade weight, blade length, blade chord, free stream velocity, blade aerodynamic coefficients, blade aerodynamic tip losses, and bearing friction.

The procedure in solving for the steady state conditions was to start with assumed initial conditions for each term. The motion of the system would then be solved for a function of time; by 1 or 2 seconds the values were essentially constant, this being the steady state condition.

A summary of the results of this study are shown in table I. This table presents the various terms of interest along the left side with the trend (increasing value or decreasing value) required to bring the analytical value more in line with the experimental value. The most important term is the hub spin rate in that it has the greatest effect on the other term values. As can be seen, altering of none of the parameters results in the desired trends for all terms considered. Even tip losses were considered. This can be done by assuming a linear lift distribution from the value at a selected blade element to a value of zero at the tip. Although the trends of the terms are all in the

Table I. Summary of Results of Initial Parameter Study to Determine Reasons for Discrepancies Between Theoretical and Experimental Data

Parameter	Required* trend	Term						
		Ω**	ω	$\frac{\omega}{\Omega}$	θ	C_{D_T}	$\frac{D}{q}$	$\hat{\Omega}$
Blade weight (wgt)	↑	↓	–	↑	↑	↓	↓	↓
Blade length (ℓ)	↑	↓	–	↑	↓	↓	↑	↓
Blade chord (C)	↑	↓	↓	↓	↑	↑	↑	↓
Blade tip speed ratio $(\hat{\omega})_{ss_0}$	↓	↓	↓	↓	↑	↓	↓	↓
Tip losses	↑	↓	↓	↑	↓	↓	↓	↓
Blade bearing friction	↑	↓	↓	↓	↓	↓	↓	↓
Desired trend to match analytical and experimental results	–	↓	↓	↑	↓	↓	↓	↓

*This column indicates whether the parameter value had to be increased (↑) or decreased (↓) relative to the nominal parameter value for the analytically determined value of the hub spin rate to equal the experimental value.

**Columns 3 through 7 indicate whether the analytically determined value of the indicated term is greater (↑) or smaller (↓) than the experimental value when the analytical hub spin rate equals the experimental value.

desired direction, matching the analytical with the experimental values for all terms could not be done. Frictional effects were simulated by limiting the blade spin rate to various fractions of the steady state value of the no friction case.

With the inability of the initial parameter study to provide an answer to the discrepancies between the theoretical and experimental results, attention was centered on the aerodynamic load distribution over the blade. It should be noted that the basic method utilized in analyzing the performance of the autorotor system was to determine the motion and forces resulting from a single blade and then to multiply this by the number of blades where required to obtain system effects. It was assumed that the blade is not influenced by the presence of the other blades.

Figure 36 shows in graphic form the conditions at several stations along the blade at the condition of steady state spin. It illustrates how the magnitude and direction of the relative velocity changes from the elements near the blade root to elements near the blade tip. It also shows how the lift and drag forces combine to give a resultant force that acts to spin the blade about the hub and also to provide the system drag. It should be noted that elements near the root result in a hub spin force tending to spin the hub faster, whereas elements near the tip tend to resist hub spin rate. This illustration shows how the lift force contributes to increasing the hub spin rate, whereas the drag force acts to decrease the hub spin rate. Also clearly shown is how both the lift and drag forces

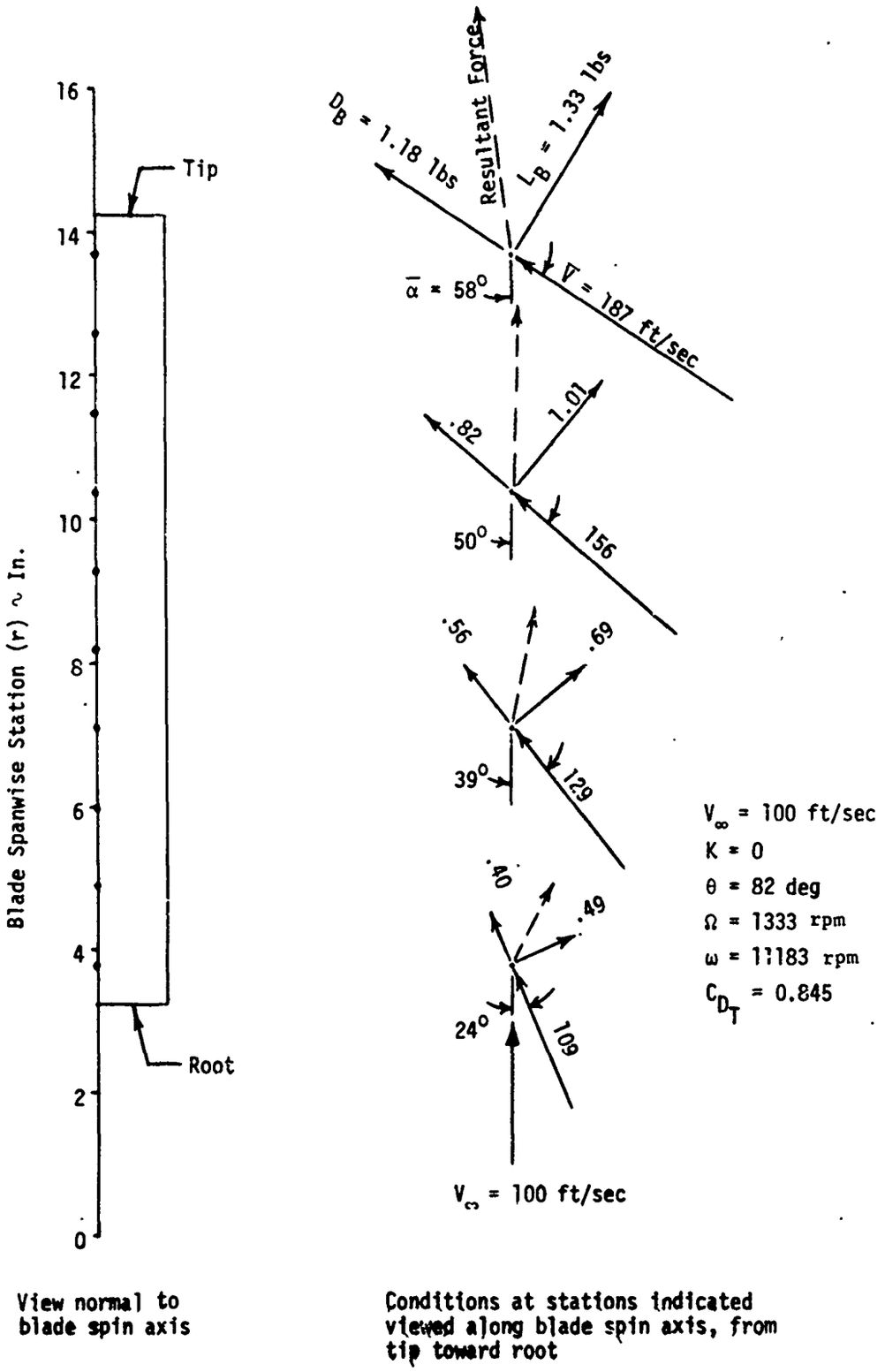

Figure 36. Aerodynamic Conditions at Various Blade Spanwise Stations at Steady State Condition for Analytical Approach With Interference Factor ($K = 0$)

contribute to the system drag, and the advantageous effect, of the high lift and high drag inherent in the autorotor blade, toward producing the high drag of the autorotor decelerator system.

Inspection of the aerodynamic load distribution over the blade reveals that a rotation of the velocity vector at each element (i.e., an incremental change in the relative angle of attack $\bar{\alpha}$) would cause a rotation of the lift and drag directional sense at each element. The general result would be to increase the magnitude of the force acting to spin down the hub, as shown in figure 37. It should also be pointed out that a decrease in hub spin rate would also decrease the magnitude of the relative velocities at each element, thus decreasing the aerodynamic forces, and influencing all the other terms in the system, and in particular, reduce the system drag. All of the resulting effects of changing the angle of attack at each element by an incremental amount $\Delta\alpha$ would seem to bring the analytical and the experimental results more in agreement.

Runs were then made in which the angle of attack at each blade element was altered a fixed amount $\Delta\alpha$

$$\bar{\alpha} = \tan^{-1}\left(\frac{r\,|\Omega|\sin\theta}{V_\infty}\right) + \Delta\alpha \tag{8-1}$$

The $\Delta\alpha$ value was a constant at all elements. Runs were made with various values for $\Delta\alpha$.

It should be pointed out that the viewing sense along the blade spin axis, indicated in figure 36, does not present the lift and drag forces truly relative to the hub torque and system drag directions due to the angle ξ, at which they are inclined. At the steady state condition being considered, however, when the blade deployment angle is large and the relative velocity at all points on the blade span is essentially normal to the blade spin axis, the effect of the angle ξ can be neglected for the purpose of this discussion. At the steady state condition, the effect of the aerodynamic side force is negligibly small; thus, only the lift and drag forces are considered.

Excellent agreement was obtained for a $\Delta\alpha$ of about 15°. A possible physical explanation for this interference effect is that it results from the flow field about a blade being influenced by the flow fields of the other blades in the system.

Figure 38 shows a typical flow field about a single autorotating shape[9] and illustrates the strong positive and negative vortices each shed periodically during one revolution. A relatively large wake is produced with a pronounced downwash angle. These flow field features are typical of all autorotating shapes. It is easy to see how the flow fields of the preceding and following blades could have a turning effect on the flow over a blade in the autorotor decelerator system. The physical reason for this angular change over the original approach was probably an interference effect or induced effect caused by the blade flow fields. It then was decided to express it as a function of the lift coefficient. This follows the usual downwash or interference practice and also makes it, in effect, proportional to the spin rate of the blade, which would seem reasonable. In addition, it allows the effect to be physically valid during the deployment sequence in that this induced angle would be zero when the blade did not have a spin rate. The new expression for angle of attack is therefore:

$$\Delta\alpha = KC_L \tag{8-2}$$

where K is an arbitrary constant of proportionality.

[9]Flow Analysis and Dynamics of Autorotating Lifting Bodies. University of Notre Dame, Notre Dame, Indiana. Contract DA 18-035 AMC-356(A). 1964.

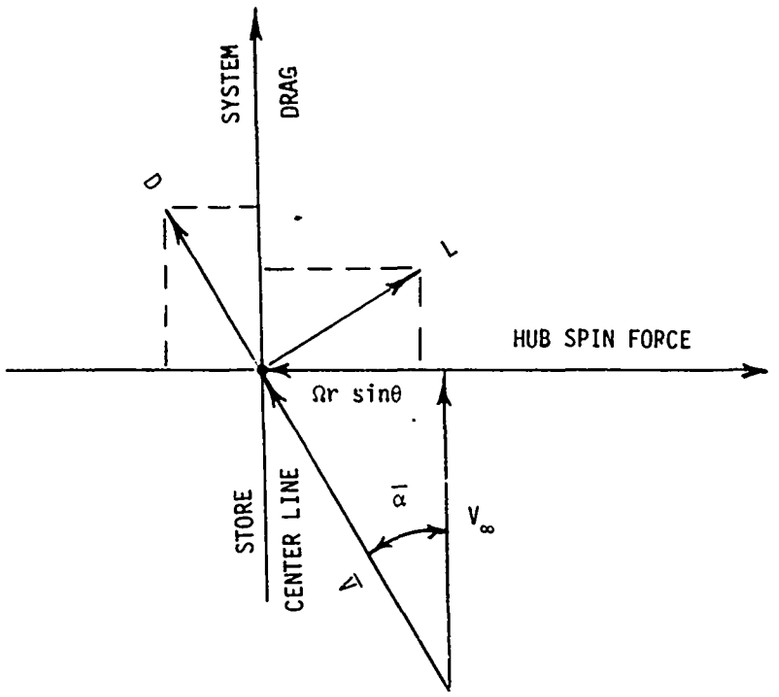

A. Conditions at a particular blade element (view along blade spin axis) with no interference effect.

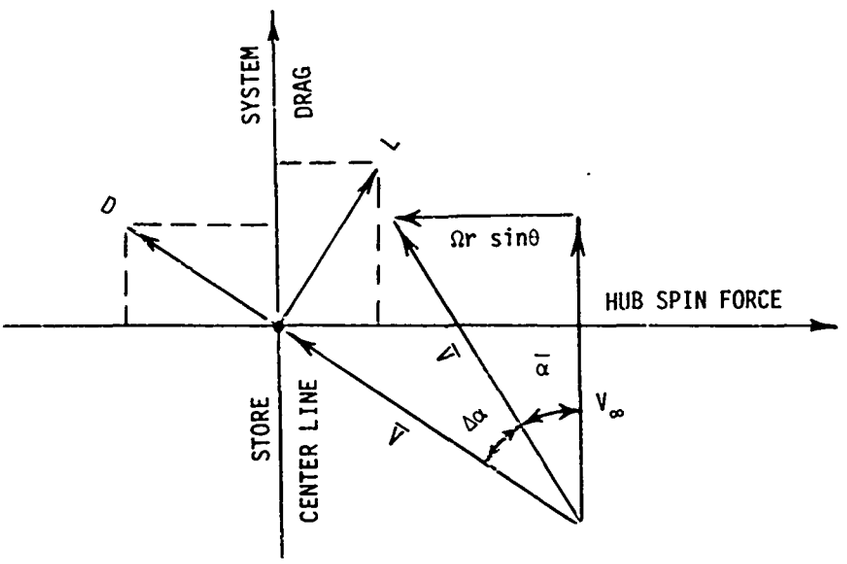

B. Conditions at the same blade element, but including an interference effect expressed as a change in the relative angle of attack (Δα).

Figure 37. Illustration of Blade Interference Effect

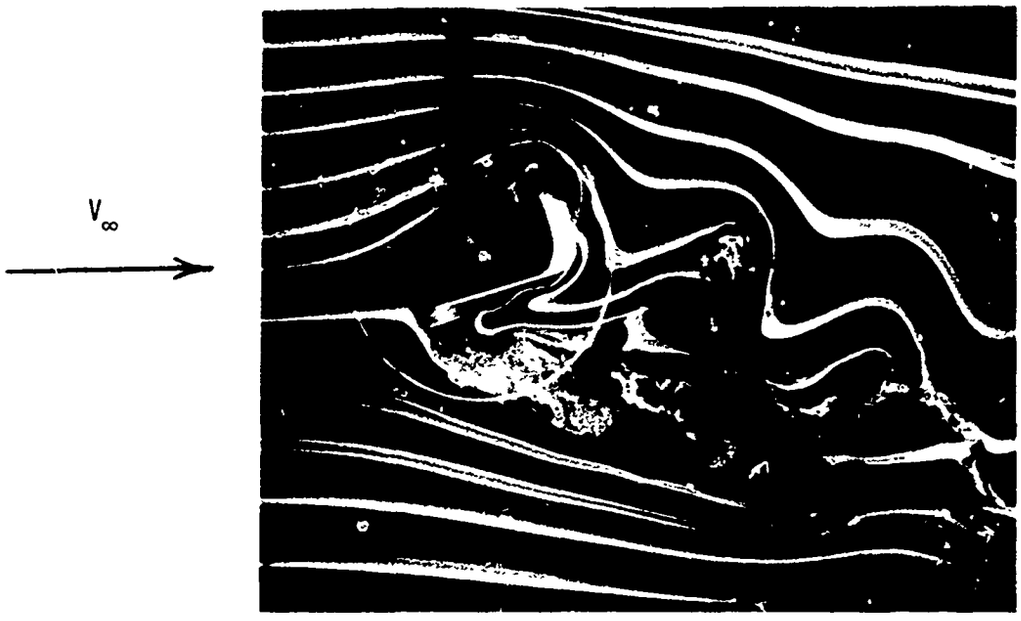

Figure 38. Typical Flow Field Around a Single Autorotor

Figures 39 through 41 show the steady state results computed for various values of K for the three velocities used during the wind tunnel test. Also indicated are the data values obtained during the test to indicate the value of K that best matches the experimental data. A value of $K = 10$ results in the values shown below as compared to the experimentally determined values:

Term	Experimental	Analytical results ($K = 10$)
Ω	850 rpm	830 rpm
ω	9650 rpm	9200 rpm
ω/Ω	11.3	11.1
θ	76.5°	76.6°
C_{D_T}	0.58	0.576
D/q	2.6 sq ft	2.55 sq ft
$\hat{\Omega}$	1.01	1.00

Table II compares the experimental results with the analytical results obtained without an interference effect ($K = 0$) and the analytical results obtained with an interference effect ($K = 10$). The aerodynamic conditions over the blade span are shown in figure 42 for the $K = 10$ case, and can be compared with $K = 0$ case shown in figure 32. Note in figure 42 that the angle of attack at each station is slightly larger than those in the $K = 0$ case (figure 36). In other words, the new angles of attack are not merely the old plus the correction angle ($\Delta\alpha$). The effect of adding the $\Delta\alpha$ term alters all other terms in a feedback type effect, resulting in all new conditions. The complete steady state conditions for the $K = 10$ case are included in appendix B.

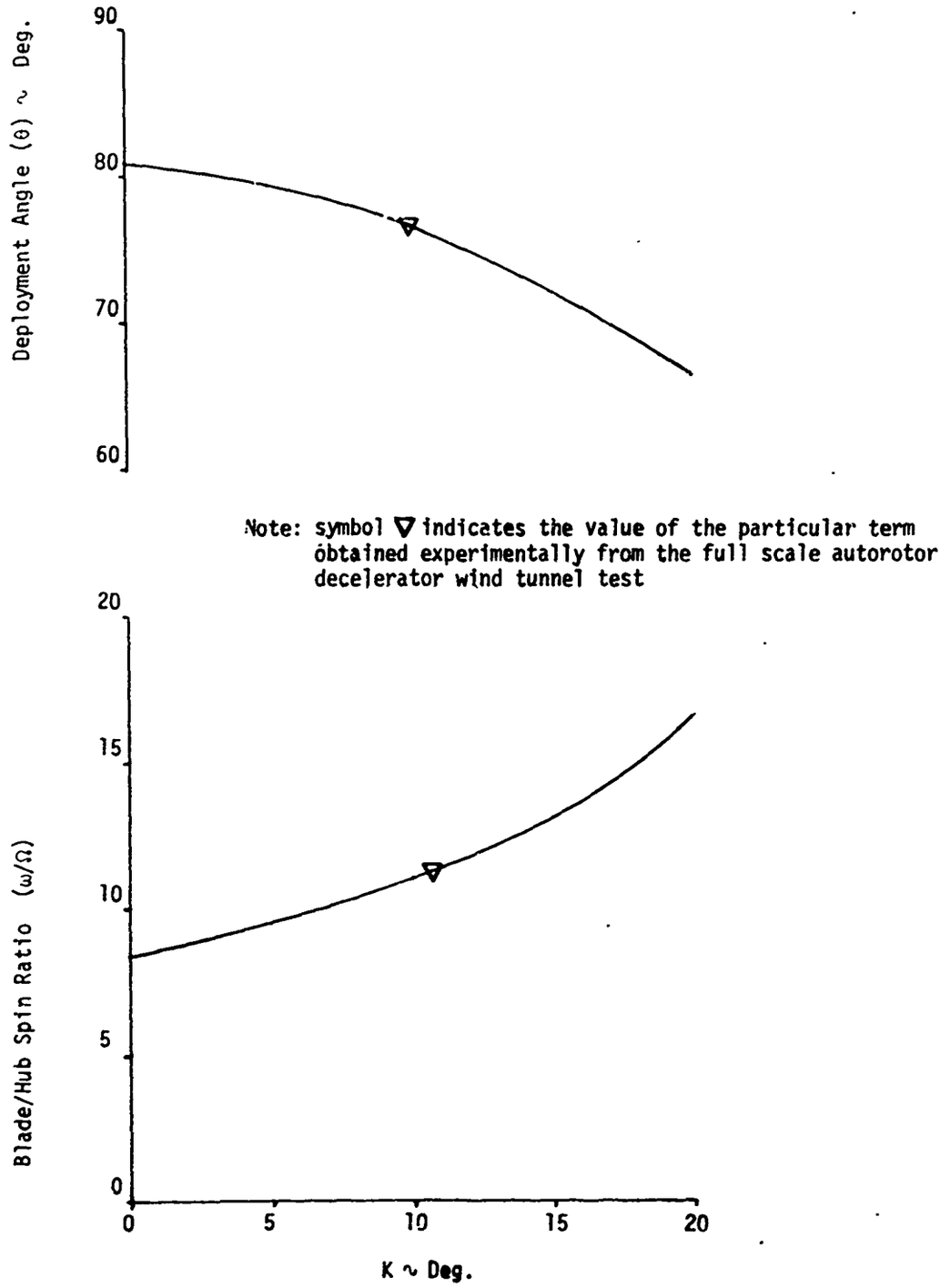

Figure 39. Steady State Performance of Full-Scale Autorotor Decelerator Computed as a Function of Interference Factor (K) for a Free Stream Velocity of 100 Ft/Sec

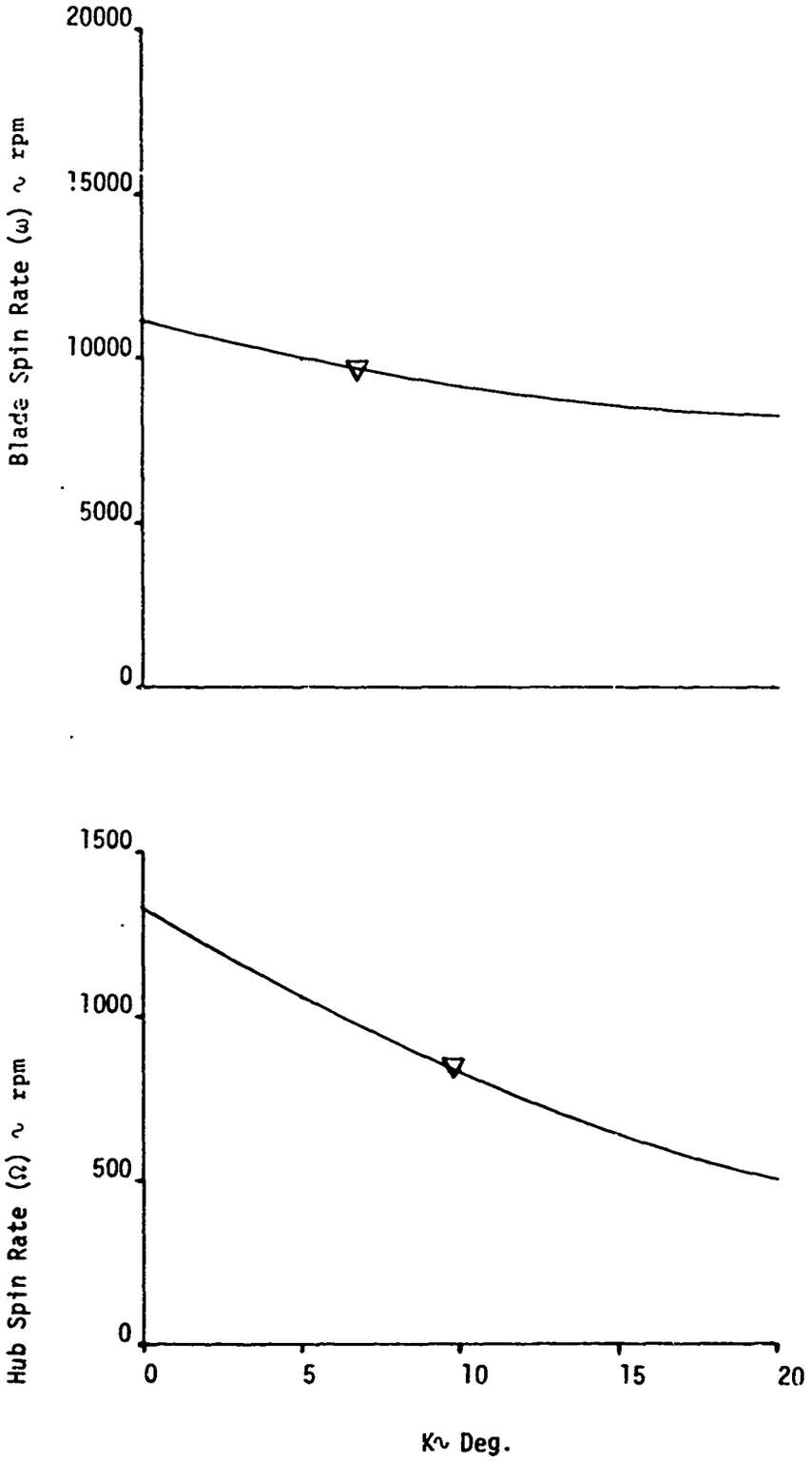

Figure 39. Continued

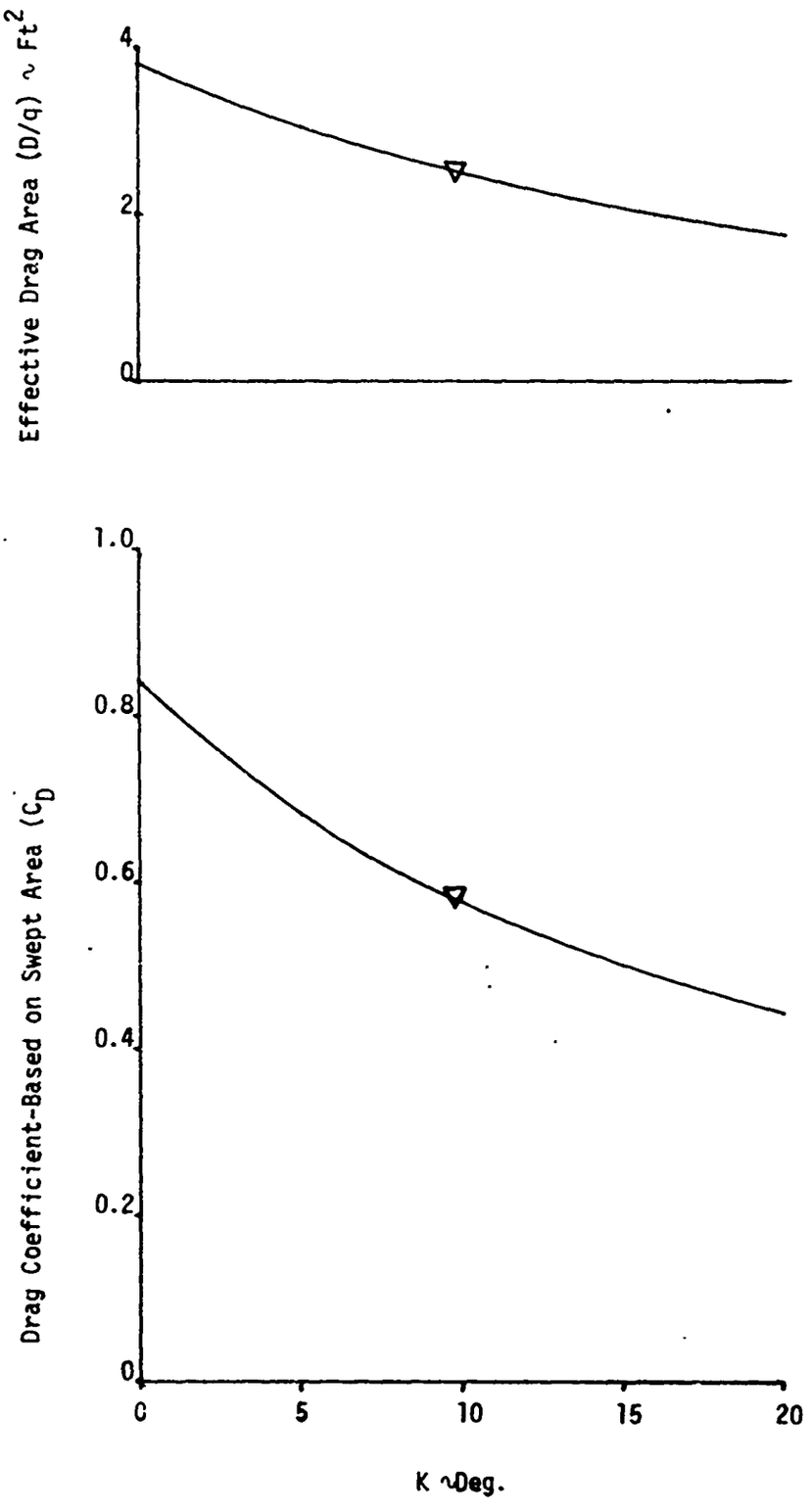

Figure 39. Continued

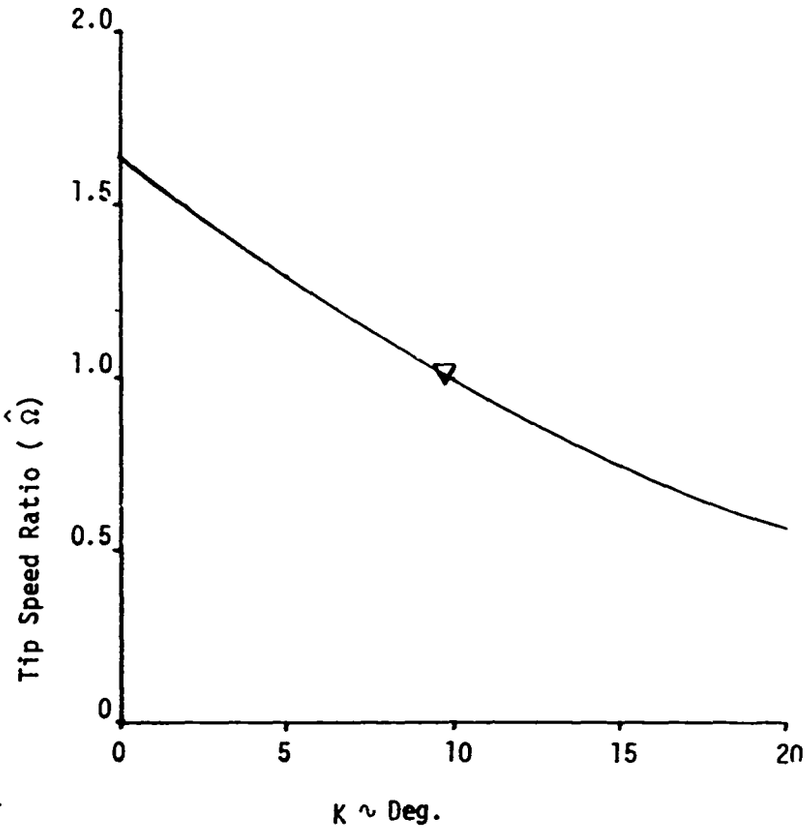

Figure 39. Continued

The value of K could be a function of other terms, such as number of blades, autorotor blade shape, solidity factor, lift coefficient, etc. It is most certainly a function of the lift coefficient. The constant nature indicated in this case could be a result of the near constant lift coefficient over the blade span.

Figures 43 through 45 indicate the transient motion during deployment determined from the computer program using $K = 10$, compared with the data obtained during the wind tunnel test.

It should be noted that the aerodynamic damping coefficient was initially selected arbitrarily to be the lowest value required to keep the system from "blowing up." Without a sufficiently large value of $C_{m_{\dot{\theta}}}$, θ was found to diverge after the system had achieved a near steady state condition. This diverging oscillatory behavior of θ resulted in the other system terms diverging.

The existence of an aerodynamic moment, which is a function of $\dot{\theta}$, is physically realistic, especially in view of the large values of $\dot{\theta}$ realized during deployment.

Several values of $C_{m_{\dot{\theta}}}$ were used in figures 43 through 45. As can be seen, the lower the damping value, the more oscillatory is the transient motion. A low value of damping would seem to be present during the initial phase of the deployment, evidenced by the large angular motion of θ in figure 43. The absence of additional oscillatory motion after this initial phase may indicate that the damping effect may be a function of factors other than those assumed in the analysis and may not be of a constant nature.

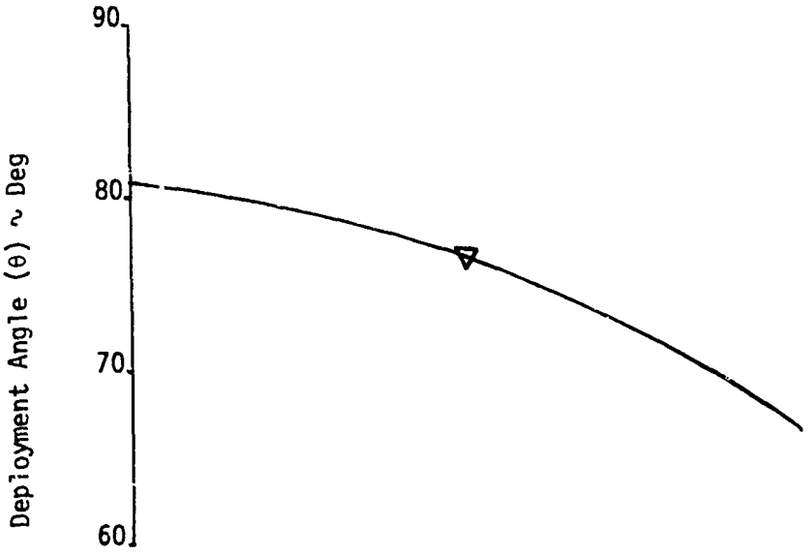

Note: symbol ▽ indicates the value of the particular term obtained experimentally from the full scale autorotor decelerator wind tunnel test

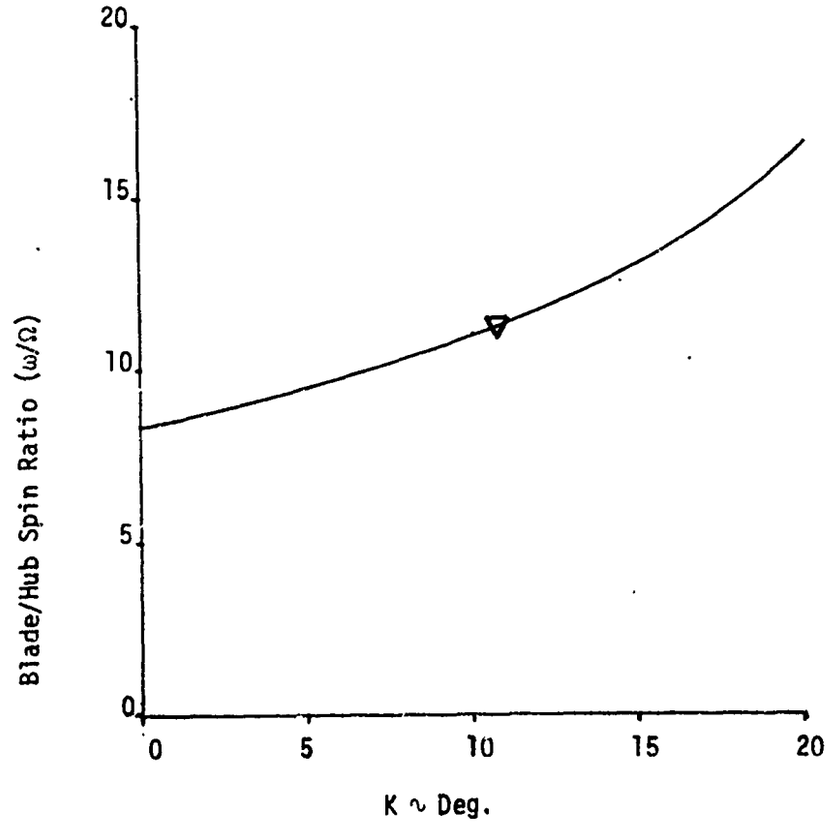

Figure 40. Steady State Performance of Full-Scale Autorotor Decelerator Computed as a Function of Interference Factor (K) for a Free Stream Velocity of 141 Ft/Sec

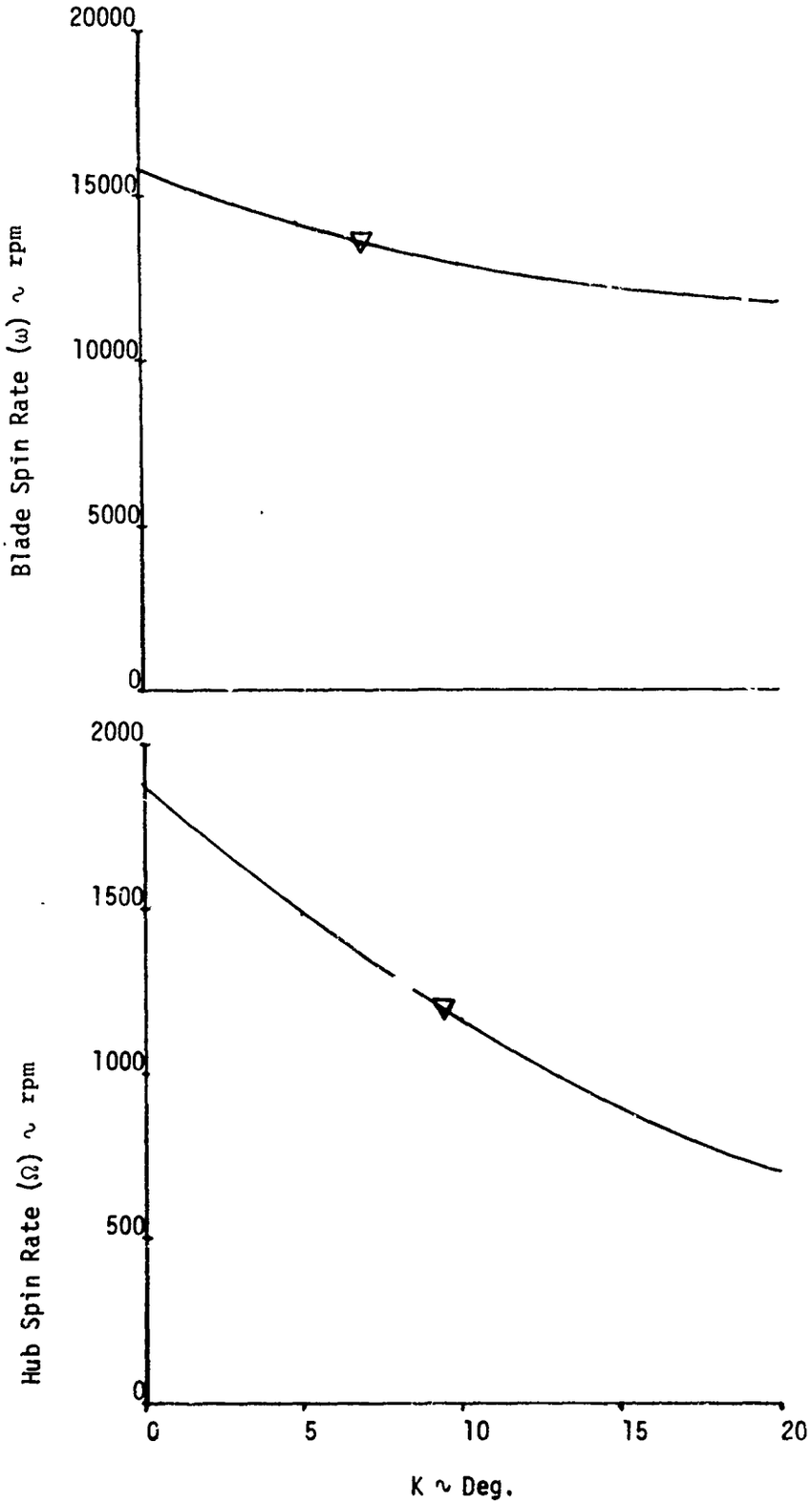

Figure 40. Continued

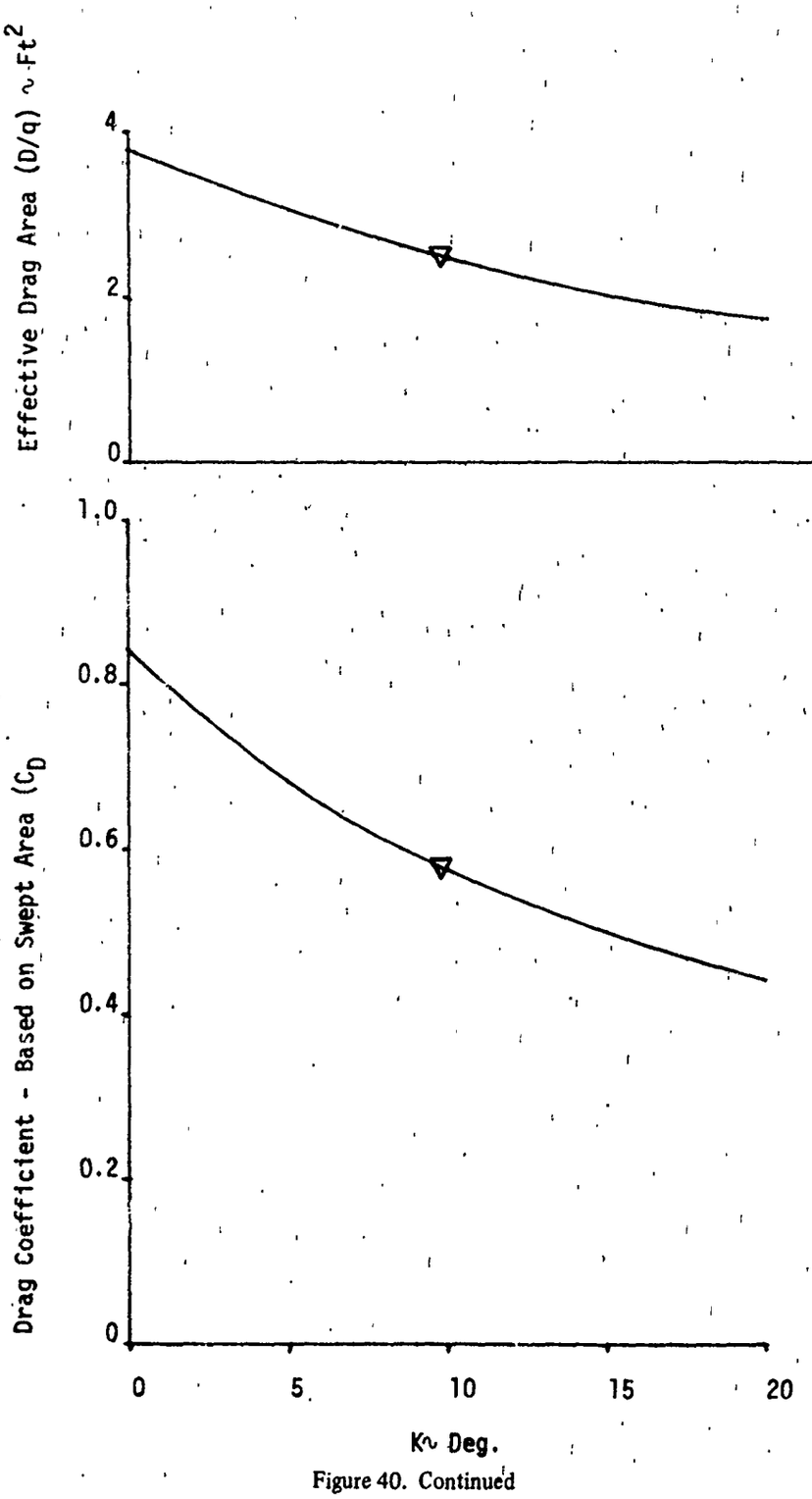

Figure 40. Continued

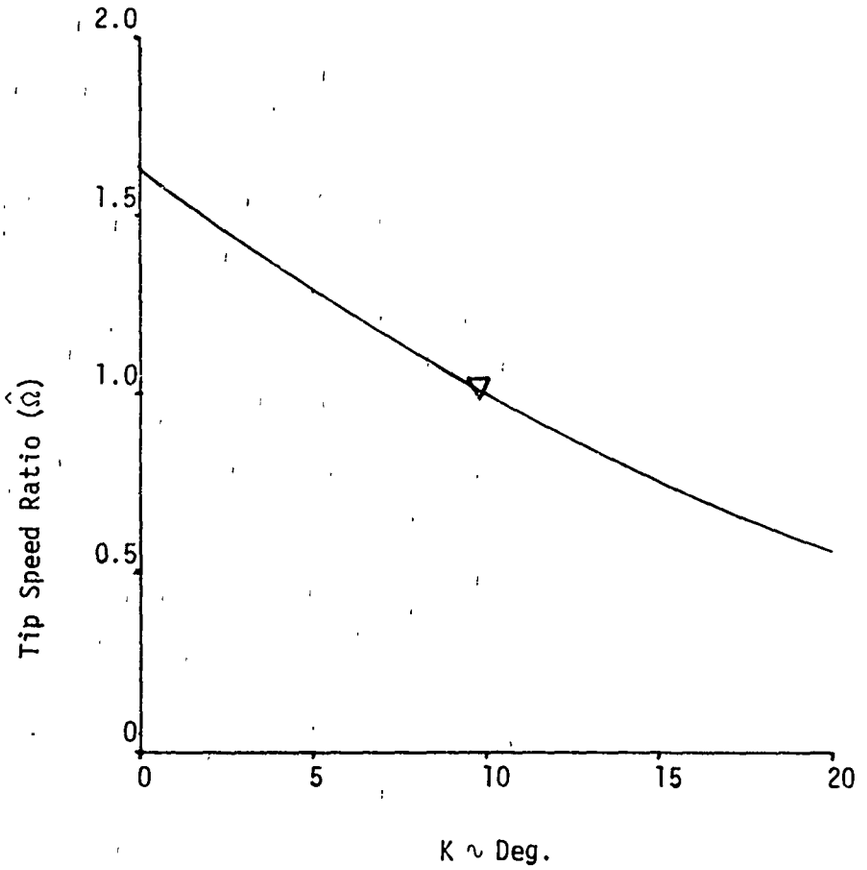

Figure 40. Continued

An appreciation of the rapidity of motion involved is gained by noting that the system achieves steady state conditions in about 1½ seconds after deployment initiation.

It should be noted from figure 43 that initial deployment motion of the blade takes about 0.1 second. From figures 44 and 45, it can be determined from the average hub and blade rotation rates during this time interval that the blade makes only one complete revolution, and the hub makes about 3/4 of a revolution during this initial deployment phase.

IX. STEADY STATE PERFORMANCE PARAMETER STUDY.

A. Method of Analysis.

A study was conducted to evaluate the effects of the various physical and aerodynamic properties on the steady state performance of the autorotor decelerator system. A nominal set of values for the rotor physical characteristics, aerodynamic characteristics, and air flow conditions were selected that were representative of a realistic physical case. The steady state performance of the rotor system for this nominal case was computed using the equations of motion programmed on the computer.

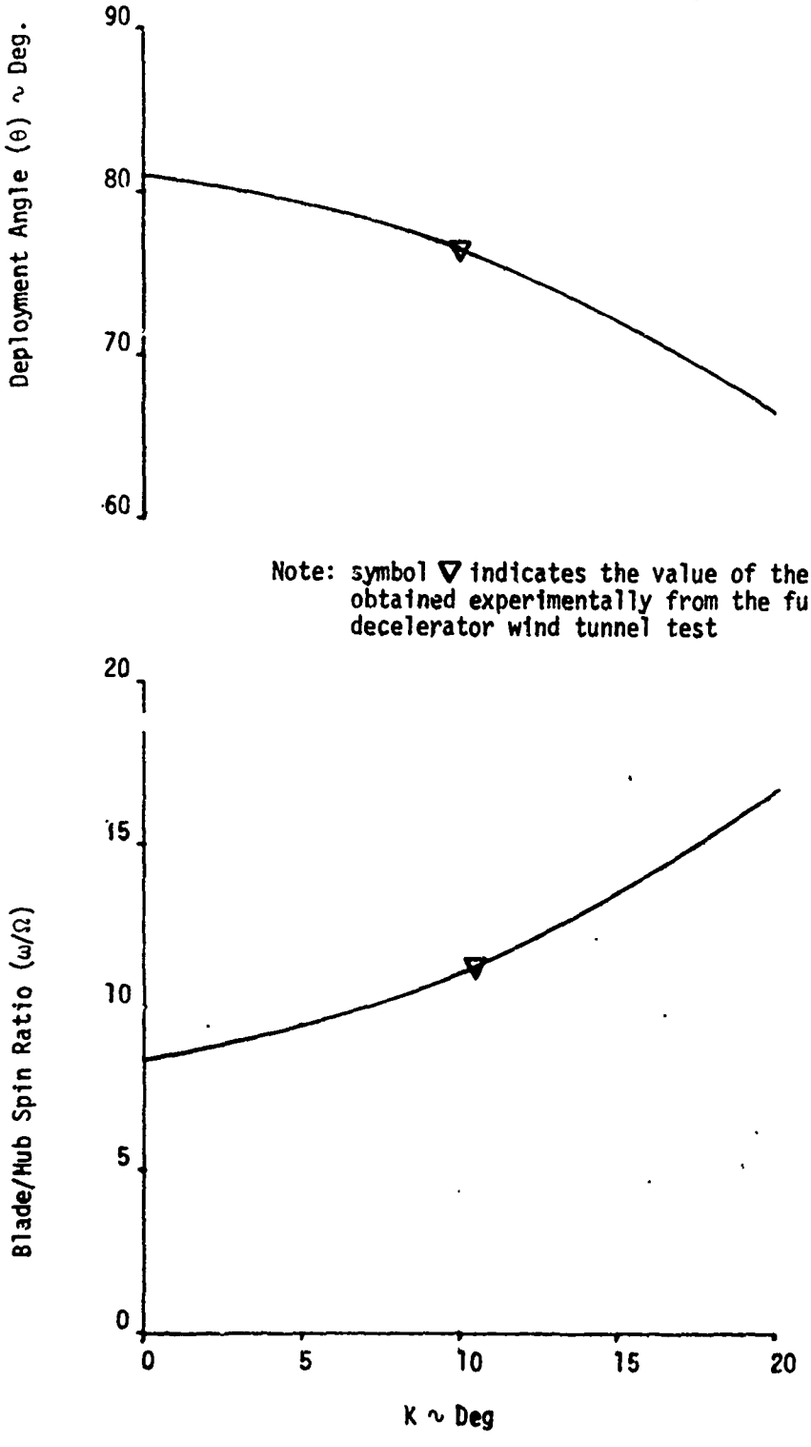

Figure 41. Steady State Performance of Full-Scale Autorotor Decelerator Computed as a Function of Interference Factor (K) for a Free Stream Velocity of 173 Ft/Sec

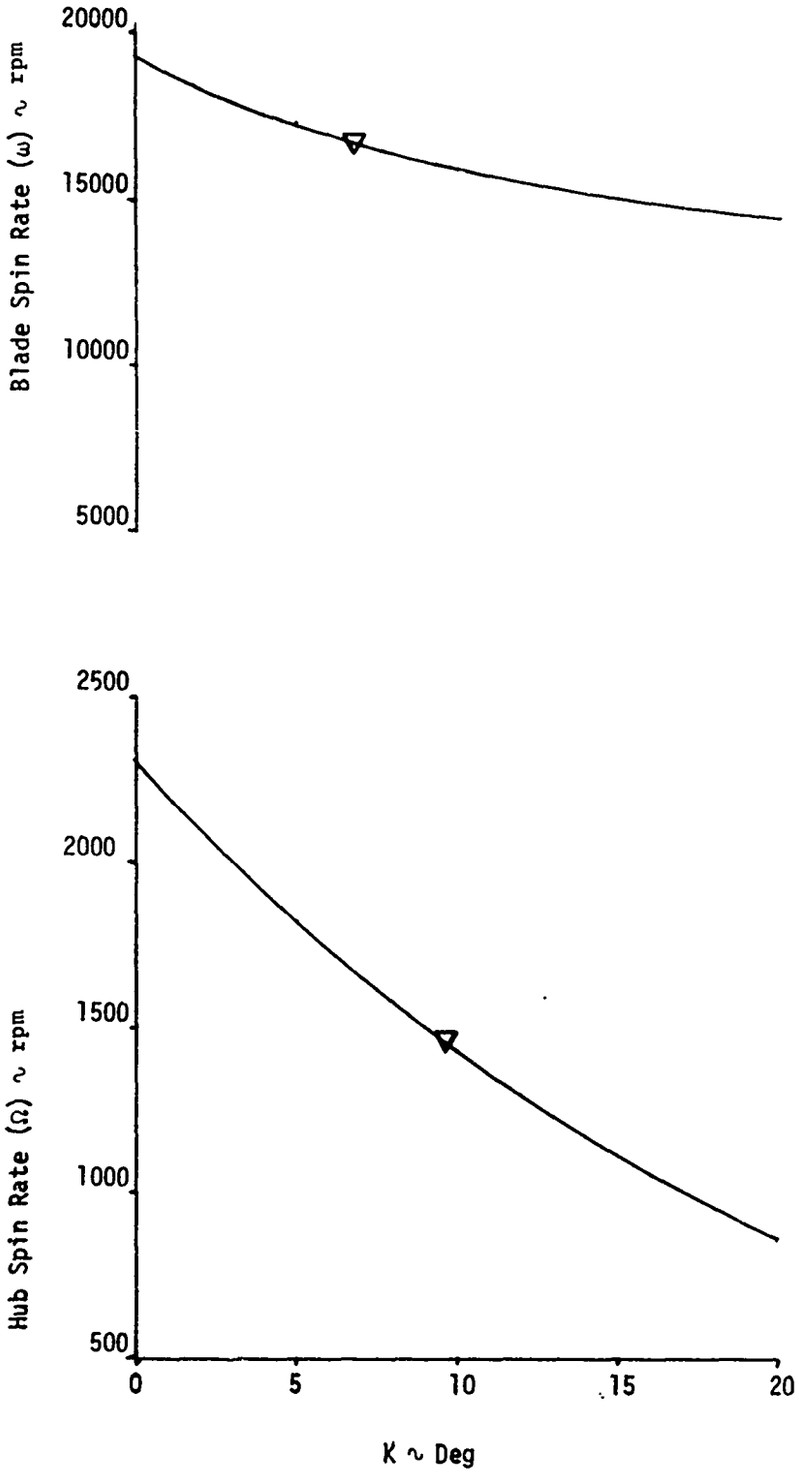

Figure 41. Continued

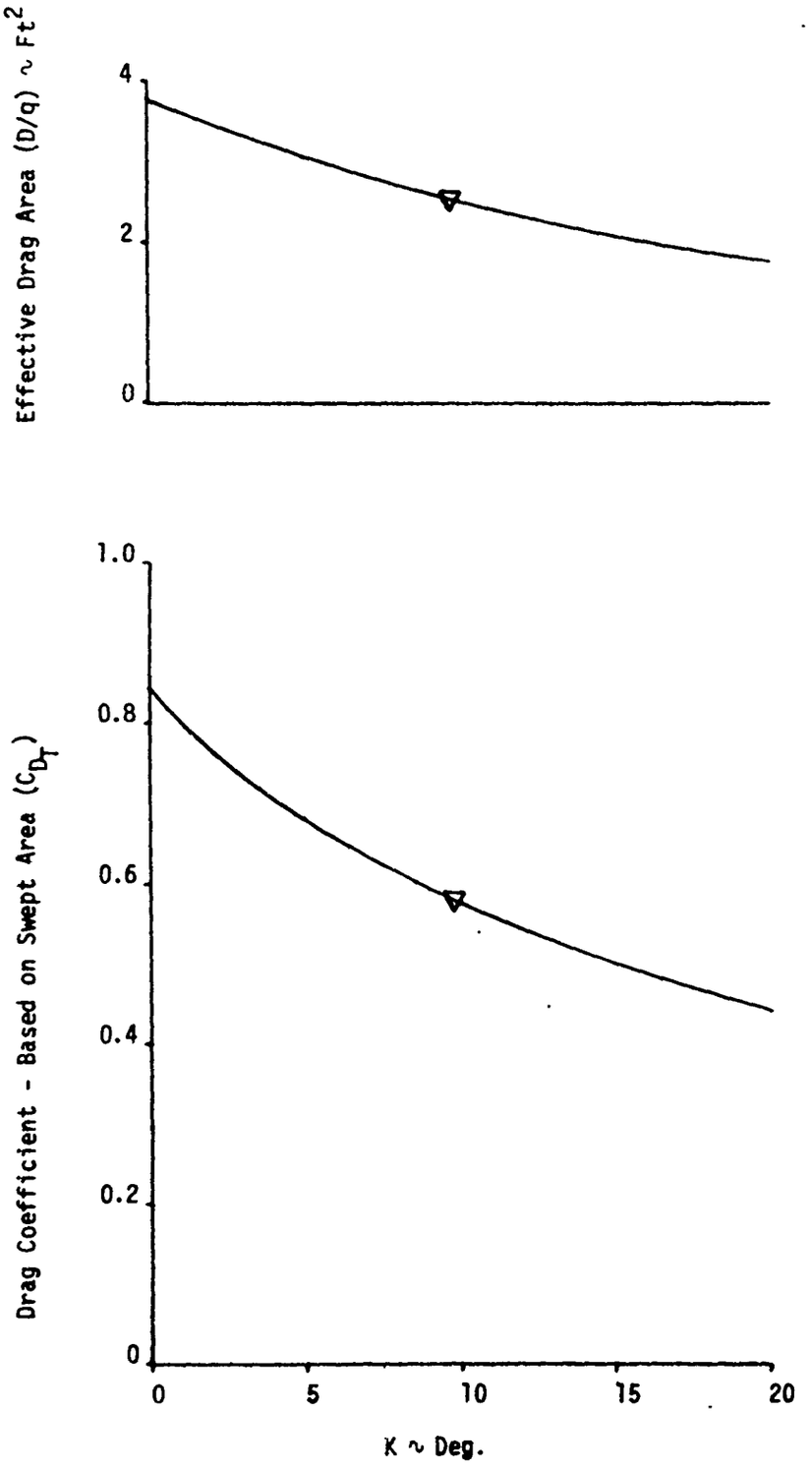

Figure 41. Continued

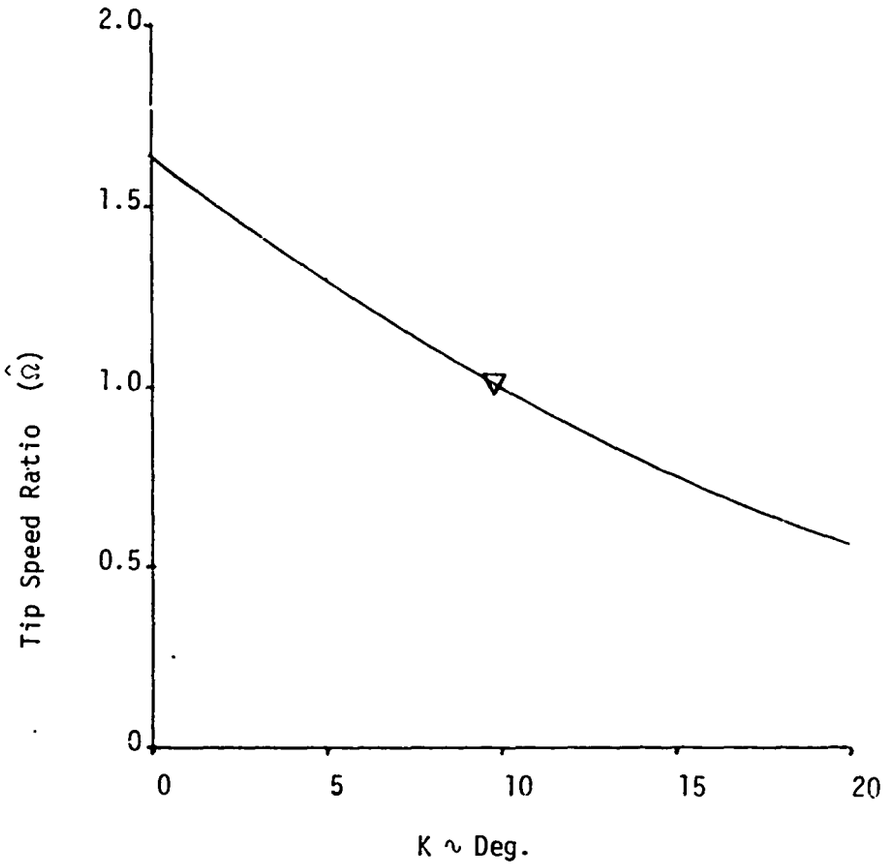

Figure 41. Continued

The steady state performance then was calculated for the cases in which a selected parameter was given a value larger than the nominal value and smaller than the nominal value. Table III contains a summary of the terms and values used in the parameter study. The high and low values selected for each term represent realistic ranges. Appendix C contains the computer printout showing the steady state conditions for each parameter run.

To facilitate discussion, the performance of the rotor system is plotted versus a specific parameter for a constant value of K. A value of $K = 10$ was selected because this value of K was determined for the full-scale autorotor decelerator, which closely resembles the nominal case for the parameter study.

As stated previously, the interference effect, and thus the value of K, may be a function of several terms. In this parameter study, however, it is assumed that the value $K = 10$ holds for the values of the parameters used. These data will be presented in three parts: rotor system physical properties, flow conditions, and rotor blade aerodynamic characteristics.

The terms with values plotted as a function of each parameter include the following:

Table II. Comparison Between Experimental Results and Analytical Results Computed With and Without an Interference Factor (K) for a Free Stream Velocity of 100 Ft/Sec

Term	Experimental results	Analytical results ($K = 0$)	Analytical results ($K = 10$)
Ω	850 rpm	1330 rpm	830 rpm
ω	9650 rpm	11200 rpm	9200 rpm
ω/Ω	11.3	8.4	11.1
θ	76.5°	80.8°	76.6°
C_{D_T}	0.58	0.84	0.576
D/q	2.6 sq ft	3.8 sq ft	2.55 sq ft
$\hat{\Omega}$	1.01	1.64	1.00

1. Tip speed ratio, $\hat{\Omega} = \dfrac{\Omega(b + \frac{\ell}{2})\sin\theta}{V_\infty}$, is the ratio of the tangential velocity of the blade tip in a plane perpendicular to the hub spin axis and the free stream velocity. This is the inverse of the advance ratio and is a common nondimensional term used in describing the rotational characteristics of autorotating or spinning type devices.

2. Deployment angle, θ, is the angle that the blade spin axis (i.e., long axis) makes with the body center line.

3. Blade spin rate, ω, is the spin rate of the blade about its long axis.

4. Hub spin rate, Ω, is the spin rate of the blade long axis about the body center line (i.e., the hub spin rate).

5. Blade/hub spin ratio, ω/Ω, is the ratio of the blade spin rate (ω) to the hub spin rate (Ω).

6. Effective drag area, D/q, is the total drag of the system expressed in terms of the free stream dynamic pressure.

7. Drag coefficient, $C_{D_T} = \dfrac{D}{qS_T}$, the drag coefficient of the system based on the total projected area swept over by the blades where:

$$S_T = \pi\left(b + \frac{\ell}{2}\right)^2 \sin^2\theta$$

This coefficient represents the efficiency of the system to produce drag for a given projected frontal area.

Although only three data points are used to construct the curves for each parameter, the curves would seem to present valid trends because of the absence of any severe nonlinearities under the assumptions used in the analysis and the relative closeness of the parameter value (i.e., same order of magnitude) used to construct the curve in each case.

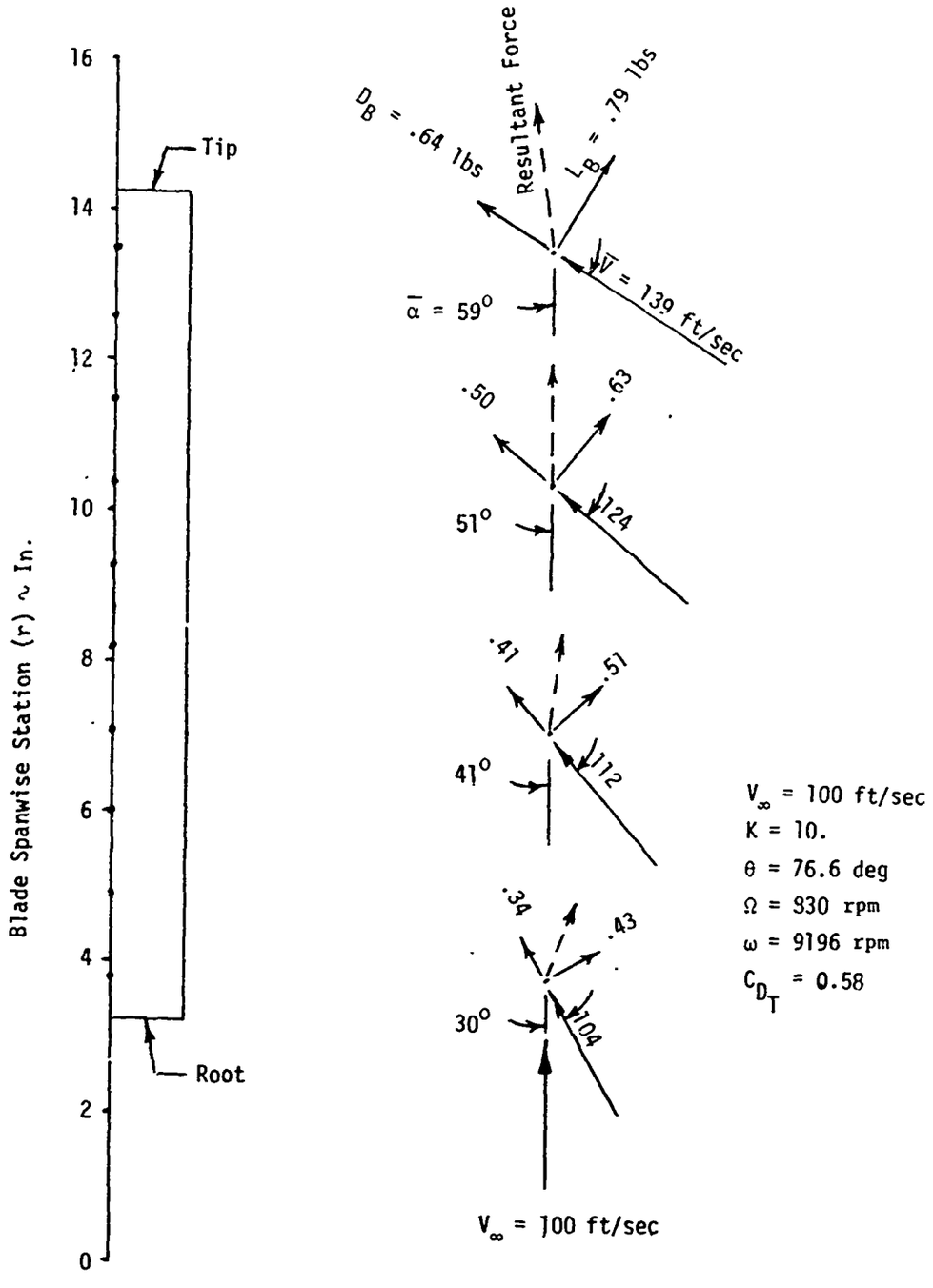

Figure 42. Aerodynamic Conditions at Various Blade Spanwise Stations at Steady Steady State Condition for Analytical Approach With Interference Factor ($K = 10$)

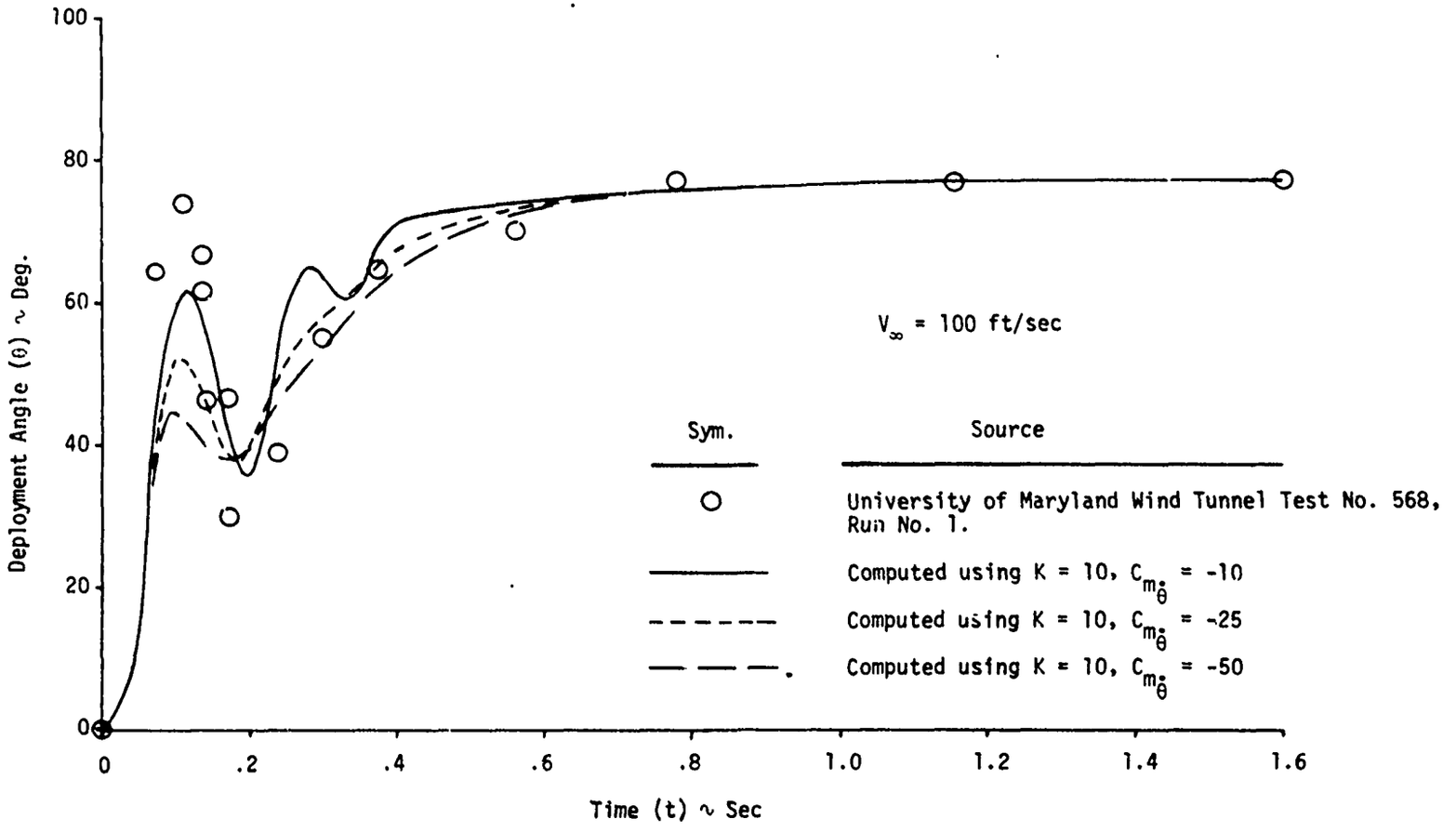

Figure 43. Deployment Angle as a Function of Time During Deployment Transient Showing Computed and Experimental Results

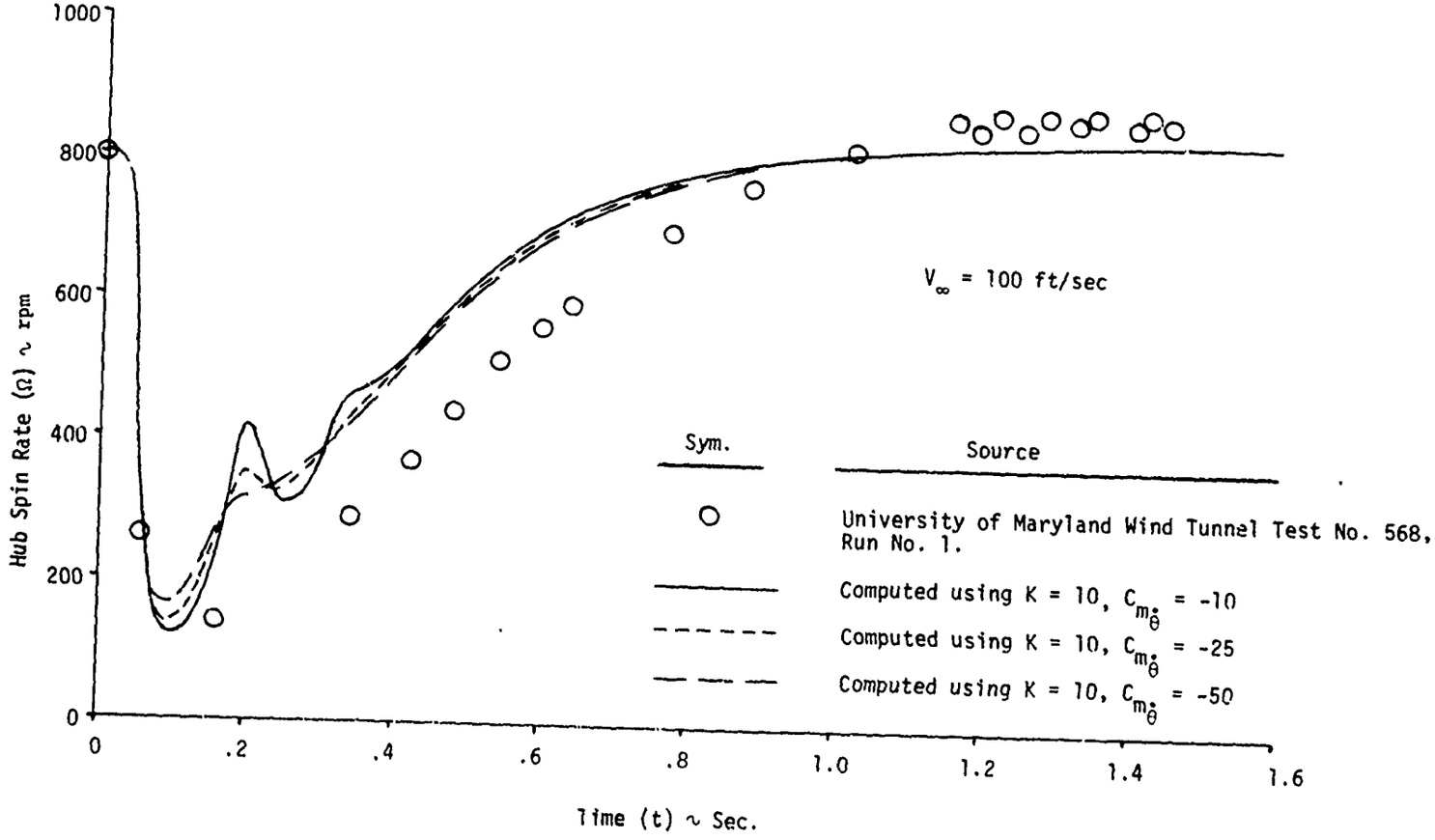

Figure 44. Hub Spin Rate as a Function of Time During Deployment Transient Showing Computed and Experimental Results

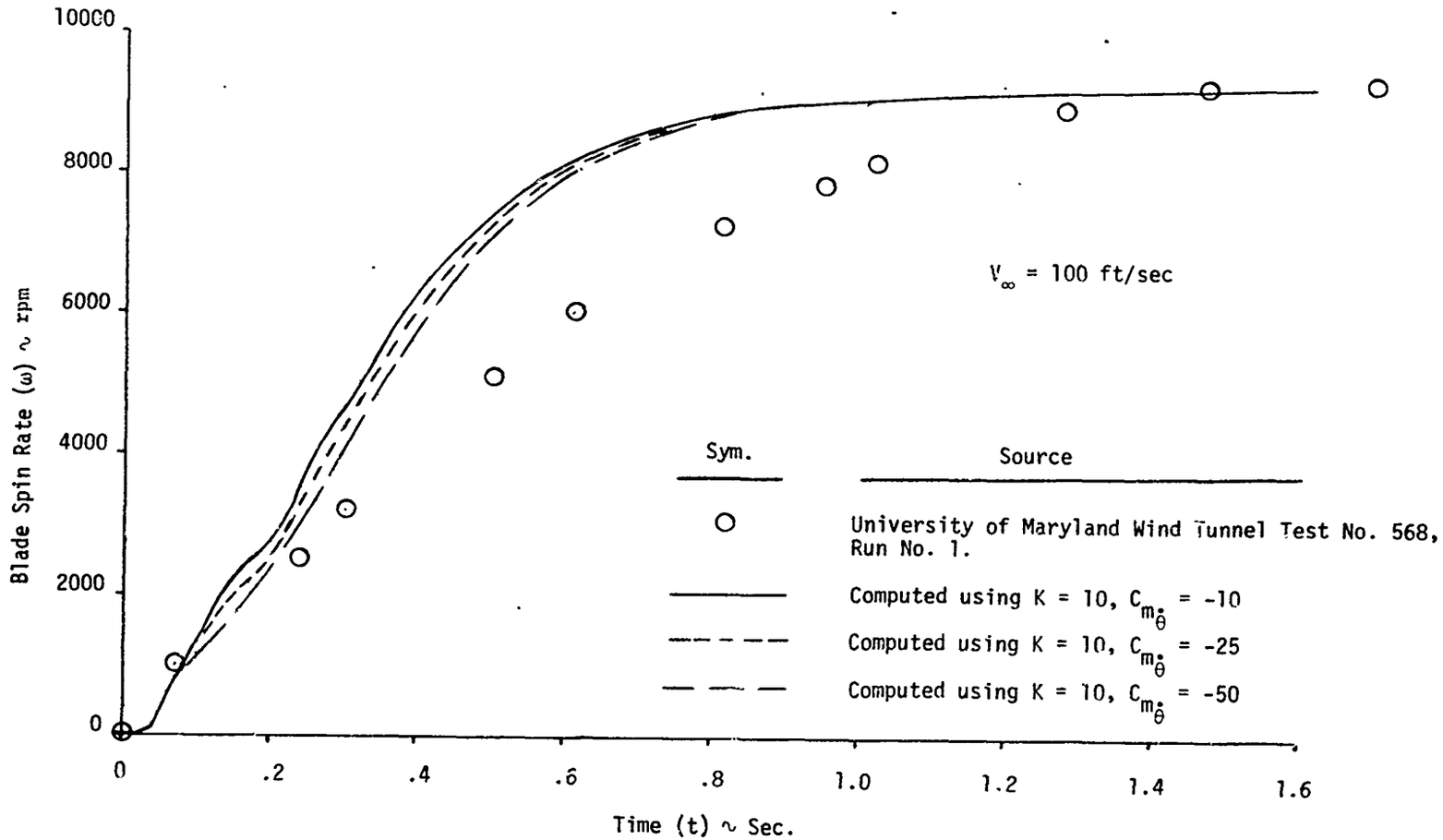

Figure 45. Blade Spin Rate as a Function of Time During Deployment Transient Showing Computed and Experimental Results

Table III. Summary of Term Values Used in Articulated Autorotor Decelerator Steady State Performance Parameter Study

Run	ρ	V_∞	Wgt	ℓ	C	s	b	I_1	I_0	r_0	Δr	$C_{L_{ss_0}}$	C_{L_1}
	slug/cu ft	ft/sec	lb	in.		sq ft	in.	slug – sq ft		ft			
1	0.002377	100	0.3290	10	3	0.2083	0.708	0.00005868	0.005740	0.3332	.0834	1.55	1.7143
2	N[a]	N	0.1645	N	N	N	N	0.00002935	0.002870	N	N	N	N
3	N	N	0.6590	N	N	N	N	0.00011730	0.011500	N	N	N	N
4	N	N	0.2300	7	N	0.1530	0.583	0.00004110	0.002651	0.3208	.0583	N	N
5	N	N	0.4275	13	N	0.2710	0.833	0.00007640	0.009225	0.3458	.1083	N	N
6	N	N	0.2194	N	2	0.1389	N	0.00003910	0.003818	N	N	N	N
7	N	N	0.4387	N	4	0.2778	N	0.00012360	0.007680	N	N	N	N
8	N	50	N	N	N	N	N	N	N	N	N	N	N
9	N	200	N	N	N	N	N	N	N	N	N	N	N
10	0.001190	N	N	N	N	N	N	N	N	N	N	N	N
11	0.004760	N	N	N	N	N	N	N	N	N	N	N	N
12	N	N	N	N	N	N	N	N	N	N	N	N	1.0
13	N	N	N	N	N	N	N	N	N	N	N	N	n[b]
14	N	N	N	N	N	N	N	N	N	N	N	N	n
15	N	N	N	N	N	N	N	N	N	N	N	1.25	n
16	N	N	N	N	N	N	N	N	N	N	N	1.75	n
17	N	N	N	N	N	N	N	N	N	N	N	N	n
18	N	N	N	N	N	N	N	N	N	N	N	N	n

N[a] denotes nominal value (run 1).
n[b] denotes nominal "linearized" coefficients value (run 12).

$$S = \ell C \qquad b = \frac{3.5 + \ell/2}{2} \qquad r_0 = 0.583 + \frac{\Delta r}{2} \qquad \Delta r = \frac{\ell}{10} \qquad AR = \frac{\ell}{C} \qquad \sigma = \frac{4\ell C}{S} \qquad \bar{S} = \frac{\pi(2\ell + 0.583)^2}{4}$$

Table III. Continued

C_{L_2}	$C_{D_{ss_0}}$	$\hat{\omega}_{ss_0}$	C_{m_0}	C_{m_1}	C_{m_2}	AR	σ	$\frac{C_{L_{ss_0}}}{C_{D_{ss_0}}}$	Parameter that is varied about nominal value
-0.7145	1.25	1.0	0.20	0.15	-0.35	3.33	0.2095	1.29	Nominal case *(N)*
N	N	N	N	N	N	N	N	N	> Blade weight (*wt*)
N	N	N	N	N	N	N	N	N	
N	N	N	N	N	N	2.33	0.2425	N	> Blade length (ℓ)
N	N	N	N	N	N	4.33	0.1825	N	
N	N	N	N	N	N	5.00	0.1395	N	> Blade chord (*C*)
N	N	N	N	N	N	2.50	0.2790	N	
N	N	N	N	N	N	N	N	N	> Free stream velocity (V_∞)
N	N	N	N	N	N	N	N	N	
N	N	N	N	N	N	N	N	N	> Air density (ρ)
N	N	N	N	N	N	N	N	N	
0	N	N	N	-0.20	0	N	N	N	Linearized coefficients (*n*)
n	N	0.75	N	n	n	N	N	N	> Maximum tip speed ratio (ω_{ss_0})
n	N	1.25	N	n	n	N	N	N	
n	N	N	N	n	n	N	N	1.00	> Maximum lift coefficient ($C_{L_{ss_0}}$)
n	N	N	N	n	n	N	N	1.40	
n	1.0	N	sN	n	n	N	N	1.55	> Maximum drag coefficient ($C_{D_{ss_0}}$)
n	1.5	N	N	n	n	N	N	1.03	

The main purpose of these curves is to indicate the general effect that varying a single parameter term has on the decelerator system performance. Of special interest is the sensitivity of the decelerator performance on a particular parametric term. Thus, the curves developed should provide valid and meaningful results.

B. Effect of Rotor System Physical Properties.

1. Effects of Blade Weight.

The effects of the weight of the autorotor blade on the steady state performance are shown in figures 46 through 49. It should be noted that the nominal value for blade weight would represent a blade fabricated from aluminum. The heavier weight would represent a steel blade, and the lighter weight would be a boron-fibre type material. The most significant effect of blade weight is that the blade deployment angle increases with increasing blade weight because of the mass effect on the centrifugal force. The hub spin rate increases slightly with decreasing blade weight. This makes up for the reduced projected frontal area from the lower deployment angle, and the result is that the total drag produced is independent of blade weight. The drag coefficient increases with reduced weight because the drag results from a reduced projected area.

It should be remembered that changes in the system weight and dimensions are also included in the moments of inertia, which, in turn, affect the inertial and gyroscopic terms.

2. Effects of Blade Length.

The effects of blade length on the performance are included in figures 50 through 53. It should be noted that the changes in blade length also affect corresponding changes in the mass and inertial properties of the blade. The deployment angle decreases slightly with blade length. The blade spin rate remains the same regardless of blade length. The hub spin rate decreases with increasing blade length; however, the tip speed ratio remains practically constant. The system drag increases with increased blade length, but the drag coefficient decreases, indicating a loss of efficiency with increased blade length. The blade-to-hub spin ratio increases with increased blade length, reflecting the reduced hub spin rate.

3. Effects of Blade Chord.

Figures 54 through 57 show the effects of the blade chord length on the performance characteristics. The mass and inertial values of the blade correspond to the changes in the blade chord. Here, the hub spin rate remains constant with chord length, but the blade spin rate decreases markedly with increasing chord length. The effect of chord length on the blade spin ratio is consistent with basic autorotor performance. Interestingly, the deployment angle exhibits a minimum value near the nominal conditions, which is a result of the interactions of the inertial gyroscopic and aerodynamic effects. These deployment angle differences, however, do not result in any effect on the tip speed ratio, which remains constant in accordance with the hub spin rate. The effective drag area increases linearly with increasing chord, as does the drag coefficient. Note that a chord of 4 inches, which is not an unrealistic size for the configuration considered, results in a relatively high drag coefficient of 0.78.

4. Effects of Solidity Factor.

The effects of blade chord and blade length also can be expressed as a function of the solidity factor (σ), which is defined as the ratio of the total areas of the blades to the maximum projected swept area.

Sym.	Run	Blade Weight (wgt) ∿ Lbs.
△	2	.1645
○	1	.3290
□	3	.6590

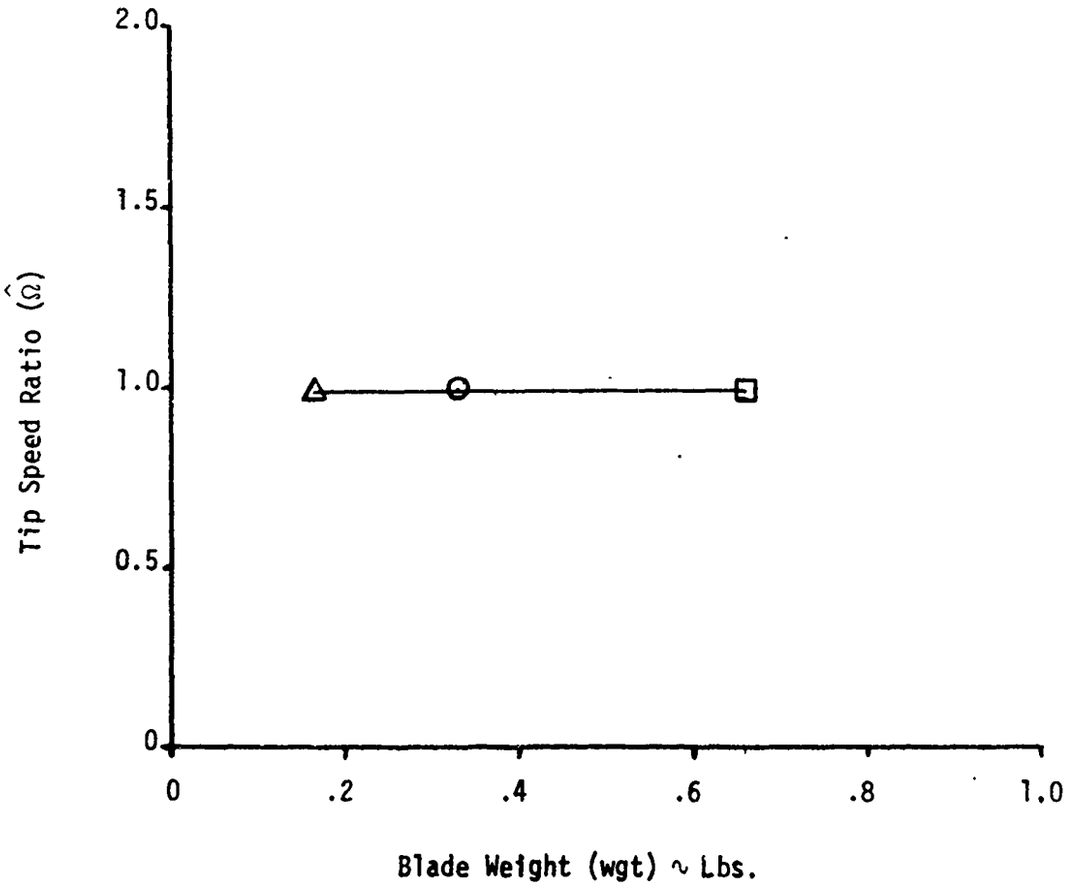

Figure 46. Effect of Blade Weight on Steady State Tip Speed Ratio

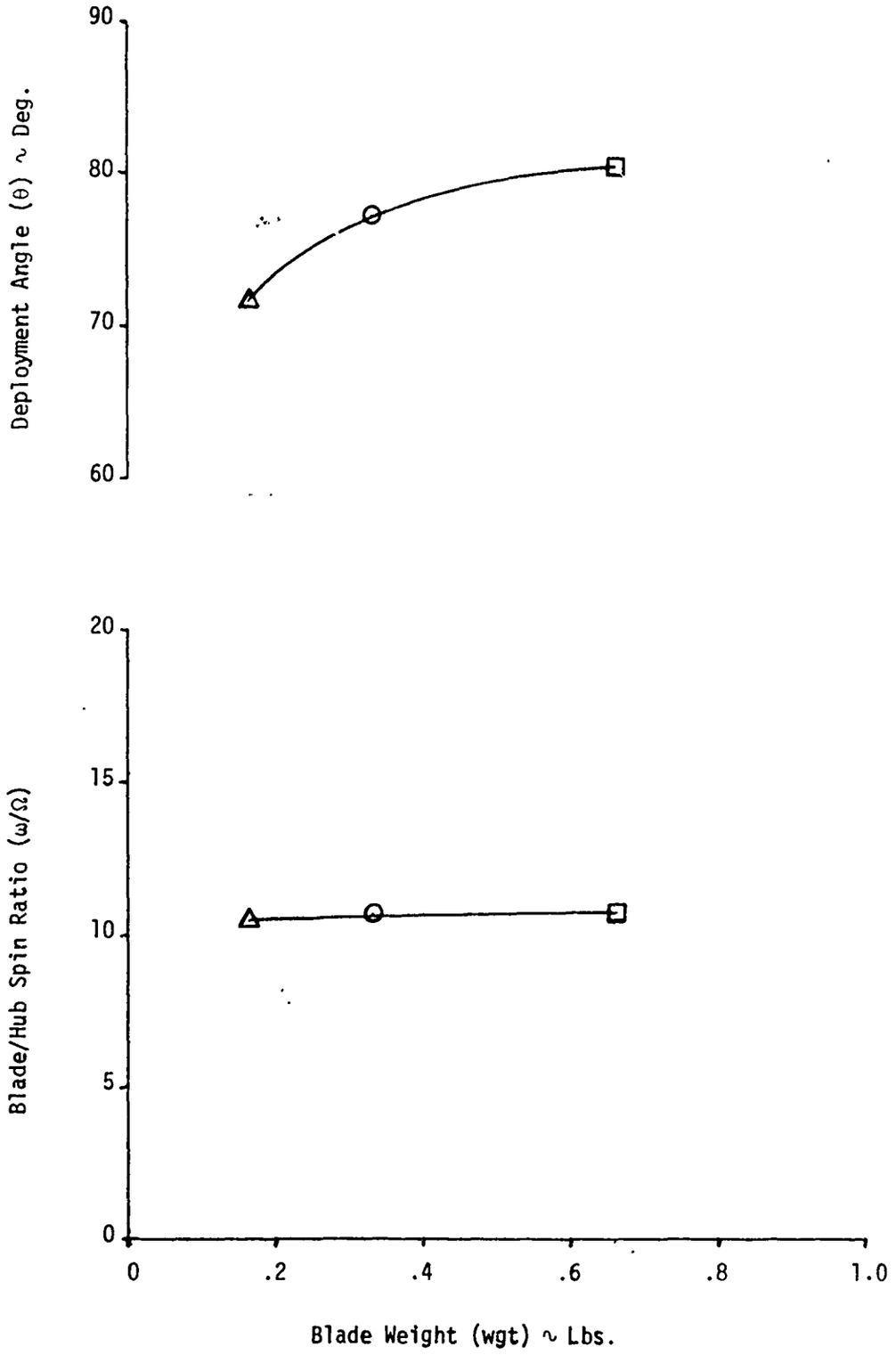

Figure 47. Effect of Blade Weight on Steady State Deployment Angle and Blade/Hub Spin Ratio

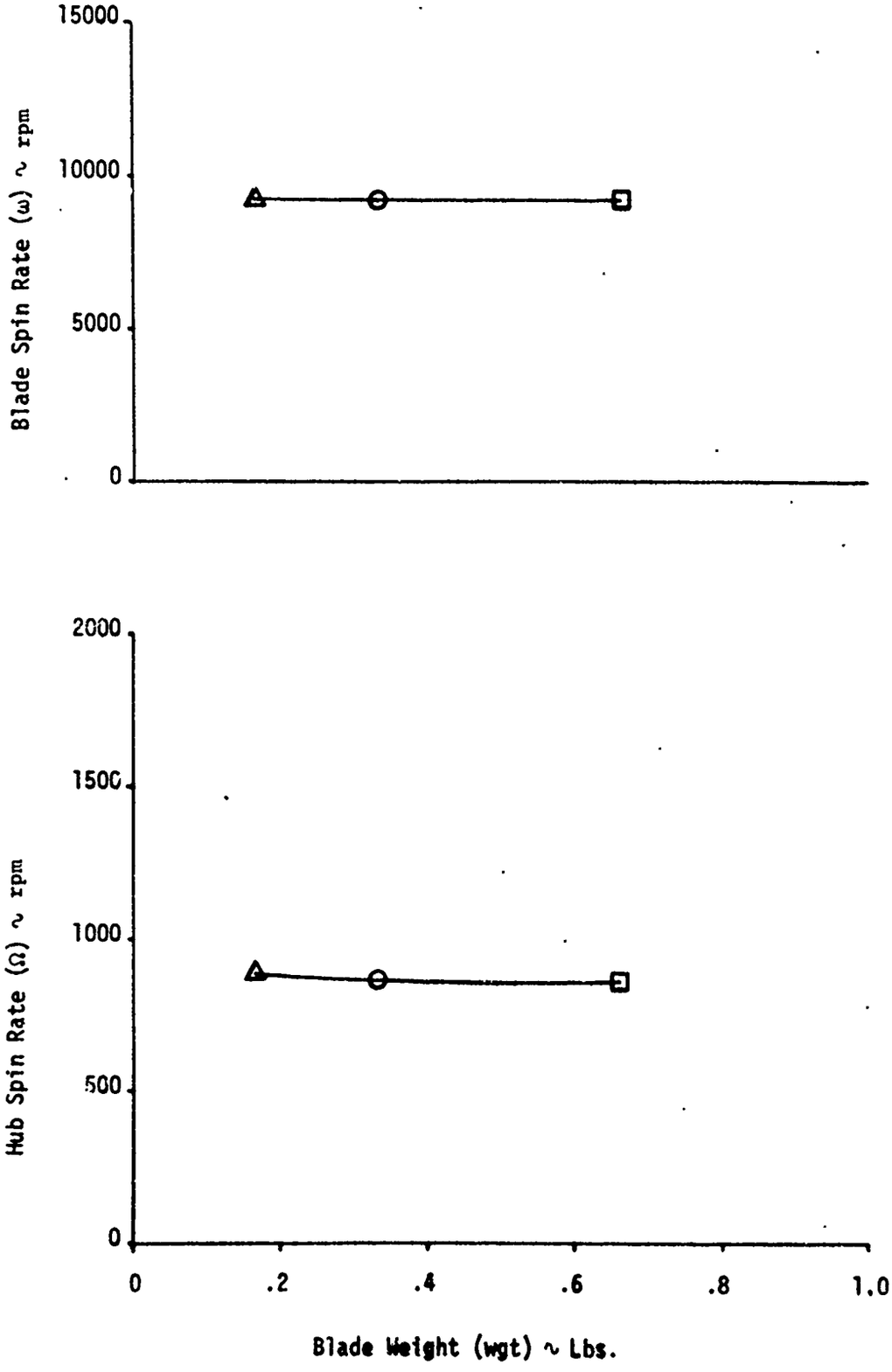

Figure 48. Effect of Blade Weight on Steady State Blade Spin Rate and Hub Spin Rate

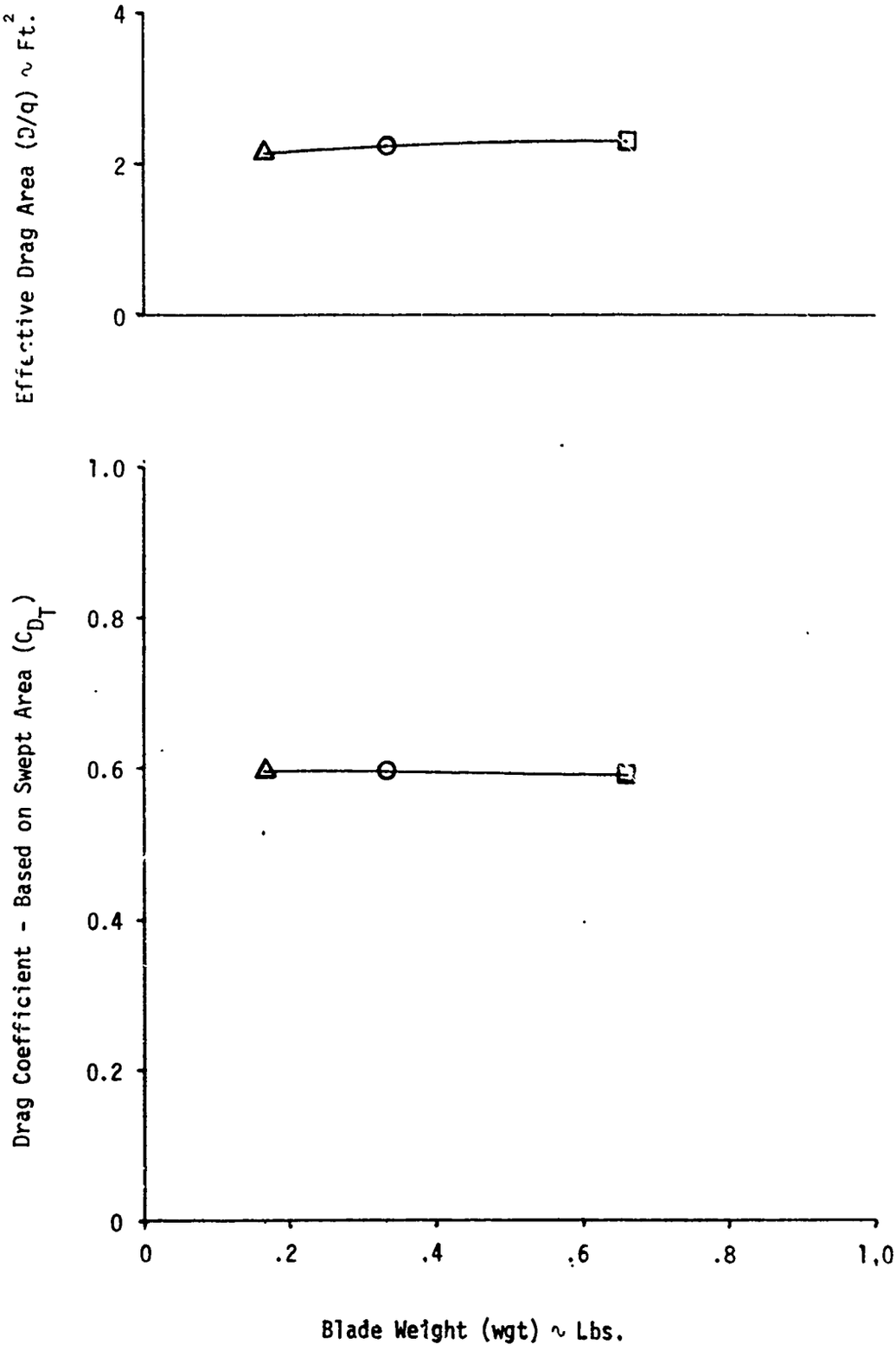

Figure 49. Effect of Blade Weight on Steady State Effective Drag Area and Drag Coefficient

Sym	Run	Blade Length (ℓ) ~ In.
△	4	7
○	1	10
□	5	13

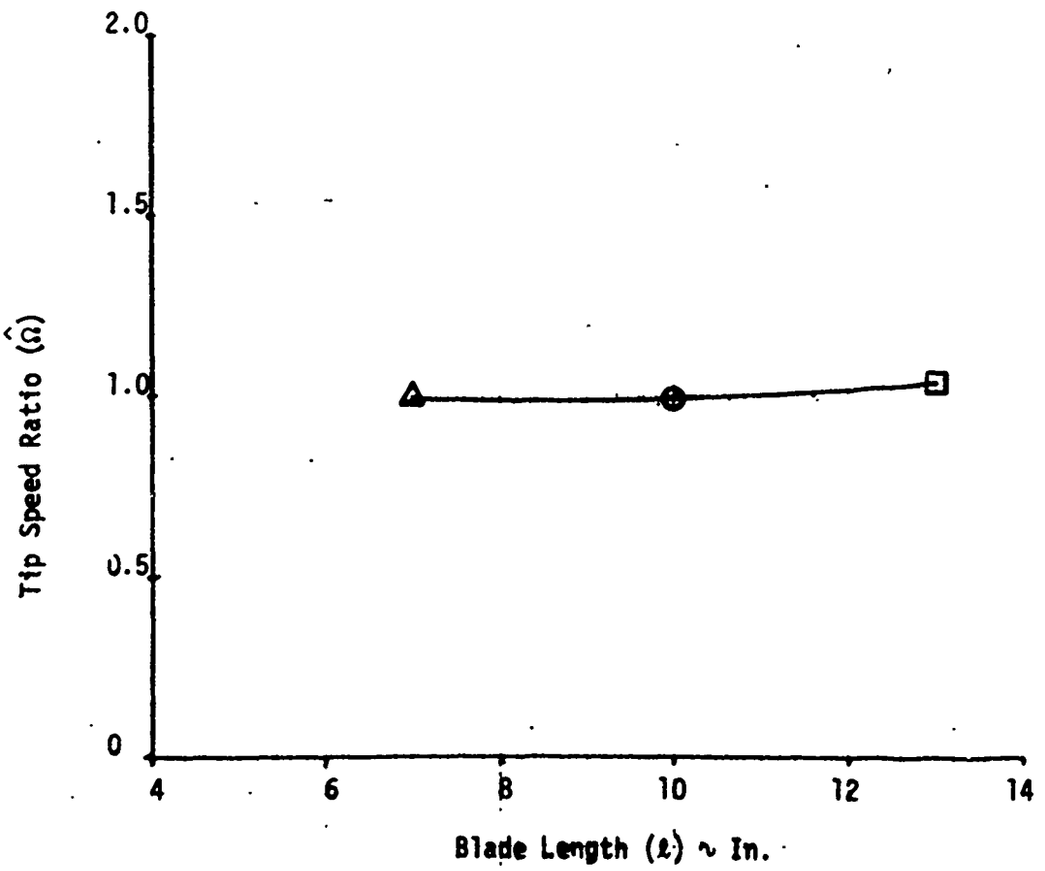

Figure 50. Effect of Blade Length on Steady State Tip Speed Ratio

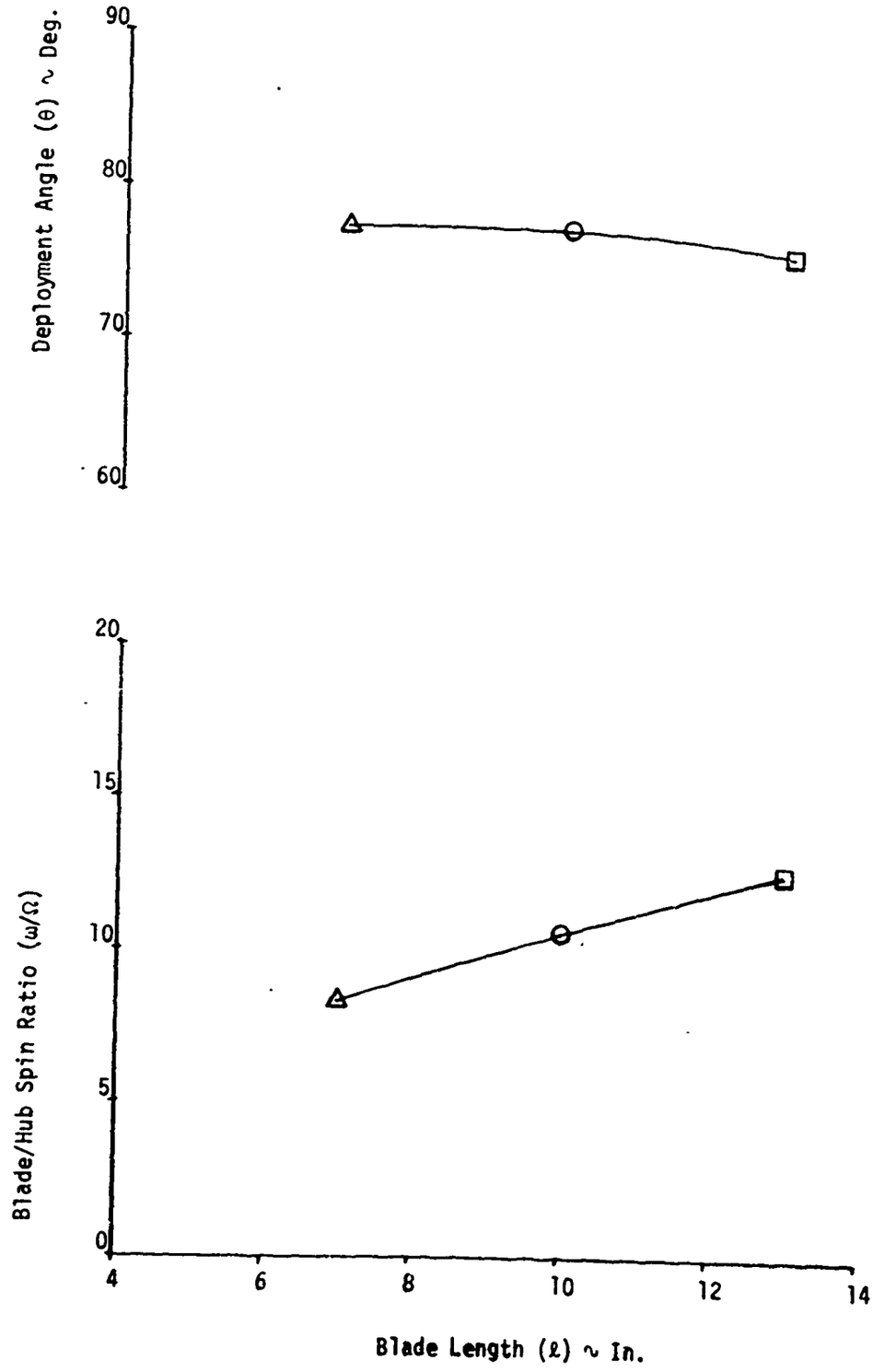

Figure 51. Effect of Blade Length on Steady State Deployment Angle and Blade/Hub Spin Ratio

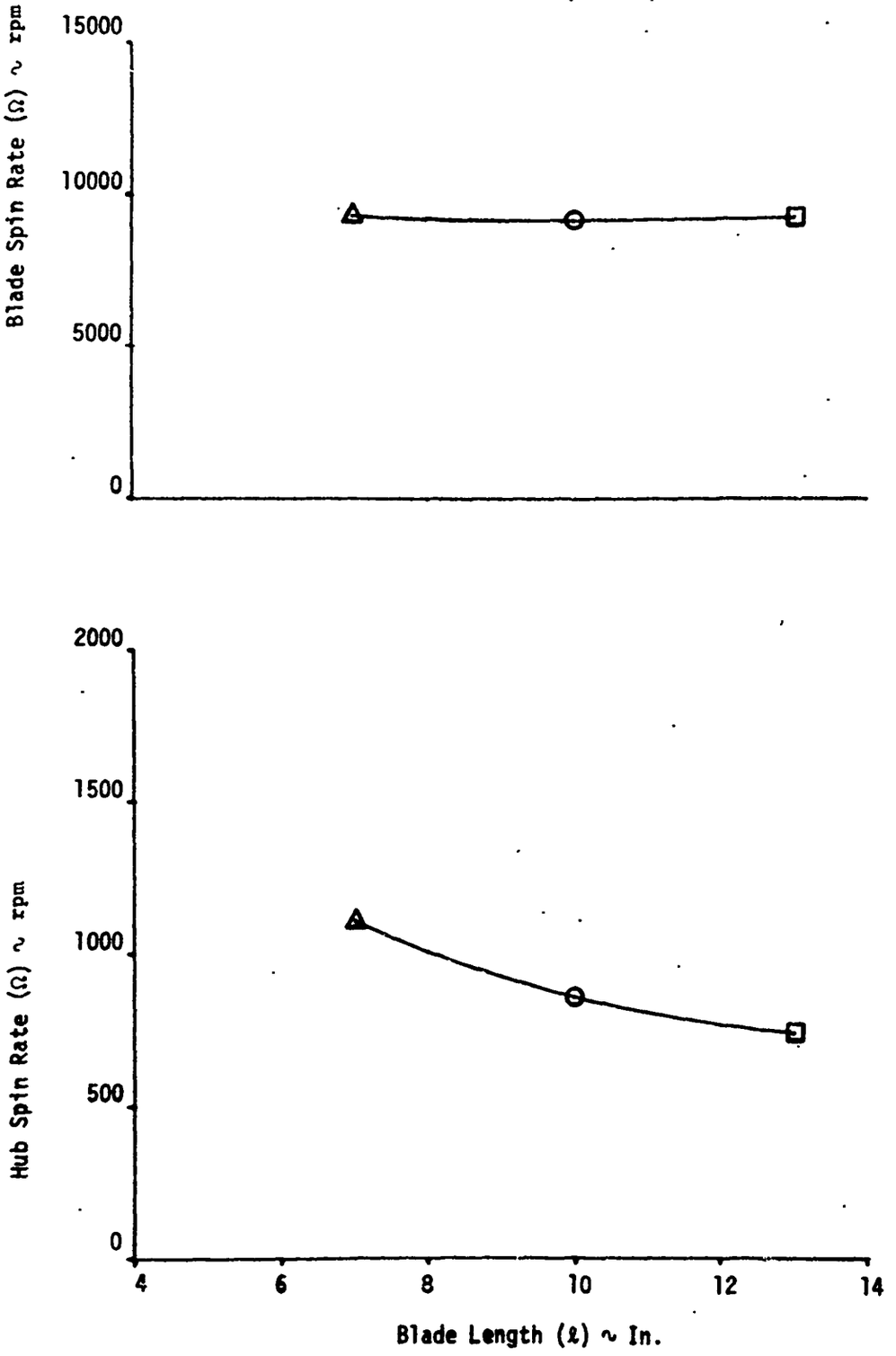

Figure 52. Effect of Blade Length on Steady State Blade Spin Rate and Hub Spin Rate

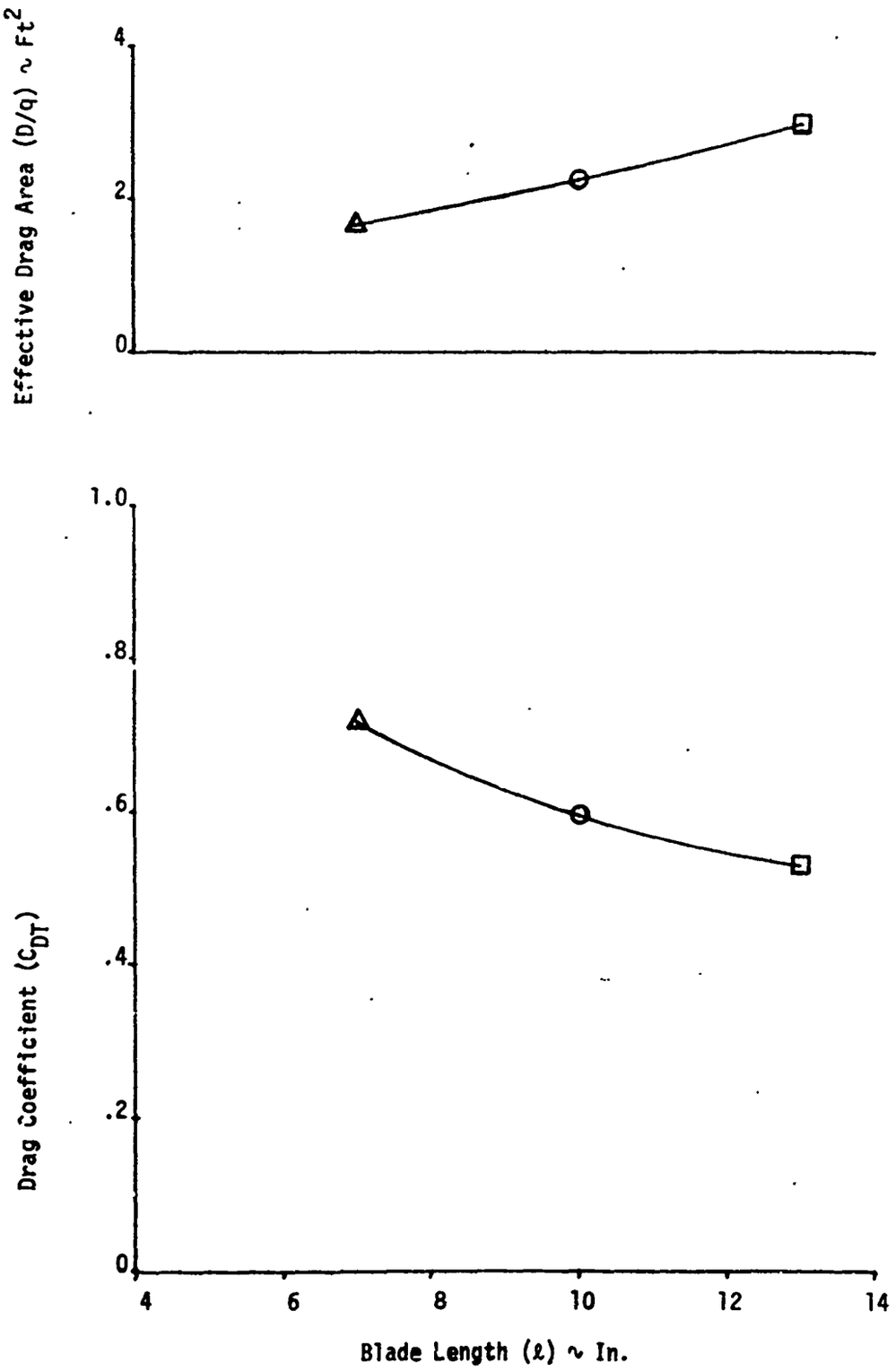

Figure 53. Effect of Blade Length on Steady State Effective Drag Area and Drag Coefficient

Sym	Run	Blade Chord (C) ∿ In.
△	6	2
○	1	3
□	7	4

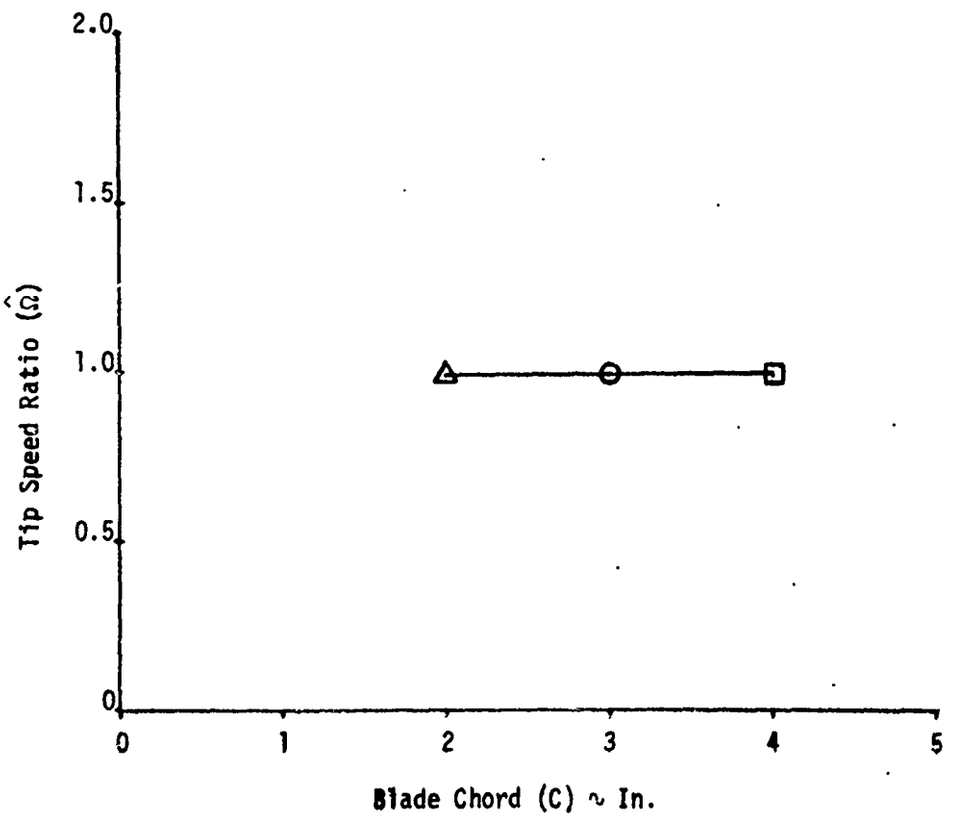

Figure 54. Effect of Blade Chord on Steady State Tip Speed Ratio

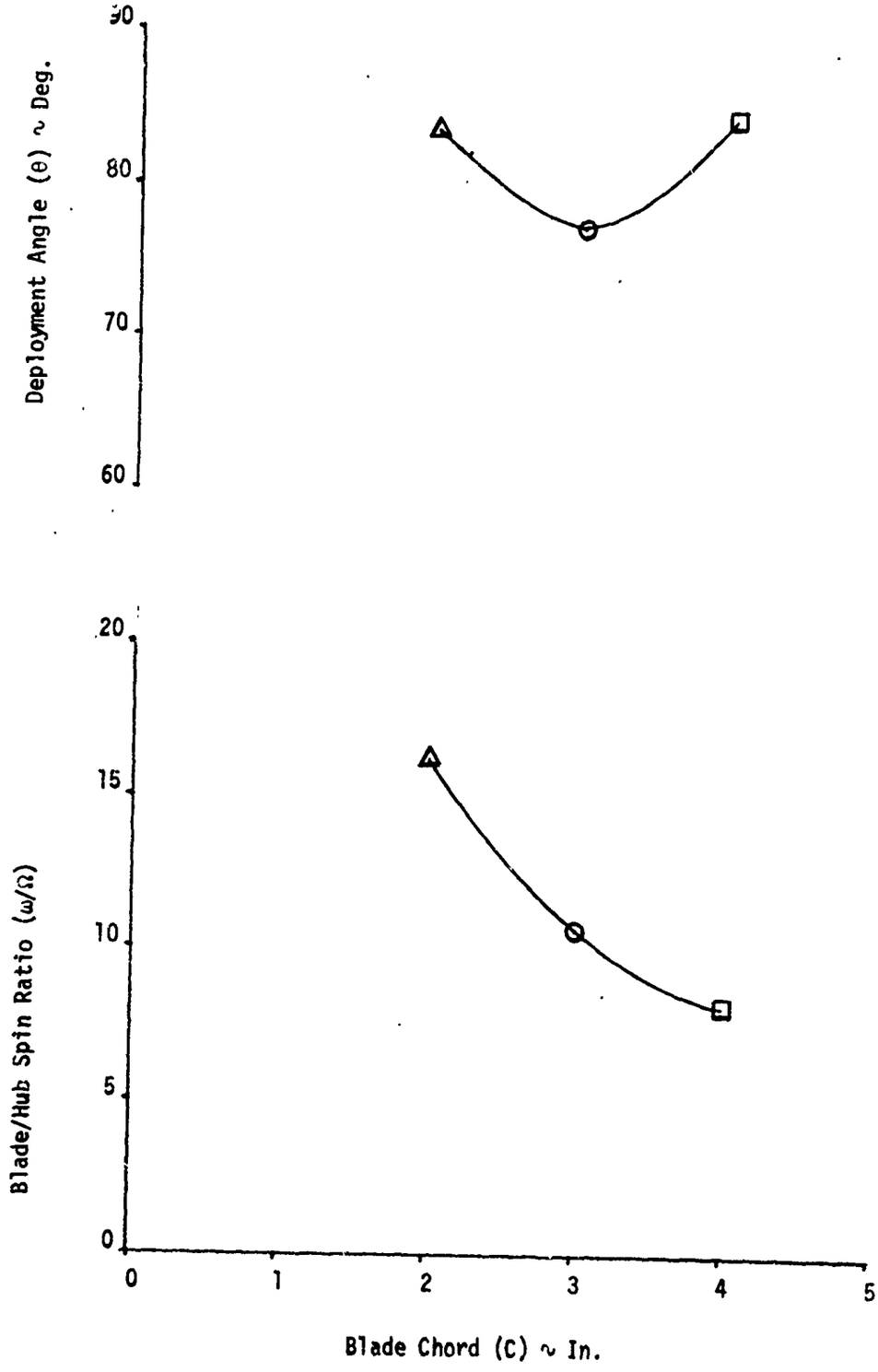

Figure 55. Effect of Blade Chord on Steady State Deployment Angle and Blade/Hub Spin Ratio

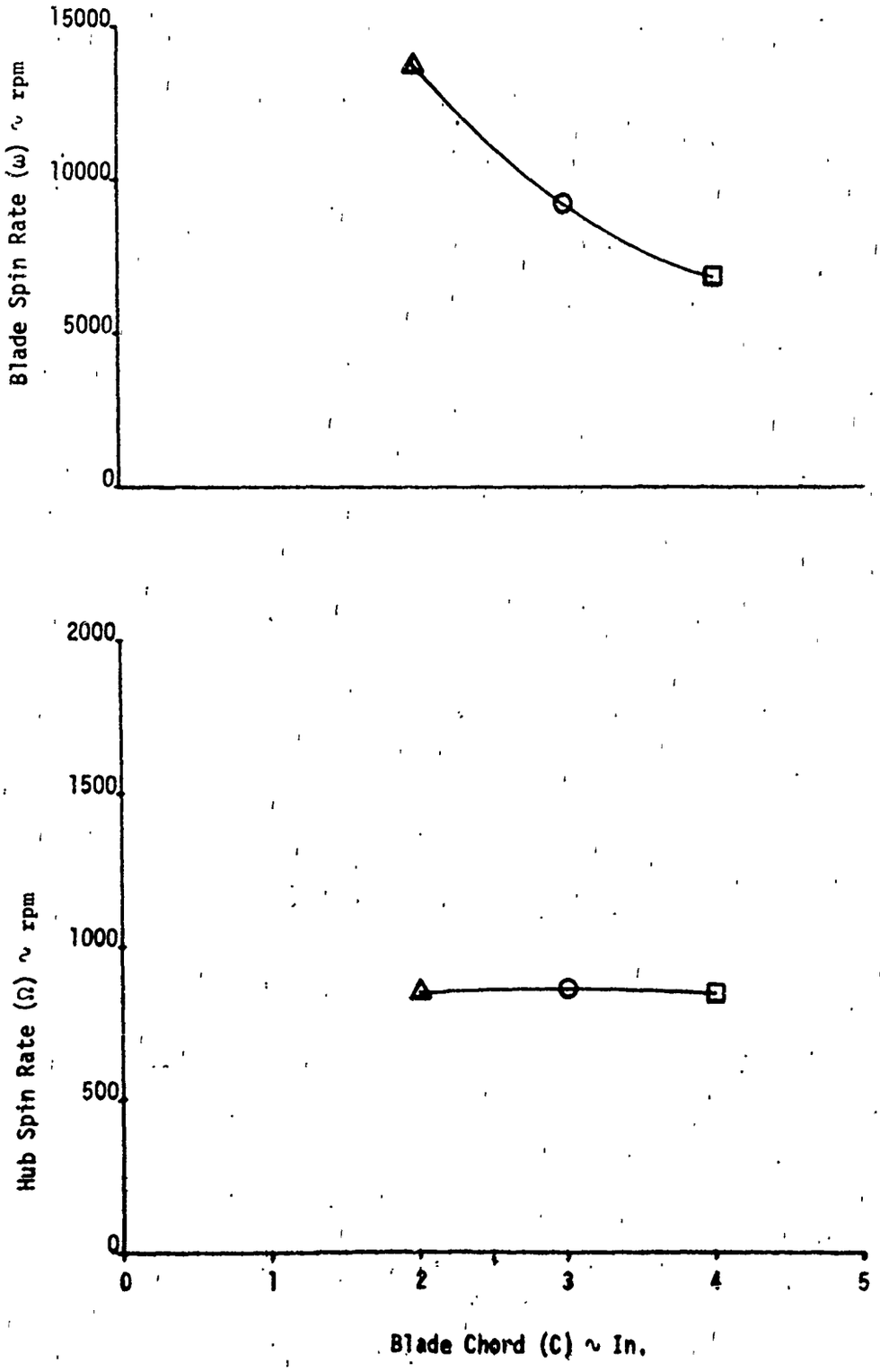

Figure 56. Effect of Blade Chord on Steady State Blade Spin Rate and Hub Spin Rate

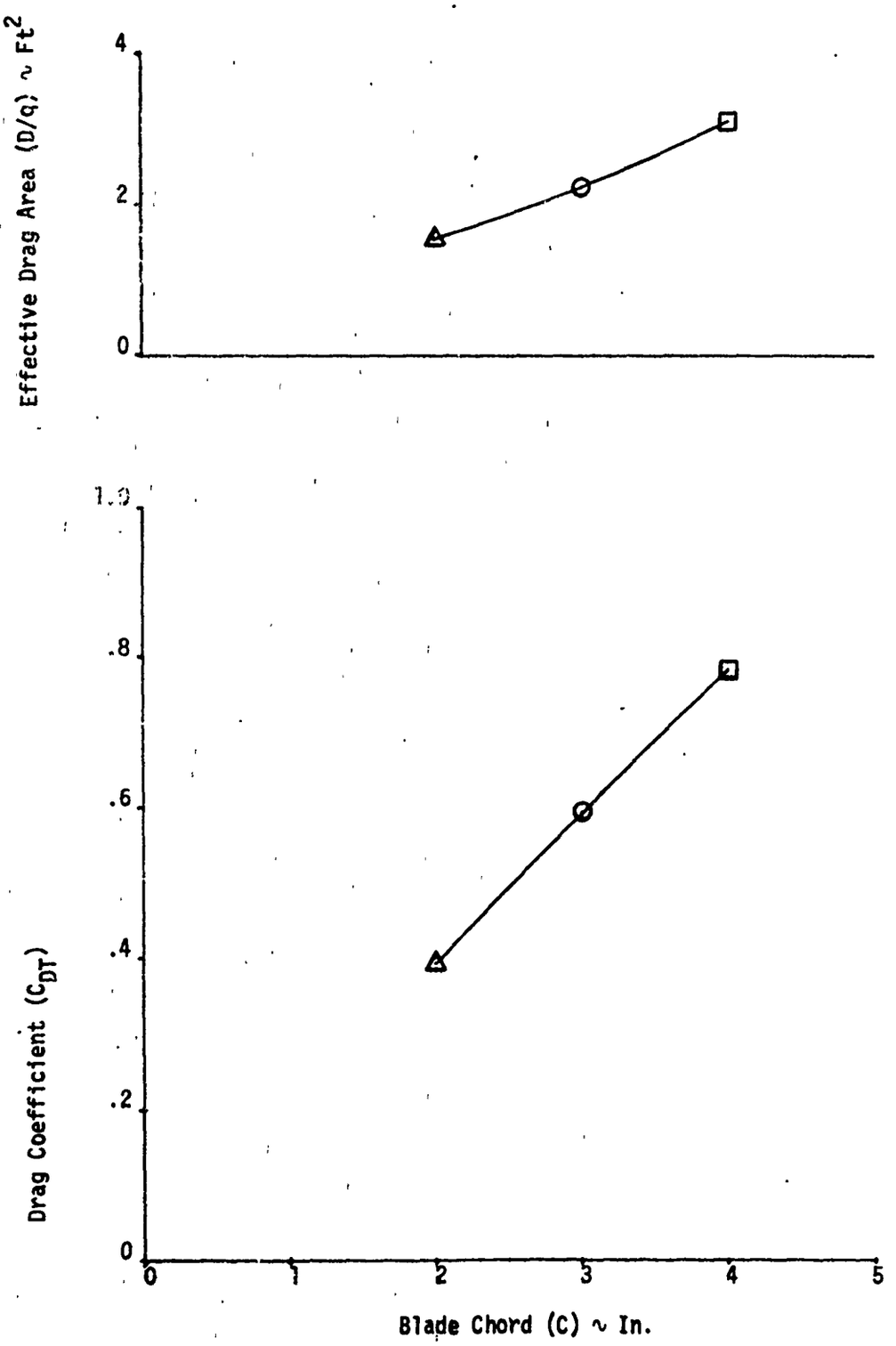

Figure 57. Effect of Blade Chord on Steady State Effective Drag Area and Drag Coefficient

$$\sigma = \frac{4\ell C}{\bar{S}}$$

where

$$\bar{S} = \pi \frac{(2\ell + .583)^2}{4} = \text{maximum swept area (blades at } \theta = 90°)$$

These data are contained in figures 58 through 61.

In effect, an increase in solidity factor gives the same results as an increase in the blade or chord length, as shown previously. However, it is interesting to note the linear nature of the drag coefficient with solidity factor. The nonlinear effects indicated can be attributed to the influence of the inertial terms (gyroscopic terms) that are present even at steady state conditions. It should be emphasized, however, that the interference factor K could be a function of the solidity factor, among other things, and could influence the shape of this curve.

C. Effect of Air Flow Conditions.

1. Effects of Free Stream Velocity.

The data showing the effects of free stream velocity are included in figures 62 through 65. Although the blade and hub spin rates increase linearly with increasing free stream velocity, the remaining terms are constant, including the blade-to-hub spin ratio.

2. Effects of Air Density.

The effects of air density are shown in figures 66 through 69. The densities investigated were half the nominal density that would correspond to an altitude of 20,000 feet and double the density that admittedly is not a realistic value for air but may have meaning for another fluid if Reynolds' number effects are not considered. The results are surprising in that the increased density results in a reduced steady state deployment angle, probably due to the large aerodynamic loads relative to the system inertial loads. This causes a slight increase in hub spin rate with increasing density, resulting in about the same effective drag area as for the lower density values. Since the frontal area is reduced slightly, the drag coefficient is constant with air density.

D. Effect of Autorotor Blade Aerodynamic Characteristics.

1. Linearized Aerodynamic Effect.

As described in section V, the aerodynamic characteristics of the autorotor blade are described as a function of the steady state tip speed ratio evaluated at zero yaw angle ($\hat{\omega}_{ss_0}$). This term not only describes the blades spin moment coefficient, but also its sectional lift and drag characteristics. As can be seen in figures 18 and 20, the aerodynamic coefficients are actually expressed by a quadratic function of the tip speed ratio. To simplify the expressions used in investigating the effects of the aerodynamic characteristics, the spin moment coefficients are expressed as a linear function of tip speed ratio, as shown in figure 70. This linearization makes it possible to understand the effects of varying the aerodynamic coefficients in a general manner without complicating the results with second order effects. The difference in the steady state performance between the linear and nonlinear nominal case is small, as shown in figures 70 through 73. This is due to the relative symmetry and the similar slope values of the coefficient curves in the vicinity of the steady state tip speed ratio. Inspection of the computer output for runs 1 and 12 in appendix C shows that the effects across the blade span are similar. The linear case, with its decreased lift coefficient in the underspin region, results in a slightly lower hub spin rate and lift

Sym	Run	Blade Length (ℓ) ~ In.	Blade Chord (C) ~ In.	Solidity Factor (σ)
○	1	10	3	.2095
◇	4	7	3	.2425
▽	5	13	3	.1825
△	6	10	2	.1395
□	7	10	4	.2790

Note: ——— Indicates Constant Blade Length (ℓ = 10 In.)

— — — — Indicates Constant Blade Chord (C = 3 In.)

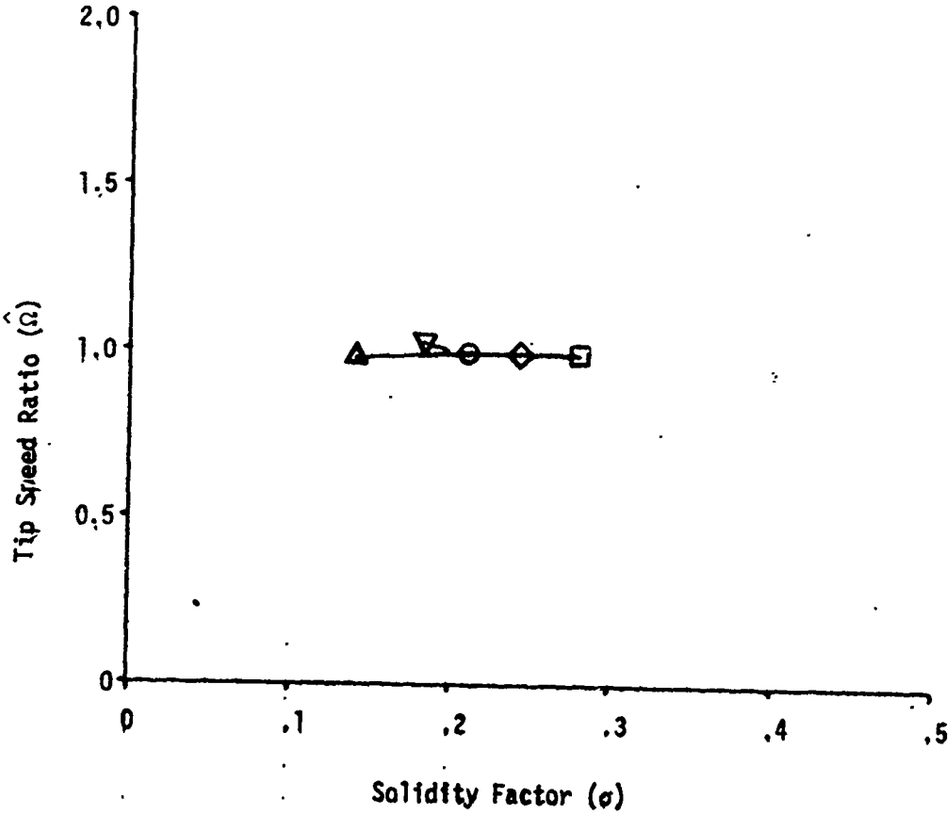

Figure 58. Effect of Solidity Factor on Steady State Tip Speed Ratio

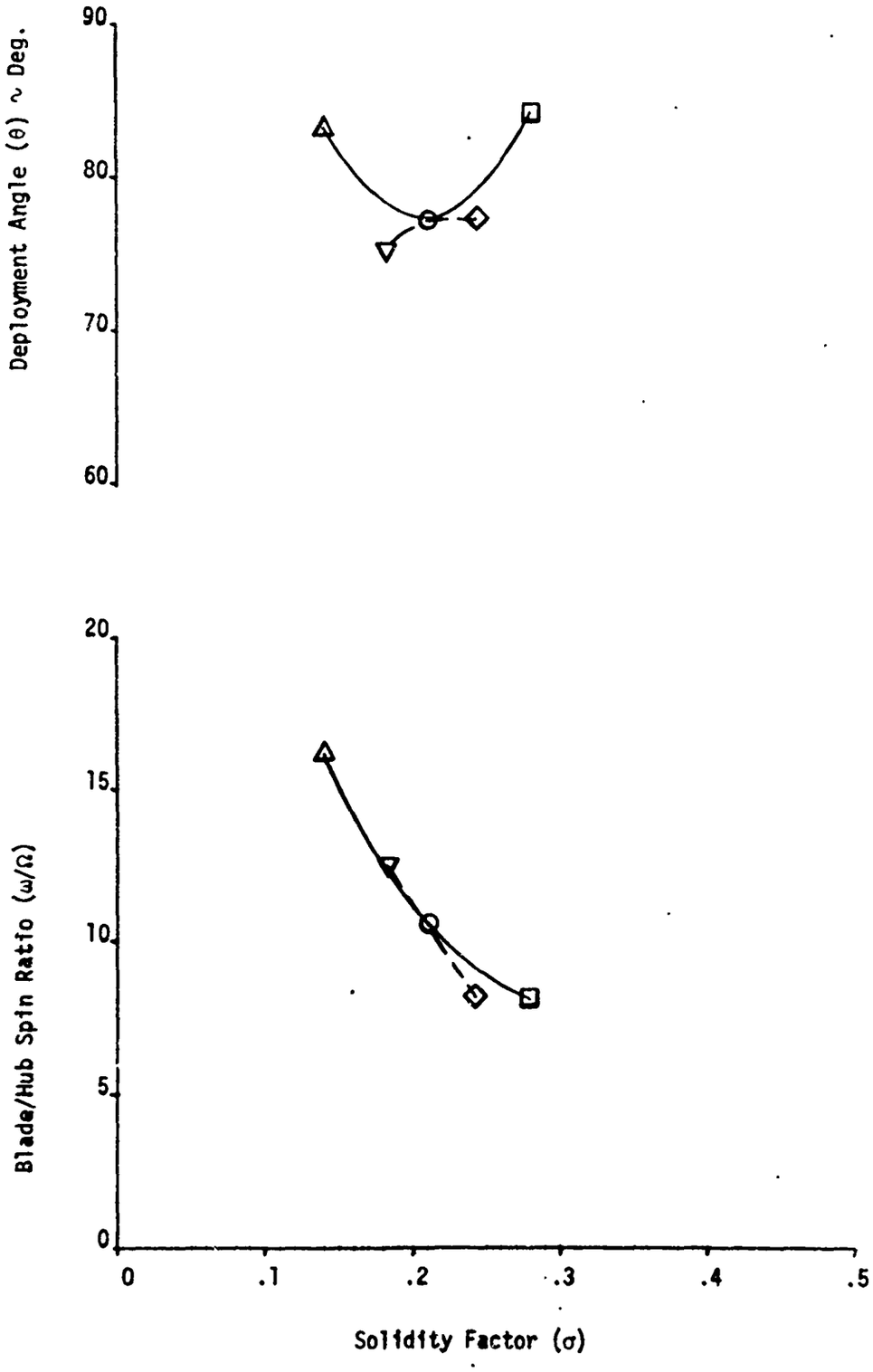

Figure 59. Effect of Solidity Factor on Steady State Deployment Angle and Blade/Hub Spin Ratio

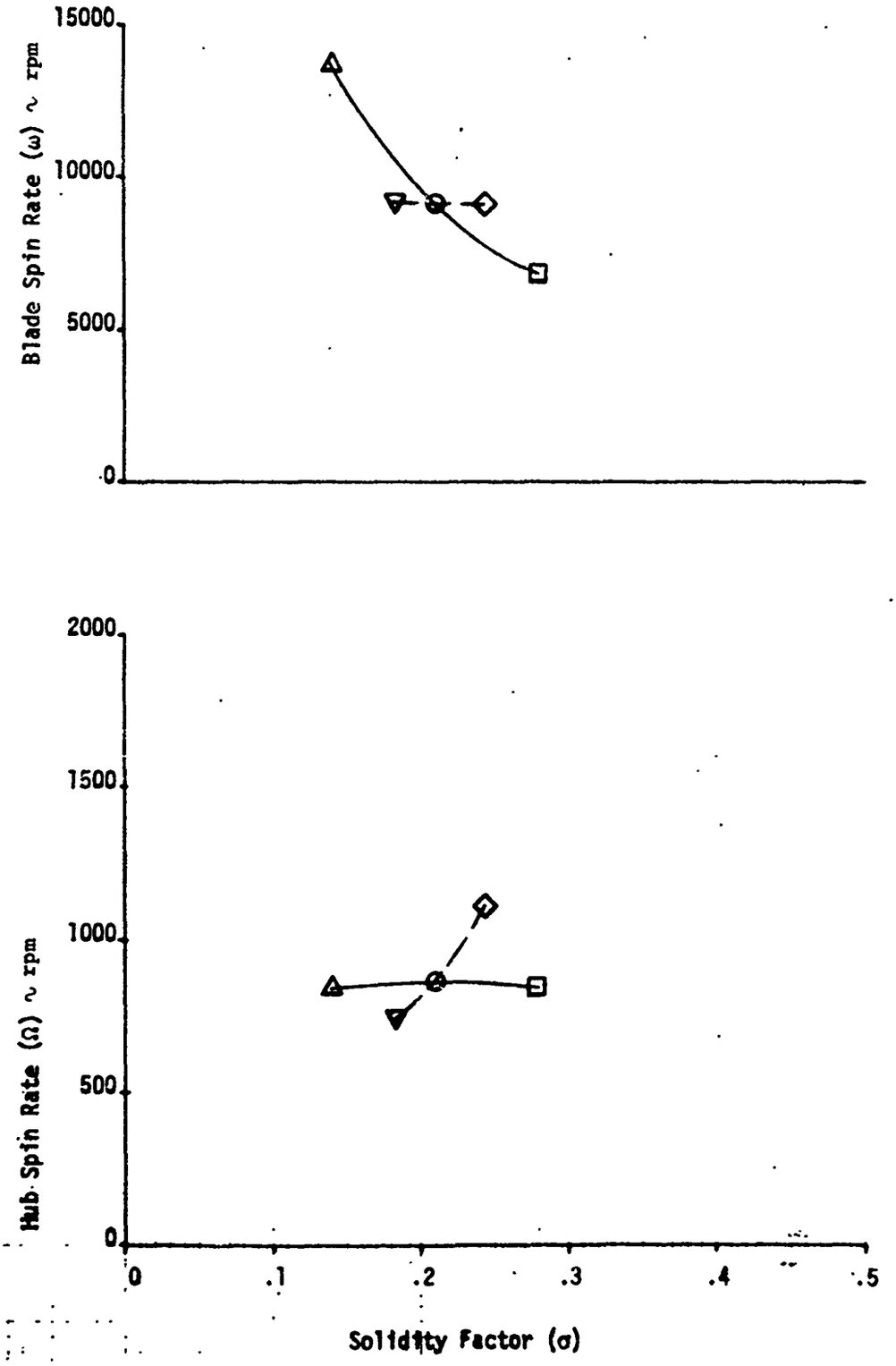

Figure 60. Effect of Solidity Factor on Steady State Blade Spin Rate and Hub Spin Rate

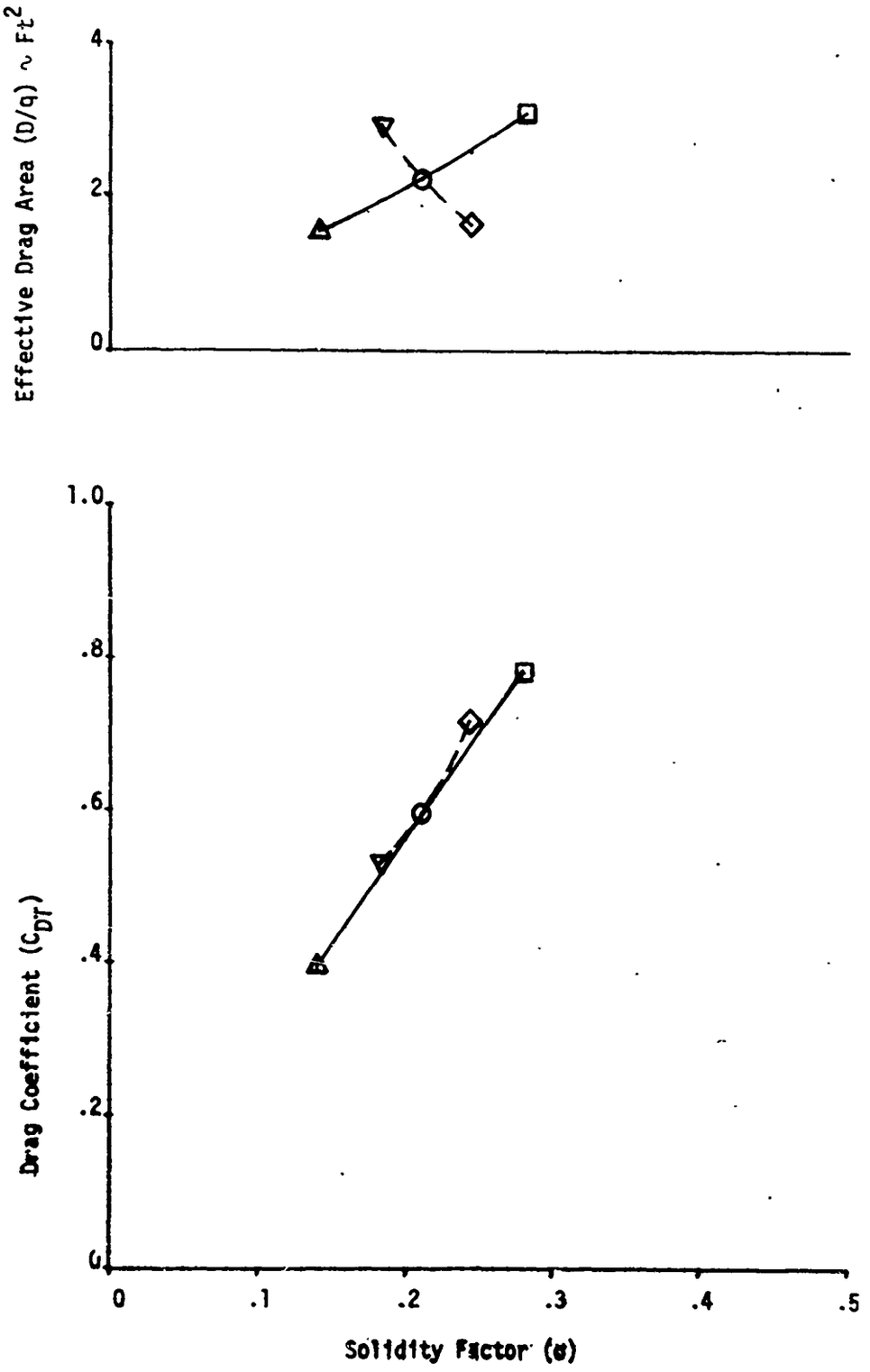

Figure 61. Effect of Solidity Factor on Steady State Effective Drag Area and Drag Coefficient

Sym	Run	Free Stream Velocity (V_∞) ~ Ft/Sec
△	8	50
○	1	100
□	9	200

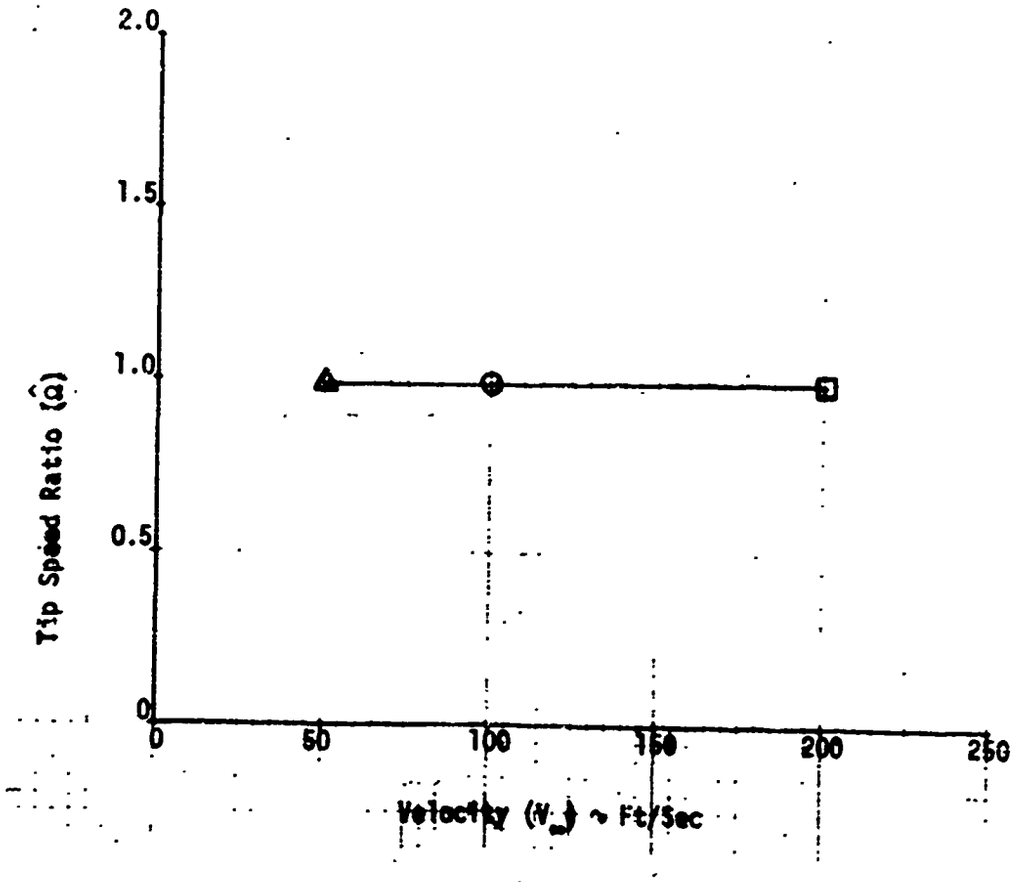

Figure 62. Effect of Free Stream Velocity on Steady State Tip Speed Ratio

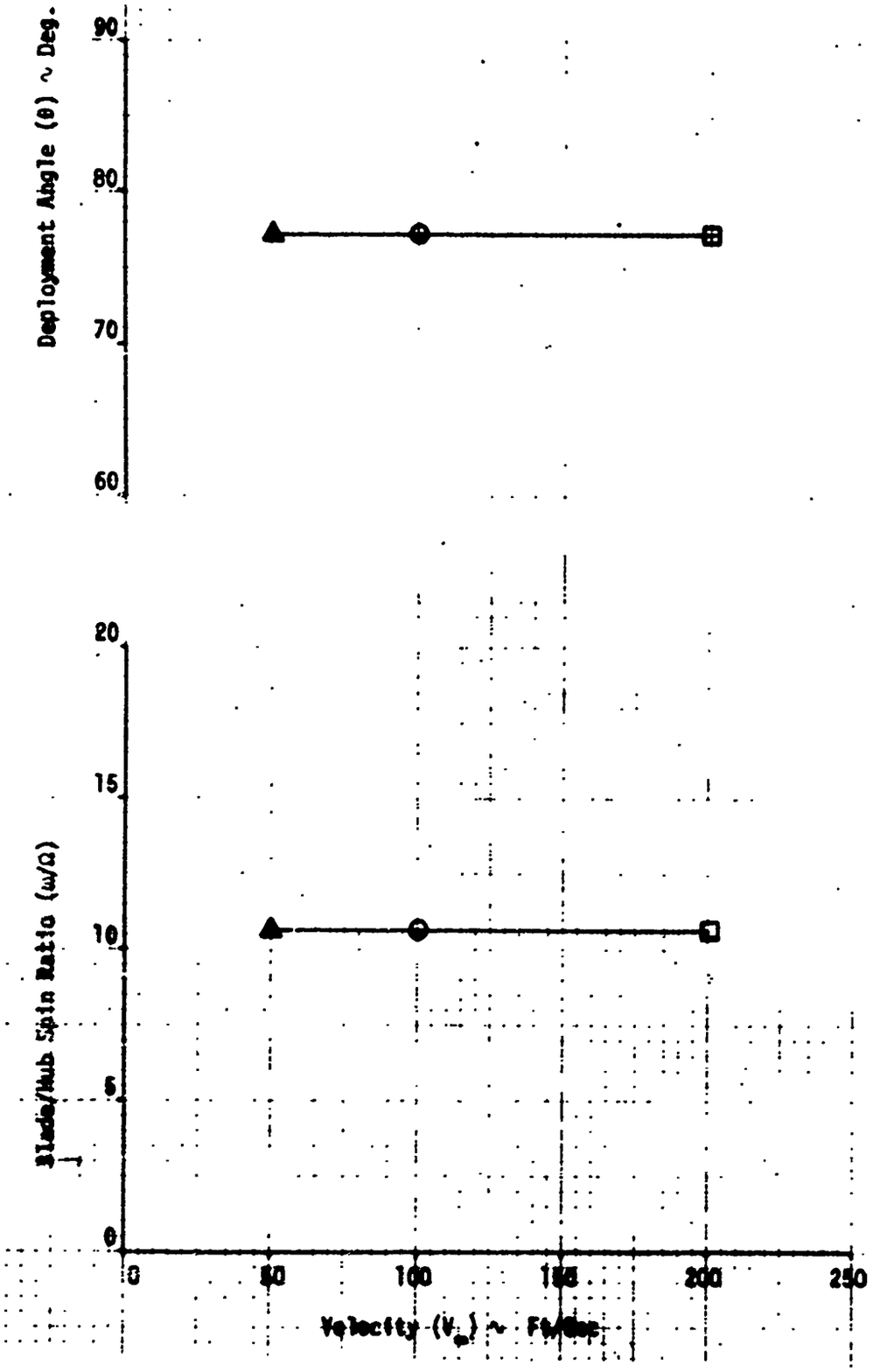

Figure 63. Effect of Free Stream Velocity on Steady State Deployment Angle and Blade/Hub Spin Ratio

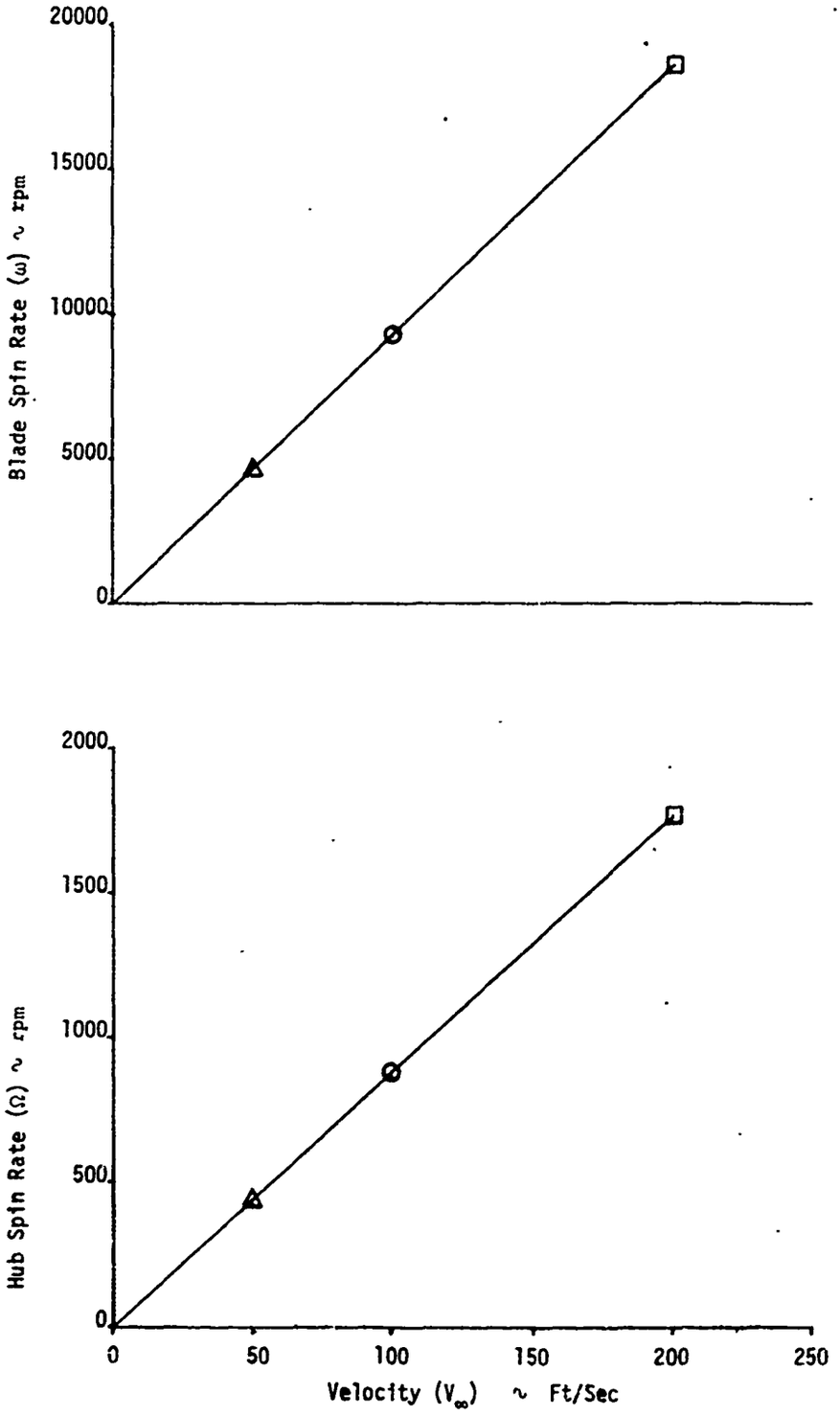

Figure 64. Effect of Free Stream Velocity on Steady State Blade Spin Rate and Hub Spin Rate

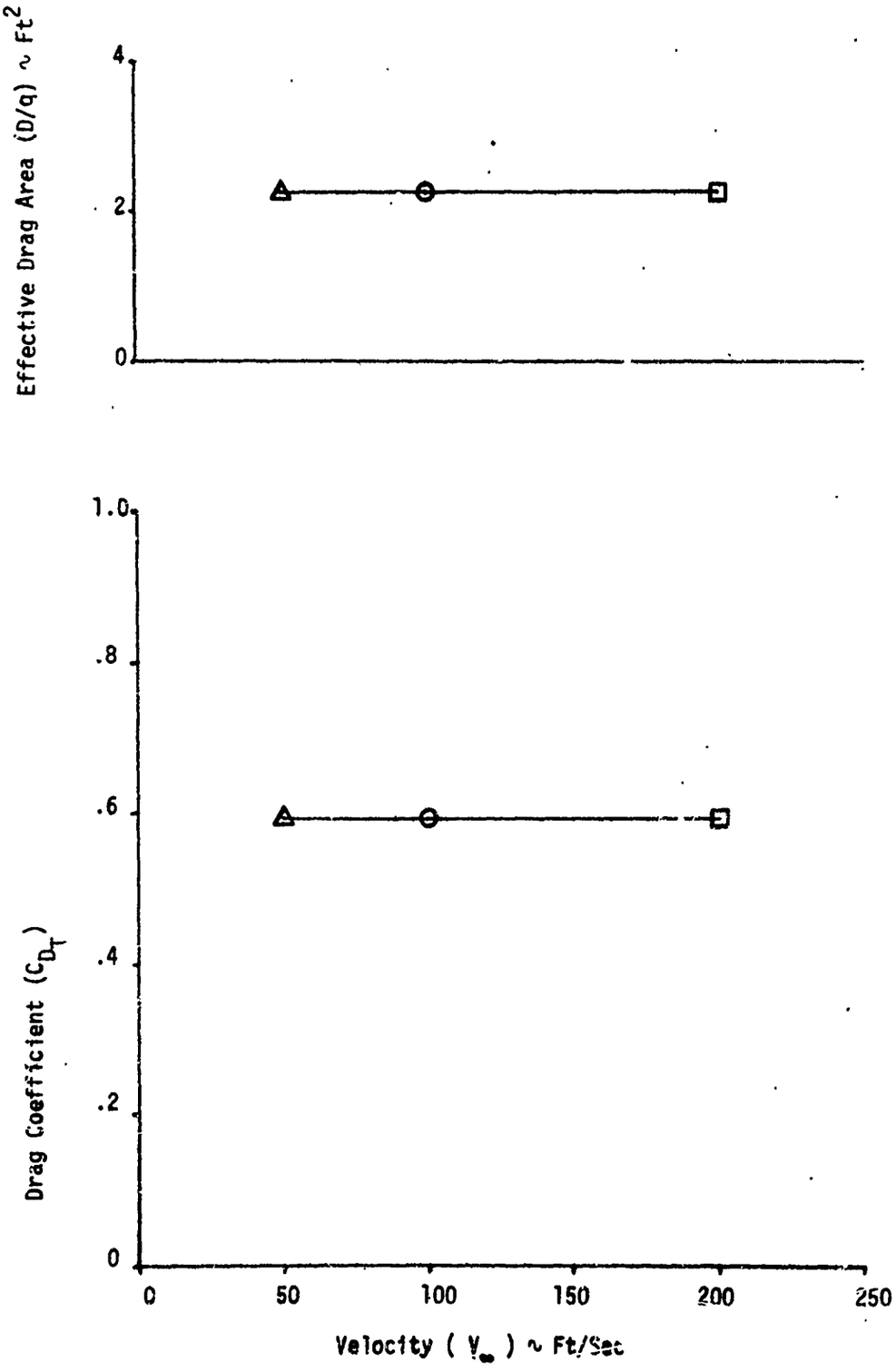

Figure 65. Effect of Free Stream Velocity on Steady State Effective Drag Area and Drag Coefficient

Sym	Run	Air Density (ρ) ∿ Slug/Ft^3
△	10	.001190
○	1	.002377
□	11	.004760

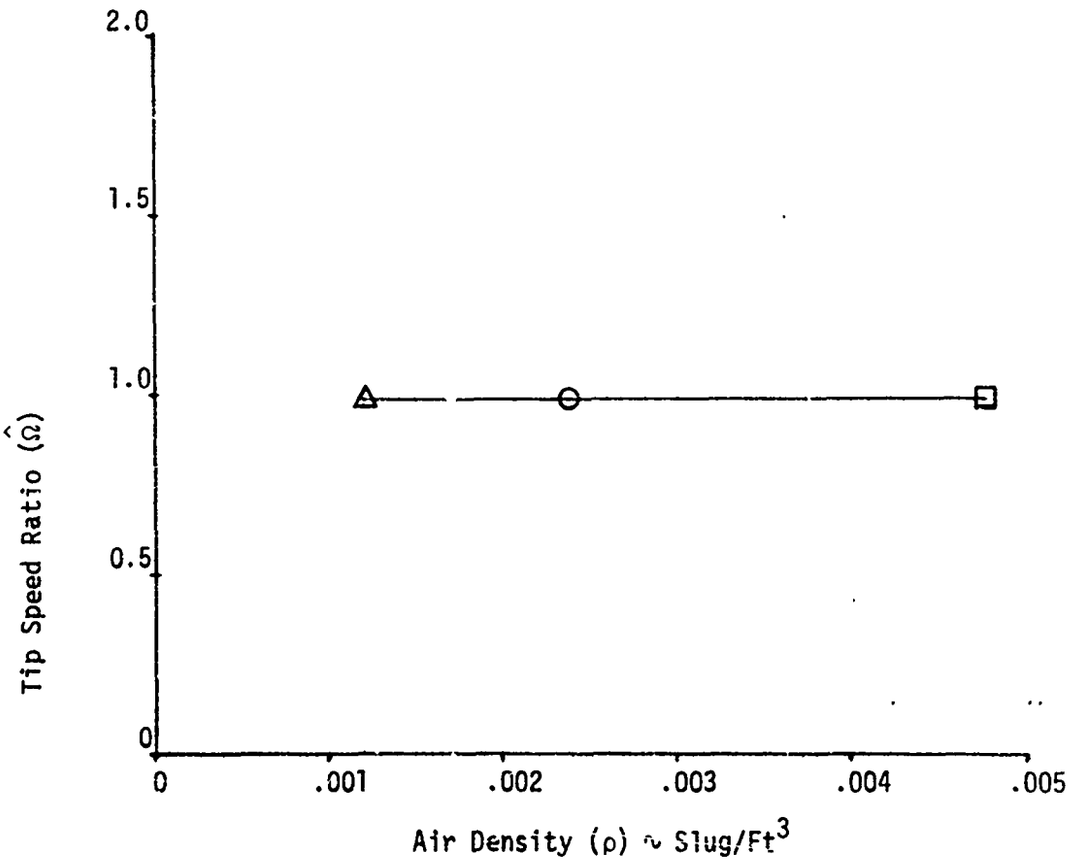

Figure 66. Effect of Air Density on Steady State Tip Speed Ratio

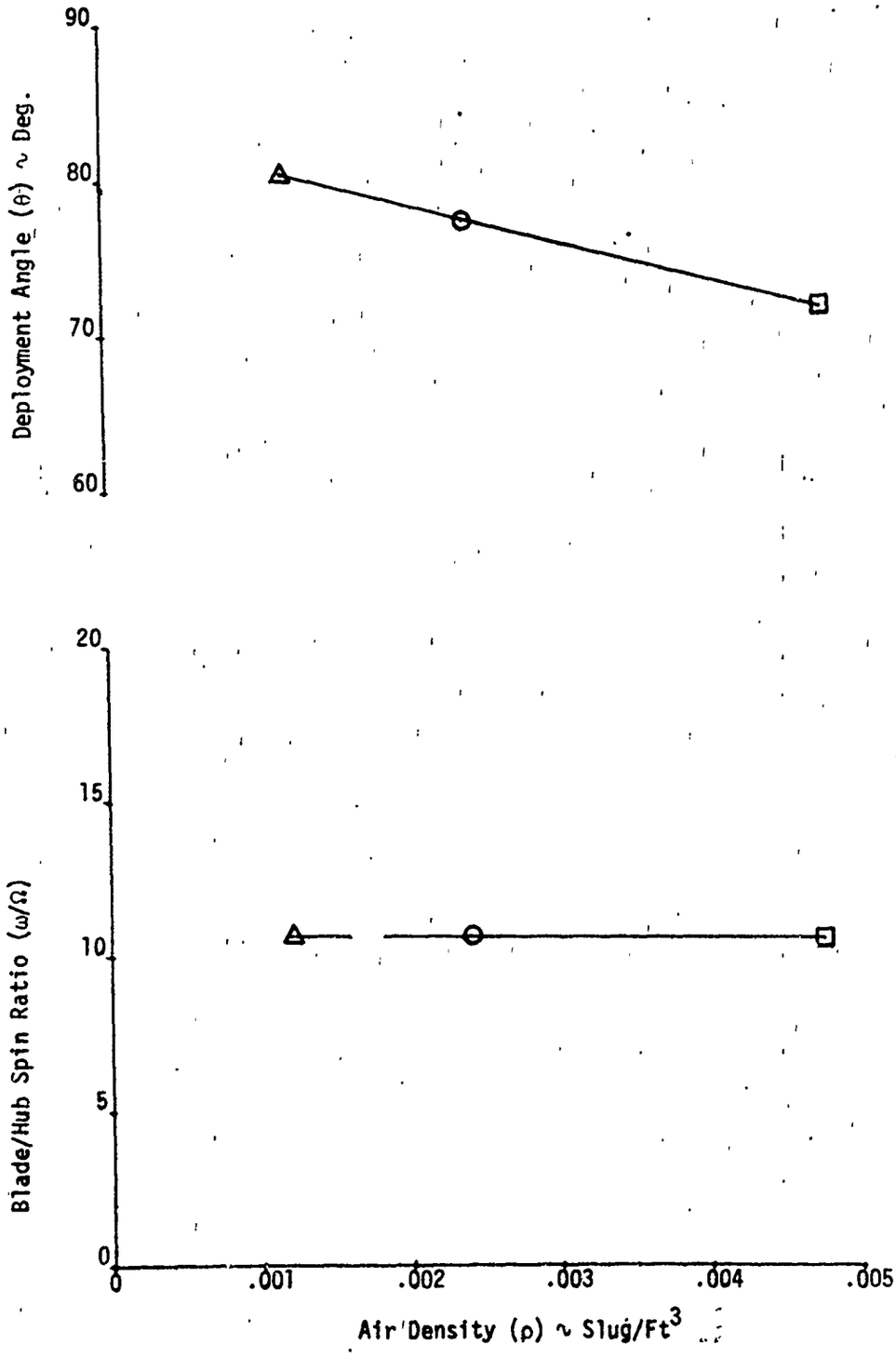

Figure 67. Effect of Air Density on Steady State Deployment Angle and Blade/Hub Spin Ratio

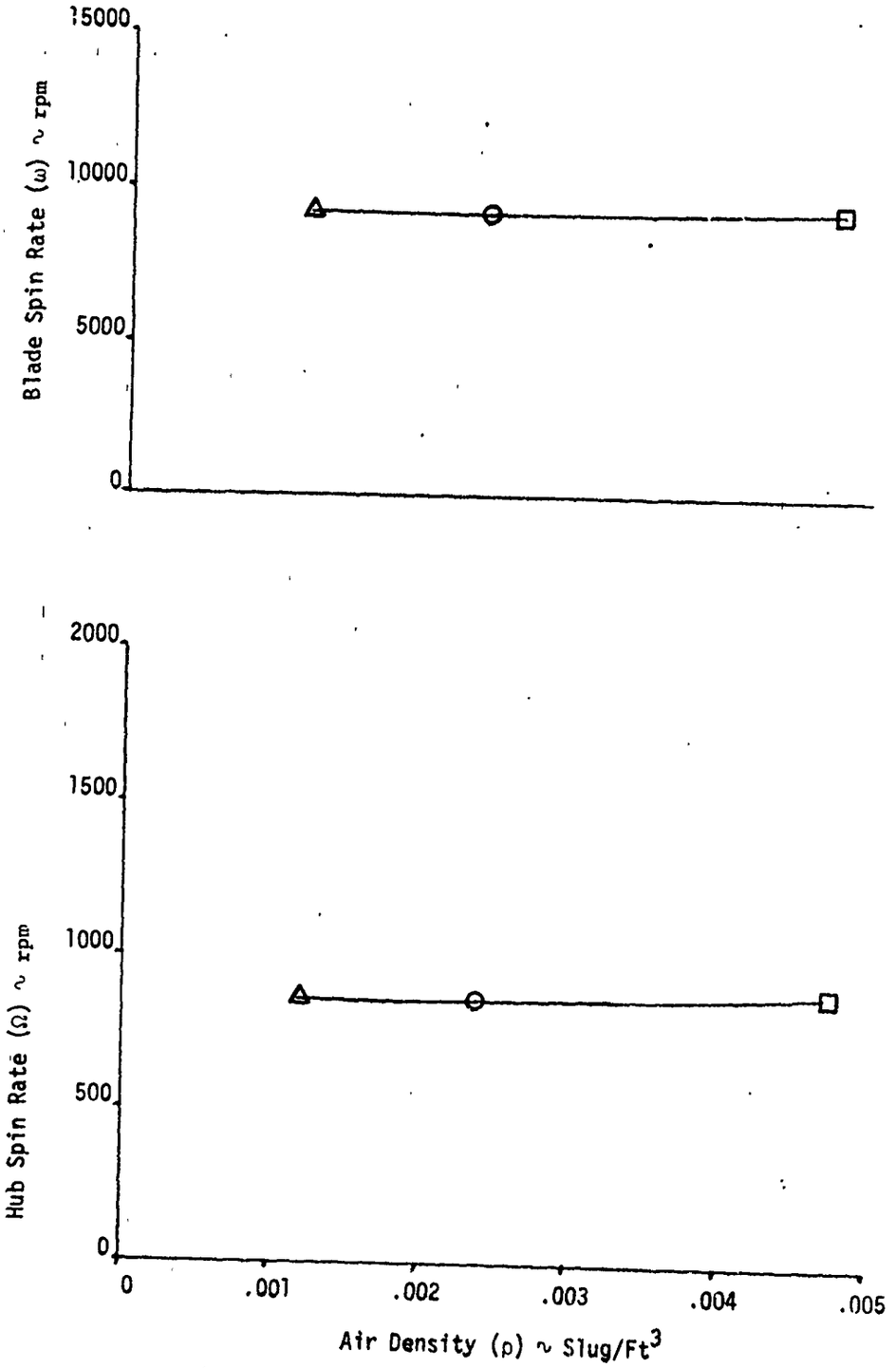

Figure 68. Effect of Air Density on Steady State Blade Spin Rate and Hub Spin Rate

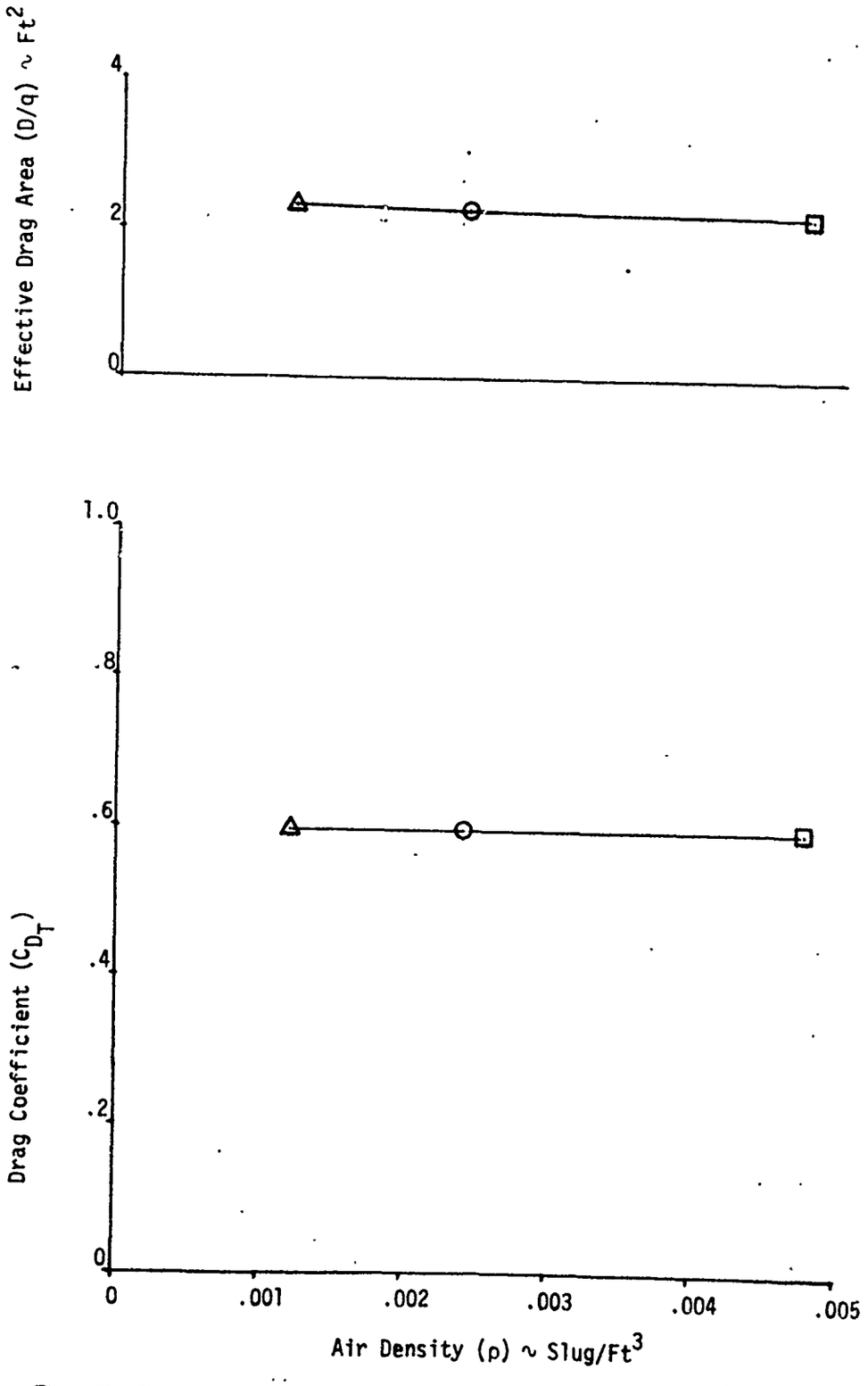

Figure 69. Effect of Air Density on Steady State Effective Drag Area and Drag Coefficient

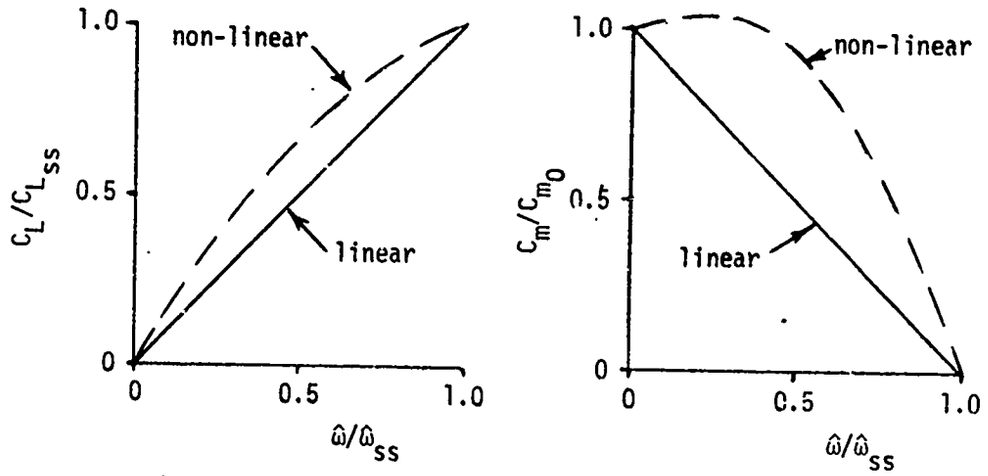

Sym	Run	C_{L_1}	C_{L_2}	C_{m_1}	C_{m_2}	ω_{ss_o}	
△	13	1.0	0.	-.20	0.	0.75	} Linear Coefficients
○	12	↓	↓	↓	↓	1.00	
□	14					1.25	
×	1	1.7143	-.7143	.15	-.35	1.00	Non-Linear Coefficients

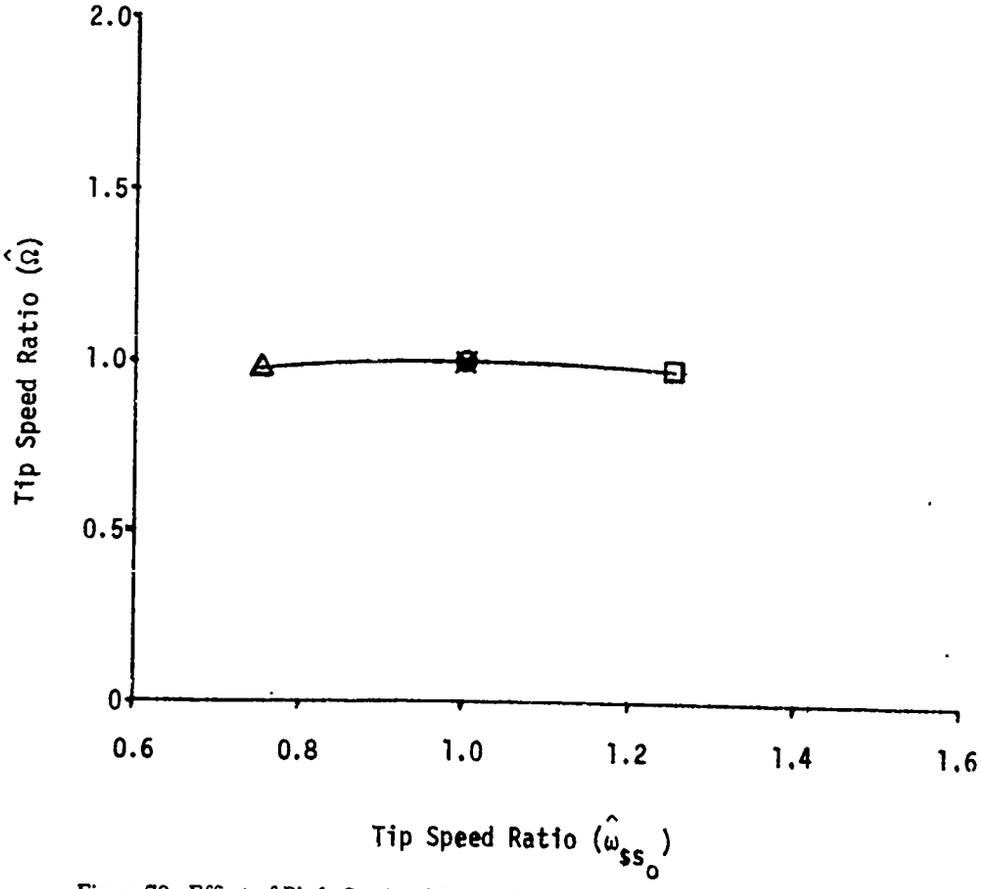

Figure 70. Effect of Blade Sectional Steady State Tip Speed Ratio on Steady State Tip Speed Ratio

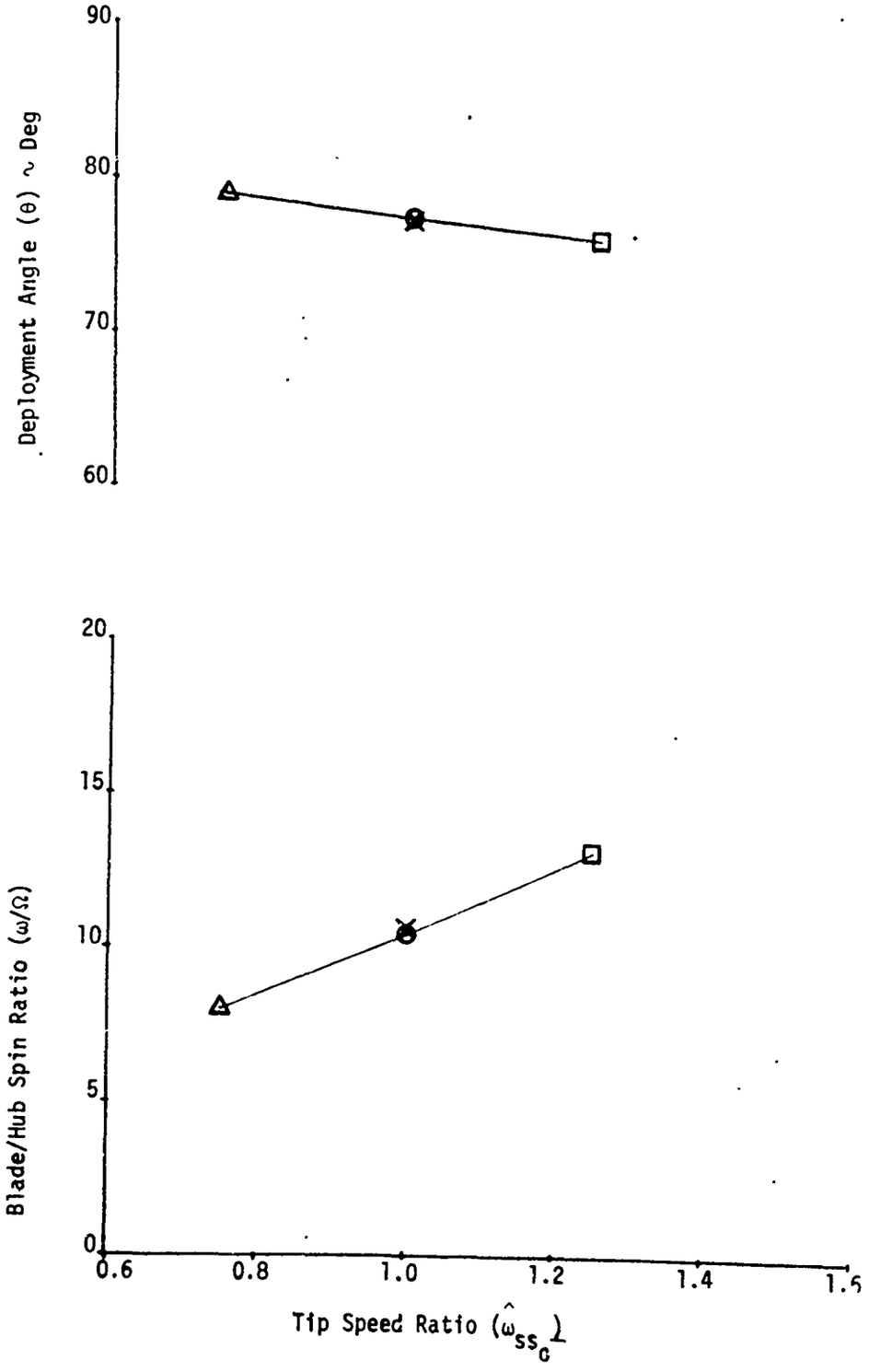

Figure 71. Effect of Blade Sectional Steady State Tip Speed Ratio on Steady State Deployment Angle and Blade/Hub Spin Ratio

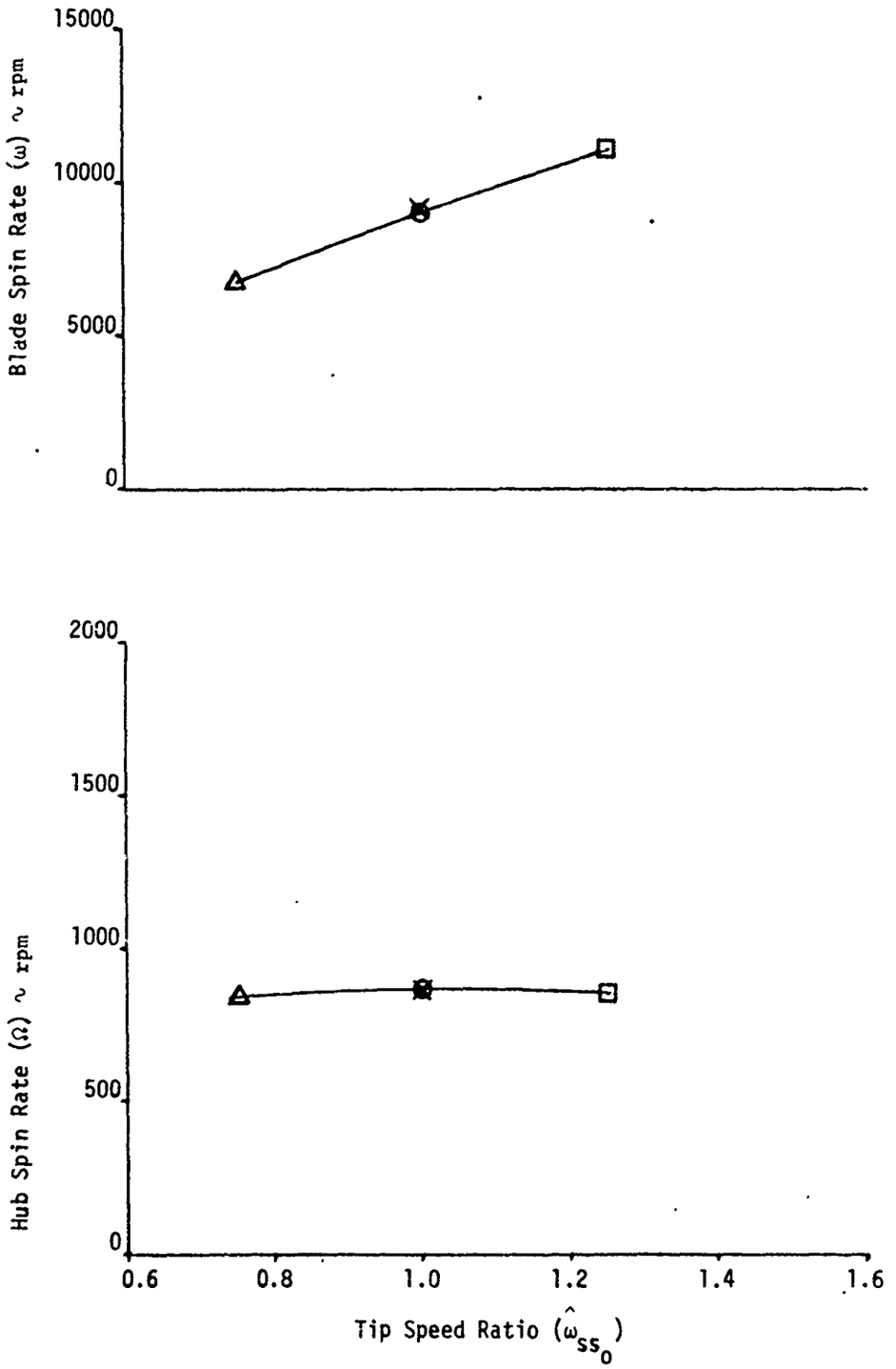

Figure 72. Effect of Blade Sectional Steady State Tip Speed Ratio on Steady State Blade Spin Rate and Hub Spin Rate

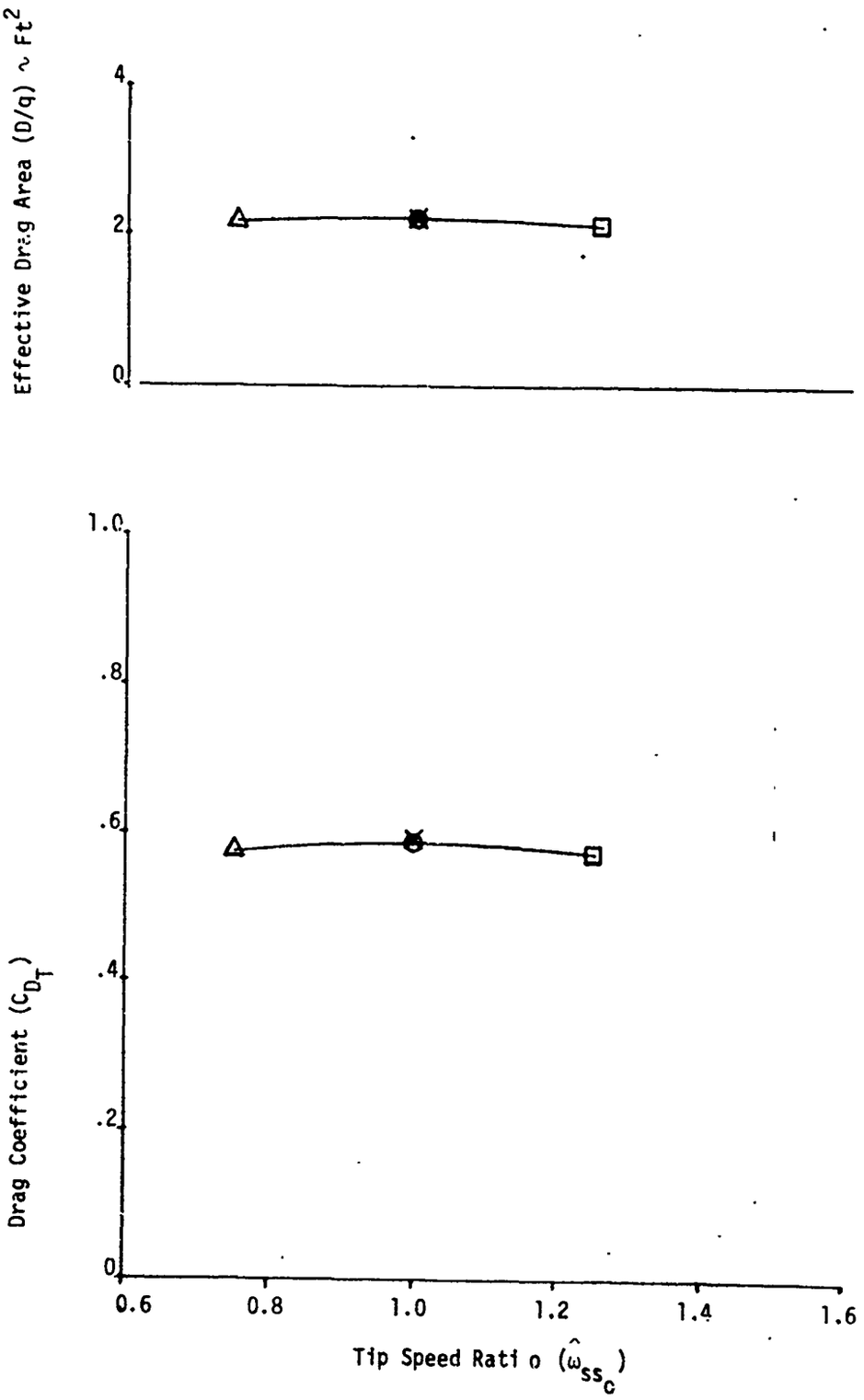

Figure 73. Effect of Blade Sectional Steady State Tip Speed Ratio on Steady State Effective Drag Area and Drag Coefficient

coefficient. The reduced spin moment coefficient of the linear case results in a slightly reduced blade spin rate.

2. Effects of Blade Steady State Tip Speel Ratio ($\hat{\omega}_{ss_0}$).

The effects of the blade sectional steady state tip speed ratio are included in figures 70 through 73. The lift coefficient is assumed to be directly proportional to the tip speed ratio, as shown in figure 70.

The final system blade spin rate is proportional to the blades section tip speed ratio. All other terms remain constant except the deployment angle, whose differences in values reflect the effect of the gyroscopic term that is proportional to the blade spin rate.

3. Effects of Blade Sectional Maximum Steady State Lift Coefficient.

The effects of the blade sectional lift coefficient are shown by varying the maximum lift coefficient value. As before, the lift coefficient is expressed as a linear function of the blade tip speed ratio. The performance data in figures 74 through 77 show that increasing the maximum lift coefficient value results in increasing hub rotation. The increased hub rotation results in a higher blade spin rate and a slightly larger deployment angle; the blade-to-hub spin rate ratio, however, decreases. The effect of increased hub spin rate and lift coefficient values results in increased system drag and drag coefficient. The hub tip speed ratio increases with increasing lift coefficient.

4. Effects of Blade Sectional Maximum Steady State Drag Coefficient.

The effects of the blade sectional drag coefficient are shown in figures 78 through 81. Increasing the sectional drag coefficient has the most marked effect of decreasing the hub spin rate and, consequently, the hub tip speed ratio.

The consequence of this effect is to decrease the blade spin rate, increase the blade to hub spin ratio, and decrease the deployment angle. The interesting result of all of these effects is that an increase in the drag coefficient of the blade results in a slight decrease in the total system drag as shown in the effective drag area and drag coefficient. The change in system drag is small compared to the relatively large change in the drag coefficient value.

5. Effects of Blade Steady State Sectional Lift to Drag Ratio.

The effects of the lift and drag coefficient can also be expressed as the ratio of the lift coefficient to the drag coefficient (i.e., the lift-to-drag ratio). These cases are shown in figures 82 through 85. Essentially increasing the lift-to-drag ratio results in an increased drag for the system. Whether the increased lift-to-drag ratio results from increasing the lift or decreasing the drag, the basic result is to increase the hub spin rate (i.e., hub tip speed ratio) with the resultant increased dynamic pressure acting on the blade. The value of the lift coefficient results in a much more pronounced effect than the value of the drag coefficient for the same lift-to-drag ratio because of the effect of the value of the lift coefficient in addition to the increased hub spin rate.

E. Aerodynamic Effects Distribution Over the Blade.

Figure 86 is a graphic representation of the manner in which the various aerodynamic terms vary at different spanwise locations (stations) on the blade. The example shown is the nominal case at steady state conditions. The velocity at each station is the vector sum of the free stream velocity and the velocity caused the blade spin about the hub. Thus, the velocity and the angle of attack increases from root to tip. The increased local velocity results in an increased

Sym	Run	C_{L_1}	C_{L_2}	C_{m_1}	C_{m_2}	$\hat{\omega}_{ss_o}$	$C_{L_{ss_o}}$
△	15	1.0	0.	-.2	0.	1.0	1.25
○	12	↓	↓	↓	↓	↓	1.55
□	16						1.75

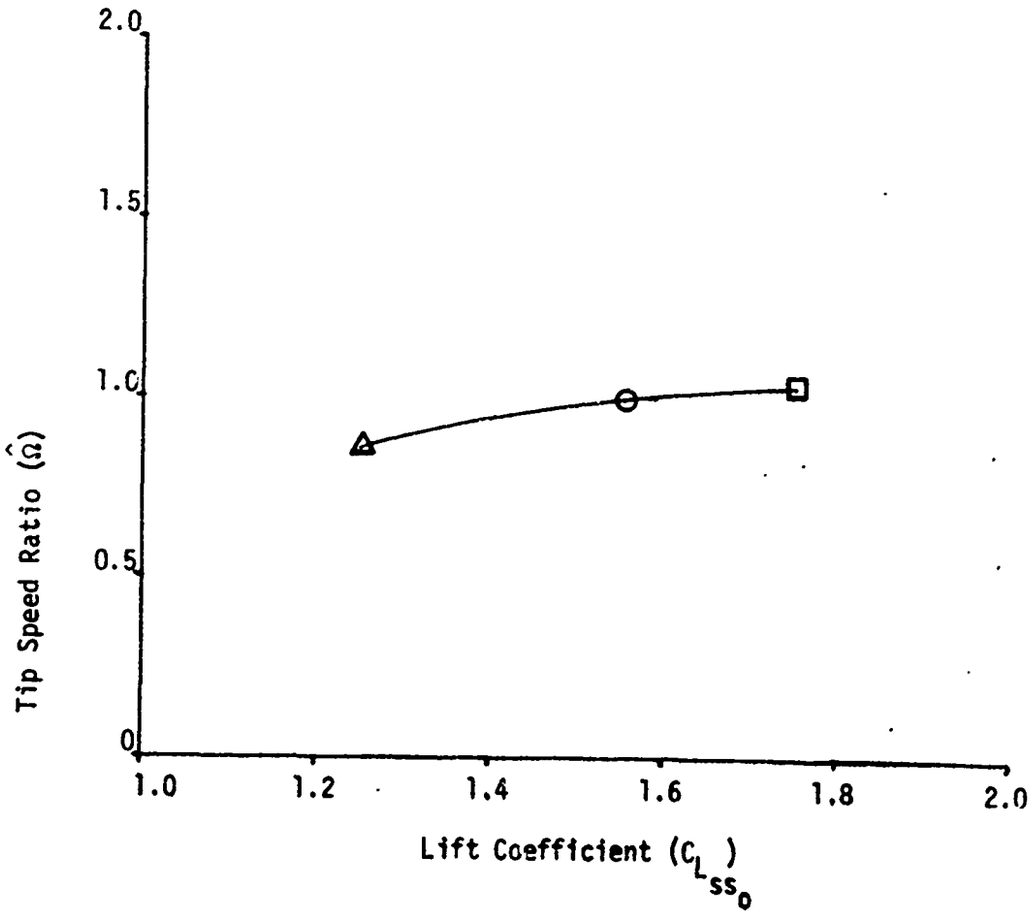

Figure 74. Effect of Blade Sectional Maximum Lift Coefficient on Steady State Tip Speed Ratio

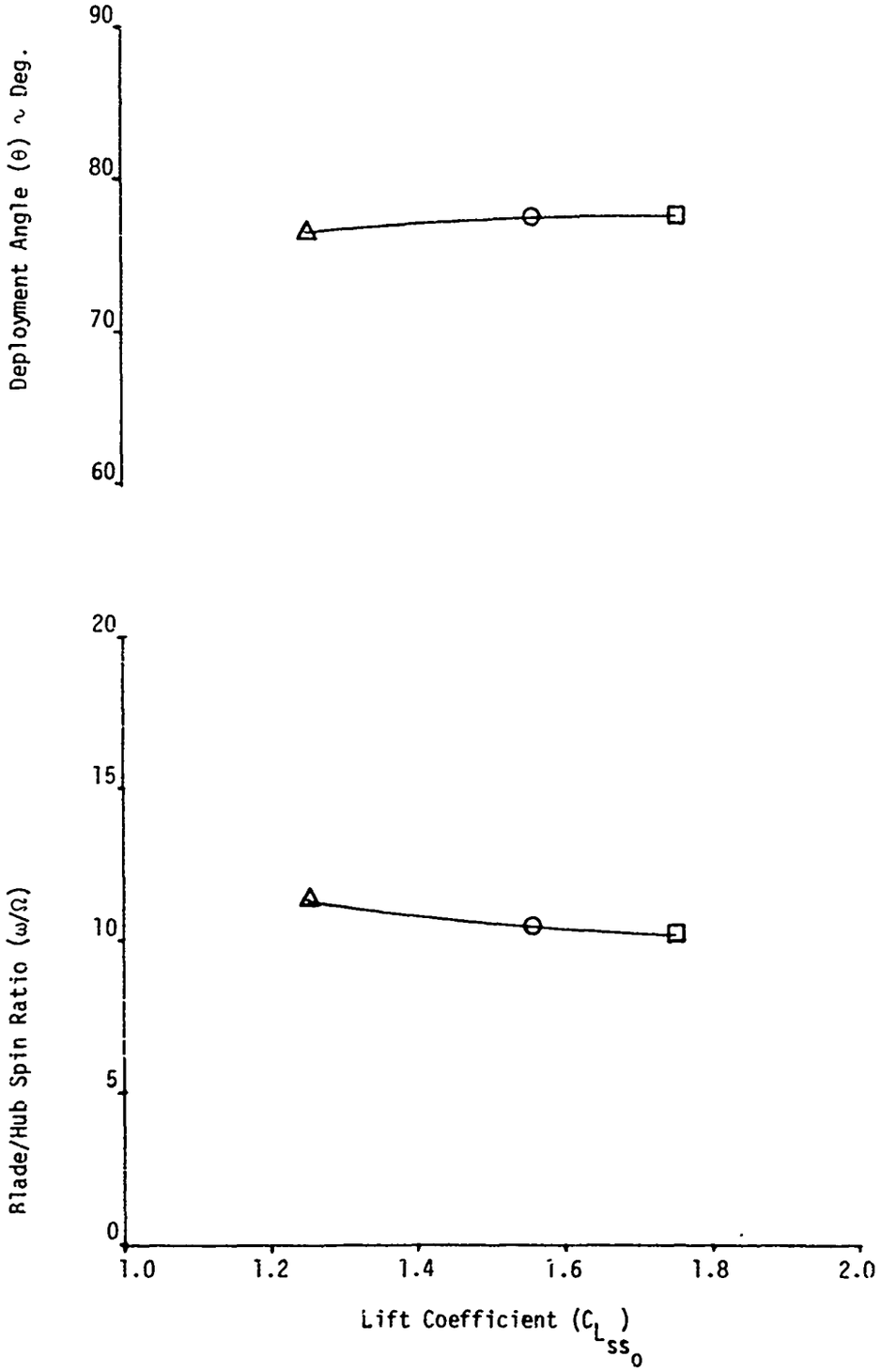

Figure 75. Effect of Blade Sectional Maximum Lift Coefficient on Steady State Deployment Angle and Blade/Hub Spin Ratio

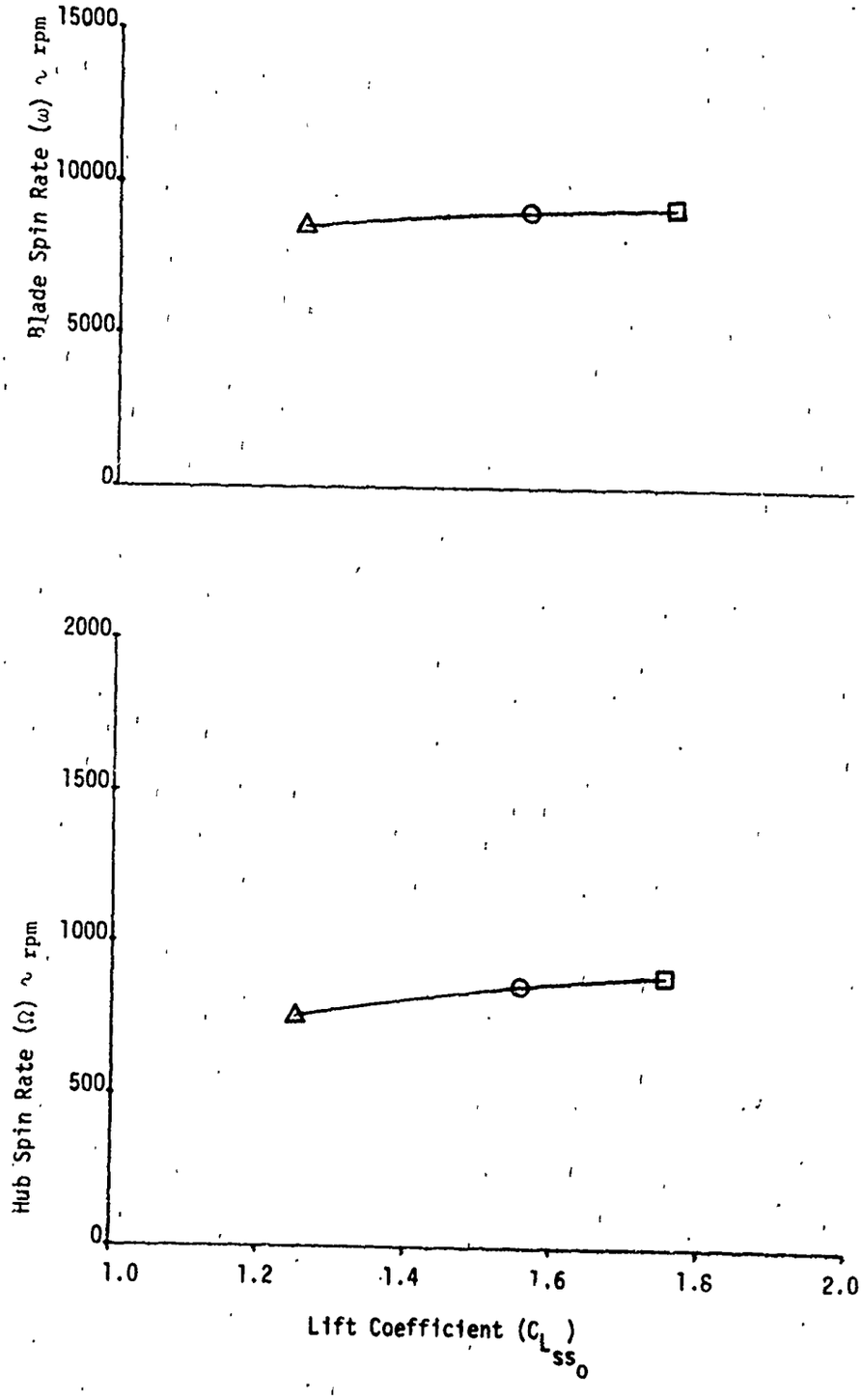

Figure 76. Effect of Blade Sectional Maximum Lift Coefficient on Steady State Blade Spin Rate and Hub Spin Rate

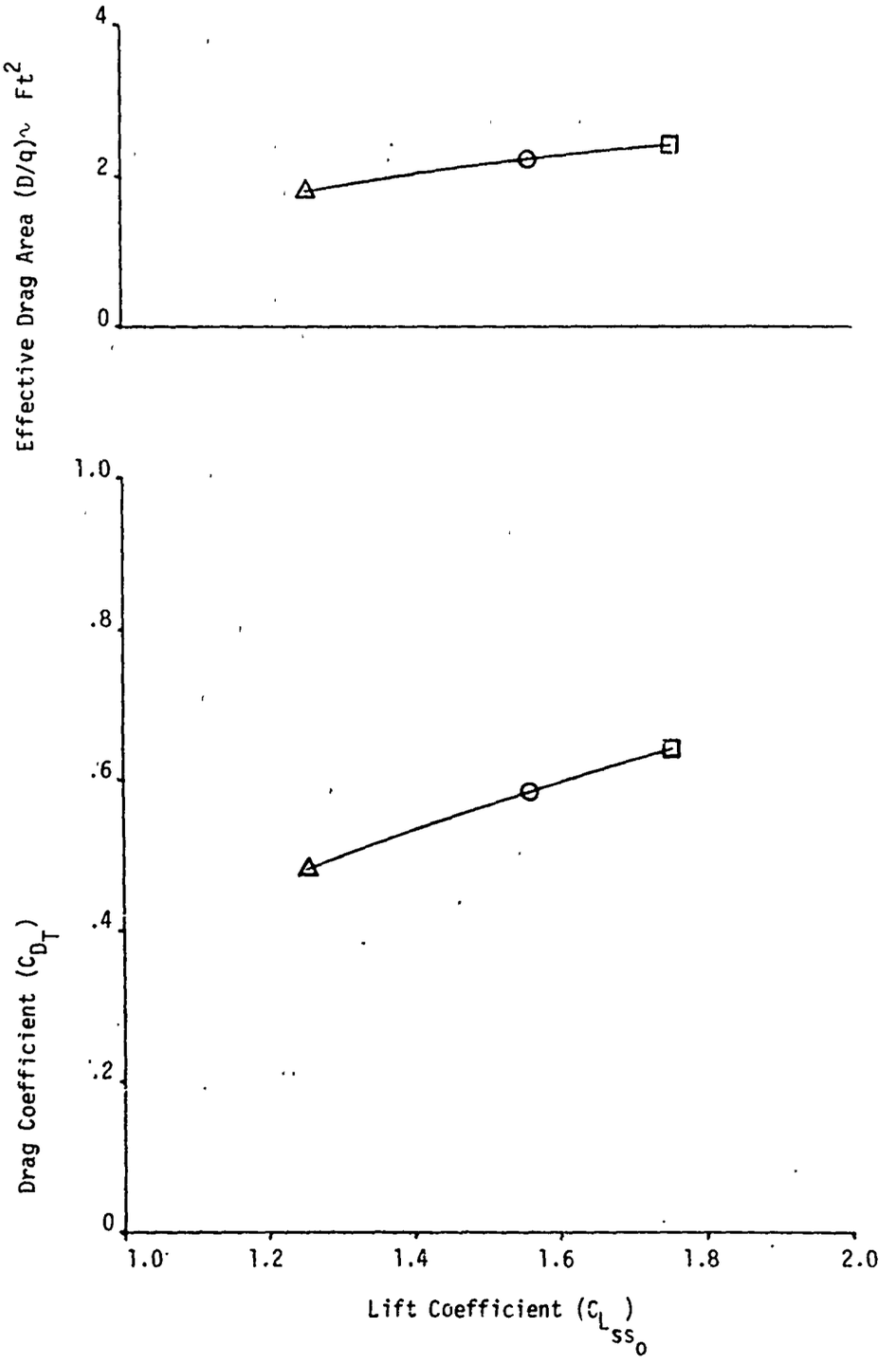

Figure 77. Effect of Blade Sectional Maximum Lift Coefficient on Steady State Effective Drag Area and Drag Coefficient

Sym	Run	C_{L_1}	C_{L_2}	C_{m_1}	C_{m_2}	$\hat{\omega}_{ss_o}$	$C_{D_{ss_o}}$
△	17	1.0	0.	-.2	0.	1.0	1.0
○	12	↓	↓	↓	↓	↓	1.25
□	18	↓	↓	↓	↓	↓	1.50

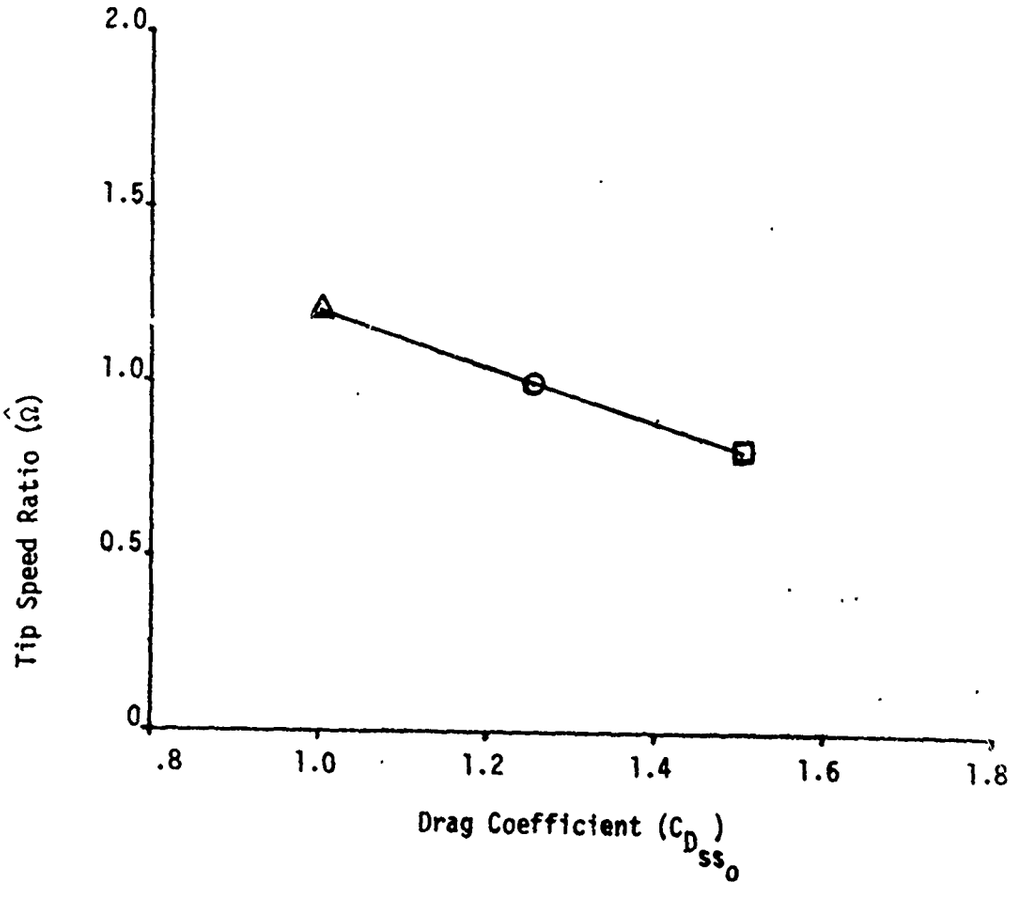

Figure 78. Effect of Blade Sectional Maximum Drag Coefficient on Steady State Tip Speed Ratio

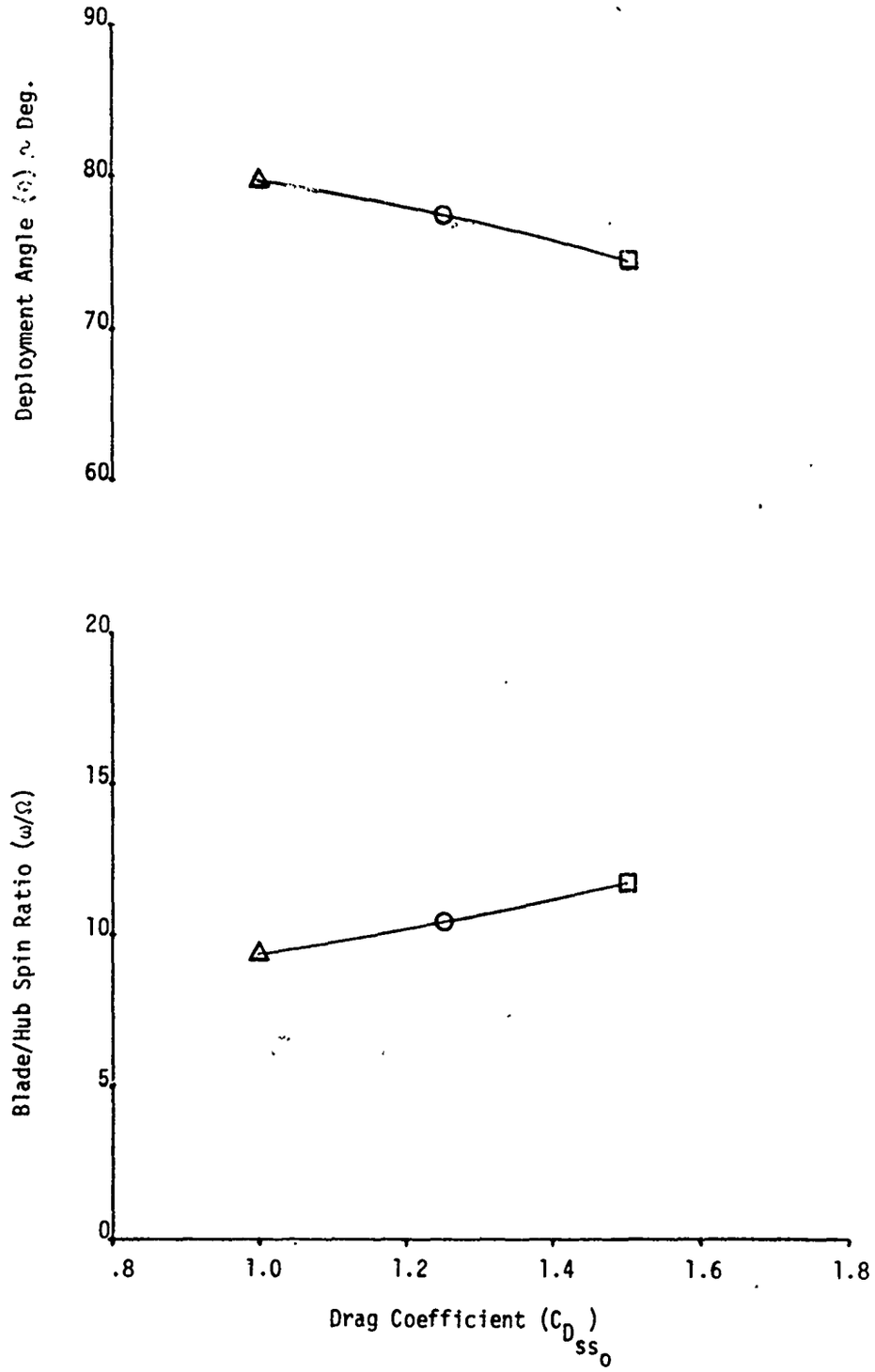

Figure 79. Effect of Blade Sectional Maximum Drag Coefficient on Steady State Deployment Angle and Blade/Hub Spin Ratio

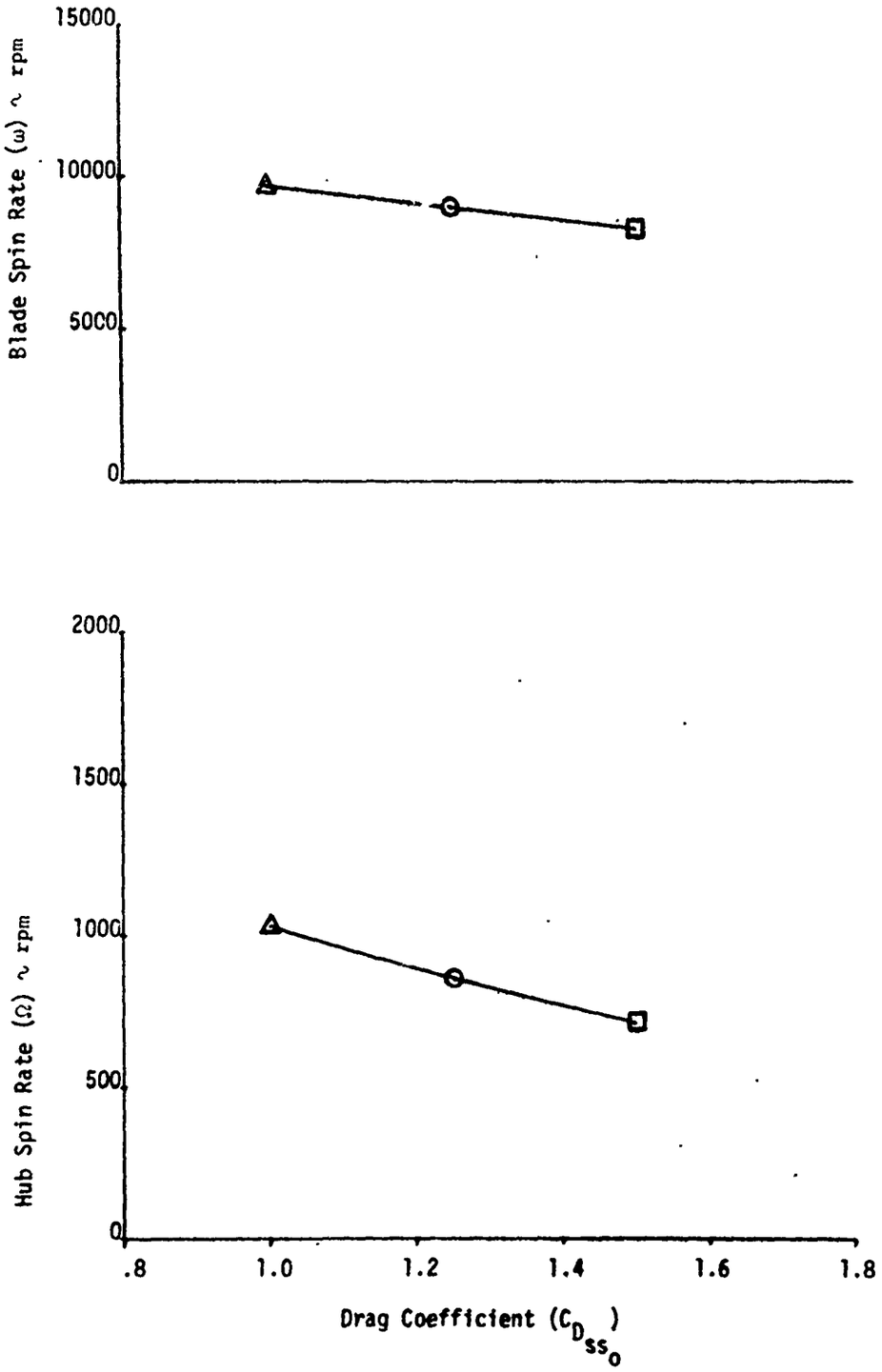

Figure 80. Effect of Blade Sectional Maximum Drag Coefficient on Steady State Blade Spin Rate and Hub Spin Rate

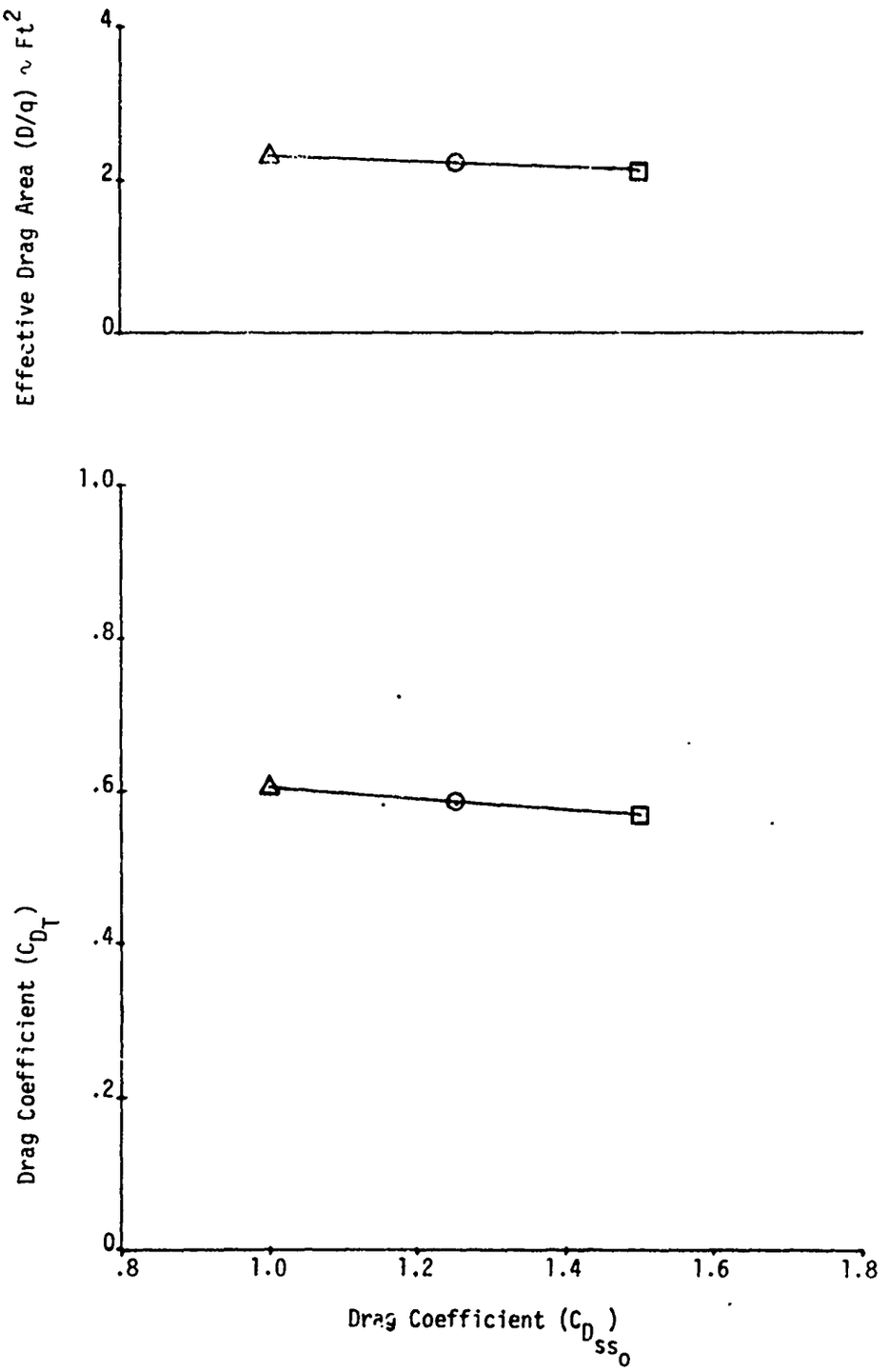

Figure 81. Effect of Blade Sectional Maximum Drag Coefficient on Steady State Effective Drag Area and Drag Coefficient

Sym	Run	$C_{L_{SS_o}}$	$C_{D_{SS_o}}$	$C_{L_{SS_o}} / C_{D_{SS_o}}$
○	12	1.55	1.25	1.24
◇	17	1.55	1.00	1.55
◁	18	1.55	1.50	1.03
△	15	1.25	1.25	1.00
□	16	1.75	1.25	1.40

Note: ———— Indicates Constant Drag Coefficient ($C_{D_{SS_o}} = 1.25$)

— — — — Indicates Constant Lift Coefficient ($C_{L_{SS_o}} = 1.55$)

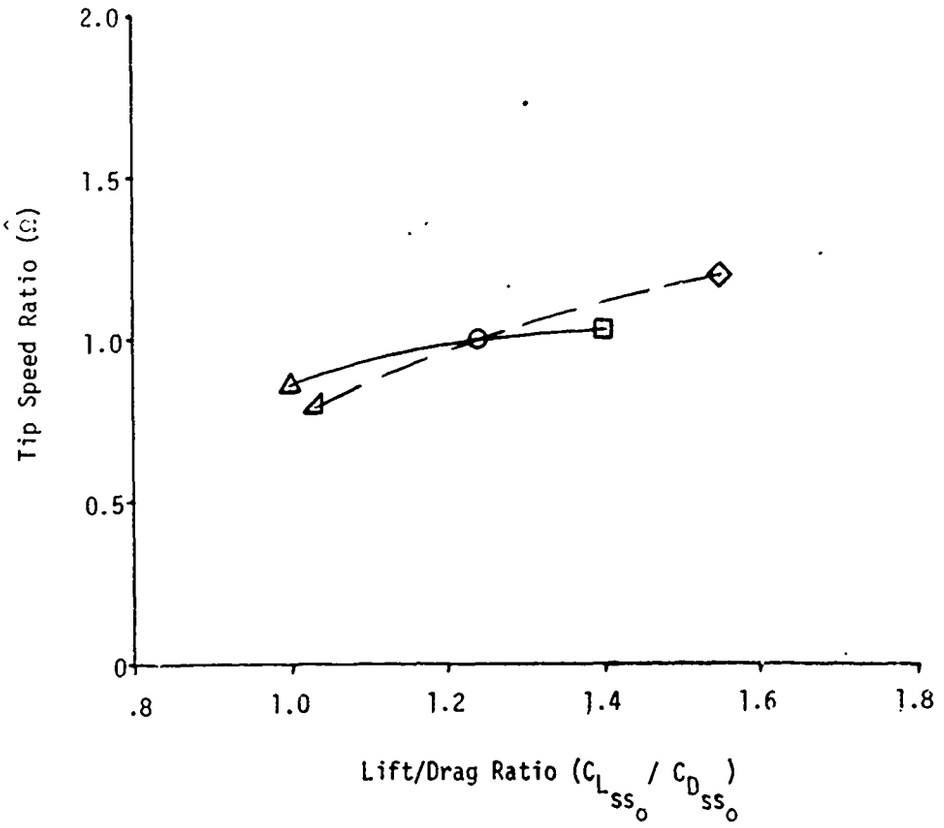

Figure 82. Effect of Blade Sectional Maximum Lift-to-Drag Ratio on Steady State Tip Speed Ratio

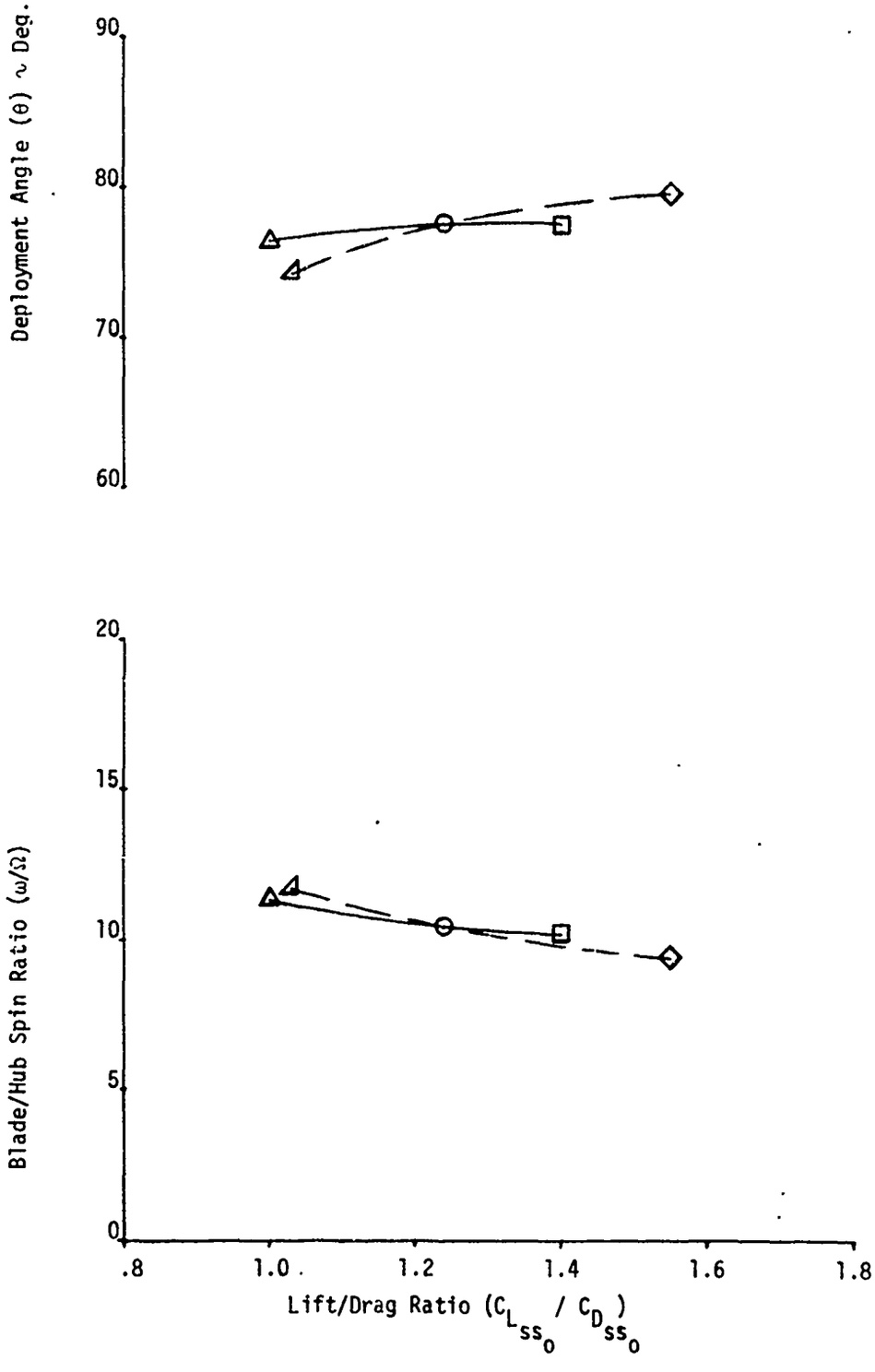

Figure 83. Effect of Blade Sectional Maximum Lift-to-Drag Ratio on Steady State Deployment Angle and Blade/Hub Spin Ratio

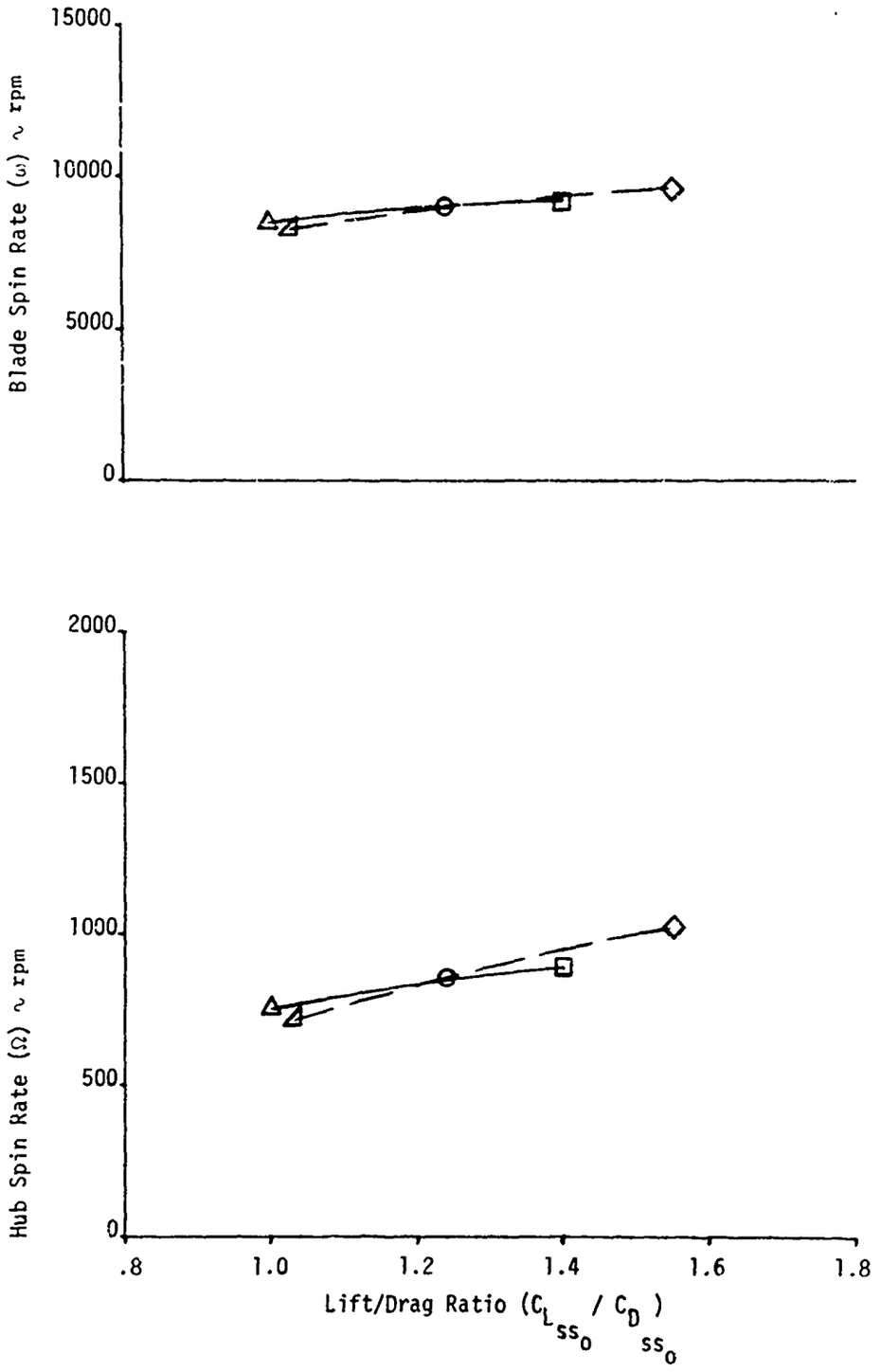

Figure 84. Effect of Blade Sectional Maximum Lift-to-Drag Ratio on Steady State Blade Spin Rate and Hub Spin Rate

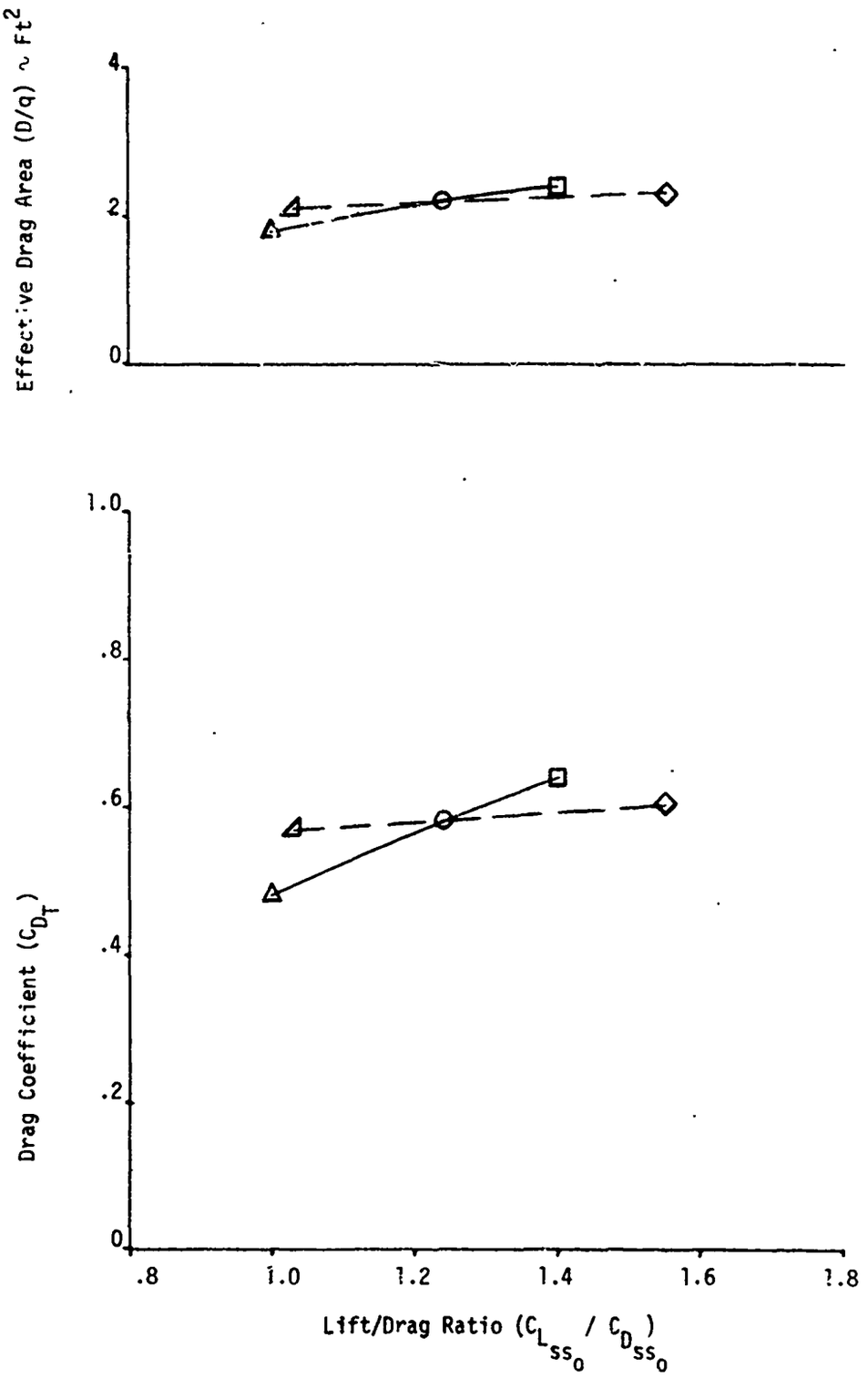

Figure 85. Effect of Blade Sectional Lift-to-Drag Ratio on Steady State Effective Drag Area and Drag Coefficient

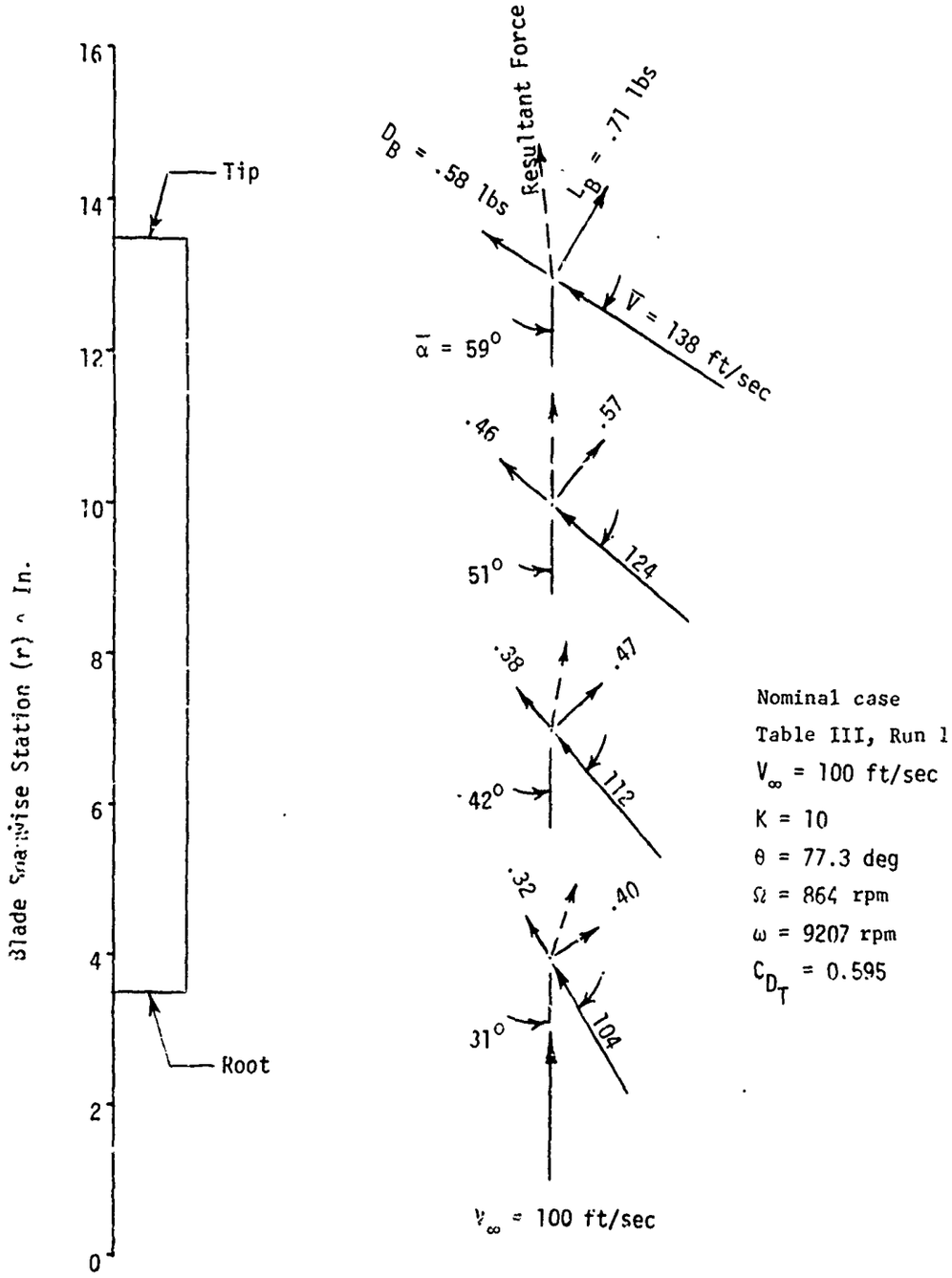

Figure 86. Steady State Aerodynamic Conditions at Various Blade Stations for the Nominal Case

dynamic pressure; consequently, the aerodynamic loads are larger at the blade tip, as indicated in figure 87, which shows the aerodynamic force distribution over the blade span. The angle of attack of the local velocity at each station determines the directional sense of the lift and drag forces, as shown in figure 86. The resultant force due to the lift and drag, shown as a dashed vector in figure 86, is seen to act to spin the hub up at stations near the blade root and to act to de-spin the hub at stations near the tip. This is also shown in figure 87. The component of this resultant force in the direction of the free stream velocity is the system drag for the blade, shown in figure 87.

The essentially constant nature of the lift coefficient distribution over the blade is shown in figure 88. Figure 88 also shows how the local blade tip speed ratio decreases from root to tip. This results in the blade spin moment acting to spin the blade up near the tip and to de-spin it near the hub.

The angle of attack distribution (including the effect of the induced angle of attack) is included in figure 88, as is the true yaw angle of the blade, β, which is used to determine the aerodynamic coefficienis values. The relative tip speed ratio, ω_R, which is a function of β, as indicated in figure 88, is also shown. The relative tip speed ratio ω_R indicates whether an overspin condition exists, and this also determines the aerodynamic coefficient. It will be noted that 60% of the blade length is in a true overspin condition.

X. DEPLOYMENT TRANSIENT CHARACTERISTICS.

A. Detailed Discussion of Equations of Motion Terms.

Before presenting the results of the analysis of the full deployment transient characteristics of the rotor system, it would be helpful to consider the meaning of each of the terms in the equations of motion. A familiarity with the basic effects of each term is helpful in understanding the consequent transient (and steady state) behavior of the system.

Consider the equations for the three degrees of freedom of the system shown in figure 10.

1. $\ddot{\theta}$-Equation.

The equation describing the angular acceleration in the θ-sense includes four basic terms, which are as follows.

a. $\omega\Omega I_1 \sin\theta$—An inertial moment term, which could be termed a "gyroscopic" moment. Because an autorotor blade spinning with a positive ω, as shown in figure 10, will create aerodynamic forces that cause a hub spin rate in the negative Ω sense, this moment will always act in a negative θ sense (i.e., to force the blade back to a smaller deployment angle). Note that the term becomes larger with increasing values of θ. This moment is present even at steady state condition.

b. $\Omega^2 (I_0 - I_1) \sin\theta \cos\theta$—The moment resulting from centrifugal force. This moment always acts to pivot the blades out normal to the hub spin axis. It has a maximum value when $\theta = 45°$.

c. M_{θ_A}—The external aerodynamic moment acting on the blade in the θ-direction. It always acts in the negative θ-sense and is composed of the blade lift, drag, and side force coefficients.

Note that all these moment terms are divided by the moment of inertia of the blade (I_0) to give the blade angular acceleration.

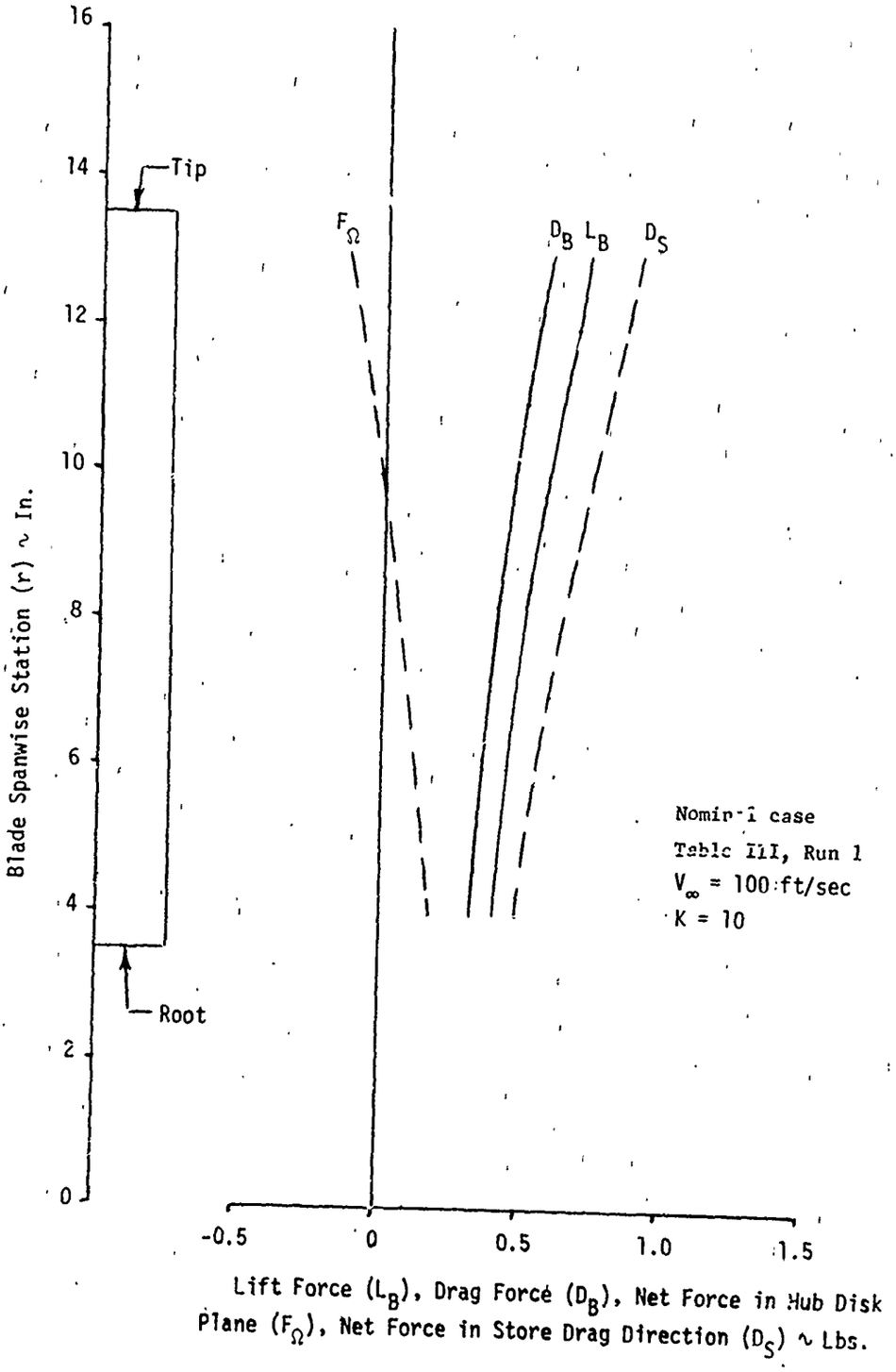

Figure 87. Steady State Aerodynamic Force Distribution Over Blade Span for the Nominal Case

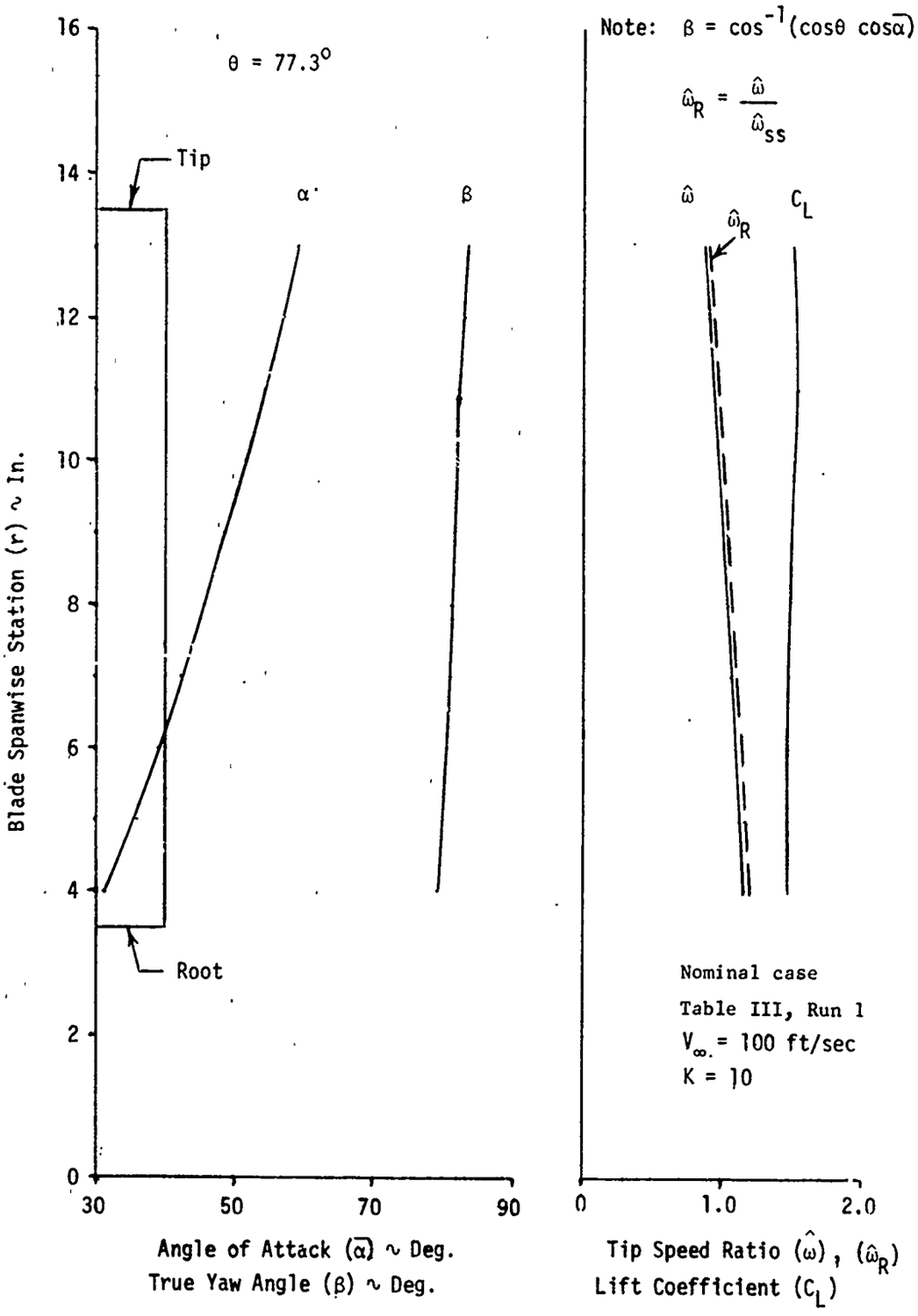

Figure 88. Steady State Conditions Spanwise Distribution for the Nominal Case

d. $M_{\dot{\theta}}$—An aerodynamic "damping" moment. This moment is proportional to, and acts in, a directional sense opposite to the rotational rate of the blade in the deployment sense ($\dot{\theta}$).

2. $\dot{\Omega}$-Equation.

The equation describing the angular acceleration of the blade about the store center line (i.e., hub spin acceleration) is composed of four terms.

a. $-\dot{\theta}\omega I_1 \sin\theta$—A "gyroscopic" moment that is effective only during the deployment transient because of the $\dot{\theta}$ term. From a consideration of the terms and their signs, it can be seen that this term results in a "spin acceleration" effect on the hub as the blade deployment angle is increasing (i.e., positive $\dot{\theta}$), because the hub spin is in the negative sense.

b. $-2\Omega\dot{\theta}(I_0 - I_1)\sin\theta\cos\theta$—This is a Coriolis moment, which acts to decelerate the hub spin rate as the blade deployment angle is increasing (i.e., positive $\dot{\theta}$).

c. $-M_{\Omega_A}$—The external aerodynamic moment acting to spin the blade about the hub. As can be seen, a positive value of the moment results in hub spin moment in the negative sense. This moment is a function of the blade sectional lift, drag, and side force coefficients.

d. $I_1\dot{\omega}\cos\theta$—This is a kinematic term that evolves from the derivation of the equation in the form where the blade spin rate ω can be considered as a relative term.

3. $\dot{\omega}$-Equation.

The equation describing the blade spin acceleration about its long axis (i.e., autorotation spin) contains three terms.

a. M_{ω_A}—An external aerodynamic spin moment. This net moment is determined by summing the spin moments acting at the various blade sections. It is only a function of the blade sectional spin moment coefficient.

b. $\Omega\dot{\theta}I_1 \sin\theta$—A "gyroscopic" moment that acts to accelerate the blade spin rate as the blade is deploying (i.e., $\dot{\theta}$ is positive).

c. $\dot{\Omega}I_1 \cos\theta$—A "kinematic" term that is a result of the derivation that makes ω a relative term.

B. Relative Contributions of Terms to the Transient and Steady State System Motion.

The relative contributions of the various terms in the equations of motion to the motion of the system during the deployment transient is shown in figures 89 through 91 for the θ, Ω, and ω equations respectively. In these figures, the terms representing the moments resulting from various means are plotted as a function of time during the deployment transient. The term values used for the system are the same as the nominal case of the parameter study of section IX, specifically, run 1. The nominal hub spin rate at blade release is 750 rpm. Note that the nominal interference factor of $K = 10$ is used. The motion of the system during the deployment transient is shown in figures 92 through 95. The complete computer printout for the nominal deployment is in appendix D. The purpose of these plots is to show the relative contributions of the inertial, gyroscopic, and aerodynamic moments to the transient and steady state motion of the system so as to facilitate a physical understanding of the system.

Figure 89 shows the three moments acting in the blade deployment (θ) direction as a function of time during a typical deployment transient. The moments are caused by centrifugal (inertial), gyroscopic, and aerodynamic forces. The aerodynamic blade damping moment $M_{\dot{\theta}}$ is also

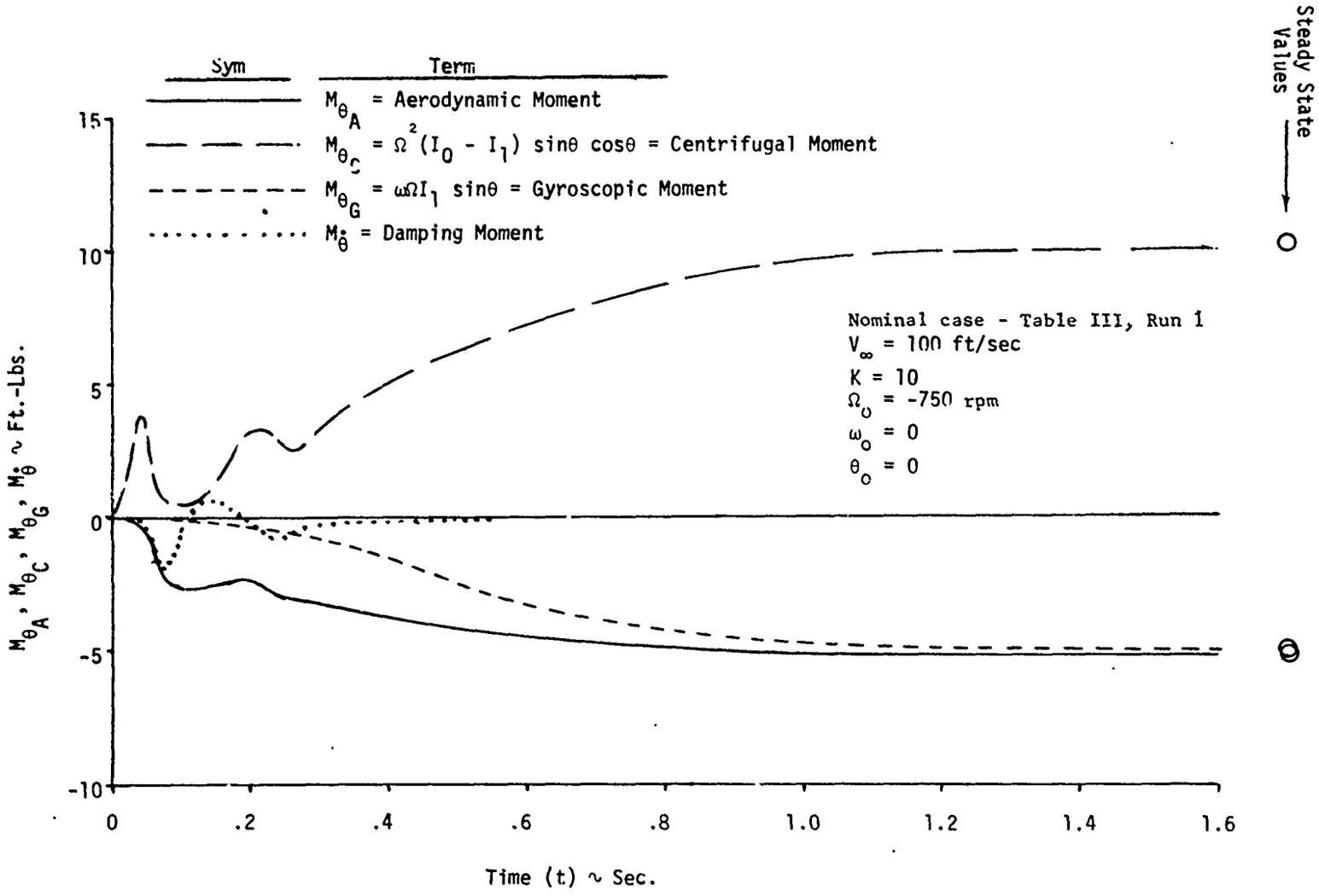

Figure 89. θ-Equation Term Values as a Function of Time During a Typical Deployment

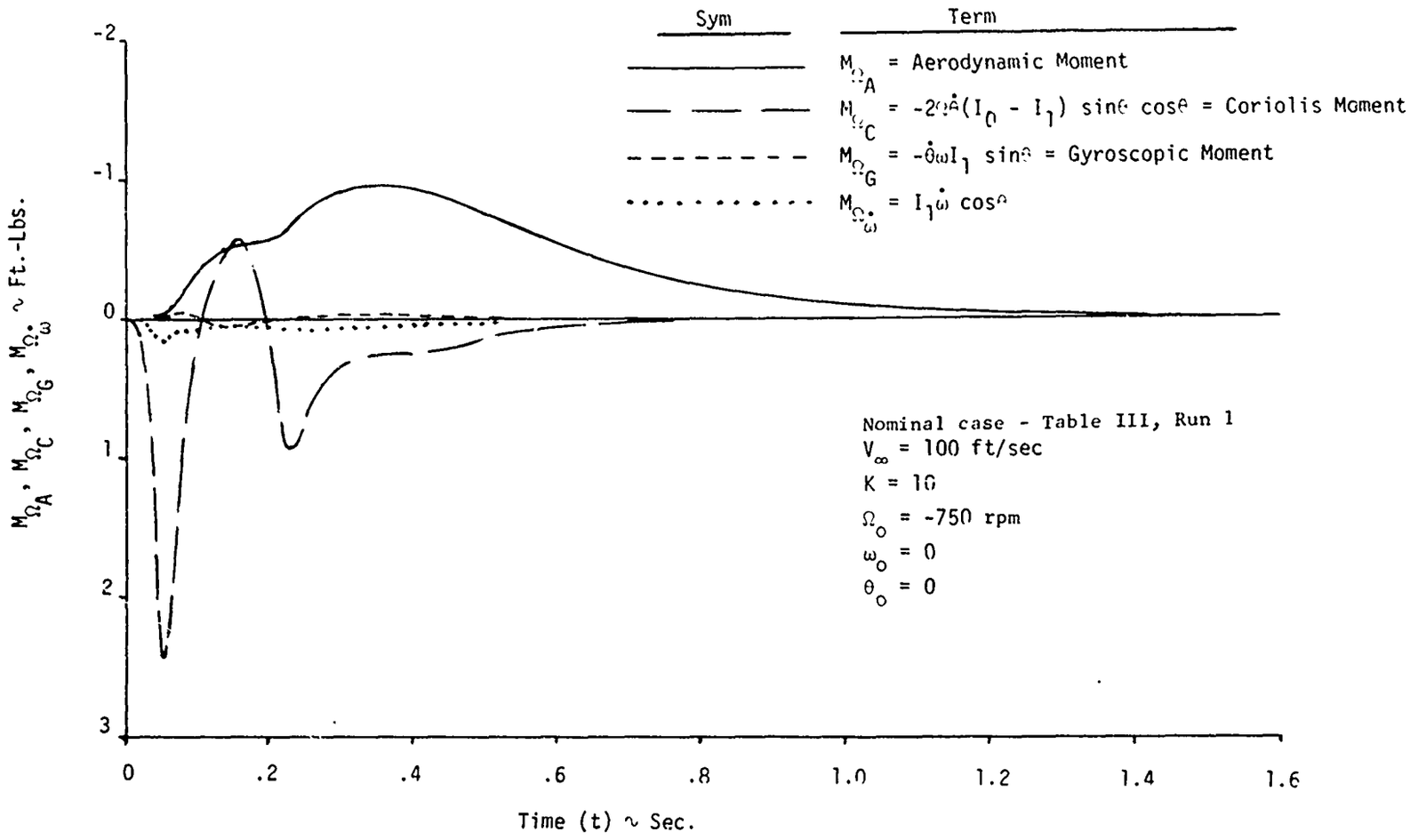

Figure 90. Ω-Equation Term Values as a Function of Time During a Typical Deployment

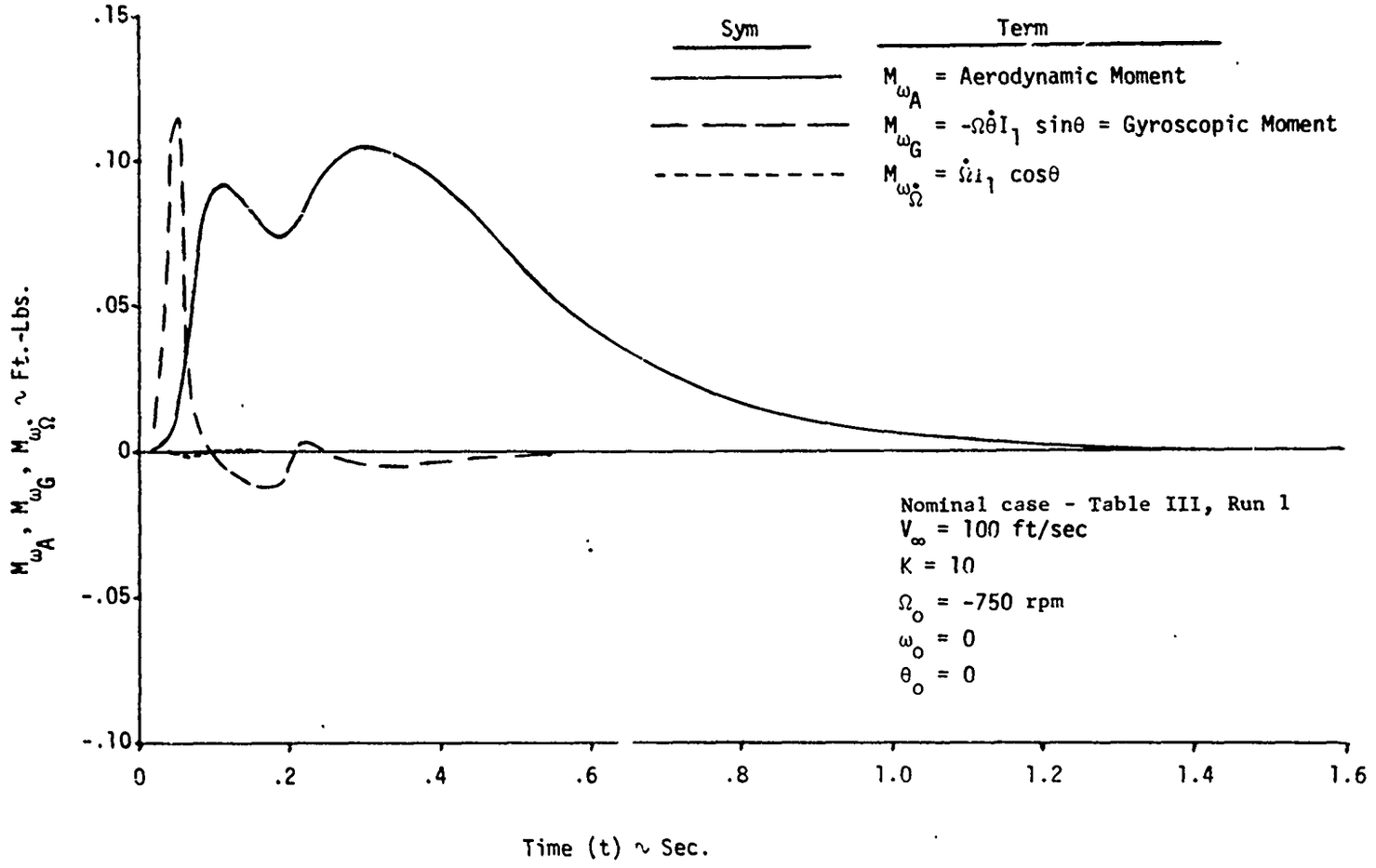

Figure 91. ω-Equation Term Values as a Function of Time During a Typical Deployment

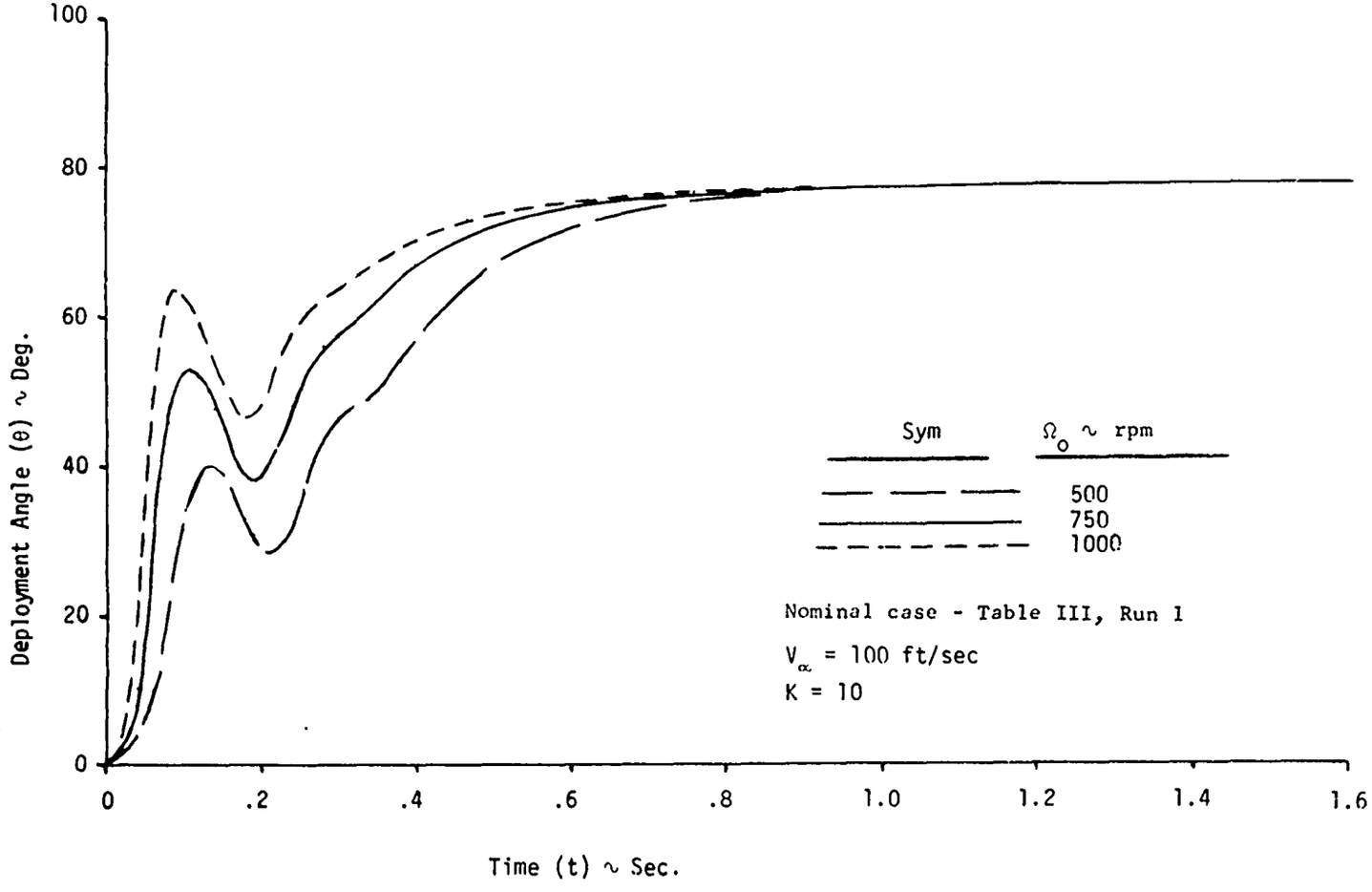

Figure 92. Effect of Initial Hub Spin Rate on the Transient Values of the Deployment Angle During Deployment

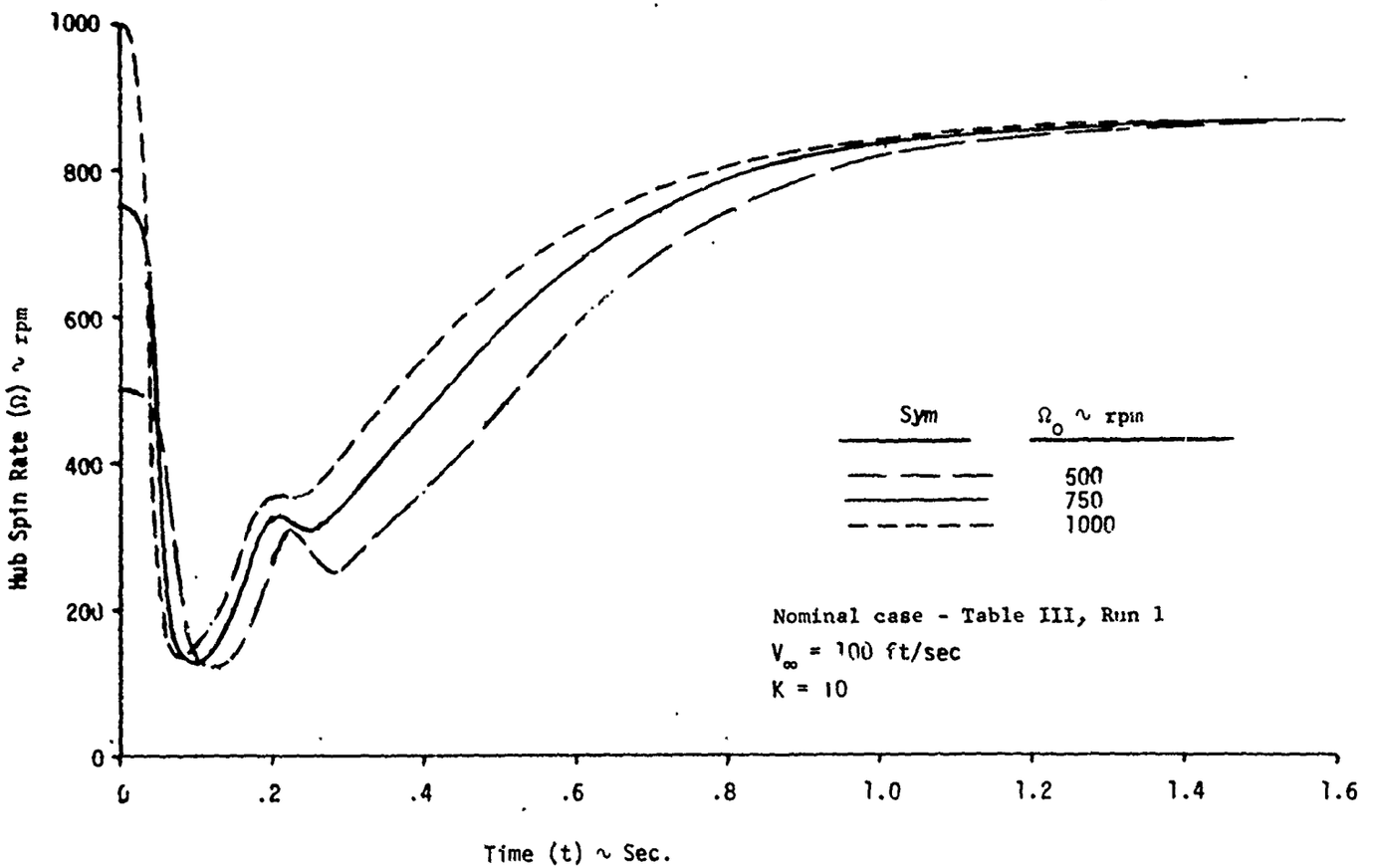

Figure 93. Effect of Initial Hub Spin Rate on the Transient Values of the Hub Spin Rate During Deployment

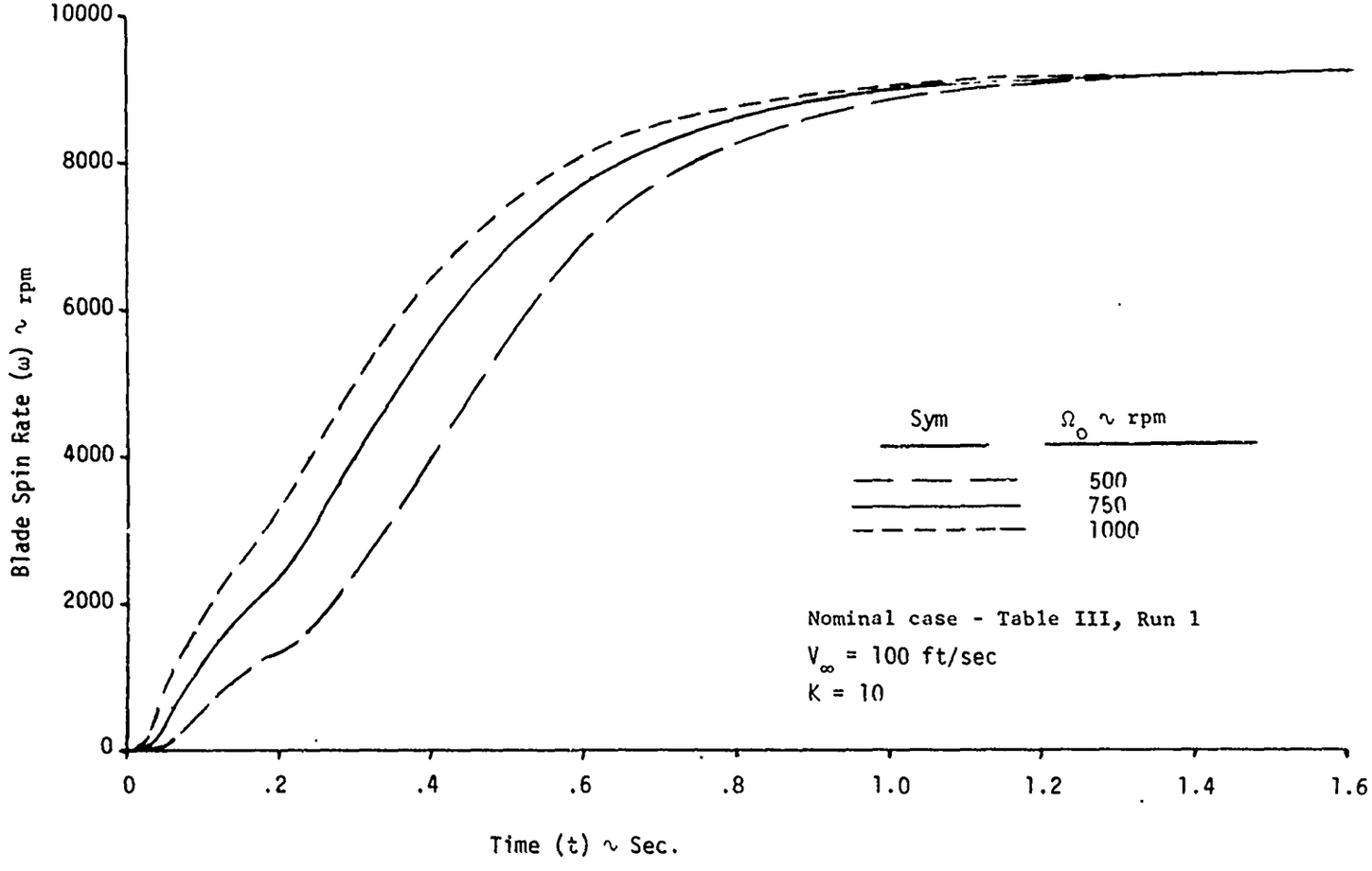

Figure 94. Effect of Initial Hub Spin Rate on the Transient Values of the Blade Spin Rate During Deployment

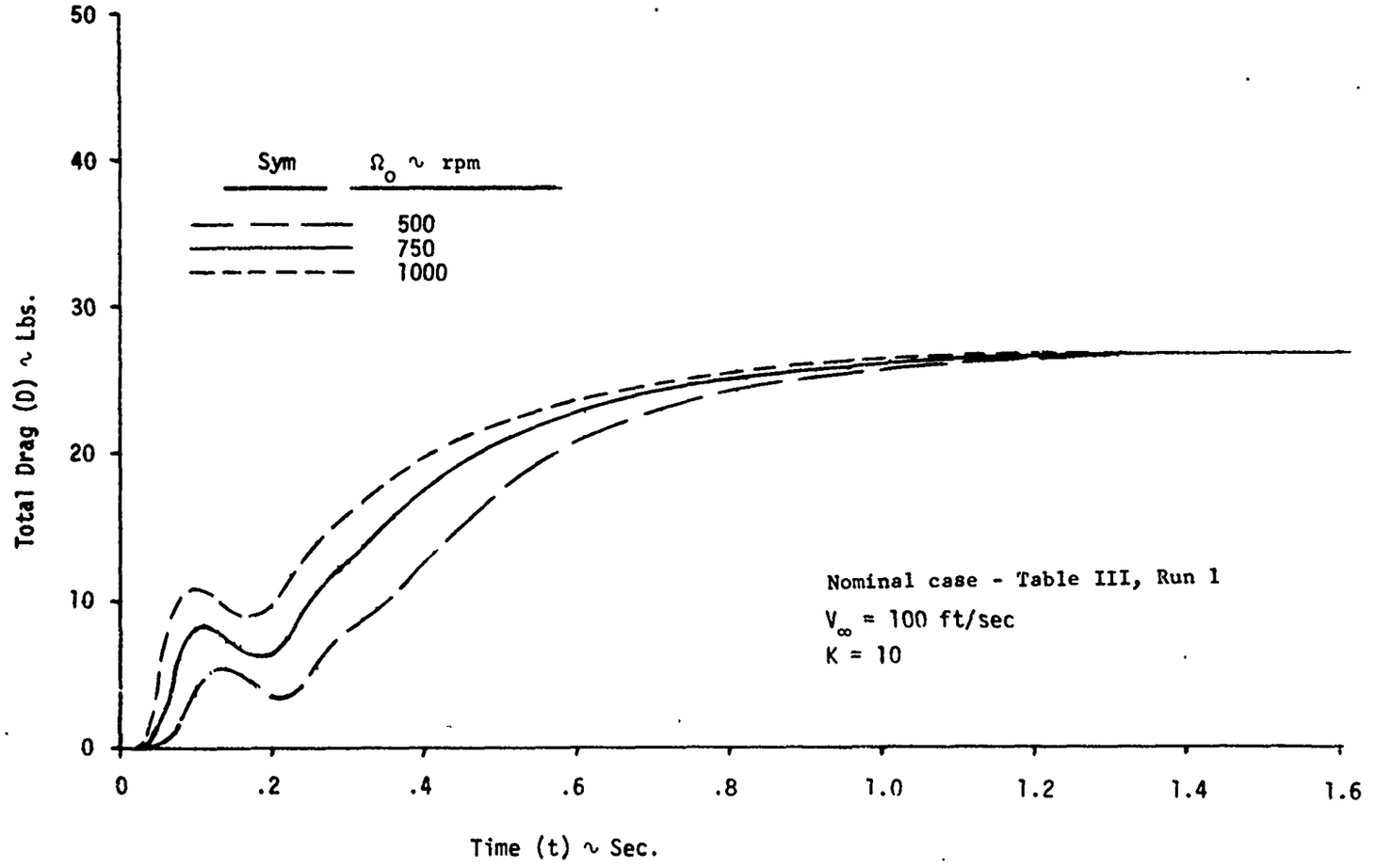

Figure 95. Effect of Initial Hub Spin Rate on the Transient Values of the Total System Drag During Deployment

included. From figure 89 it can be seen that the centrifugal moment always acts in a positive sense in that it acts to pivot the blade out to larger values of θ. The net aerodynamic and gyroscopic moments always act to force the blade back toward the undeployed position. In the initial deployment phase, the centrifugal and aerodynamic moments are prevalent; but when the system has assumed a steady state condition, the gyroscopic and aerodynamic moments are of about the same magnitude and together balance out the centrifugal moment, thereby holding the blade at the steady state deployment angle. The sharp increase, decrease, and steady increase of the values of the centrifugal and aerodynamic moments during the initial deployment phase reflect the corresponding fluctuation in the hub spin rate during this time.

The time histories of the moments in the hub spin (Ω) direction for the nominal deployment transient are shown in figure 90. The moments considered are the Coriolis (inertial), gyroscopic, and aerodynamic. It should be noted that because of the defined positive sense of the blade spin rate, ω, the resulting aerodynamic moments acting on the blade will cause the hub to spin in a negative sense (as defined in figure 10). Thus, a negative moment value tends to spin the hub faster, whereas a positive value tends to resist the hub spin rate.

From figure 90 it can be seen that the gyroscopic moment is small relative to the aerodynamic and Coriolis terms. Thus, the hub spin acceleration is essentially due entirely to the aerodynamic and Coriolis moments. The net aerodynamic moment always tends to increase the hub spin rate. The large Coriolis moment resulting from the initial rapid deployment motion of the blade is the main reason for the abrupt decrease in hub spin rate. The consequent oscillation of the blade deployment angle in reaction to the hub spin rate change results in the Coriolis moment fluctuating between a negative and positive value. With the transient effect of $\dot{\theta}$ diminished, the net aerodynamic moment then continues to accelerate the hub spin up to its steady state value where the net value of the aerodynamic moment is zero.

In addition to the external moments acting on the system, the moment of inertia for the Ω-equation also varies during the deployment phase, becoming larger as the blades deploy to larger angles.

Figure 91 shows the moments affecting the blade spin acceleration. As can be seen in figure 91, the initial blade deployment motion, combined with the hub spin rate, results in a large positive value for the gyroscopic moment, which acts to give a large positive spin moment to the blade. This is the most significant effect in initiating blade spin (autorotation). The aerodynamic moment, acting to spin the blade, increases as the blade is deployed to larger values of θ.

As will be noted in figures 89, 90, and 91, the deployment transient effects are essentially over by 1 second after deployment initiation.

C. Illustrative Examples of Deployment Transients.

In order to investigate the general transient behavior of the system during deployment, deployments were simulated using the computer program. Selected variables were varied to show their effect on the resulting motion, using the nominal case terms (table III, run 1) as the basic input. Figures 92 through 95 show the effects of varying the initial hub spin rate on the system motion as a function of time. Figure 92 shows the characteristic deployment motion of the blade where the blade is initially thrown out to a large deployment angle, hesitates momentarily, and then deploys to the final steady state value. Figure 93 illustrates the severe hub spin deceleration that occurs during the initial deployment phase. Note that the hub spin rate decreases to about the same minimum value regardless of the initial spin rate value. Figure 94 shows how the blade spin rate steadily increases throughout the deployment transient. The total system drag is shown as a function of time in figure 95. Although these data are for nominal conditions selected to illustrate

the system performances, they show the same characteristic behavior as was obtained experimentally in figures 43 through 45.

The effect of free stream velocity (or free stream dynamic pressure) is illustrated in figures 96 through 99. It should be noted that a steady state condition is achieved more quickly at the high velocities, although the associated spin rates are higher.

XI. SUMMARY.

Equations have been evolved that describe the aerodynamic and dynamic performance of a self-deploying articulated autorotor decelerator system. These equations describe the transient motion during the deployment sequence whereby the decelerator system goes from a stowed (low drag) configuration to a fully deployed, high drag configuration; they also fully describe the motions of the various system components and the overall system performance during both the transient phase and the final steady state conditions. These equations were formulated using the modified Euler's equations approach and include the inertial, gyroscopic, and aerodynamic forces.

The aerodynamic force distribution and the resulting moment acting on the decelerator blades are determined by means of the blade element propeller theory. The sectional aerodynamic characteristics of the decelerator blade are determined from wind tunnel tests of the autorotor section utilized in the blade. The wind tunnel data thus obtained can be utilized directly in the equations.

General expressions were evolved to describe the transient and steady state aerodynamic characteristics of the autorotor configuration and were verified by wind tunnel tests. The expressions derived permit the complete transient behavior of an autorotor to be determined with a minimum of wind tunnel testing.

A condition of overspin exists at certain spanwise locations of the decelerator blade, where the term overspin denotes a condition in which the tip speed ratio of the blade at that location is greater than the steady state tip speed ratio corresponding to the conditions at that location. Wind tunnel tests on an autorotor in an overspin condition were conducted to determine the aerodynamic characteristics of the autorotor for inclusion in the decelerator system analysis. These tests revealed that, for an autorotor in an overspin condition (1) the lift and drag coefficients remain at their steady state values, and (2) the spin moment coefficient follows the general expression determined for the underspin condition.

Wind tunnel data obtained on a nonspinning autorotor are presented to explain the spin initiating difficulties characteristic of autorotors in general and to illustrate the effect of spin in increasing the lift and spin moment coefficients of the basic shape.

The complete equations were programmed to be solved on a digital computer. In addition to the transient and steady state performance, the distribution of the various terms over the blade span is also determined.

Data from a wind tunnel test of a representative full scale autorotor decelerator are presented and used as the basis of comparison with the analytical results. Excellent correlation between analytical and experimental results are achieved when a mutual blade interference effect is included in the analytical equations. The blade interference effect utilized is in the form of a local flow directional change, similar to a downwash, which would seem to be physically valid.

The analytical results, which were verified by the experimental data, indicate the following for a particular autorotor decelerator system under steady conditions.

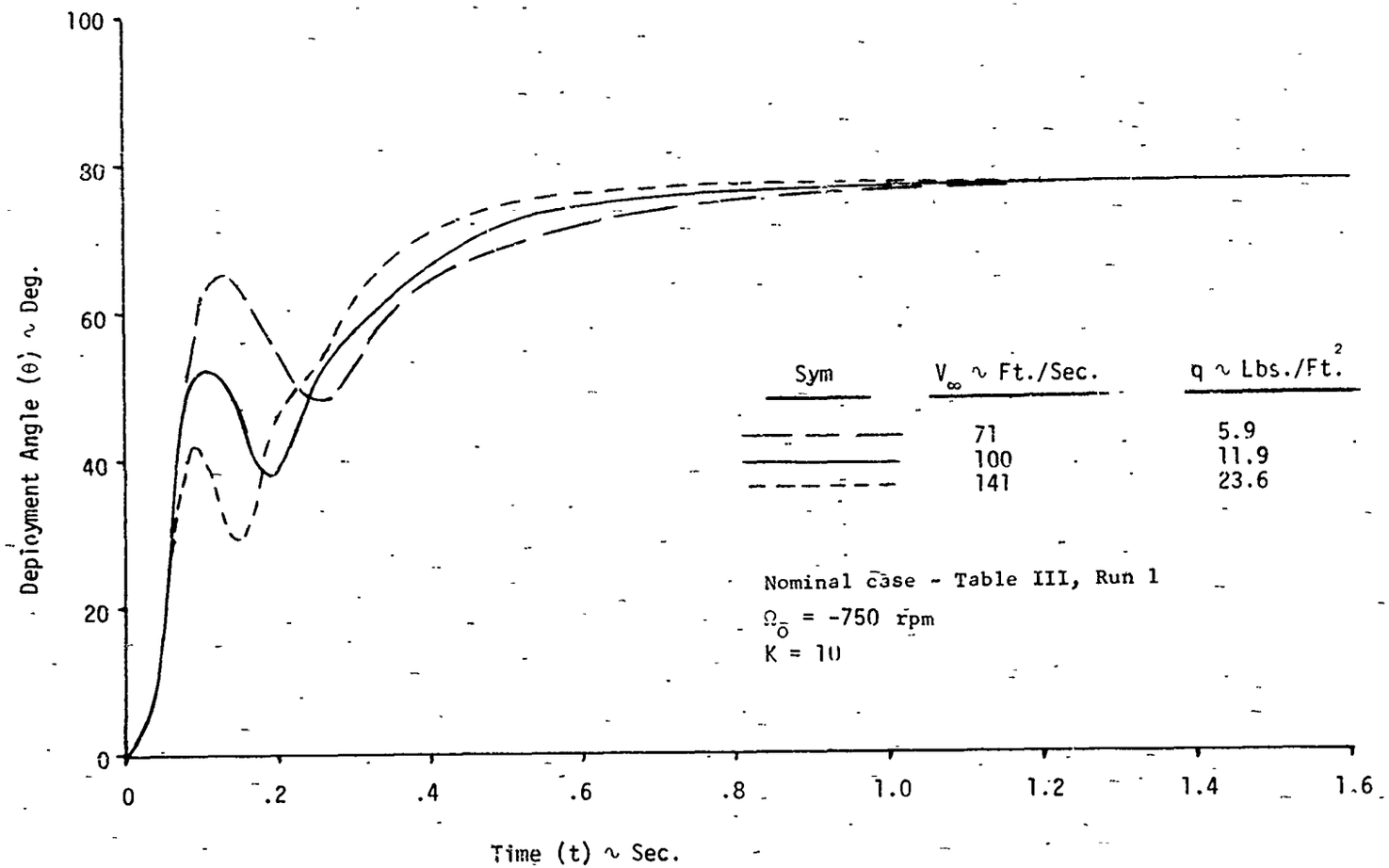

Figure 96. Effect of Free Stream Velocity Magnitude on the Transient Values of the Deployment Angle During Deployment

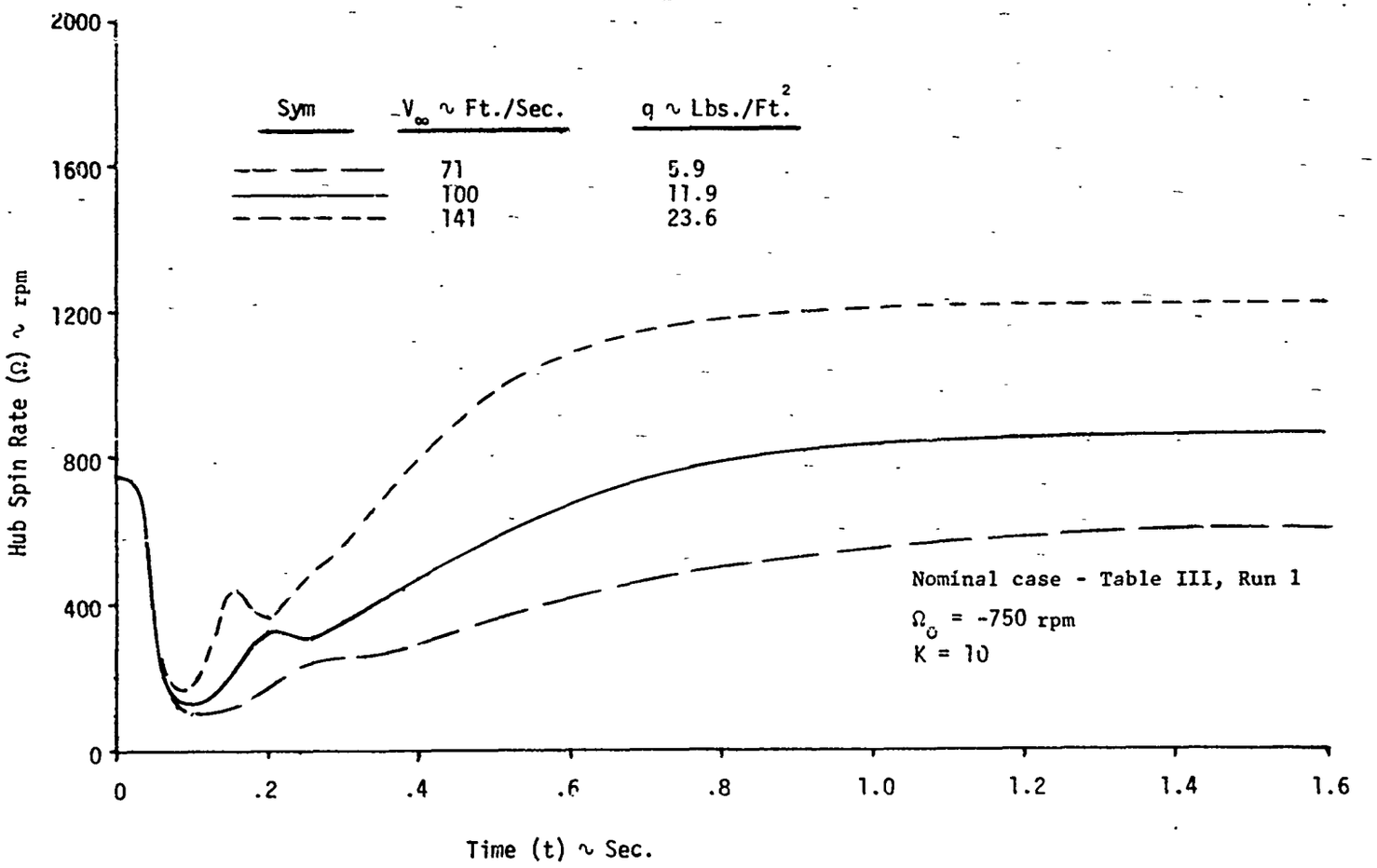

Figure 97. Effect of Free Stream Velocity Magnitude on the Transient Values of the Hub Spin Rate During Deployment

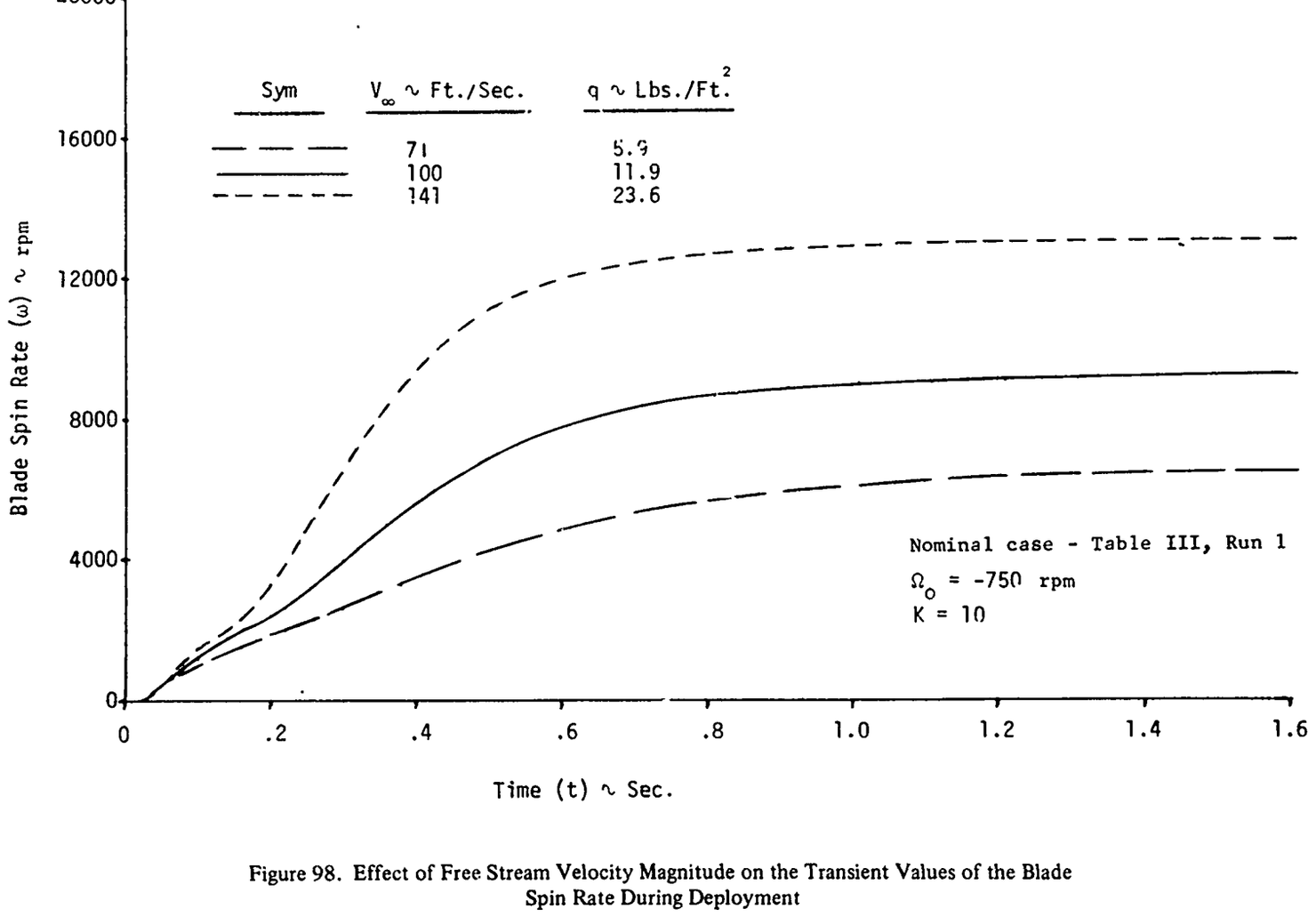

Figure 98. Effect of Free Stream Velocity Magnitude on the Transient Values of the Blade Spin Rate During Deployment

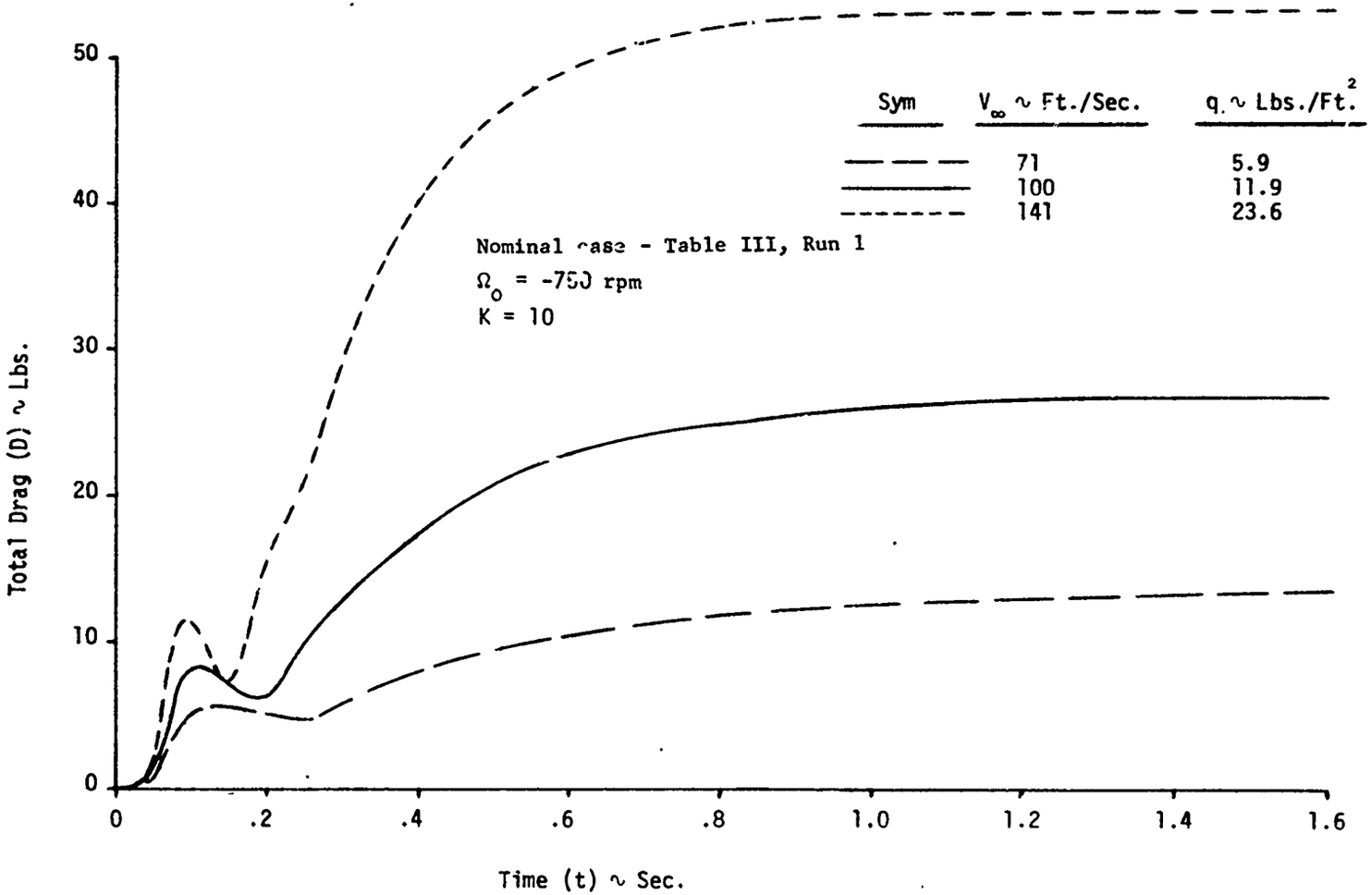

Figure 99. Effect of Free Stream Velocity Magnitude on the Transient Values of the Total System Drag During Deployment

1. The blade deployment angle is independent of free stream velocity.

2. The blade spin rate and hub spin rate are linear with velocity.

3. The ratio of the blade spin rate to hub spin rate is a constant with velocity.

4. The drag coefficient is a constant with velocity.

A parametric study is included in which the steady state performance of the decelerator system is investigated analytically by investigating the effect on the decelerator performance by varying a single term value about a nominal case value. Plots of these effects indicate specific qualitative trends and illustrate the contribution of the inertial and especially the gyroscopic effects on the system performance. The presence of the gyroscopic effects, which are a function of the inertial properties of the system, does not permit the non-dimensionalization of the system performance that would be possible if only the aerodynamic terms were used.

A nominal deployment transient is presented in detail to illustrate the relative contribution of the various terms of the basic equations of motion.

Only one gyroscopic moment is present under steady state spin conditions; namely, a moment that acts to push the blades back. This moment, which is a function of the blade spin rate and hub spin rate, is of the same magnitude and directional sense as the aerodynamic moment. During the deployment transient, only one gyroscopic moment is of consequence. This moment, which is a function of the hub spin rate and the blade deployment rate, acts to initiate blade autorotation and is the major reason for the autorotor blade self-starting feature during the deployment sequence.

LITERATURE CITED

1. Flatau, A., and Brunk, J. E. Free Spinning Articulated Rotor. US Patent 3,291,418. 13 December 1966.

2. Greenwood, D. F. Principals of Dynamics. Prentice-Hall Inc., Englewood Cliffs, New Jersey. 1965.

3. Von Mises, R. Theory of Flight. Dover Publications Inc., New York, New York. 1959.

4. Flatau, A. CRDL Technical Memorandum 15-49. Preliminary Investigation of Modified Autorotating Finned Cylinders. 17 August 1961. UNCLASSIFIED Memorandum.

5. Brunk, J. E. Final Summary Report. Contract DA-18-108 AMC 236(A). Analytical and Aerodynamic Studies of Rotating Bomblet Motion. 31 January 1965. UNCLASSIFIED Report.

6. Dupleich, P. NASA TM 1201. Rotation in Free Fall of Rectangular Wings of Elongated Shape. April, 1949.

7. Kreyszic, E. Advanced Engineering Mathematics. John Wiley and Sons Inc., New York, New York. 1962.

8. Autorotor Decelerator Retardation System. All American Engineering Company, Wilmington, Delaware. Contract DA 18-035 AMC-356(A). 1969.

9. Flow Analysis and Dynamics of Autorotating Lifting Bodies. University of Notre Dame, Notre Dame, Indiana. Contract DA 18-035 AMC-356(A). 1964.

GLOSSARY

AR	Blade aspect ratio
α	Angle of attack for nonspinning autorotor
$\bar{\alpha}$	Angle of attack resulting from hub spin rate
$\Delta\alpha$	Flow angular change (interference effect)
b	Distance between blade center of gravity and hub spin axis–measured along blade
β	Yaw angle used in decelerator system
C	Blade chord
C_D	Drag coefficient
$C_{D_{ss}}$	Steady state drag coefficient
$C_{D_{ss_0}}$	Maximum steady state drag coefficient
C_L	Lift coefficient
C_{L_1}, C_{L_2}	Transient lift coefficient constants
$C_{L_{ss}}$	Steady state lift coefficient
$C_{L_{ss_0}}$	Maximum steady state lift coefficient
C_m	Spin moment coefficient
$C_{m_{\bar{0}}}$	Spin moment coefficient evaluated at condition of zero spin and zero yaw
C_{m_1}, C_{m_2}	Transient spin moment coefficient constants
$C_{m_0}, C_{m_1}, C_{m_2}$	Combined transient spin moment coefficient constants
$C_{m_{\dot{\theta}}}$	Deployment damping moment coefficient
C_{D_T}	Drag coefficient based on swept area
C_Y	Side force coefficient
$C_{Y_{ss}}$	Steady state side force coefficient
$C_{Y_{ss_0}}$	Maximum steady state side force coefficient
D	Drag force
D_B	Blade drag force directed along wind axes

D_S	Aerodynamic force acting on blade in the direction of the store center line
D/q	Effective drag area
δ	Euler angle defining blade orientation in plane containing the store center line
$F_{\overline{A}}$	Total force along blade spin axis
F	Total force acting at blade pivot point
F_Ω, T_S	Aerodynamic force acting normal to blade and in a plane perpendicular to the store center line
F_N, F_c	Aerodynamic force acting normal to blade and in a plane containing the store center line
$F_{\overline{N}}$	Total force normal to blade spin axis
$F_{\overline{X}}$, $F_{\overline{Y}}$, $F_{\overline{Z}}$	Aerodynamic force acting on blade referred to inertial axes system
g	Gravitational acceleration constant
γ	Euler angle defining blade orientation in plane perpendicular to store center line
H	Angular momentum
H_x, H_y, H_z	Absolute angular momentum referred to body axes system
I	Moment of inertia
I_0	Moment of inertia of blade about transverse axis through blade/hub pivot point
I_1	Moment of inertia of blade about the blade long axis
I_x, I_y, I_z	Total moment of inertia referred to body axes system
I_H	Moment of inertia of hub
i	Subscript indicating conditions at a particular blade element or spanwise station
$\overline{i}, \overline{j}, \overline{k}$	Unit vectors for body axes system
K	Blade interference factor
ℓ	Blade length
$\overline{\ell}$	Distance between store center line and root edge of blade—measured along blade
L	Lift force
L_B	Blade lift force directed along wind axes
m_b	Blade mass

M_B	Spin moment
$M_\gamma, M_\delta, M_\phi$	Total moment acting on blade–referred to the Euler axes system
$M_{\omega_A}, M_{\theta_A}, M_{\Omega_A}$	Aerodynamic moment acting on blade–referred to the modified Euler axes system
$M_\omega, M_\theta, M_\Omega$	Total moment acting on blade–referred to the modified Euler axes system
M	Total moment
M_x, M_y, M_z	Total moment–referred to body axes system
$M_{\dot{\theta}}$	Deployment damping moment
Ω	Hub spin rate
$\hat{\Omega}$	Ratio of tip velocity of blade about the store center line to the free stream velocity
ϕ	Euler angle defining blade orientation in plane perpendicular to the blade long axis
ψ	Yaw angle used in wind tunnel
π	Ratio of circle circumference to radius
q	Dynamic pressure
q_∞	Free stream dynamic pressure
$\bar{q}$	Total dynamic pressure
r	Distance from store center line to particular blade element–measured along blade
R	Radius of curvature of S-section autorotor
r_0	Blade station located nearest root of blade
r_f	Blade station located nearest tip of blade
r_{B_θ}	Blade center of pressure location for force F_N
r_{B_Ω}	Blade center of pressure location for force T_S
s	Spin rate of the blade relative to the x-component of the body axes
S	Blade aerodynamic reference area
$\bar{S}$	Total blade area
Δr	Spanwise interval used in blade element method
ρ	Air density

σ	Solidity factor
SF	Side force
SF_B	Blade side force directed along wind axes
t	Time
T	Blade thickness
Δt	Integration time interval
θ	Deployment angle
$V, \bar{V}$	Total velocity
V_∞	Free stream velocity
wgt	Blade weight
ω	Blade spin rate about the blade long axis
$\bar{\omega}'$	Total angular velocity
$\bar{\omega}_x, \bar{\omega}_y, \bar{\omega}_z$	Total angular velocity
$\omega'_x, \omega'_y, \omega'_z$	Total angular velocity–referred to body axes system
$\omega_x, \omega_y, \omega_z$	Angular velocity of the body axes system, relative to the inertial axes system–referred to the body axes system
$\bar{\omega}$	Total angular velocity of the body axes system
ω/Ω	Ratio of the blade spin rate to the hub spin rate
$\hat{\omega}$	Ratio of tip velocity of blade about the blade long axis to the total velocity (tip speed ratio)
$\hat{\omega}_K$	Ratio of actual blade sectional tip speed ratio to the steady state tip speed ratio corresponding to the local sectional flow conditions
$\hat{\omega}_{ss}$	Steady state tip speed ratio
$\hat{\omega}_{ss_0}$	Maximum steady state tip speed ratio
ξ	Angle used to relate the wind axes to the inertial axes in the decelerator system
$\bar{X}, \bar{Y}, \bar{Z}$	Inertial axes system
x, y, z	Body axes system
$x_\omega, y_\omega, z_\omega$	Wind axes system

Subscripts:

$\bar{X}, \bar{Y}, \bar{Z}$	Term referred to inertial axes system
x, y, z	Term referred to body axes system
γ, δ, ϕ	Term referred to Euler angle system
Ω, θ, ω	Term referred to modified Euler angle system
ss	Steady state condition
B	Refers to aerodynamic force or moment acting on blade in the decelerator system
i	Denotes condition at a particular blade element

Superscripts:

$'$	Denotes absolute value of angular momentum
-	Denotes a vector (except in the case of $\bar{q}, \bar{S}$, and $\bar{\alpha}$)
.	Denotes the first derivative with respect to time
..	Denotes the second derivative with respect to time
$( )_r$	Denotes absolute value of term expressed in terms of the body axis components

APPENDIXES

APPENDIX A

COMPUTER PROGRAM DETAILED LISTING AND SYMBOL DEFINITIONS

```
00100     1*    C     SDAD PARAMETER STUDY
00100     2*    C     ELAINE J WESTERVELT
00100     3*    C     MARCH 1969
00101     4*          DIMENSION AMACH(20),WSSR(20),DEN(20),WGT(20),DRI(10),ALRI(10),DSI(
00101     5*         1101),TORT(10),AMRT(10),SFBT(10),FAI(10),FNI(10)
00103     6*          DATA PAD,G,REV,SS/.01745329,32.174,9.5492964,1100./
00110     7*          NP=1
00110     8*    C     INPUT
00111     9*          READ 1010,NRUN
00114    10*    10    READ 1000,WGT,WGTS,ALTO,VINF,GH
00123    11*          READ 1000,A,AL,S,C,RHO
00132    12*          READ 1000,AIO,AI1,AIM,SV,DV
00141    13*          READ 1000,CLSS,CDSS,CYSS,COS,DFR
00150    14*          READ 1000,CM0,CM1,CM2,CL1,CL2
00157    15*          READ 1000,CMV1,CMV2,CMDT,CMD0,WI
00166    16*          READ 1000,THETA,THETT,OMG,OMGI,W
00175    17*          READ 1000,VLIM,TO,XO,ZO,THETIO
00204    18*          READ 1000,ALFT,RINT,DR,DT,DT2
00213    19*          READ 1000,TIME1,TIMF2,TIME3,TSTP,AST*
00222    20*          READ 1010,NF,NM2,NM3,NDP,NRAN,IDEN,IVFL,TEMD,TL
00235    21*          READ 1000,AN,AK
00241    22*          PRINT 2070
00243    23*          PRINT 2040
00245    24*          CALL CSUB2(AMACH,WSS*,AMCN,0,WSSR,I1,N1)
00246    25*          IF(IDEN.EQ.0)GO TO 15
00250    26*          PRINT 2040
00252    27*          CALL CSUB2(WGT,DEN,ALT,0,RHO,I2,N2)
00257    28*    15    PRINT 2010,WGT,WGTS,ALTO,VINF,RHO
00262    29*          PRINT 2020,S,C,AL,R,GH
00271    30*          PRINT 2030,AIM,AII,AIO,SV,DV
00300    31*          PRINT 2040,CLSS,CDSS,CYSS,OMG,OMGI
00307    32*          PRINT 2050,DFR,CMV1,CMV2,CMDT,CMD0
00316    33*          OMG=OMG/REV
00317    34*          PRINT 2065,CM0,CM1,CM2,CL1,CL2
00326    35*          PRINT 2060,THETA,THETT,W,WI,CD,*THETIO,VLI*
00337    36*          PRINT 2400,*INT,DR,AN,AK,TL
00337    37*    C     INITIAL CONDITIONS
00345    38*          ISTOP=0
00347    39*          T1=1
00350    40*          T2=1
00351    41*          THETA=THETA*PAD
00352    42*          GH=GH*PAD
00353    43*          XI=VINF*COS(GH)
00354    44*          ZI=VINF*SIN(GH)
00355    45*          AMASS=WGTS/G
00356    46*          AMASS=WGT/G
00357    47*          W=W/REV
00360    48*          VLIM=VLIM/REV
00361    49*          Y=YO
00362    50*          Z=ZO
00363    51*          ALI=ALIO
00365    52*          THETII=THETIO
00365    53*    C     ITERATION
00366    54*    50    DO 100 J=1,NM
00371    55*          T1=SIN(GH)
00372    56*          T2=COS(GH)
00373    57*          C1=SIN(THETA)
00374    58*          C2=COS(THETA)
00375    59*          CMV=CMV1+CMV2*OMG*DV/(2.*VINF)
00377    60*          IF(IDEN.EQ.0)GO TO 60
00400    61*          CALL CSUB2(WGT,DEN,ALT,1,RHO,I2,N2)
00401    62*    60    Q=RHO*VINF**2/2.
00402    63*          CD=AIO-AII
00403    64*          CR=0.5*S**2*C1**2/VINF
00404    65*          DR=0.
00405    66*          ALS=0.
00406    67*          DS=0.
00407    68*          TORQ=0.
00410    69*          AMB=0.
00411    70*          AMO=0.
00412    71*          AMT=0.
00413    72*          AMTSF=0.
00414    73*          SFR=0.
00415    74*          FB=0.
00416    75*          FN=0.
00417    76*          FMS=0.
00420    77*          R=RINT
00421    78*          IF(J.NE.NM)GO TO 65
00423    79*          PRINT 2300,T
00426    80*          DO 75 I=1,NDP
00431    81*    65    ALPHA=ATAN(ABS(OMG)*C1*R/VINF)
00432    82*          CS=SIN(ALPHA)
00433    83*          CC=COS(ALPHA)
00434    84*          BETA=ATAN(SQRT(1.-C2**2*CC**2)/(C2*CC))
00435    85*          CB=SIN(BETA)
00436    86*          VB=SQRT(VINF**2+OMG**2*C1**2*R**2)
00437    87*          QB=RHO*VB**2/2.
00440    88*          CS=QB*C*DR
00441    89*          WSS=W*C/(2.*VB)
00442    90*          AMCN=VB*CB/SS
00443    91*          CALL CSUB2(AMACH,WSS*,AMCN,1,WSSR,I1,N1)
00444    92*          CD=CDSS*CB**2
00445    93*          VB=WSSR*CB**2
00446    94*          CL=CLSS*(CL1*WSS/WSS*+CL2*WSS**2/WSSR**2*CB**2)
00447    95*          IF(WSS.GE.VB)CL=CLSS*CB**2
```

```
      IF(CL.LT.0.)CL=0.
      IF(AMCN.GE.1.)CL=0.
      ALPHA=ALPHA+AK*CL*RAD
      C5=SIN(ALPHA)
      C6=COS(ALPHA)
      BETA=ATAN(SQRT(1.-C2**2*C6**2)/(C2*C6))
      C4=SIN(BETA)
      CM=(CM0*C4**2+CM1*WSS/WSSB+CM2*WSS**2/WSSB**2*C4**2)
      CY=CYSS*SIN(2.*BETA)**2
      DBI(I)=CD*C3
      ALBI(I)=CL*C3
      SFBI(I)=CY*C3
      IF(I.GT.IL)ALBI(I)=FLOAT(NDR-I+1)*ALBI(IL)/FLOAT(NDR+1-IL)
      CTNT=C2/C1
      SQS=SQRT(1.+CTNT**2*C5**2)
      C11=CTNT*C5/SQS
      C12=1./SQS
      DSI(I)=ALBI(I)*C12*C5+DBI(I)*C6-SFBI(I)*C11*C5
      TORI(I)=ALBI(I)*C12*C6-DBI(I)*C5-SFBI(I)*C11*C5
      AMBI(I)=CM*C3*C
      FAI(I)=DBI(I)*C6*C2-SFBI(I)*C12*C1-SFBI(I)*C11*C5*C2
      FNI(I)=ALBI(I)*C12*C5*C1+ALBI(I)*C11*C2+DBI(I)*C6*C1+SFBI(I)*C12*C
     12-SFBI(I)*C11*C5*C1
      DB=DB+DBI(I)
      ALB=ALB+ALBI(I)
      DS=DS+DSI(I)
      TORQ=TORQ+TORI(I)
      AMB=AMB+AMBI(I)
      SFB=SFB+SFBI(I)
      FA=FA+FAI(I)
      FN=FN+FNI(I)
      FNS=FNS+FNI(I)*R
      AMT=AMT+DSI(I)*R
      AMQ=AMQ+TORI(I)*R
      AMTSF=AMTSF+SFBI(I)*R
      IF(J.NE.NN)GO TO 75
      ALPHA=ALPHA/RAD
      PRINT 2100,I,R,VB,WSS,DBI(I),ALBI(I),DSI(I),TORI(I),AMBI(I),SFBI(I
     1),CL,FNI(I),ALPHA
   75 R=R+DR
      IF(J.NE.NN)GO TO 80
      PRINT 2200,DB,ALB,DS,TORQ,AMB,SFB,FA,FN
   80 DRAG=AN*DS
      DF=CUS*Q*SV
      OM=OMG
      OMI=OMGI
      TH=THETI
      TA=THETA
      WF=W
      WIF=WI
      XII=(-DRAG-DF)*T2/AMASS
      XT1=XT+XII*DT
      DX=(XT1+XT)*DT*.5
      X=X+DX
      XT=XT1
      ZII=(-DRAG*T1+WGTS-DF*T1)/AMASS
      ZT1=ZT+ZII*DT
      DZ=(ZT1+ZT)*DT*.5
      Z=Z+DZ
      ZT=ZT1
      WT=AMB/AT1-OM*TH*C1*OMI*C2
      W=W+WT*DT
      IF(T.GE.TIME3)W=WLTM
      IF(T.GE.TIME3)WI=0.
      OMGI=      (-AMQ+AT1*WIE*C2-2.*OM*TH*C7*C1*C2-TH*WE*AT1*C1+CMV*Q*
     1SV*DV+CMDO*C8)/(ATH/4.+AT1*C2**2+ATO*C1**2)
      OMG=OMG+OMGI*DT
      THETI=(-AMT*C1-AMTSF*C2+WE*OM*AT1*C1+OM**2*C7*C1*C2+CMDT*TH*C8+AMA
     1SR*DEB*B*OMG**2*C2)/AIO
      THET1=THETT+THETI*DT
      DTH=(THET1+THETT)*DT*.5
      THETA=THETA+DTH
      THETT=THET1
      GH=ATAN(ZT/XT)
      ALT=ALTO-Z
      IF(IVEL.EQ.0)GO TO 85
      VINF=SQRT(XT*XT+ZT*ZT)
   85 IF(IEND.EQ.0)GO TO 90
      IF(ALT.LE.ASTP)GO TO 175
      GO TO 95
   90 IF(T.GE.TSTP)GO TO 175
   95 T=T+DT
  100 CONTINUE
      IF(T.GE.TIME1)NN=NN2
      IF(T.LT.TIME2)GO TO 125
      NN=NN3
        DT=DT2
  125 C9=SIN(THETA)
      C10=COS(THETA)
      OMGR=OMG*RFV
      OMSS=OMG*(R+AL/2.)*C9/VINF
      WR=W*RFV
      THETD=THETA/RAD
      GHD=GH/RAD
```

```
      GV=90.-GHO
      AMCH=VINF/SS
      AMI=ATI*WT
      AMTT=AIO*THETT
      AMX=(ATH/8.+AI1*CIO**2+AIO*C9**2)*OMGT
      PRT=FNC/FN
      RRO=AMO/TOOO
      FA=DS*C10-SFB*C9*AMACR*R*(OMG**2*C9**2*THETI**2)
      FN=DS*C9*SFB*C10-AMACR*R*OMG**2*C9*C10
      FX=FA*C10+FN*C9
      FZ=FA*C9-FN*C10
      F=SQRT(FX*FX+FZ*FZ)
      XIG=XII/G
      ZIG=ZII/G
      ATT=AMT+AMTSF
      ST=3.14*(R+AL*.5)**2*C9**2
      CDT=(DRAG+DF)/(Q*ST)
      CDD=(DRAG+DF)/(Q*SV)
  150 PRINT 2000, X,Z,THETO,OMSS,WO,XI,ZI,THETI,OMGO,WI,XIG,ZIG,THETI,O
     1MGI,Q,FA,FN,FX,FZ,F,AMCH,AMI,AMTT,AMX,DRAG,VINF,ALT,CDD,GV,DF,ATT,
     2AMG,CDT,PRT,RRO
      IF(ISTOP.EQ.1)GO TO 200
      GO TO 50
  175 PRINT 2500,T
      ISTOP=1
      GO TO 175
  200 IF(NRUN.EQ.NR)CALL EXIT
      NR=NR+1
      GO TO 10
C     FORMATS
 1000 FORMAT(5E15.8)
 1010 FORMAT(5I4,3I1,I2)
 2000 FORMAT(13H               ,5H   X=,E15.8,6H    Z=,E15.8,6H   TH=,E15
     1.8,7H  OMSS=,E15.8,6H    W=,E15.8,/5H  XI=,E15.8,6H   ZI=,E15.8,6H
     2  THI=,E15.8,7H  . ,E15.8,6H   WI=,E15.8,/5H XIG=,E15.8,6H  ZIG
     3=,E15.8,6H THIT=,E15.8,7H  OMGT=,E15.8,6H    Q=,E15.8,/5H  FA=,E15
     4.8,6H   FN=,E15.8,6H   FX=,E15.8,7H   FZ=,E15.8,6H    F=,E15.8/5H
     5 MCH=,E15.8,6H   MV=,E15.8,6H   MT=,E15.8,7H   MO=,E15.8,6H DRAG=
     6,E15.8,/5H VIN=,E15.8,6H  ALT=,E15.8,6H   CD=,E15.8,7H   GV=,E15.
     78,6H   DF=,E15.8,/5H ATT=,E15.8,6H  AMO=,E15.8,6H  CDT=,E15.8,7H
     8 PRT=,E15.8,6H  RRO=,E15.8,/)
 2010 FORMAT(6H0 WGT=,E15.8,6H WGTS=,E15.8,6H ALTO=,E15.8,6H VINF=,E15.8
     1,6H  RHO=,E15.8,/)
 2020 FORMAT(6H    S=,E15.8,6H    C=,E15.8,6H    L=,E15.8,6H   ..=,E15.8
     1,6H   GH=,E15.8,/)
 2030 FORMAT(6H   TH=,E15.8,6H   TI=,E15.8,6H   TO=,E15.8,6H   SV=,E15.8
     1,6H   DV=,E15.8,/)
 2040 FORMAT(6H CLSS=,E15.8,6H COSS=,E15.8,6H CYSS=,E15.8,6H  OMG=,E15.8
     1,6H OMGT=,E15.8,/)
 2050 FORMAT(6H  DEB=,E15.8,6H CMV1=,E15.8,6H CMV2=,E15.8,6H CMOT=,E15.8
     1,6H CMOO=,E15.8,/)
 2045 FORMAT(6H  CMO=,E15.8,6H CM1=,E15.8,6H CM2=,E15.8,6H CL1=,E15.8,6H
     1 CL2=,E15.8,/)
 2060 FORMAT(6H  THO=,E15.8,6H  THI=,E15.8,6H    W=,E15.8,6H   WI=,E15.8
     1,6H  COS=,E15.8,//6H THIT=,E15.8,6H WITH=,E15.8,/)
 2070 FORMAT(6H INPUT//)
 2080 FORMAT(5X,5HMACHN,11X,7HUSS,/)
 2090 FORMAT(1H0,5X,6HHEIGHT,8X,7HDENSITY/)
 2100 FORMAT(I3,11(1PE10.3),0PF6.2)
 2200 FORMAT(33X,8(1PE10.3))
 2300 FORMAT(55X,5HTIME=,F7.3//3H I ,8X,1HP,9X,2HVB,7X,3HUSS,8X,2HDR,8X,
     12HLR,8X,2HDS,7X,4HTORQ,7X,2HMR,7X,3HSFR,8X,2HCL,8X,2HFN,5X,5HALPHA
     2/)
 2400 FORMAT(6H PINT=,E15.8,6H   DO=,E15.8,6H   AN=,E15.8,6H   AK=,E15.8
     1,6H   TI=,I3,/)
 2500 FORMAT(55X,5HTIME=,F7.3,//)
      END
```


NOT REPRODUCIBLE

DEFINITIONS OF COMPUTER TERMS

SYSTEM PHYSICAL CHARACTERISTICS:

MACHN - MACH NUMBER OF VELOCITY COMPONENT NORMAL TO BLADE SPIN AXIS ... $\bar{M}$

WSS - ROTOR BLADE TIP SPEED RATIO CORRESPONDING TO MACH NUMBER OF AIRFLOW NORMAL TO BLADE ... Ω_{ss_0}

WGT - WEIGHT OF BLADE (LBS) ... wgt

WGTS - WEIGHT OF STORE (LBS) . . . W_s

ALTO - INITIAL LAUNCH ALTITUDE (FT)

VINF - INITIAL FREE STREAM VELOCITY (FT/SEC) ... V_{∞_0}

RHO - DENSITY OF AIR (CONSTANT OR VARIABLE WITH ALTITUDE) (SLUG/FT^3) ... ρ

S - BLADE PLAN FORM AREA (FT^2) ... S

C - BLADE CHORD (FT) ... C

L BLADE LENGTH (FT) ... ℓ

B - LOCATION OF BLADE MIDPOINT FROM HUB SPIN AXIS, MEASURED ALONG BLADE (FT) ... B

GH - INITIAL FLIGHT PATH ANGLE, OFF HORIZONTAL (DEG.) ... γ_{H_0}

IH - MOMENT OF INERTIA OF HUB ABOUT HUB SPIN AXIS (SLUG-FT^2) ... I_H

II - MOMENT OF INERTIA OF BLADE ABOUT BLADE SPIN AXIS (SLUG-FT^2) ... I_1

IO - MOMENT OF INERTIA OF BLADE ABOUT BLADE/HUB PIVOT POINT (SLUG-FT^2) ... I_0

SV - REFERENCE AREA OF STORE - BUTT END CROSS AREA (FT^2) ... S_v

DV - REFERENCE DIAMETER OF STORE-BUTT END DIAMETER (5 INCHES) (FT) ... d_v

CLSS MAXIMUM BLADE LIFT COEFFICIENT ... $C_{L_{ss_0}}$

CDSS MAXIMUM BLADE DRAG COEFFICIENT ... $C_{D_{ss_0}}$

CYSS MAXIMUM BLADE SIDE FORCE COEFFICIENT ... $C_{Y_{ss_0}}$

OMG - INITIAL HUB SPIN RATE (REV/MIN) ... Ω_0

OMGI - INITIAL HUB SPIN ACCELERATION (RAD/SEC^2) ... $\dot{\Omega}_0$

DEB - RADIUS DISTANCE OF BLADE PIVOT POINT FROM HUB SPIN AXIS (FT)... $\bar{d}$

CMV1 - TURBINE VANE SPIN MOMENT COEFFICIENT ... $C_{m_{V_1}}$ } evaluated in terms of one vane

CMV2 - TURBINE VANE SPIN DAMPING MOMENT COEFFICIENT... $C_{m_{V_2}}$ }

CMDT - BLADE ROTATION DAMPING COEFFICIENT IN θ - PLANE ... $C_{m_{\dot{\theta}}}$

CMO - MAXIMUM BLADE SPIN MOMENT COEFFICIENT ... C_{m_0}

CM1 - BLADE SPIN TRANSIENT COEFFICIENT ... C_{m_1}

CM2 - BLADE SPIN TRANSIENT COEFFICIENT ... C_{m_2}

CL1 BLADE LIFT TRANSIENT COEFFICIENT ... C_{L_1}

CL2 BLADE LIFT TRANSIENT COEFFICIENT ... C_{L_2}

THO - INITIAL BLADE DEPLOYMENT ANGLE (DEG.) ... θ_0

THI - INITIAL BLADE DEPLOYMENT RATE (RAD/SEC) ... $\dot{\theta}_0$

W - INITIAL BLADE SPIN RATE (REV/MIN) ... ω_0

WI - INITIAL BLADE SPIN ACCELERATION (RAD/SEC^2) ... $\dot{\omega}_0$

CDS - STORE BODY DRAG COEFFICIENT ... C_{D_s}

THII - INITIAL BLADE DEPLOYMENT ANGULAR ACCELERATION (RAD/SEC^2) ... $\ddot{\theta}_0$

WLIM - BLADE SPIN RATE LIMIT (REV/MIN) ... ω_{LIM}

RINT - DISTANCE FROM HUB SPIN AXIS TO INITIAL BLADE STATION FOR EVALUATION OF AERODYNAMIC LOADS - MEASURED ALONG BLADE (FT) ... r_0

DR - DISTANCE BETWEEN BLADE STATIONS - MEASURED ALONG BLADE (FT) ... Δr

AN - NUMBER OF BLADES IN SYSTEM ... N

AK - INTERFERENCE FACTOR (DEG) ... K

IL - BLADE STATION AT WHICH LINEAR TIP LOSSES INITIATE

AERODYNAMIC CONDITIONS OVER BLADE SPAN:

NOTE: THE SUBSCRIPT (1) REFERS TO THE PARTICULAR BLADE STATION NUMBER FOR WHICH THE TERM IS COMPUTED.

TIME - TIME AFTER STORE RELEASE (SEC) ... t

I - BLADE STATION (INTEGER) ... 1

R - BLADE STATION AT WHICH AERODYNAMICS ARE EVALUATED - MEASURED ALONG BLADE (FT) ... r_1

VB - TOTAL VELOCITY OVER BLADE AT STATION I (FT/SEC) ... $\bar{V}_1$

WSS - BLADE TIP SPEED RATIO AT STATION I ... $\hat{\omega}_1$

DB - BLADE DRAG FORCE AT STATION I (ACTING OVER A Δr SPAN AREA AROUND STATION I) (LBS) ... D_{B_1}

LB - BLADE LIFT FORCE AT STATION I (LBS) ... L_{B_1}

DS - BLADE DRAG FORCE (IN DIRECTION OF FREE STREAM VELOCITY) AT STATION I - (LBS) ... D_{S_1}

TORQ - BLADE TORQUE FORCE (IN HUB DISK PLANE) AT STATION I(LBS) ... T_{S_1}

MB - BLADE SPIN MOMENT AT STATION I (FT-LBS) ... M_{B_1}

SFB - BLADE SIDE FORCE AT STATION I (LBS) ... SF_{B_1}

CL - BLADE LIFT COEFFICIENT AT STATION I ... C_{L_1}

FN - BLADE NORMAL FORCE (DUE TO AERODYNAMICS) AT STATION I (LBS) ... F_{N_1}

ALPHA - ANGLE OF ATTACK AT STATION I (DEG.) ... $\bar{\alpha}_1$

NOTE: THE SUMMATION OF THE TERMS AT THE VARIOUS STATIONS REPRESENTS THE TOTAL LOAD ACTING ON THE BLADE. THESE TOTAL OR NET LOADS APPEAR BENEATH THE CORRESPONDING COLUMNS FOR DB, LB, DS, TORQ, MB, SFB, FA, AND FN

SYSTEM PERFORMANCE:

X - HORIZONTAL DISTANCE TRAVELED BY STORE (FT) ... X

Z - VERTICAL DISTANCE TRAVELED BY STORE (FT) ... Z

TH - DEPLOYMENT ANGLE OF BLADE (DEG) ... θ

OMSS - TIP SPEED RATIO OF BLADE TIP ABOUT HUB ... $\hat{\Omega}$

W - BLADE SPIN RATE (REV/MIN) ... ω

XI - HORIZONTAL VELOCITY COMPONENT OF STORE (FT/SEC) ... $\dot{X}$

ZI - VERTICAL VELOCITY COMPONENT OF STORE (FT/SEC) ... $\dot{Z}$

THI - DEPLOYMENT RATE OF BLADE (RAD/SEC) ... $\dot{\theta}$

OMG - SPIN RATE OF HUB (REV/MIN) ... Ω

WI - SPIN ACCELERATION OF BLADE (RAD/SEC^2) ... $\dot{\omega}$

XIG - HORIZONTAL ACCELERATION OF STORE (g's) ... $\dot{X}/g$

ZIG - VERTICAL ACCELERATION OF STORE (g's) ... $\dot{Z}/g$

THII - DEPLOYMENT ANGULAR ACCELERATION OF BLADE (RAD/SEC^2) ... $\ddot{\theta}$

OMGI - ANGULAR SPIN ACCELERATION OF HUB (RAD/SEC^2) ... $\dot{\Omega}$

Q - FREE STREAM DYNAMIC PRESSURE (LBS/FT^2) ... q, q_∞

F_A - TOTAL AXIAL FORCE ALONG BLADE SPIN AXIS ACTING AT BLADE BEARING (LBS) ... F_A

F_N - TOTAL NORMAL FORCE TO BLADE SPIN AXIS ACTING AT BLADE BEARING (LBS) ... F_N

F_X - TOTAL FORCE COMPONENT PARALLEL TO STORE CENTER LINE ACTING AT BLADE BEARING (LBS) ... F_X

F_Z - TOTAL FORCE COMPONENT PERPENDICULAR TO STORE CENTER LINE ACTING AT BLADE BEARING (LBS) ... F_Z

F - TOTAL FORCE ACTING AT BLADE BEARING (LBS) ... F

MACH - FREE STREAM MACH NUMBER ... M_∞

MW - TOTAL (NET) SPIN MOMENT ACTING ON BLADE SPIN BEARING (FT-LBS) ... M_ω

MT - TOTAL (NET) MOMENT ACTING ON BLADE BEARING IN DEPLOYMENT ANGLE PLANE (FT-LBS) ... M_θ

MO - TOTAL (NET) MOMENT ACTING ON BLADE BEARING in HUB/DISK PLANE (FT-LBS) ... M_Ω

DRAG - STORE DRAG DUE TO ALL BLADES (LBS) ... D

VINF - FREE STREAM VELOCITY (FT/SEC) ... V_∞

ALT - ALTITUDE (FT) - ... ALT

CD - TOTAL DRAG COEFFICIENT BASED ON STORE DIAMETER ... C_D

GV - FLIGHT PATH ANGLE OFF VERTICAL (DEG) ... γ_v

DF - STORE DRAG DUE TO BODY (LBS) ... D_F

ATT - MOMENT ABOUT BLADE BEARING IN BLADE DEPLOYMENT PLANE DUE TO AERODYNAMIC LOADS ON BLADE (FT-LBS) ... M_{θ_A}

AMO - MOMENT ABOUT BLADE BEARING IN HUB/DISK PLANE DUE TO AERODYNAMIC LOADS ON BLADE (FT-LBS) ... M_{Ω_A}

CDT - TOTAL DRAG COEFFICIENT BASED ON TOTAL SWEPT AREA ... C_{D_T}

RBT - CENTER OF PRESSURE FOR BLADE DEPLOYMENT MOMENT (FT) ... r_{B_θ}

RBO - CENTER OF PRESSURE FOR HUB SPIN MOMENT (FT) ... r_{B_Ω}

APPENDIX B

INPUT CONDITIONS AND SOLUTION PRINTOUTS FOR THE ANALYTICAL SOLUTIONS OF THE STEADY STATE CONDITIONS FOR THE FULL-SCALE AUTOROTOR DECELERATOR IN THE UNIVERSITY OF MARYLAND SUBSONIC WIND TUNNEL

Computer Program Input for the Analytical Computation of the Performance of the Full Scale Autorotor Decelerator as Tested in the University of Maryland Wind Tunnel :

MACHN	WSS
.00000000	.10000000+01
.40000000+00	.10000000+01
.50000000+00	.94000001+00
.60000000+00	.83000000+00
.70000000+00	.65000000+00
.80000000+00	.41000000+00
.90000000+00	.28000000+00
.10000000+01	.20000000+00
.12000000+01	.13000000+00
.20000000+01	.13000000+00

WGT=	.37400000+00	WGTS=	.40000000+00	ALTO=	.50000000+03	VINF=	.10000000+03	RHO=	.23770000-02
S=	.22917000+00	C=	.25000000+00	L=	.91670000+00	R=	.72900000+00	GH=	.00000000
IH=	.27500000-02	II=	.50680000-02	IO=	.61720000-02	SV=	.13628500+00	DV=	.41670000+00
CLSS=	.15500000+01	COSS=	.12500000+01	CYSS=	.67500000+00	OMG=	-.75000000+03	OMGI=	.00000000
DEP=	.00000000	CMY1=	-.34375000-01	CMY2=	-.12971750+00	CMDT=	-.50000000+02	CMD3=	.00000000
CMO=	.20000000+00	CM1=	.15000000+00	CM2=	-.35000000+00	CL1=	.17143000+01	CL2=	-.71430000+00
THO=	.78000000+02	THI=	.00000000	W=	.84000000+04	WI=	.00000000	COS=	.60000000+00
THTI=	.00000000	WLIM=	.10000000+05	RINT=	.31685000+00	RP=	.91700000-01	OFGO=	-.10000000+02
AM=	.60000000+01	AK=	.00000000	TL=	10				

Steady State Conditions, K = 0 :

I	R	VR	WSS	DB	LR	DS	TORQ	MR	SFB	CL	FN	ALPHA
1	3.164-01	1.091+02	1.342+00	3.971-01	4.924-01	5.602-01	2.994-01	-1.783-02	1.779-02	1.518+00	5.609-01	23.59
2	4.085-01	1.148+02	1.276+00	4.402-01	5.458-01	6.499-01	2.570-01	-1.576-02	1.783-02	1.521+00	6.523-01	29.39
3	5.007-01	1.215+02	1.205+00	4.991-01	6.127-01	7.527-01	2.205-01	-1.230-02	1.787-02	1.524+00	7.544-01	34.59
4	5.919-01	1.291+02	1.134+00	5.589-01	6.930-01	8.678-01	1.796-01	-8.678-03	1.790-02	1.527+00	8.708-01	39.21
5	6.836-01	1.374+02	1.065+00	6.346-01	7.869-01	9.970-01	1.327-01	-4.449-03	1.793-02	1.530+00	1.001+00	43.30
6	7.753-01	1.464+02	1.000+00	7.212-01	8.942-01	1.140+00	7.989-02	2.358-04	[illegible]	1.532+00	1.145+00	45.90
7	8.670-01	1.559+02	9.394-01	8.186-01	1.012+00	1.294+00	1.520-02	5.481-03	[illegible]	1.529+00	1.300+00	50.00
8	9.587-01	1.657+02	8.834-01	9.270-01	1.116+00	1.440+00	-7.254-02	1.123-02	[illegible]	1.491+00	1.407+00	52.89
9	1.050+00	1.760+02	8.319-01	1.046+00	1.224+00	1.591+00	-1.726-01	1.768-02	1.823-02	1.453+00	.599+00	55.37
10	1.142+00	1.865+02	7.849-01	1.176+00	1.335+00	1.745+00	-2.849-01	2.422-02	1.899-02	1.404+00	1.754+00	57.58
				7.214+00	8.711+00	1.174+01	6.400-01	7.977-02	1.793-01	5.863-01	1.108+01	

X=	.16445777+03	Z=	.87982165+02	TH=	.80957794+02	OMSS=	-.16366157+01	W=	.11183591+05
XI=	.14955232+02	ZI=	.40754085+02	THI=	.14678259-04	OMG=	-.13378156+04	WI=	.15144347-01
XTG=	-.45717774+00	ZTG=	-.31273499-01	THTI=	.00000000	OMGI=	-.18461846-02	Θ=	.11885000+02
FA=	.16718712+03	FN=	-.11619608+02	FX=	.11937257+02	FZ=	.14323745+03	F=	.14365709+03
MCH=	.90909091-01	MU=	.44866998-05	MT=	.00000000	MO=	-.12653472-04	DRAG=	.44149078+02
VTN=	.10000000+03	ALT=	.41201784+03	CD=	.27856749+02	GV=	.23892636+02	DF=	.97184832+00
ATT=	.91966757+01	AMO=	.72784983-02	COT=	.88543207+00	RBT=	.82162844+00	RHO=	.35316226-02

Steady State Conditions, K = 10 :

I	R	VR	WSS	DB	LR	DS	TORQ	MR	SFB	CL	FN	ALPHA
1	3.164-01	1.035+02	1.163+00	3.466-01	4.298-01	5.108-01	1.959-01	-6.394-03	3.080-02	1.472+00	5.157-01	29.71
2	4.085-01	1.058+02	1.134+00	3.628-01	4.499-01	5.474-01	1.555-01	-5.565-03	2.955-02	1.475+00	5.530-01	33.80
3	5.002-01	1.086+02	1.109+00	3.831-01	4.750-01	5.881-01	1.383-01	-4.597-03	2.831-02	1.479+00	5.944-01	37.71
4	5.919-01	1.118+02	1.076+00	4.074-01	5.052-01	6.329-01	1.016-01	-3.226-03	2.708-02	1.483+00	6.401-01	41.41
5	6.836-01	1.155+02	1.042+00	4.359-01	5.405-01	6.820-01	6.689-02	-1.724-03	2.586-02	1.487+00	6.901-01	44.89
6	7.753-01	1.196+02	1.007+00	4.685-01	5.809-01	7.353-01	2.959-02	-2.994-06	2.466-02	1.491+00	7.445-01	48.15
7	8.670-01	1.240+02	9.709-01	5.051-01	6.263-01	7.930-01	-1.038-02	1.432-03	2.347-02	1.496+00	8.033-01	51.19
8	9.587-01	1.287+02	9.352-01	5.458-01	6.969-01	8.721-01	-4.487-02	4.076-03	2.178-02	1.508+00	8.662-01	54.50
9	1.050+00	1.337+02	9.001-01	5.907-01	7.415-01	9.284-01	-9.856-02	6.430-03	2.093-02	1.522+00	9.415-01	56.82
10	1.142+00	1.390+02	8.660-01	6.396-01	7.860-01	9.865-01	-1.527-01	8.900-03	2.014-02	1.534+00	1.001+00	58.93
				4.606+00	5.874+00	7.276+00	3.039-01	3.959-02	2.526-01	4.757-01	[illegible]	

X=	.20162825+03	Z=	.19875097+02	TH=	.76565117+02	OMSS=	-.10035631+01	W=	.91557299+04
XI=	.40139339+02	ZI=	.61934159+02	THI=	.10314691-04	OMG=	-.82942712+03	WI=	.75685994-02
XTG=	-.44918074+00	ZTG=	.36913570+00	THTI=	.00000000	OMGI=	-.93942723-03	Θ=	.11885000+02
FA=	.54694718+02	FN=	-.55959825+01	FX=	.72764687+01	FZ=	.54899503+02	F=	.54983113+02
MCH=	.90909091-01	MU=	.44412591-05	MT=	.00000000	MO=	-.61339815-05	DRAG=	.29105873+02
VTN=	.10000000+03	ALT=	.39124993+03	CD=	.18569397+02	GV=	.32953956+02	DF=	.97184837+00
ATT=	.59413833+01	AMO=	-.73496587-02	COT=	.57791567+00	RBT=	.78599787+00	RHO=	-.19119574-01

APPENDIX C

COMPUTER SOLUTION PRINTOUTS FOR THE STEADY STATE PERFORMANCE PARAMETER STUDY RUNS LISTED IN TABLE III

RUN 1

I	R	VR	VSS	DB	LR	DS	TORQ	PR	SFB	CL	FN	ALPHA
1	3.332-01	1.042+02	1.156+00	3.216-01	3.988-01	9.788-01	1.599-01	-5.720-03	7.675-02	1.681+00	9.826-01	31.20
2	4.166-01	1.065+02	1.131+00	3.367-01	4.175-01	5.116-01	1.673-01	-4.930-03	2.377-02	1.638+00	5.161-01	35.03
3	5.000-01	1.093+02	1.103+00	3.551-01	4.404-01	5.078-01	1.154-01	-3.956-03	2.280-02	1.687+00	5.523-01	38.69
4	5.834-01	1.125+02	1.071+00	3.769-01	4.674-01	5.874-01	8.721-02	-2.800-03	2.185-02	1.691+00	5.992-01	42.15
5	6.668-01	1.160+02	1.039+00	4.021-01	4.986-01	6.305-01	5.680-02	-1.863-03	2.090-02	1.696+00	6.370-01	45.42
6	7.502-01	1.199+02	1.005+00	4.306-01	5.340-01	6.772-01	2.630-02	5.231-05	1.996-02	1.698+00	6.845-01	48.49
7	8.336-01	1.241+02	9.707-01	4.625-01	5.735-01	7.274-01	-1.059-02	1.741-03	1.903-02	1.701+00	7.355-01	51.36
8	9.170-01	1.286+02	9.368-01	4.977-01	6.170-01	7.842-01	-4.613-02	3.602-03	1.777-02	1.586+00	8.037-01	54.44
9	1.000+00	1.338+02	9.039-01	5.363-01	6.709-01	8.430-01	-8.734-02	5.636-03	1.710-02	1.521+00	8.533-01	56.66
10	1.084+00	1.384+02	8.709-01	5.782-01	7.097-01	8.957-01	-1.338-01	7.435-03	1.648-02	1.495+00	9.044-01	58.68
				6.298+00	5.345+00	6.691+00	3.219-01	-3.824-07	2.044-01	9.237-01	6.763+00	

DIVIDE CHECK FAULT AT 016029

XI=	.27546668+03	ZI=	.26990725+07	THI=	.77312387+02
XIG=	.26879057+02	ZIG=	.90897688+02	THIG=	-.19130436-09
XIGI=	-.18980000+00	ZIGI=	.34037391+00	THIGI=	-.99035346-10
FAI=	.57667198+02	FNI=	-.61291945+01	FRI=	.66910597+01
MCHI=	.90909091-01	MWI=	-.49343125-06	MTI=	-.56803418-12
VINI=	.10000000+03	ALTI=	.23009275+07	CDI=	.00000000
ATTI=	.52027761+01	AMOI=	-.81884628-05	CDTI=	.59538241+00
				OMSSI=	-.9929298?+00
				OMGI=	-.86392016+03
				OMGTI=	.94476548-03
				FZI=	.57604172+02
				GWI=	.16477772+02
				RBTI=	.75717772+00
				WI=	.92065084+06
				MI=	-.75567698-02
				QI=	.11885000+02
				FI=	.57991477+02
				DRAGI=	.26764397+02
				PMOI=	-.25427244-06

RUN 2

I	R	VR	VSS	DB	LR	DS	TORQ	PR	SFB	CL	FN	ALPHA
1	3.332-01	1.042+02	1.163+00	3.060-01	3.794-01	9.692-01	1.612-01	-5.333-03	9.484-02	1.411+00	9.632-01	30.39
2	4.166-01	1.065+02	1.138+00	3.209-01	3.979-01	9.805-01	1.359-01	-4.629-03	9.715-02	1.417+00	9.936-01	34.23
3	5.000-01	1.092+02	1.110+00	3.391-01	4.204-01	5.159-01	1.098-01	-3.744-03	9.546-02	1.423+00	5.297-01	37.92
4	5.834-01	1.123+02	1.079+00	3.606-01	4.471-01	5.532-01	8.746-02	-2.674-03	9.376-02	1.430+00	5.685-01	41.38
5	6.668-01	1.158+02	1.046+00	3.858-01	4.778-01	5.967-01	5.334-02	-1.430-03	9.205-02	1.437+00	6.114-01	44.68
6	7.502-01	1.197+02	1.013+00	4.135-01	5.127-01	6.397-01	2.225-02	-3.101-07	9.033-02	1.445+00	6.578-01	47.77
7	8.336-01	1.238+02	9.786-01	4.449-01	5.517-01	6.887-01	-1.126-02	1.608-03	3.460-02	1.452+00	7.079-01	50.67
8	9.170-01	1.283+02	9.486-01	4.797-01	5.948-01	7.402-01	-4.742-02	3.393-03	3.688-02	1.458+00	7.615-01	53.37
9	1.000+00	1.330+02	9.112-01	5.177-01	6.405-01	8.251-01	-7.875-02	5.334-03	3.962-02	1.553+00	8.503-01	56.77
10	1.084+00	1.379+02	8.787-01	5.591-01	7.183-01	8.737-01	-1.240-01	7.474-03	3.248-02	1.524+00	9.004-01	58.77
				9.127+00	5.181+00	6.369+00	3.040-01	-1.955-07	9.092-01	9.630-01	6.582+00	

XI=	.25037831+03	ZI=	.18957115+07	THI=	.71809355+02
XIG=	.32353142+02	ZIG=	.82070398+02	THIG=	-.18155938-09
XIGI=	-.26353825+00	ZIGI=	.42119403+00	THIGI=	.79724276-10
FAI=	.29404116+02	FNI=	-.29679191+01	FRI=	.63597857+01
MCHI=	.90909091-01	MWI=	-.27313849-06	MTI=	.22737367-12
VINI=	.10000000+03	ALTI=	.31042885+07	CDI=	.00000000
ATTI=	.51087770+01	AMOI=	-.49564987-05	CDTI=	.59576090+00
				OMSSI=	-.98602072+00
				OMGI=	-.88098958+03
				OMGTI=	.95365758-03
				FZI=	.28861109+02
				GWI=	.30690072-05
				RBTI=	.75997507+00
				WI=	.92583033+06
				MI=	-.76026748-02
				QI=	.11885000+02
				FI=	.59553519+02
				DRAGI=	.25439143+02
				PMOI=	-.16304135-06

RUN 3

I	R	VR	VSS	DB	LR	DS	TORQ	PR	SFB	CL	FN	ALPHA
1	3.332-01	1.042+02	1.153+00	3.279-01	4.066-01	9.906-01	1.729-01	-5.850-03	1.445-02	1.510+00	9.921-01	31.50
2	4.166-01	1.066+02	1.128+00	3.430-01	4.258-01	5.239-01	1.460-01	-5.029-03	1.385-02	1.512+00	5.257-01	35.32
3	5.000-01	1.093+02	1.099+00	3.615-01	4.483-01	5.605-01	1.187-01	-4.074-03	1.326-02	1.514+00	5.628-01	38.96
4	5.834-01	1.125+02	1.068+00	3.833-01	4.753-01	6.006-01	8.901-02	-2.836-03	1.268-02	1.516+00	6.033-01	42.42
5	6.668-01	1.161+02	1.036+00	4.085-01	5.066-01	6.482-01	5.814-02	-1.470-03	1.211-02	1.518+00	6.473-01	45.67
6	7.502-01	1.200+02	1.002+00	4.371-01	5.420-01	6.913-01	2.520-02	7.296-05	1.155-02	1.520+00	6.949-01	48.73
7	8.336-01	1.242+02	9.678-01	4.690-01	5.936-01	7.519-01	-6.854-03	1.787-03	1.085-02	1.553+00	7.556-01	51.90
8	9.170-01	1.287+02	9.339-01	5.043-01	6.297-01	7.989-01	-4.724-02	3.674-03	1.042-02	1.532+00	8.037-01	54.33
9	1.000+00	1.339+02	9.006-01	5.429-01	6.659-01	8.487-01	-9.037-02	5.726-03	1.001-02	1.509+00	8.535-01	56.55
10	1.084+00	1.384+02	8.682-01	5.849-01	7.049-01	8.991-01	-1.369-01	7.542-03	9.643-03	1.485+00	9.049-01	58.59
				6.363+00	5.397+00	6.809+00	3.286-01	-7.351-06	1.188-01	3.639-01	6.884+00	

XI=	.23796276+03	ZI=	.18183328+07	THI=	.80383328+02
XIG=	.32948747+02	ZIG=	.77276569+07	THIG=	-.18574169-09
XIGI=	-.26091678+00	ZIGI=	.37112966+00	THIGI=	.51860347-09
FAI=	.11413462+07	FNI=	-.12493063+02	FRI=	.68788988+01
MCHI=	.90909091-01	MWI=	-.73284435-05	MTI=	.59639398-06
VINI=	.10000000+03	ALTI=	.31816672+07	CDI=	.00000000
ATTI=	.52227453+01	AMOI=	-.10908395-07	CDTI=	.59315739+00
				OMSSI=	-.99358906+00
				OMGI=	-.85600990+03
				OMGTI=	.88563896-02
				FZI=	.11460775+03
				GWI=	.22957153+07
				RBTI=	.75553710+00
				WI=	.91810777+06
				MI=	-.62476074-01
				QI=	.11885000+02
				FI=	.11480940+03
				DRAGI=	.27233994+02
				PMOI=	-.33195472-03

RUN 4

I	R	VR	VSS	DB	LR	DS	TORQ	PR	SFB	CL	FN	ALPHA
1	3.708-01	1.064+02	1.146+00	2.389-01	2.912-01	3.591-01	1.051-01	-3.909-03	1.649-02	1.485+00	3.580-01	38.80
2	3.792-01	1.088+02	1.121+00	7.462-01	3.053-01	3.821-01	8.833-02	-3.310-03	1.589-02	1.488+00	3.763-01	38.10
3	3.875-01	1.116+02	1.093+00	2.598-01	3.217-01	4.071-01	7.083-02	-2.608-03	1.529-02	1.491+00	4.005-01	41.25
4	3.958-01	1.147+02	1.064+00	2.745-01	3.408-01	4.341-01	5.739-02	-1.803-03	1.470-02	1.494+00	4.269-01	44.23
5	5.542-01	1.180+02	1.033+00	2.915-01	3.615-01	4.632-01	3.283-02	-8.974-04	1.411-02	1.497+00	4.551-01	47.06
6	6.125-01	1.217+02	1.002+00	3.109-01	3.849-01	4.947-01	1.199-02	1.077-04	1.354-02	1.500+00	4.853-01	49.73
7	6.708-01	1.256+02	9.715-01	3.312-01	4.106-01	5.274-01	-1.030-02	1.211-03	1.296-02	1.503+00	5.175-01	52.23
8	7.291-01	1.296+02	9.408-01	3.538-01	4.509-01	5.721-01	-3.126-02	2.408-03	1.215-02	1.506+00	5.611-01	55.00
9	7.875-01	1.339+02	9.106-01	3.789-01	4.745-01	6.040-01	-5.852-02	3.705-03	1.173-02	1.226+00	5.920-01	56.97
10	8.458-01	1.384+02	8.811-01	4.068-01	5.992-01	6.367-01	-8.740-02	5.094-03	1.135-02	1.501+00	6.238-01	58.78
				3.085+00	3.840+00	4.880+00	1.740-01	-2.552-07	1.582-01	5.018-01	4.793+00	

DIVIDE CHECK FAULT AT 016071

XI=	.23291595+03	ZI=	.12232520+07	THI=	.77383507+02
XIG=	.59123695+02	ZIG=	.75236296+07	THIG=	-.19173358-09
XIGI=	-.30162970+00	ZIGI=	.61633387+00	THIGI=	-.56270910-06
FAI=	.59303655+07	FNI=	-.71535907+01	FRI=	.48803776+01
MCHI=	.90909091-01	MWI=	-.31266799-06	MTI=	-.18917818-08
VINI=	.10000000+03	ALTI=	.37767485+07	CDI=	.00000000
ATTI=	.30759776+01	AMOI=	-.43231994-05	CDTI=	.71828207+00
				OMSSI=	-.9896705?+00
				OMGI=	-.11073840+04
				OMGTI=	.96588505-03
				FZI=	.56554451+02
				GWI=	.29803427-05
				RBTI=	.61490989+00
				WI=	.93136014+06
				MI=	-.76029535-02
				QI=	.11885000+02
				FI=	.59.72810+02
				DRAGI=	.19521455+02
				PMOI=	-.29889817-06

RUN 5

I	R	VR	WSS	DB	LB	DS	TORQ	MR	SFB	CL	FN	ALPHA
1	3.458-01	1.033+02	1.173+00	4.043-01	5.014-01	5.973-01	2.410-01	-7.919-03	4.208-02	1.459+00	5.889-01	29.15
2	4.542-01	1.057+02	1.147+00	4.240-01	5.257-01	6.436-01	2.049-01	-6.976-03	4.033-02	1.463+00	6.332-01	33.46
3	5.625-01	1.085+02	1.11[illegible]+00	4.489-01	5.567-01	6.953-01	1.675-01	-5.642-03	3.859-02	1.468+00	6.829-01	37.57
4	6.708-01	1.120+02	1.082+00	4.792-01	5.942-01	7.526-01	1.281-01	-4.057-03	3.687-02	1.473+00	7.379-01	41.45
5	7.792-01	1.158+02	1.046+00	5.148-01	6.384-01	8.156-01	8.595-02	-2.202-03	3.516-02	1.478+00	7.985-01	45.10
6	8.875-01	1.202+02	1.009+00	5.558-01	6.891-01	8.844-01	4.041-02	-5.267-05	3.346-02	1.483+00	8.647-01	48.50
7	9.958-01	1.248+02	9.707-01	6.020-01	7.465-01	9.590-01	-9.045-03	2.378-03	3.177-02	1.488+00	9.365-01	51.66
8	1.104+00	1.299+02	9.331-01	6.536-01	8.422-01	1.065+00	-5.534-02	5.075-03	2.926-02	1.551+00	1.038+00	55.16
9	1.212+00	1.352+02	8.962-01	7.105-01	8.960-01	1.137+00	-1.164-01	8.056-03	2.808-02	1.523+00	1.108+00	57.53
10	1.321+00	1.408+02	8.606-01	7.727-01	9.526-01	1.212+00	-1.860-01	1.130-02	2.699-02	1.493+00	1.181+00	59.68
				5.566+00	6.943+00	8.762+00	4.990-01	-5.246-07	3.426-01	5.858-01	8.570+00	

X=	.20104146+03	Z=	.15700931+03	TH=	.75529745+02	OMSS=	-.10317025+01	W=	.92578031+04
XI=	.18927508+02	ZI=	.59879966+02	THI=	-.12630048-04	OMG=	-.74025486+03	WI=	-.75761836-02
XIG=	-.25784232+00	ZIG=	.16259466+00	THII=	.11091399-09	OMGI=	.95205228-03	Q=	.11885000+02
FA=	.64216200+02	FN=	-.75227962+01	FX=	.87620223+01	FZ=	.64058876+02	F=	.64655336+02
MCH=	.90909091-01	MW=	-.57882043-06	MT=	.10231815-11	MO=	.88338769-05	DRAG=	.35048090+02
VIN=	.10000000+03	ALT=	.34299069+03	CO=	.00000000	GV=	.17105265+02	DF=	.00000000
ATT=	.81959686+01	AMO=	-.12407079-04	COT=	.53020814+00	RBT=	.90341644+00	RBO=	-.24863491-04

RUN 6

I	R	VR	WSS	DB	LB	DS	TORQ	MR	SFB	CL	FN	ALPHA
1	3.332-01	1.042+02	1.150+00	2.217-01	2.749-01	3.327-01	1.168-01	-2.629-03	4.409-03	1.532+00	3.329-01	31.69
2	4.166-01	1.065+02	1.125+00	2.317-01	2.873-01	3.550-01	9.870-02	-2.256-03	4.221-03	1.533+00	3.553-01	35.49
3	5.000-01	1.093+02	1.097+00	2.440-01	3.026-01	3.795-01	7.995-02	-1.801-03	4.036-03	1.534+00	3.800-01	39.12
4	5.834-01	1.124+02	1.065+00	2.585-01	3.205-01	4.060-01	6.076-02	-1.266-03	3.855-03	1.534+00	4.070-01	42.56
5	6.668-01	1.160+02	1.033+00	2.752-01	3.413-01	4.355-01	3.964-02	-6.520-04	3.677-03	1.535+00	4.363-01	45.80
6	7.502-01	1.199+02	9.997-01	2.942-01	3.648-01	4.670-01	1.756-02	3.974-05	3.504-03	1.536+00	4.680-01	48.84
7	8.336-01	1.241+02	9.658-01	3.159-01	3.927-01	5.010-01	-5.747-03	8.051-04	3.326-03	1.542+00	5.030-01	51.73
8	9.170-01	1.286+02	9.321-01	3.398-01	4.158-01	5.328-01	-3.299-02	1.648-03	3.192-03	1.522+00	5.350-01	54.17
9	1.000+00	1.333+02	8.989-01	3.645-01	4.405-01	5.668-01	-6.107-02	2.552-03	3.067-03	1.500+00	5.682-01	56.41
10	1.084+00	1.383+02	8.666-01	3.903-01	4.655-01	6.072-01	-9.156-02	3.547-03	2.95[illegible]-03	1.477+00	6.074-01	58.46
				2.976+00	3.607+00	4.579+00	2.272-01	-2.734-06	3.624-02	1.827-01	4.588+00	

DIVIDE CHECK FAULT AT 01F074

X=	.33593602+03	Z=	.31449130+03	TH=	.83573321+02	OMSS=	-.99161901+00	W=	.13737412+05
XI=	.45659757+02	ZI	.11476456+03	THI=	-.15191648-04	OMG=	-.84710204+03	WI=	-.70462155-01
XIG=	-.16429423+00	ZIG=	.57450895+00	THII=	-.51362410-04	OMGI=	.70322219-02	Q=	.11885000+02
FA=	.37994924+02	FN=	.39322799+02	FX=	.95297507+01	FZ=	.37708995+02	F=	.37986033+02
MCH=	.90909091-01	MW=	-.27550707-05	MT=	-.40137285-06	MO=	-.70815572-04	DRAG=	.18317403+02
VIN=	.10000000+03	ALT=	.18550813+03	CD=	.00000000	GV=	.21691547+02	DF=	.00000000
ATT=	.34769028+01	AMO=	-.73144712-04	COT=	.39280235+00	RBT=	.75407093+00	RBO=	-.32920742-03

RUN 7

I	R	VR	WSS	DB	LB	DS	TORQ	MR	SFB	CL	FN	ALPHA
1	3.332-01	1.042+02	1.149+00	4.495-01	5.512-01	6.673-01	2.342-01	-1.053-02	6.817-03	1.536+00	6.676-01	31.72
2	4.166-01	1.065+02	1.124+00	4.695-01	5.760-01	7.120-01	1.979-01	-9.035-03	6.524-03	1.537+00	7.124-01	35.52
3	5.000-01	1.093+02	1.096+00	4.891-01	6.064-01	7.611-01	1.603-01	-7.210-03	6.237-03	1.537+00	7.618-01	39.15
4	5.834-01	1.124+02	1.065+00	5.190-01	6.427-01	8.148-01	1.211-01	-5.064-03	5.956-03	1.538+00	8.157-01	42.58
5	6.668-01	1.160+02	1.033+00	5.514-01	6.838-01	8.731-01	7.959-02	-2.605-03	5.680-03	1.539+00	8.74[illegible]-01	45.82
6	7.502-01	1.199+02	9.993-01	5.893-01	7.308-01	9.352-01	3.539-02	1.679-04	5.411-03	1.539+00	9.375-01	48.86
7	8.336-01	1.241+02	9.654-01	6.317-01	7.831-01	1.004+00	-1.197-02	3.237-03	5.148-03	1.540+00	1.006+00	51.69
8	9.170-01	1.286+02	9.317-01	6.795-01	8.301-01	1.068+00	-6.535-02	6.599-03	4.939-03	1.520+00	1.070+00	54.14
9	1.000+00	1.333+02	8.986-01	7.297-01	8.797-01	1.174+00	-1.224-01	1.025-02	4.745-03	1.499+00	1.136+00	56.38
10	1.084+00	1.383+02	8.663-01	7.954-01	9.317-01	1.207+00	-1.837-01	1.429-02	4.566-03	1.475+00	1.204+00	58.43
				5.892+00	7.215+00	9.172+00	4.455-01	-7.355-06	5.602-02	3.294-01	9.184+00	

X=	.19764756+03	Z=	.20384695+03	TH=	.84720434+02	OMSS=	-.99113984+00	W=	.68636815+04
XI=	.86210250+01	ZI=	.57056799+02	THI=	-.13807627-04	OMG=	-.84595605+03	WI=	-.19762982-01
XIG=	-.13570762+00	ZIG=	.92911612-01	THII=	.12277594-03	OMGI=	.52101953-02	Q=	.11885000+02
FA=	.75782794+02	FN=	.16807475+01	FX=	.91718365+01	FZ=	.75244484+02	F=	.75801417+02
MCH=	.90909091-01	MW=	-.24427046-05	MT=	.23545971-05	MO=	.10220519-03	DRAG=	.36687347+02
VIN=	.10000000+03	ALT=	.25615305+03	CD=	.00000000	GV=	.85081142+01	DF=	.00000000
ATT=	.69501340+01	AMO=	-.10584481-05	COT=	.78443495+00	RBT=	.75374725+00	RBO=	-.23760853-03

RUN 8

I	R	VR	WSS	DB	LB	DS	TORQ	MR	SFB	CL	FN	ALPHA
1	3.332-01	5.212+01	1.156+00	8.040-02	9.970-02	1.197-01	4.244-02	-1.430-03	6.188-03	1.461+00	1.207-01	31.20
2	4.166-01	5.327+01	1.131+00	8.417-02	1.044-01	1.279-01	3.582-02	-1.233-03	5.943-03	1.484+00	1.290-01	35.03
3	5.000-01	5.465+01	1.103+00	8.878-02	1.101-01	1.369-01	2.898-02	-9.897-04	5.701-03	1.487+00	1.382-01	38.69
4	5.834-01	5.624+01	1.071+00	9.423-02	1.169-01	1.469-01	2.181-02	-7.001-04	5.462-03	1.491+00	1.483-01	42.15
5	6.668-01	5.802+01	1.039+00	1.005-01	1.247-01	1.576-01	1.420-02	-3.656-04	5.724-03	1.494+00	1.593-01	45.42
6	7.502-01	5.997+01	1.005+00	1.077-01	1.335-01	1.693-01	6.074-03	1.301-05	4.990-03	1.498+00	1.711-01	48.49
7	8.336-01	6.208+01	9.707-01	1.156-01	1.434-01	1.818-01	-2.649-03	4.357-04	4.758-03	1.501+00	1.839-01	51.36
8	9.170-01	6.432+01	9.368-01	1.244-01	1.585-01	1.985-01	-1.103-02	9.004-04	4.442-03	1.546+00	2.009-01	54.44
9	1.000+00	6.670+01	9.034-01	1.341-01	1.677-01	2.107-01	-2.184-02	1.409-03	4.275-03	1.521+00	2.133-01	56.66
10	1.084+00	6.919+01	8.709-01	1.436-01	1.774-01	2.233-01	-3.335-02	1.959-03	4.120-03	1.495+00	2.261-01	58.68
				1.074+00	1.336+00	1.673+00	8.046-02	-7.361-07	5.110-02	1.059-01	1.691+00	

X=	.19029092+03	Z=	.35641003+03	TH=	.77312570+02	OMSS=	-.99294665+00	W=	.46033008+04
XI=	.32614803+02	ZI=	.13957520+03	THI=	-.14915292-04	OMG=	-.43196709+03	WI=	-.12790693-01
XIG=	-.38071476-01	ZIG=	.83711050+00	THII=	-.66907714-04	OMGI=	.16577209-02	Q=	.29712500+01
FA=	.14417278+02	FN=	-.15310890+01	FX=	.16727949+01	FZ=	.14401524+02	F=	.14498350+02
MCH=	.45454545-01	MW=	-.75055789-06	MT=	-.38400[illegible]8-06	MO=	.11315271-04	DRAG=	.66911798+01
VIN=	.50000000+02	ALT=	.14358997+03	CO=	.00000000	GV=	.13152416+02	DF=	.00000000
ATT=	.13005353+01	AMO=	-.12706034-04	COT=	.59538873+00	RBT=	.75712305+00	RBO=	-.15792339-03

RUN 9

I	R	VR	VSS	DB	LR	DS	TORQ	MR	SFB	CL	FN	ALPHA
1	3.332-01	2.088+02	1.161+00	1.293+00	1.603+00	1.940+00	6.895-01	-2.392-02	9.626-02	1.483+00	1.915+00	31.55
2	4.166-01	2.136+02	1.135+00	1.355+00	1.681+00	2.079+00	5.832-01	-2.061-02	9.235-02	1.486+00	2.050+00	35.44
3	5.000-01	2.194+02	1.105+00	1.432+00	1.776+00	2.232+00	4.728-01	-1.653-02	8.849-02	1.489+00	2.198+00	39.16
4	5.834-01	2.260+02	1.073+00	1.523+00	1.889+00	2.400+00	3.564-01	-1.169-02	8.466-02	1.493+00	2.362+00	42.67
5	6.668-01	2.334+02	1.039+00	1.628+00	2.019+00	2.584+00	2.325-01	-6.107-03	8.088-02	1.496+00	2.540+00	45.97
6	7.502-01	2.414+02	1.004+00	1.747+00	2.167+00	2.787+00	9.939-02	2.325-04	7.715-02	1.500+00	2.732+00	49.07
7	8.336-01	2.502+02	9.694-01	1.880+00	2.430+00	3.072+00	-1.747-02	7.272-03	7.143-02	1.567+00	3.015+00	52.59
8	9.170-01	2.595+02	9.346-01	2.027+00	2.575+00	3.272+00	-1.844-01	1.506-02	6.659-02	1.543+00	3.209+00	55.01
9	1.000+00	2.693+02	9.005-01	2.188+00	2.729+00	3.479+00	-3.629-01	2.356-02	6.596-02	1.518+00	3.411+00	57.23
10	1.084+00	2.796+02	8.673-01	2.363+00	2.890+00	3.692+00	-5.535-01	3.274-02	6.352-02	1.492+00	3.618+00	59.25
				1.744+01	2.176+01	2.753+01	1.316+00	7.679-07	7.493-01	1.704+00	2.705+01	

X=	.89692713+01	Z=	.15509317+03	TH=	.77474646+02	OMSS=	-.10141413+01	W=	.18526594+05		
XI=	-.19051329+03	ZI=	.12610684+03	THI=	.13709333-04	OMG=	-.17636339+04	WI=	.15158137-01		
XIG=	-.22960742+01	ZIG=	.25194570+01	THII=	.79724276-10	OMGI=	-.18414609-02	Q=	.47539999+02		
FA=	.24052992+03	FN=	-.25231547+02	FX=	.27533082+02	FZ=	.24027734+03	F=	.24184969+03		
MCH=	.18181818+00	MW=	.88947916-06	MT=	.45474734-12	MO=	-.11228839-04	DRAG=	.11013233+03		
VIN=	.20000000+03	ALT=	.34490683+03	CO=	.00000000	GV=	.12350195+03	OF=	.00000000		
ATT=	.21015813+02	AMO=	.15988946-04	COT=	.61170673+00	RBT=	.75792917+00	RRO=	.12153708-04		

RUN 10

I	R	VR	VSS	DB	LR	DS	TORQ	MR	SFB	CL	FN	ALPHA
1	3.332-01	1.042+02	1.153+00	1.597-01	2.036-01	2.456-01	8.656-02	-2.929-03	7.269-03	1.510+00	2.463-01	31.50
2	4.166-01	1.066+02	1.129+00	1.717-01	2.179-01	2.622-01	7.708-02	-2.518-03	5.968-03	1.512+00	2.632-01	35.32
3	5.000-01	1.093+02	1.099+00	1.910-01	2.244-01	2.806-01	5.915-02	-2.014-03	6.671-03	1.514+00	2.817-01	38.96
4	5.834-01	1.125+02	1.068+00	1.919-01	2.380-01	2.906-01	4.655-02	-1.420-03	6.379-03	1.516+00	3.020-01	42.42
5	6.668-01	1.161+02	1.036+00	2.085-01	2.535-01	3.225-01	2.910-02	-7.360-04	5.092-03	1.518+00	3.240-01	45.67
6	7.502-01	1.200+02	1.002+00	2.188-01	2.713-01	3.461-01	1.261-02	3.633-05	5.810-03	1.520+00	3.479-01	48.73
7	8.336-01	1.242+02	9.678-01	2.348-01	2.972-01	3.761-01	-3.027-03	9.043-04	5.057-03	1.553+00	3.783-01	51.90
8	9.170-01	1.287+02	9.379-01	2.524-01	3.148-01	3.920-01	-2.365-02	1.839-03	5.239-03	1.532+00	4.024-01	54.33
9	1.000+00	1.334+02	9.006-01	2.718-01	3.334-01	4.285-01	-4.524-02	2.857-03	5.037-03	1.509+00	4.273-01	56.55
10	1.084+00	1.384+02	8.692-01	2.928-01	3.579-01	4.501-01	-6.827-02	3.876-03	4.859-03	1.485+00	4.530-01	58.59
				2.184+00	2.702+00	3.408+00	1.695-01	-4.959-06	5.977-02	1.825-01	3.026+00	

X=	.31597862+03	Z=	.22259469+03	TH=	.80359987+02	OMSS=	-.99361884+00	W=	.91813983+04
XI=	.63421371+03	ZI=	.10519984+03	THI=	-.28059820-04	OMG=	-.85649096+03	WI=	-.84921103-01
XIG=	-.17612133+00	ZIG=	.70820012+00	THII=	.85278336-04	OMGI=	.12396698-01	Q=	.59499999+01
FA=	.56987137+02	FN=	-.52228709+01	FX=	.74983111+01	FZ=	.57274438+02	F=	.57325848+02
MCH=	.90909091-01	MW=	-.49976835-05	MT=	.25989766-05	MO=	.76929993-04	DRAG=	.13633247+02
VIN=	.10000000+03	ALT=	.27741551+03	CO=	.00000000	GV=	.31106114+02	OF=	.00000000
ATT=	.26147276+01	AMO=	-.50026344-05	COT=	.59319865+00	RBT=	.75554708+00	RRO=	-.49207426-03

RUN 11

I	R	VR	VSS	DB	LR	DS	TORQ	MR	SFB	CL	FN	ALPHA
1	3.332-01	1.042+02	1.163+00	6.127-01	7.597-01	8.995-01	3.227-01	-1.068-02	9.791-02	1.411+00	9.235-01	30.39
2	4.166-01	1.066+02	1.138+00	6.475-01	7.967-01	9.621-01	2.772-01	-9.268-03	9.453-02	1.417+00	9.883-01	34.22
3	5.000-01	1.092+02	1.110+00	6.789-01	8.418-01	1.031+00	2.189-01	-7.497-03	9.114-02	1.423+00	1.060+00	37.90
4	5.834-01	1.123+02	1.079+00	7.219-01	8.952-01	1.109+00	1.651-01	-5.362-03	8.774-02	1.430+00	1.138+00	41.38
5	6.668-01	1.158+02	1.046+00	7.716-01	9.558-01	1.191+00	1.059-01	-2.863-03	8.431-02	1.437+00	1.224+00	44.68
6	7.502-01	1.197+02	1.017+00	8.279-01	1.027+00	1.281+00	4.454-02	-8.619-07	8.386-02	1.444+00	1.317+00	47.77
7	8.336-01	1.238+02	9.786-01	8.909-01	1.105+00	1.378+00	-2.256-02	3.220-03	7.740-02	1.451+00	1.418+00	50.67
8	9.170-01	1.283+02	9.446-01	9.604-01	1.191+00	1.482+00	-9.496-02	6.798-03	7.394-02	1.458+00	1.525+00	53.37
9	1.000+00	1.330+02	9.113-01	1.037+00	1.363+00	1.652+00	-1.569-01	1.069-02	6.740-02	1.557+00	1.703+00	56.77
10	1.084+00	1.379+02	8.787-01	1.119+00	1.438+00	1.749+00	-2.483-01	1.496-02	6.511-02	1.524+00	1.803+00	58.77
				8.263+00	1.037+01	1.273+01	6.097-01	-3.860-07	8.203-01	9.272-01	1.310+01	

X=	.17755083+03	Z=	.97577703+03	TH=	.71798363+02	OMSS=	-.98600245+00	W=	.92584244+04
XI=	.13695484+03	ZI=	.10519912+03	THI=	-.14458818-04	OMG=	-.88102870+03	WI=	-.75506211-02
XIG=	-.80707042-01	ZIG=	-.27028756+00	THII=	-.79724276-10	OMGI=	.94515401-03	Q=	.23800000+02
FA=	.58811210+02	FN=	-.59371598+01	FX=	.17734110+02	FZ=	.57721773+02	F=	.59109773+02
MCH=	.90909091-01	MW=	-.94307044-05	MT=	-.45474730-12	MO=	.54920590-05	DRAG=	.50936442+02
VIN=	.10000000+03	ALT=	.40242780+03	CO=	.00000000	GV=	.49104647+01	OF=	.00000000
ATT=	.10730030+02	AMO=	-.93467574-05	COT=	.59676527+00	RBT=	.75998674+00	RRO=	-.15355739-04

RUN 12

I	R	VR	VSS	DB	LR	DS	TORQ	MR	SFB	CL	FN	ALPHA
1	3.332-01	1.042+02	1.130+00	3.221-01	3.995-01	4.825-01	1.747-01	-2.201-03	2.381-02	1.484+00	4.763-01	31.22
2	4.166-01	1.065+02	1.105+00	3.372-01	4.187-01	5.162-01	1.487-01	-1.915-03	2.287-02	1.487+00	5.090-01	35.04
3	5.000-01	1.093+02	1.077+00	3.556-01	4.410-01	5.533-01	1.219-01	-1.361-03	2.193-02	1.490+00	5.450-01	38.70
4	5.834-01	1.125+02	1.047+00	3.774-01	4.680-01	5.939-01	9.356-02	-1.134-03	2.101-02	1.493+00	5.845-01	42.16
5	6.668-01	1.160+02	1.015+00	4.026-01	4.992-01	6.381-01	6.354-02	-6.284-04	2.009-02	1.497+00	6.275-01	45.43
6	7.502-01	1.199+02	9.819-01	4.310-01	5.345-01	6.859-01	3.140-02	-3.960-05	1.919-02	1.500+00	6.740-01	48.49
7	8.336-01	1.241+02	9.485-01	4.629-01	5.613-01	7.275-01	-6.849-03	6.321-04	1.856-02	1.470+00	7.194-01	51.03
8	9.170-01	1.286+02	9.154-01	4.981-01	5.816-01	7.641-01	-4.982-02	1.392-03	1.814-02	1.415+00	7.501-01	53.16
9	1.000+00	1.334+02	8.828-01	5.366-01	6.031-01	8.016-01	-9.516-02	2.249-03	1.778-02	1.368+00	7.857-01	55.11
10	1.084+00	1.383+02	8.510-01	5.785-01	6.256-01	8.400-01	-1.430-01	3.205-03	1.746-02	1.319+00	8.241-01	56.90
				4.302+00	5.132+00	6.603+00	3.389-01	-1.998-06	2.008-01	4.261-01	6.492+00	

X=	.24570680+03	Z=	.18552439+03	TH=	.77565451+02	OMSS=	-.99235535+00	W=	.89945038+04
XI=	.34513720+02	ZI=	.79541170+02	THI=	.14598123-04	OMG=	-.86257104+03	WI=	-.32337609-01
XIG=	-.26293357+00	ZIG=	.39928192+00	THII=	-.29218681-03	OMGI=	.19071725-02	Q=	.11885000+02
FA=	.57557488+02	FN=	-.59293659+01	FX=	.66032450+01	FZ=	.57494076+02	F=	.57862093+02
MCH=	.90909091-01	MW=	-.18975730-05	MT=	-.13901523-05	MO=	.11636781-04	DRAG=	.26412980+02
VIN=	.10000000+03	ALT=	.31397561+03	CO=	.00000000	GV=	.23956509+02	OF=	.00000000
ATT=	.50958462+01	AMO=	-.96447766-05	COT=	.58640970+00	RBT=	.75097798+00	RRO=	-.28462277-04

RUN 13

I	Q	VB	WSS	DB	LB	DS	TORQ	MR	SFB	CL	FN	ALPHA
1	3.332-01	1.041+02	8.471-01	3.240-01	4.018-01	4.828-01	1.735-01	-2.106-03	1.931-02	1.497+00	4.853-01	31.07
2	4.166-01	1.063+02	8.294-01	3.386-01	4.198-01	5.150-01	1.473-01	-1.834-03	1.854-02	1.499+00	5.189-01	34.84
3	5.000-01	1.090+02	8.091-01	3.564-01	4.419-01	5.505-01	1.203-01	-1.496-03	1.778-02	1.501+00	5.539-01	38.44
4	5.834-01	1.121+02	7.869-01	3.774-01	4.680-01	5.892-01	9.204-02	-1.087-03	1.704-02	1.504+00	5.931-01	41.86
5	6.668-01	1.155+02	7.634-01	4.016-01	4.980-01	6.313-01	6.219-02	-6.037-04	1.630-02	1.507+00	6.358-01	45.09
6	7.502-01	1.193+02	7.392-01	4.291-01	5.321-01	6.768-01	3.038-02	-4.023-05	1.557-02	1.509+00	6.820-01	48.13
7	8.336-01	1.234+02	7.147-01	4.599-01	5.571-01	7.157-01	-7.458-03	6.033-04	1.507-02	1.477+00	7.213-01	50.62
8	9.170-01	1.277+02	6.903-01	4.938-01	5.763-01	7.507-01	-4.945-02	1.333-03	1.473-02	1.427+00	7.567-01	52.74
9	1.000+00	1.324+02	6.662-01	5.311-01	5.977-01	7.866-01	-9.368-02	2.154-03	1.443-02	1.377+00	7.929-01	54.70
10	1.084+00	1.372+02	6.427-01	5.715-01	6.196-01	8.234-01	-1.403-01	3.072-03	1.417-02	1.328+00	8.299-01	56.49
				4.283+00	5.113+00	6.572+00	3.348-[illegible]	-5.282-06	1.629-01	3.987-01	6.569+00	

DIVIDE CHECK FAULT AT 016074

X=	.20699200+03	Z=	.11246792+07	TH=	.78859309+02	OMSS=	-.97505148+00	W=	.67361490+04
XI=	.45054379+02	ZI=	.56470791+02	THI=	-.14508287-04	OMG=	-.84354543+03	WI=	-.89839245-01
XIG=	-.36620606+00	ZIG=	.46037602+00	THII=	.14363512-03	OMGI=	.75157646-02	Q=	.11885000+02
FA=	.55489689+02	FN=	-.42792380+01	FX=	.65220891+01	FZ=	.55265987+02	F=	.55649461+02
MCH=	.90909091-01	MW=	-.52717669-05	MT=	.82446558-06	MO=	.45243719-04	DRAG=	.26088357+02
VIN=	.10000000+03	ALT=	.38703208+03	CD=	.00000000	GV=	.34145720+02	DF=	.00000000
ATT=	.49988593+01	AMO=	-.49473718-04	COT=	.57376892+00	RBT=	.74957654+00	PRO=	-.14778069-03

RUN 14

I	Q	VB	WSS	DB	LB	DS	TORQ	MR	SFB	CL	FN	ALPHA
1	3.332-01	1.041+02	1.396+00	3.173-01	3.934-01	4.702-01	1.702-01	-2.150-03	2.999-02	1.466+00	4.755-01	30.72
2	4.166-01	1.063+02	1.367+00	3.317-01	4.114-01	5.018-01	1.445-01	-1.867-03	2.886-02	1.470+00	5.077-01	34.49
3	5.000-01	1.089+02	1.334+00	3.494-01	4.333-01	5.366-01	1.183-01	-1.518-03	2.774-02	1.474+00	5.432-01	38.10
4	5.834-01	1.120+02	1.297+00	3.703-01	4.592-01	5.747-01	9.042-02	-1.099-03	2.662-02	1.478+00	5.821-01	41.53
5	6.668-01	1.154+02	1.259+00	3.944-01	4.891-01	6.161-01	6.114-02	-6.050-04	2.552-02	1.482+00	6.244-01	44.76
6	7.502-01	1.192+02	1.219+00	4.217-01	5.230-01	6.610-01	2.992-02	-3.126-05	2.442-02	1.486+00	6.701-01	47.81
7	8.336-01	1.232+02	1.179+00	4.523-01	5.502-01	7.012-01	-6.683-03	6.212-04	2.361-02	1.462+00	7.110-01	50.38
8	9.170-01	1.276+02	1.139+00	4.860-01	5.696-01	7.356-01	-4.830-02	1.356-03	2.310-02	1.412+00	7.460-01	52.51
9	1.000+00	1.322+02	1.099+00	5.230-01	5.901-01	7.709-01	-9.214-02	2.183-03	2.265-02	1.363+00	7.817-01	54.47
10	1.084+00	1.370+02	1.061+00	5.632-01	6.116-01	8.070-01	-1.383-01	3.104-03	2.226-02	1.315+00	8.184-01	56.27
				4.209+00	5.031+00	6.375+00	3.289-01	-6.106-06	2.548-01	4.417-01	6.460+00	

X=	.25184932+03	Z=	.18867010+07	TH=	.75998818+02	OMSS=	-.97192156+00	W=	.11099306+05
XI=	.36584755+02	ZI=	.81638395+02	THI=	.14997276-04	OMG=	-.85025304+03	WI=	-.10187094+00
XIG=	-.26138422+00	ZIG=	.41854378+00	THII=	-.13873732-03	OMGI=	.36713722-02	Q=	.11885000+02
FA=	.55330981+02	FN=	-.72265263+01	FX=	.63750533+01	FZ=	.55435537+02	F=	.55800897+02
MCH=	.90909091-01	MW=	-.59777865-05	MT=	-.79635219-06	MO=	.22147086-04	DRAG=	.25500214+02
VIN=	.10000000+03	ALT=	.31132990+07	CD=	.00000000	GV=	.24197083+02	DF=	.00000000
ATT=	.49552525+01	AMO=	-.21019951-04	COT=	.57346904+00	RBT=	.75013691+00	PRO=	-.63921646-04

RUN 15

I	Q	VB	WSS	DB	LB	DS	TORQ	MR	SFB	CL	FN	ALPHA
1	3.332-01	1.032+02	1.085+00	3.132-01	3.132-01	4.172-01	1.386-01	-1.699-03	2.960-02	1.187+00	4.202-01	26.18
2	4.166-01	1.050+02	1.067+00	3.246-01	3.246-01	4.397-01	1.172-01	-1.472-03	2.883-02	1.189+00	4.432-01	29.58
3	5.000-01	1.071+02	1.046+00	3.385-01	3.385-01	4.585-01	9.525-02	-1.194-03	2.807-02	1.191+00	4.684-01	32.86
4	5.834-01	1.095+02	1.023+00	3.549-01	3.549-01	4.915-01	7.255-02	-8.609-04	2.731-02	1.194+00	4.978-01	36.01
5	6.668-01	1.123+02	9.975-01	3.738-01	3.738-01	5.207-01	4.887-02	-4.700-04	2.656-02	1.197+00	5.265-01	39.02
6	7.502-01	1.153+02	9.712-01	3.953-01	3.953-01	5.572-01	2.382-02	-1.808-05	2.581-02	1.199+00	5.575-01	41.87
7	8.336-01	1.186+02	9.441-01	4.193-01	4.116-01	5.807-01	-5.789-03	4.942-04	2.524-02	1.180+00	5.864-01	44.35
8	9.170-01	1.222+02	9.165-01	4.458-01	4.239-01	6.068-01	-3.913-02	1.070-03	2.484-02	1.146+00	6.127-01	46.54
9	1.000+00	1.260+02	8.891-01	4.749-01	4.371-01	6.335-01	-7.420-02	1.716-03	2.447-02	1.111+00	6.397-01	48.57
10	1.084+00	1.300+02	8.619-01	5.069-01	4.509-01	6.510-01	-1.111-01	2.433-03	2.414-02	1.077+00	6.674-01	50.47
				3.947+00	3.824+00	5.368+00	2.659-01	-5.610-07	2.649-01	4.273-01	5.417+00	

DIVIDE CHECK FAULT AT 016074

X=	.31215656+03	Z=	.29826134+03	TH=	.76574246+02	OMSS=	-.86152701+00	W=	.85567069+04
XI=	.38055373+02	ZI=	.10605711+07	THI=	-.12251565-04	OMG=	-.75183324+03	WI=	-.10278474-01
XIG=	-.18133711+00	ZIG=	.49978211+00	THII=	.19764749-04	OMGI=	.95442105-03	Q=	.11885000+02
FA=	.43446428+02	FN=	-.48524681+01	FX=	.53677578+01	FZ=	.43385777+02	F=	.43716570+02
MCH=	.90909091-01	MW=	-.60364088-05	MT=	.11057966-06	MO=	.57825700-05	DRAG=	.21471033+02
VIN=	.10000000+03	ALT=	.20173862+07	CD=	.00000000	GV=	.19738981+02	DF=	.00000000
ATT=	.41766545+01	AMO=	-.77746809-05	COT=	.49049748+00	RBT=	.74411083+00	PRO=	-.29236204-04

RUN 16

I	Q	VB	WSS	DB	LB	DS	TORQ	MR	SFB	CL	FN	ALPHA
1	3.332-01	1.045+02	1.142+00	3.242-01	4.539-01	5.182-01	1.927-01	-2.354-03	2.256-02	1.676+00	5.227-01	33.70
2	4.166-01	1.070+02	1.116+00	3.404-01	4.765-01	5.562-01	1.639-01	-2.050-03	2.148-02	1.680+00	5.615-01	37.64
3	5.000-01	1.099+02	1.086+00	3.602-01	5.042-01	5.982-01	1.340-01	-1.673-03	2.042-02	1.683+00	6.042-01	41.39
4	5.834-01	1.133+02	1.053+00	3.836-01	5.370-01	6.442-01	1.026-01	-1.217-03	1.937-02	1.687+00	6.510-01	44.94
5	6.668-01	1.171+02	1.019+00	4.105-01	5.747-01	6.943-01	6.915-02	-6.760-04	1.834-02	1.691+00	7.020-01	48.27
6	7.502-01	1.212+02	9.846-01	4.411-01	6.176-01	7.496-01	3.331-02	-4.545-05	1.733-02	1.695+00	7.572-01	51.35
7	8.336-01	1.257+02	9.496-01	4.753-01	6.508-01	7.954-01	-8.477-03	6.747-04	1.662-02	1.662+00	8.048-01	53.92
8	9.170-01	1.305+02	9.149-01	5.131-01	6.755-01	8.354-01	-5.505-02	1.490-03	1.619-02	1.601+00	8.454-01	55.98
9	1.000+00	1.355+02	8.810-01	5.544-01	7.015-01	8.765-01	-1.041-01	2.410-03	1.581-02	1.542+00	8.869-01	57.86
10	1.084+00	1.408+02	8.481-01	5.994-01	7.287-01	9.184-01	-1.557-01	3.438-03	1.548-02	1.484+00	9.294-01	59.57
				4.492+00	5.920+00	7.185+00	3.723-01	-1.357-06	1.836-01	4.182-01	7.265+00	

X=	.23330691+03	Z=	.17823694+07	TH=	.77607396+02	OMSS=	-.10282121+01	W=	.91197034+04
XI=	.24939612+02	ZI=	.74489667+02	THI=	.13488410-04	OMG=	-.89359430+03	WI=	-.21629372-01
XIG=	-.26807119+00	ZIG=	.31332774+00	THII=	-.45580381-04	OMGI=	.12094983-02	Q=	.11885000+02
FA=	.61838953+02	FN=	-.62309946+01	FX=	.71854994+01	FZ=	.61735312+02	F=	.62152072+02
MCH=	.90909091-01	MW=	-.12692116-05	MT=	-.25220539-06	MO=	.73819725-05	DRAG=	.28791999+02
VIN=	.10000000+03	ALT=	.32176306+07	CD=	.00000000	GV=	.21896659+02	DF=	.00000000
ATT=	.55297297+01	AMO=	-.53793192-05	COT=	.63791196+00	RBT=	.75207203+00	PRO=	-.14449774-04

RUN 17

I	R	VR	VRS	DB	LR	DS	TORQ	MR	SFB	CL	FN	ALPHA
1	3.732-01	1.051+02	1.200+00	2.715-01	4.208-01	4.605-01	1.887-01	-3.088-03	1.545-02	1.507+00	4.636-01	34.66
2	4.166-01	1.095+02	1.160+00	2.892-01	4.482-01	4.907-01	1.621-01	-2.711-03	1.467-02	1.510+00	5.078-01	39.08
3	5.000-01	1.134+02	1.124+00	3.108-01	4.817-01	5.528-01	1.387-01	-2.234-03	1.390-02	1.513+00	5.569-01	43.23
4	5.834-01	1.178+02	1.081+00	3.363-01	5.214-01	6.063-01	1.046-01	-1.646-03	1.318-02	1.515+00	6.110-01	47.08
5	6.668-01	1.228+02	1.034+00	3.658-01	5.670-01	6.689-01	7.233-02	-9.381-04	1.240-02	1.518+00	6.703-01	50.64
6	7.502-01	1.281+02	9.843-01	3.992-01	6.187-01	7.287-01	3.719-02	-1.021-04	1.167-02	1.521+00	7.349-01	53.91
7	8.336-01	1.339+02	9.316-01	4.365-01	6.552-01	7.799-01	-6.248-03	8.651-04	1.125-02	1.475+00	7.867-01	56.43
8	9.170-01	1.400+02	9.107-01	4.778-01	6.889-01	8.255-01	-5.459-02	1.974-03	1.098-02	1.411+00	8.327-01	58.51
9	1.000+00	1.463+02	8.706-01	5.230-01	7.161-01	8.721-01	-1.058-01	3.232-03	1.075-02	1.389+00	8.798-01	60.39
10	1.084+00	1.530+02	8.379-01	5.721-01	7.485-01	9.197-01	-1.601-01	4.647-03	1.055-02	1.291+00	9.277-01	62.08
				3.982+00	5.862+00	6.915+00	3.724-01	-1.363-06	1.247-01	2.961-01	6.971+00	

X=	.24099120+03	Z=	.1818[illegible]02+07	THI=	.79867119+02	OMGS=	-.12014172+01
XI=	.32366460+02	ZI=	.77019575+02	THT=	.13027610-08	OMG=	-.10359530+00
XIG=	-.26708619+00	ZIG=	.36257188+00	THII=	.67505026-05	OMGI=	.10849027-02
FA=	.83660760+02	FN=	-.7925261+01	FX=	.69147067+01	FY=	.83750552+02
MCH=	.90909091-01	MW=	-.17659905-05	MT=	.9747888-07	MA=	.91907481-05
WING=	.10000000+03	ALT=	.31401098+07	CG=	.00000000	GV=	.22794189+02
ATT=	.57445421+01	AMO=	-.74002892-05	CDT=	.6747028n+00	RRT=	.76085100+00
U=	.97327903+00						
WI=	-.21574480-01						
Q=	.11885000+02						
F=	.84035517+02						
DRAG=	.27658826+02						
DF=	.00000000						
RPO=	-.19871899-04						

RUN 18

I	R	VR	VRS	DB	LR	DS	TORQ	MR	SFB	CL	FN	ALPHA
1	3.332-01	1.028+02	1.061+00	3.657-01	3.779-01	4.960-01	1.561-01	-1.547-03	3.809-02	1.487+00	5.011-01	27.88
2	4.166-01	1.064+02	1.045+00	3.776-01	3.909-01	5.200-01	1.314-01	-1.338-03	3.697-02	1.486+00	5.256-01	31.06
3	5.000-01	1.062+02	1.027+00	3.922-01	4.052-01	5.462-01	1.061-01	-1.075-03	3.585-02	1.450+00	5.525-01	34.19
4	5.834-01	1.084+02	1.006+00	4.094-01	4.230-01	5.767-01	8.005-02	-7.691-04	3.476-02	1.454+00	5.817-01	37.20
5	6.668-01	1.108+02	9.844-01	4.292-01	4.435-01	6.056-01	5.288-02	-4.175-04	3.363-02	1.458+00	6.133-01	40.09
6	7.502-01	1.135+02	9.609-01	4.517-01	4.668-01	6.388-01	2.439-02	-3.370-06	3.252-02	1.462+00	6.476-01	42.86
7	8.336-01	1.164+02	9.367-01	4.769-01	4.879-01	6.711-01	-7.306-03	8.577-04	3.157-02	1.452+00	6.803-01	45.38
8	9.170-01	1.196+02	9.118-01	5.047-01	5.011-01	6.982-01	-4.374-02	9.697-04	3.096-02	1.413+00	7.079-01	47.41
9	1.000+00	1.230+02	8.868-01	5.351-01	5.153-01	7.262-01	-8.186-02	1.589-03	3.041-02	1.375+00	7.362-01	49.35
10	1.084+00	1.266+02	8.618-01	5.683-01	5.302-01	7.549-01	-1.218-01	2.172-03	2.991-02	1.336+00	7.653-01	51.16
				4.511+00	4.581+00	6.272+00	2.969-01	-4.251-07	3.347-01	5.750-01	6.311+00	

X=	.28594187+03	Z=	.27933761+07	THI=	.78716721+02	OMGS=	-.8052787n+00
XI=	.30268162+02	ZI=	.96046067+02	THT=	-.87058011-05	OMG=	-.70997727+03
XIG=	-.18776142+00	ZIG=	.40566928+00	THII=	.99030346-10	OMGI=	.9507617?-03
FA=	.38856966+02	FN=	-.8325[illegible]77+01	FX=	.62716393+01	FY=	.38198[illegible]+02
MCH=	.90909091-01	MW=	-.44060740-05	MT=	.5[illegible]83418-12	MA=	.56568908-05
WING=	.10000000+03	ALT=	.22[illegible]62394+07	CG=	.00000000	GV=	.17891835+02
ATT=	.4888255n+01	AMO=	-.72628534-05	CDT=	.5693544?+00	RRT=	.74126475+00
U=	.83325616+00						
WI=	-.76108368-02						
Q=	.11885000+02						
F=	.38699[illegible]+02						
DRAG=	.24926558+02						
DF=	.00000000						
RPO=	-.28513783-04						

APPENDIX D

COMPUTER SOLUTION PRINTOUT OF THE DEPLOYMENT TRANSIENT FOR THE NOMINAL CASE–TABLE III, RUN 1

INPUT

MACHN	VSS
.00000000	.10000000+01
.20000000+01	.10000000+01

WGT=	.32900000+00	WGTS=	.40000000+00	ALTO=	.50000000+03	VINF=	.10000000+03	RHO=	.23770000-02
S=	.20830000+00	C=	.25000000+00	L=	.83400000+00	R=	.70800000+00	GH=	.00000000
TH=	.25000000-02	II=	.38680000-04	YO=	.57400000-02	SV=	.00000000	RV=	.00000000
CLSS=	.15500000+01	CDSS=	.12500000+01	CYSS=	.67500000+00	OMG=	-.75000000+03	OMGI=	.00000000
DFR=	.00000000	CMV1=	.00000000	CMV2=	.00000000	CMOT=	-.25000000+00	CMDO=	.00000000
CMO=	.20000000+00	CM1=	.15000000+00	CM2=	-.35000000+00	CL1=	.17143000+01	CL2=	-.71430000+00
THO=	.10000000+01	THI=	.00000000	W=	.00000000	WI=	.00000000	CDS=	.00000000
THTT=	.00000000	VLIM=	.10000000+05						
RINT=	.33320000+00	DR=	.83400000-01	AM=	.40000000+01	AK=	.10000000+02	IL=	10

TIME= .009

I	R	VR	VSS	DR	LR	DS	TORQ	MR	SFR	CL	FN	ALPHA
1	3.332-01	1.000+02	1.357-04	1.586-04	8.934-05	1.586-04	-2.091-06	7.614-06	3.429-04	3.605-04	3.577-04	.33
2	4.166-01	1.000+02	1.357-04	1.643-04	8.934-05	1.641-04	-2.752-05	7.884-06	3.553-04	3.605-04	3.689-04	.41
3	5.000-01	1.000+02	1.357-04	1.713-04	8.934-05	1.708-04	-5.445-05	8.126-06	3.705-04	3.605-04	3.811-04	.50
4	5.830-01	1.000+02	1.357-04	1.795-04	8.934-05	1.787-04	-8.304-05	8.458-06	3.884-04	3.605-04	3.940-04	.58
5	6.668-01	1.000+02	1.357-04	1.891-04	8.934-05	1.878-04	-1.134-04	8.841-06	4.091-04	3.605-04	4.077-04	.66
6	7.502-01	1.000+02	1.357-04	1.998-04	8.935-05	1.980-04	-1.457-04	9.275-06	4.325-04	3.605-04	4.220-04	.74
7	8.336-01	1.000+02	1.357-04	2.119-04	8.935-05	2.093-04	-1.800-04	9.759-06	4.586-04	3.605-04	4.369-04	.82
8	9.170-01	1.000+02	1.357-04	2.252-04	8.935-05	2.219-04	-2.168-04	1.029-05	4.875-04	3.605-04	4.523-04	.91
9	1.000+00	1.000+02	1.357-04	2.398-04	8.935-05	2.355-04	-2.549-04	1.088-05	5.191-04	3.605-04	4.682-04	.99
10	1.084+00	1.000+02	1.357-04	2.557-04	8.935-05	2.502-04	-2.957-04	1.152-05	5.534-04	3.605-04	4.843-04	1.07
				1.995-03	8.935-04	1.975-03	-1.377-03	9.261-05	4.317-03	1.884-03	4.173-03	

DIVIDE CHECK FAULT AT 016074

X=	.99999978+00	Z=	.16086937-02	TH=	.13167814+01	OMSS=	-.20264197-01	V=	.13307029+01
XI=	.99999956+02	ZI=	.37173992+00	THI=	.11539197+01	OMG=	-.74852901+03	VI=	.31226585+02
XIG=	-.19748171-03	ZIG=	.99999943+00	THII=	.13262277+03	OMGI=	.33006097+02	Q=	.11885000+02
FA=	.35004769-01	FN=	-.10175787+01	FX=	.11617231-01	FZ=	.10181099+01	F=	.10181761+01
MCH=	.90909091-01	MW=	.18323759-02	MT=	.76125839+00	MO=	.72664628-01	DRAG=	.78893014-02
VIN=	.10000000+03	ALT=	.49999839+03	CD=	.00000000	GV=	.89815658+02	DF=	.00000000
ATT=	.46889648-02	AMO=	-.31966977-02	CDT=	.31677507+00	RBT=	.73183710+00	RBO=	.87148668+00

TIME= .019

I	R	VR	VSS	DR	LR	DS	TORQ	MR	SFR	CL	FN	ALPHA
1	3.332-01	1.000+02	1.008-03	5.253-04	6.638-04	5.249-04	3.378-04	3.050-05	1.139-03	2.678-03	1.293-03	.62
2	4.166-01	1.000+02	1.008-03	5.438-04	6.638-04	5.432-04	2.470-04	3.127-05	1.181-03	2.678-03	1.351-03	.77
3	5.000-01	1.000+02	1.008-03	5.666-04	6.638-04	5.690-04	1.502-04	3.221-05	1.231-03	2.678-03	1.411-03	.91
4	5.834-01	1.000+02	1.008-03	5.934-04	6.639-04	5.948-04	4.734-05	3.332-05	1.291-03	2.678-03	1.473-03	1.06
5	6.668-01	1.000+02	1.008-03	6.244-04	6.639-04	6.232-04	-6.292-05	3.459-05	1.359-03	2.678-03	1.535-03	1.21
6	7.502-01	1.000+02	1.008-03	6.595-04	6.639-04	6.554-04	-1.780-04	3.602-05	1.436-03	2.678-03	1.599-03	1.36
7	8.336-01	1.000+02	1.008-03	6.987-04	6.640-04	6.911-04	-3.009-04	3.762-05	1.522-03	2.678-03	1.663-03	1.51
8	9.170-01	1.000+02	1.008-03	7.421-04	6.640-04	7.309-04	-4.308-04	3.939-05	1.617-03	2.677-03	1.727-03	1.65
9	1.000+00	1.000+02	1.008-03	7.896-04	6.641-04	7.722-04	-5.678-04	4.132-05	1.721-03	2.677-03	1.792-03	1.80
10	1.084+00	1.001+02	1.007-03	8.413-04	6.641-04	8.175-04	-7.121-04	4.341-05	1.833-03	2.677-03	1.857-03	1.95
				6.585-03	6.639-03	6.529-03	-1.469-03	3.596-04	1.433-02	5.908-03	1.570-02	

DIVIDE CHECK FAULT AT 016074

X=	.19999988+01	Z=	.64347964-02	TH=	.28482787+01	OMSS=	-.37261419-01	V=	.90939182+01
XI=	.99999833+02	ZI=	.64347926+00	THI=	.29727485+01	OMG=	-.74041010+03	VI=	.14587490+03
XIG=	-.65787590-03	ZIG=	.99999601+00	THII=	.23579857+03	OMGI=	.15777949+03	Q=	.11885000+02
FA=	.14931168+00	FN=	-.18429323+01	FX=	.70449915-01	FZ=	.18476287+01	F=	.18489708+01
MCH=	.90909091-01	MW=	.85599330-02	MT=	.13534838+01	MO=	.10565445+00	DRAG=	.76115579-01
VIN=	.10000000+03	ALT=	.49999357+03	CD=	.00000000	GV=	.89631318+02	DF=	.00000000
ATT=	.15529839-01	AMO=	-.18424452-02	CDT=	.39300728+00	RBT=	.73670548+00	RBO=	.12539131+01

TIME= .029

I	R	VR	VSS	DR	LR	DS	TORQ	MR	SFR	CL	FN	ALPHA
1	3.332-01	1.000+02	4.796-03	2.182-03	3.159-03	2.222-03	1.740-03	1.330-04	4.743-03	1.274-02	5.573-03	1.29
2	4.166-01	1.000+02	4.795-03	2.254-03	3.159-03	2.292-03	1.355-03	1.362-04	4.909-03	1.274-02	5.829-03	1.58
3	5.000-01	1.000+02	4.795-03	2.341-03	3.160-03	2.370-03	9.668-04	1.400-04	5.110-03	1.274-02	6.090-03	1.87
4	5.834-01	1.001+02	4.794-03	2.444-03	3.160-03	2.466-03	5.434-04	1.444-04	5.344-03	1.274-02	6.356-03	2.16
5	6.668-01	1.001+02	4.793-03	2.563-03	3.161-03	2.570-03	9.464-05	1.494-04	5.612-03	1.274-02	6.625-03	2.45
6	7.502-01	1.001+02	4.792-03	2.698-03	3.162-03	2.683-03	-3.807-04	1.551-04	5.913-03	1.273-02	6.897-03	2.74
7	8.336-01	1.001+02	4.791-03	2.849-03	3.162-03	2.807-03	-8.914-04	1.614-04	6.248-03	1.273-02	7.169-03	3.03
8	9.170-01	1.002+02	4.789-03	3.016-03	3.163-03	2.939-03	-1.411-03	1.684-04	6.616-03	1.273-02	7.443-03	3.31
9	1.000+00	1.002+02	4.788-03	3.199-03	3.164-03	3.081-03	-1.957-03	1.760-04	7.017-03	1.272-02	7.717-03	3.60
10	1.084+00	1.002+02	4.786-03	3.397-03	3.165-03	3.231-03	-2.551-03	1.842-04	7.451-03	1.272-02	7.991-03	3.89
				2.694-02	3.162-02	2.667-02	-2.490-03	1.548-03	5.896-02	2.127-02	6.769-02	

DIVIDE CHECK FAULT AT 016074

Y:	.29999951+01	Z:	.14478274-01	TH:	.59742604+01	OMSS:	-.72846578-01	W:	.42374782+02
YI:	.99999345+02	ZI:	.96521516+00	THI:	.63595489+01	OMG:	-.70608956+03	WI:	.60007777+03
YIG:	-.26663859-02	ZIG:	.99997513+00	THII:	.43636574+03	OMGI:	.61411465+03	Q:	.11885000+02
FA:	.61775756+00	FN:	-.33917401+01	FX:	.31834377+00	FZ:	.34728097+01	F:	.34475390+01
MCH:	.90909091-01	MW:	.35298606-01	MT:	.25087397+01	MO:	.44661778+00	DRAG:	.10666008+00
VIN:	.10000000+03	ALT:	.49998552+03	CO:	.00000000	GV:	.89446986+02	DF:	.00000000
ATT:	.63511802-01	AMO:	-.59346053-02	COT:	.29443031+00	RBT:	.73588797+00	RRO:	.20297009+01

TIME= .039

I	R	VR	VCS	DR	LR	DS	TORQ	MR	SFR	CL	FN	ALPHA
1	3.332-01	1.001+02	1.827-02	8.815-03	1.204-02	9.101-03	6.501-03	5.304-04	1.891-02	4.852-02	2.254-02	2.50
2	4.166-01	1.001+02	1.826-02	9.030-03	1.205-02	9.316-03	5.217-03	5.409-04	1.984-02	4.852-02	2.338-02	3.00
3	5.000-01	1.001+02	1.826-02	9.293-03	1.205-02	9.547-03	3.859-03	5.532-04	2.096-02	4.850-02	2.424-02	3.50
4	5.834-01	1.002+02	1.825-02	9.604-03	1.206-02	9.799-03	2.449-03	5.675-04	2.078-02	4.847-02	2.511-02	4.00
5	6.668-01	1.002+02	1.824-02	9.962-03	1.206-02	1.007-02	9.598-04	5.837-04	2.160-02	4.845-02	2.600-02	4.50
6	7.502-01	1.003+02	1.822-02	1.037-02	1.207-02	1.035-02	-6.030-04	6.019-04	2.250-02	4.841-02	2.689-02	5.00
7	8.336-01	1.004+02	1.821-02	1.082-02	1.208-02	1.065-02	-2.240-03	6.219-04	2.351-02	4.838-02	2.780-02	5.50
8	9.170-01	1.005+02	1.820-02	1.132-02	1.209-02	1.097-02	-3.953-03	6.439-04	2.460-02	4.834-02	2.871-02	6.00
9	1.000+00	1.006+02	1.818-02	1.187-02	1.210-02	1.130-02	-5.742-03	6.678-04	2.578-02	4.830-02	2.962-02	6.50
10	1.084+00	1.006+02	1.816-02	1.247-02	1.211-02	1.163-02	-7.609-03	6.936-04	2.706-02	4.825-02	3.053-02	7.00
				1.036-01	1.207-01	1.029-01	-1.153-03	6.005-03	2.242-01	5.982-02	2.548-01	

Y:	.39999807+01	Z:	.25739090-01	TH:	.17158788+02	OMSS:	-.12329747+00	W:	.15674134+03
YI:	.99997387+02	ZI:	.12459326+01	THI:	.11843335+02	OMG:	-.59337823+03	WI:	.17887891+04
YIG:	-.10274215-01	ZIG:	.99987109+00	THII:	.50799657+03	OMGI:	.17079313+04	Q:	.11885000+02
FA:	.19466851+01	FN:	-.46143093+01	FX:	.11023119+01	FZ:	.48853108+01	F:	.50081286+01
MCH:	.90909091-01	MW:	.10496615+00	MT:	.74899003+01	MO:	.14695363+01	DRAG:	.41100096+00
VIN:	.10000000+03	ALT:	.49997426+03	CO:	.00000000	GV:	.89267564+02	DF:	.00000000
ATT:	.23985175+00	AMO:	-.11593483-01	COT:	.27972170+00	RBT:	.73161645+00	RRO:	.10056092+02

TIME= .049

I	R	VR	VCS	DR	LR	DS	TORQ	MR	SFR	CL	FN	ALPHA
1	3.332-01	1.001+02	4.655-02	2.862-02	3.066-02	3.092-02	1.684-02	1.611-03	5.773-02	1.235-01	6.887-02	3.75
2	4.166-01	1.002+02	4.653-02	2.921-02	3.067-02	3.036-02	1.394-02	1.629-03	5.856-02	1.234-01	7.028-02	4.38
3	5.000-01	1.002+02	4.650-02	2.962-02	3.069-02	3.072-02	1.118-02	1.651-03	5.951-02	1.233-01	7.174-02	5.00
4	5.834-01	1.003+02	4.646-02	3.011-02	3.071-02	3.109-02	8.431-03	1.676-03	6.059-02	1.232-01	7.322-02	5.63
5	6.668-01	1.004+02	4.642-02	3.067-02	3.074-02	3.147-02	5.606-03	1.704-03	6.180-02	1.231-01	7.474-02	6.25
6	7.502-01	1.005+02	4.637-02	3.131-02	3.077-02	3.186-02	2.698-03	1.735-03	6.312-02	1.230-01	7.629-02	6.87
7	8.336-01	1.006+02	4.632-02	3.202-02	3.080-02	3.225-02	-2.981-04	1.769-03	6.457-02	1.228-01	7.784-02	7.49
8	9.170-01	1.007+02	4.626-02	3.280-02	3.084-02	3.265-02	-3.372-03	1.806-03	6.614-02	1.227-01	7.942-02	8.11
9	1.000+00	1.009+02	4.620-02	3.366-02	3.088-02	3.305-02	-6.538-03	1.846-03	6.783-02	1.225-01	8.102-02	8.73
10	1.084+00	1.010+02	4.613-02	3.459-02	3.093-02	3.345-02	-9.792-03	1.889-03	6.963-02	1.223-01	8.262-02	9.35
				3.129-01	3.077-01	3.169-01	3.819-02	1.732-02	.295-01	9.279-02	7.560-01	

DIVIDE CHECK FAULT AT 016074

Y:	.49999270+01	Z:	.40216684-01	TH:	.19551109+02	OMSS:	-.14859607+00	W:	.38022531+03
YI:	.99990783+02	ZI:	.16085761+01	THI:	.17005418+02	OMG:	-.39605476+03	WI:	.25402462+04
YIG:	-.31685943-01	ZIG:	.99950087+00	THII:	.37149672+03	OMGI:	.29778571+04	Q:	.11885000+02
FA:	.30568772+01	FN:	-.39662223+01	FX:	.23017387+01	FZ:	.40067091+01	F:	.46207919+01
MCH:	.90909091-01	MW:	.14906165+00	MT:	.21074388+01	MO:	.25154851+01	DRAG:	.12675952+01
VIN:	.10000000+03	ALT:	.49995479+03	CO:	.00000000	GV:	.89078749+02	DF:	.00000000
ATT:	.68225088+00	AMO:	.70210157-02	COT:	.26518391+00	RBT:	.72243524+00	RRO:	.18382986+00

TIME= .059

I	R	VR	VCS	DR	LR	DS	TORQ	MR	SFR	CL	FN	ALPHA
1	3.332-01	1.001+02	7.545-02	6.782-02	4.942-02	7.009-02	2.717-02	3.427-03	1.157-01	1.991-01	1.402-01	4.36
2	4.166-01	1.001+02	7.541-02	6.812-02	4.944-02	7.045-02	2.403-02	3.446-03	1.163-01	1.990-01	1.414-01	4.95
3	5.000-01	1.002+02	7.537-02	6.848-02	4.947-02	7.082-02	2.087-02	3.468-03	1.169-01	1.989-01	1.427-01	5.54
4	5.834-01	1.003+02	7.532-02	6.891-02	4.951-02	7.120-02	1.767-02	3.492-03	1.177-01	1.987-01	1.439-01	6.12
5	6.668-01	1.003+02	7.526-02	6.941-02	4.954-02	7.159-02	1.443-02	3.519-03	1.185-01	1.986-01	1.452-01	6.71
6	7.502-01	1.004+02	7.519-02	6.997-02	4.959-02	7.197-02	1.116-02	3.549-03	1.195-01	1.984-01	1.466-01	7.30
7	8.336-01	1.005+02	7.511-02	7.060-02	4.963-02	7.236-02	7.842-03	3.581-03	1.205-01	1.982-01	1.479-01	7.88
8	9.170-01	1.006+02	7.503-02	7.129-02	4.969-02	7.275-02	4.488-03	3.617-03	1.215-01	1.980-01	1.493-01	8.46
9	1.000+00	1.008+02	7.494-02	7.205-02	4.974-02	7.314-02	1.092-03	3.654-03	1.227-01	1.977-01	1.507-01	9.05
10	1.084+00	1.009+02	7.484-02	7.288-02	4.981-02	7.352-02	-2.345-03	3.695-03	1.239-01	1.974-01	1.521-01	9.63
				6.995-01	4.958-01	7.179-01	1.264-01	3.545-02	1.193+00	4.221-02	1.460+00	

Y:	.59987612+01	Z:	.57908888-01	TH:	.25817950+02	OMSS:	-.13779455+00	W:	.59557138+03
YI:	.99973981+02	ZI:	.19309171+01	THI:	.18945865+02	OMG:	-.24264898+03	WI:	.19574839+04
YIG:	-.21775261-01	ZIG:	.99863787+00	THII:	-.10491748+03	OMGI:	.11938335+04	Q:	.11885000+02
FA:	.34975979+01	FN:	-.54270576+00	FX:	.27835513+01	FZ:	.21964760+01	F:	.35457956+01
MCH:	.90909091-01	MW:	.11486516+00	MT:	-.60222635+00	MO:	.23712945+01	DRAG:	.28715278+01
VIN:	.10000000+03	ALT:	.49994279+03	CO:	.00000000	GV:	.88898032+02	DF:	.00000000
ATT:	.13629882+01	AMO:	.67001633-01	COT:	.26165818+00	RBT:	.71474770+00	RRO:	.53907372+00

TIME= .069

I	R	VR	VCS	DR	LR	DS	TORQ	MR	SFR	CL	FN	ALPHA
1	3.332-01	1.001+02	9.724-02	1.156-01	6.715-02	1.190-01	3.676-02	5.494-03	1.572-01	2.545-01	2.017-01	4.66
2	4.166-01	1.001+02	9.721-02	1.159-01	6.717-02	1.194-01	3.372-02	5.510-03	1.575-01	2.544-01	2.026-01	5.18
3	5.000-01	1.002+02	9.716-02	1.162-01	6.720-02	1.199-01	3.057-02	5.528-03	1.578-01	2.543-01	2.035-01	5.71
4	5.834-01	1.002+02	9.711-02	1.165-01	6.723-02	1.202-01	2.751-02	5.548-03	1.582-01	2.541-01	2.044-01	6.24
5	6.668-01	1.003+02	9.704-02	1.169-01	6.727-02	1.206-01	2.453-02	5.570-03	1.586-01	2.539-01	2.054-01	6.76
6	7.502-01	1.003+02	9.697-02	1.173-01	6.732-02	1.210-01	2.144-02	5.595-03	1.590-01	2.538-01	2.063-01	7.28
7	8.336-01	1.004+02	9.690-02	1.178-01	6.737-02	1.215-01	1.834-02	5.622-03	1.595-01	2.535-01	2.073-01	7.31
8	9.170-01	1.005+02	9.681-02	1.184-01	6.742-02	1.219-01	1.527-02	5.651-03	1.601-01	2.533-01	2.083-01	8.33
9	1.000+00	1.006+02	9.672-02	1.190-01	6.748-02	1.223-01	1.208-02	5.682-03	1.606-01	2.531-01	2.093-01	8.85
10	1.084+00	1.007+02	9.662-02	1.197-01	6.754-02	1.228-01	8.931-03	5.715-03	1.612-01	2.528-01	2.103-01	9.37
				1.173+00	6.731-01	1.209+00	2.203-01	5.591-02	1.590+00	-5.976-02	2.058+00	

Y:	.69993547+01	Z:	.74815789-01	TH:	.30457848+02	OMSS:	-.12339589+00	W:	.75836919+03
YI:	.99942183+02	ZI:	.22519935+01	THI:	.15118137+02	OMG:	-.16441159+03	WI:	.15698374+04
YIG:	-.12092249+00	ZIG:	.99731750+00	THII:	-.41061341+03	OMGI:	.51389118+03	Q:	.11885000+02
FA:	.24432867+01	FN:	.44990695+00	FX:	.25042641+01	FZ:	.83976556+00	F:	.26413150+01
MCH:	.90909091-01	MW:	.92004588-01	MT:	-.23569719+01	MO:	.14826577+01	DRAG:	.48349870+01
VIN:	.10000000+03	ALT:	.49997118+03	CO:	.00000000	GV:	.88709591+02	DF:	.00000000
ATT:	.19485923+01	AMO:	.14119930+00	COT:	.26454777+00	RBT:	.71168841+00	RRO:	.61577789+00

TIME= .07

I	R	VR	VCS	DR	LR	DS	TORQ	MR	SFR	CL	FN	ALPHA
1	3.332-01	1.001+02	1.164-01	1.563-01	7.484-02	1.609-01	4.629-02	7.275-03	1.674-01	3.016-01	2.363-01	5.00
2	4.166-01	1.001+02	1.163-01	1.565-01	7.486-02	1.614-01	4.343-02	7.239-03	1.675-01	3.015-01	2.370-01	5.49
3	5.000-01	1.001+02	1.163-01	1.568-01	7.489-02	1.619-01	4.057-02	7.255-03	1.677-01	3.014-01	2.378-01	5.98
4	5.834-01	1.002+02	1.162-01	1.571-01	7.493-02	1.623-01	3.771-02	7.277-03	1.678-01	3.013-01	2.386-01	6.48
5	6.668-01	1.002+02	1.162-01	1.574-01	7.497-02	1.628-01	3.483-02	7.292-03	1.680-01	3.011-01	2.394-01	6.97
6	7.502-01	1.003+02	1.161-01	1.578-01	7.502-02	1.633-01	3.195-02	7.314-03	1.682-01	3.009-01	2.402-01	7.46
7	8.336-01	1.004+02	1.160-01	1.582-01	7.507-02	1.638-01	2.907-02	7.337-03	1.684-01	3.007-01	2.410-01	7.95
8	9.170-01	1.005+02	1.159-01	1.587-01	7.512-02	1.643-01	2.617-02	7.363-03	1.686-01	3.004-01	2.418-01	8.44
9	1.000+00	1.005+02	1.158-01	1.593-01	7.519-02	1.649-01	2.327-02	7.390-03	1.689-01	3.002-01	2.427-01	8.93
10	1.084+00	1.006+02	1.157-01	1.598-01	7.525-02	1.654-01	2.036-02	7.419-03	1.692-01	2.999-01	2.435-01	9.41
				1.578+00	7.501-01	1.631+00	3.337-01	7.311-02	1.662+00	-1.000-01	2.398+00	

X=	.79985539+01	Z=	.10293020+00	TH=	.45900262+02	OMSS=	-.11673814+00	V=	.90397247+03
XI=	.99895506+02	ZI=	.25717197+01	THI=	.10812775+02	OMG=	-.13773508+03	WI=	.15152863+04
XIG=	-.16306400+00	ZIG=	.99585461+00	THIT=	-.49901254+03	OMGT=	.20028842+03	Q=	.11885000+02
FA=	.14905255+01	FN=	.15899941+01	FX=	.21783836+01	FZ=	-.39125383-01	F=	.21787350+01
MCH=	.90909091-01	MU=	.88917001-01	MT=	-.29149680+01	MQ=	.72171097+00	DRAG=	.65246673+01
VIN=	.10000000+03	ALT=	.99989707+03	CQ=	.00000000	GV=	.88525303+02	NF=	.00000000
ATT=	.23519858+01	AMO=	.21650737+00	COT=	.26873961+00	RRT=	.71081569+00	RRO=	.64910911+00

TIME= .08

I	R	VR	VCS	DR	LR	DS	TORQ	MR	SFR	CL	FN	ALPHA
1	3.332-01	1.001+02	1.354-01	1.825-01	8.632-02	1.886-01	5.554-02	8.364-03	1.618-01	3.479-01	2.526-01	5.44
2	4.166-01	1.001+02	1.354-01	1.827-01	8.635-02	1.892-01	5.285-02	8.377-03	1.619-01	3.478-01	2.533-01	5.92
3	5.000-01	1.001+02	1.353-01	1.829-01	8.638-02	1.897-01	5.006-02	8.393-03	1.619-01	3.477-01	2.541-01	6.41
4	5.834-01	1.002+02	1.353-01	1.832-01	8.643-02	1.903-01	4.727-02	8.410-03	1.619-01	3.475-01	2.549-01	6.90
5	6.668-01	1.002+02	1.352-01	1.836-01	8.647-02	1.909-01	4.448-02	8.429-03	1.620-01	3.473-01	2.557-01	7.39
6	7.502-01	1.003+02	1.351-01	1.840-01	8.652-02	1.915-01	4.167-02	8.450-03	1.621-01	3.471-01	2.565-01	7.87
7	8.336-01	1.004+02	1.350-01	1.844-01	8.658-02	1.921-01	3.887-02	8.473-03	1.622-01	3.469-01	2.573-01	8.36
8	9.170-01	1.004+02	1.349-01	1.849-01	8.665-02	1.927-01	3.605-02	8.498-03	1.623-01	3.466-01	2.582-01	8.84
9	1.000+00	1.005+02	1.348-01	1.854-01	8.672-02	1.933-01	3.324-02	8.524-03	1.624-01	3.463-01	2.590-01	9.32
10	1.084+00	1.006+02	1.347-01	1.859-01	8.680-02	1.940-01	3.041-02	8.553-03	1.626-01	3.460-01	2.599-01	9.80
				1.839+00	8.652-01	1.912+00	4.305-01	8.447-02	1.621+00	-8.107-02	2.562+00	

X=	.89972270+01	Z=	.13024847+00	TH=	.50898109+02	OMSS=	-.11551167+00	V=	.10500573+04
XI=	.99837631+02	ZI=	.28818759+01	THI=	.57650920+01	OMG=	-.32723710+03	WI=	.15028466+04
XIG=	-.19113189+00	ZIG=	.99452531+00	THIT=	-.43114346+03	OMGT=	.51077870+02	Q=	.11885000+02
FA=	.97322974+00	FN=	.18754152+01	FX=	.20650557+01	FZ=	-.44575596+00	F=	.21129078+01
MCH=	.90909091-01	MU=	.97534739-01	MT=	-.24747635+01	MQ=	.20726418+00	DRAG=	.76484115+01
VIN=	.10000000+03	ALT=	.99986975+03	CQ=	.00000000	GV=	.88308848+02	NF=	.00000000
ATT=	.25079675+01	AMO=	.28575875+00	COT=	.27769394+00	RRT=	.71069142+00	RRO=	.66371366+00

TIME= .09

I	R	VR	VCS	DR	LR	DS	TORQ	MR	SFR	CL	FN	ALPHA
1	3.332-01	1.001+02	1.548-01	1.951-01	9.791-02	[illegible]	6.453-02	8.951-03	1.557-01	3.946-01	2.602-01	5.95
2	4.166-01	1.001+02	1.547-01	1.954-01	9.795-02	2.036-01	6.169-02	8.975-03	1.556-01	3.945-01	2.611-01	6.45
3	5.000-01	1.001+02	1.547-01	1.956-01	9.799-02	2.042-01	5.885-02	8.991-03	1.556-01	3.943-01	2.619-01	6.95
4	5.834-01	1.002+02	1.546-01	1.959-01	9.803-02	2.049-01	5.600-02	9.009-03	1.557-01	3.941-01	2.628-01	7.45
5	6.668-01	1.002+02	1.545-01	1.963-01	9.809-02	2.056-01	5.315-02	9.029-03	1.557-01	3.939-01	2.637-01	7.95
6	7.502-01	1.003+02	1.544-01	1.967-01	9.815-02	2.063-01	5.029-02	9.052-03	1.557-01	3.936-01	2.646-01	8.45
7	8.336-01	1.004+02	1.543-01	1.971-01	9.822-02	2.070-01	4.743-02	9.076-03	1.558-01	3.934-01	2.655-01	8.95
8	9.170-01	1.005+02	1.542-01	1.976-01	9.830-02	2.078-01	4.457-02	9.102-03	1.558-01	3.930-01	2.664-01	9.44
9	1.000+00	1.006+02	1.540-01	1.982-01	9.839-02	2.085-01	4.169-02	9.130-03	1.559-01	3.927-01	2.674-01	9.94
10	1.084+00	1.006+02	1.539-01	1.988-01	9.848-02	2.093-01	3.881-02	9.160-03	1.560-01	3.923-01	2.683-01	10.43
				1.967+00	9.815-01	2.050+00	5.170-01	9.048-02	1.557+00	-5.687-02	2.642+00	

X=	.99952849+01	Z=	.16076640+00	TH=	.52585697+02	OMSS=	-.11885010+00	V=	.11981245+04
XI=	.99773275+02	ZI=	.32116551+01	THI=	.29117003+01	OMG=	-.12701304+03	WI=	.15518655+04
XIG=	-.20591905+00	ZIG=	.99343795+00	THIT=	-.32811989+03	OMGT=	-.31531870+02	Q=	.11885000+02
FA=	.85198790+00	FN=	.19645696+01	FX=	.20780366+01	FZ=	-.51688717+00	F=	.21413566+01
MCH=	.90909091-01	MU=	.91039998-01	MT=	-.18834058+01	MQ=	-.13457350+00	DRAG=	.82409873+01
VIN=	.10000000+03	ALT=	.99983024+03	CQ=	.00000000	GV=	.88155713+02	NF=	.00000000
ATT=	.25682250+01	AMO=	.34664657+00	COT=	.27656863+00	RRT=	.71085586+00	RRO=	.67087875+00

TIME= .10

I	R	VR	VCS	DR	LR	DS	TORQ	MR	SFR	CL	FN	ALPHA
1	3.332-01	1.001+02	1.740-01	1.977-01	1.094-01	2.073-01	7.282-02	9.158-03	1.541-01	4.411-01	2.636-01	6.52
2	4.166-01	1.001+02	1.740-01	1.979-01	1.095-01	2.081-01	6.987-02	9.174-03	1.540-01	4.409-01	2.646-01	7.05
3	5.000-01	1.002+02	1.739-01	1.982-01	1.095-01	2.089-01	6.682-02	9.192-03	1.540-01	4.407-01	2.656-01	7.57
4	5.834-01	1.002+02	1.738-01	1.986-01	1.096-01	2.096-01	6.382-02	9.212-03	1.540-01	4.405-01	2.666-01	8.09
5	6.668-01	1.003+02	1.737-01	1.990-01	1.097-01	2.105-01	6.081-02	9.234-03	1.540-01	4.402-01	2.676-01	8.62
6	7.502-01	1.003+02	1.736-01	1.994-01	1.097-01	2.113-01	5.780-02	9.259-03	1.540-01	4.399-01	2.686-01	9.14
7	8.336-01	1.004+02	1.734-01	1.999-01	1.098-01	2.121-01	5.478-02	9.286-03	1.541-01	4.395-01	2.697-01	9.66
8	9.170-01	1.005+02	1.733-01	2.005-01	1.099-01	2.130-01	5.176-02	9.315-03	1.541-01	4.391-01	2.708-01	10.18
9	1.000+00	1.006+02	1.731-01	2.011-01	1.100-01	2.138-01	4.873-02	9.346-03	1.542-01	4.387-01	2.719-01	10.70
10	1.084+00	1.007+02	1.729-01	2.017-01	1.102-01	2.147-01	4.569-02	9.379-03	1.543-01	4.382-01	2.730-01	11.21
				1.994+00	1.097+00	2.109+00	5.929-01	9.255-02	1.541+00	-5.152-02	2.682+00	

X=	.10992682+02	Z=	.19998053+00	TH=	.52911026+02	OMSS=	-.12509672+00	V=	.13450216+04
XI=	.99705945+02	ZI=	.35311294+01	THI=	-.72007135+00	OMG=	-.13311391+03	WI=	.15218096+04
XIG=	-.21079546+00	ZIG=	.99269761+00	THIT=	-.23076250+03	OMGT=	-.88133859+02	Q=	.11885000+02
FA=	.94178502+00	FN=	.19359231+01	FX=	.21115156+01	FZ=	-.41566256+00	F=	.21520393+01
MCH=	.90909091-01	MU=	.89290778-01	MT=	-.13245770+01	MQ=	-.37887396+00	DRAG=	.84770026+01
VIN=	.10000000+03	ALT=	.99980552+03	CQ=	.00000000	GV=	.87971693+02	NF=	.00000000
ATT=	.25919132+01	AMO=	.39939078+00	COT=	.28077137+00	RRT=	.71117751+00	RRO=	.67351999+00

TIME= .119

I	R	VR	WCS	DB	L*	DS	TORQ	HP	SFB	CL	FN	ALPHA
1	3.332-01	1.001+02	1.927-01	1.932-01	1.207-01	2.047-01	8.039-02	9.040-03	1.565-01	4.864-01	2.643-01	7.11
2	4.166-01	1.001+02	1.926-01	1.935-01	1.208-01	2.056-01	7.716-02	9.088-03	1.565-01	4.862-01	2.656-01	7.68
3	5.000-01	1.002+02	1.925-01	1.938-01	1.208-01	2.065-01	7.392-02	9.119-03	1.565-01	4.860-01	2.667-01	8.23
4	5.834-01	1.002+02	1.924-01	1.942-01	1.209-01	2.074-01	7.068-02	9.143-03	1.565-01	4.857-01	2.679-01	8.79
5	6.668-01	1.003+02	1.923-01	1.946-01	1.210-01	2.084-01	6.743-02	9.169-03	1.565-01	4.853-01	2.692-01	9.35
6	7.502-01	1.004+02	1.921-01	1.951-01	1.211-01	2.093-01	6.418-02	9.197-03	1.566-01	4.849-01	2.704-01	9.91
7	8.336-01	1.005+02	1.919-01	1.957-01	1.212-01	2.103-01	6.092-02	9.228-03	1.566-01	4.845-01	2.716-01	10.46
8	9.170-01	1.006+02	1.917-01	1.963-01	1.213-01	2.112-01	5.765-02	9.262-03	1.567-01	4.840-01	2.729-01	11.01
9	1.000+00	1.007+02	1.915-01	1.970-01	1.215-01	2.122-01	5.437-02	9.297-03	1.568-01	4.834-01	2.742-01	11.56
10	1.084+00	1.008+02	1.913-01	1.978-01	1.216-01	2.132-01	5.109-02	9.336-03	1.569-01	4.829-01	2.754-01	12.11
				1.951+00	1.211+00	2.089+00	6.578-01	9.193-02	1.566+00	-6.411-02	2.698+00	

X=	.11989802+02	Z=	.27138821+00	TH=	.51928595+02	OMSS=	-.13361991+00	W=	.14871988+04
XI=	.99638380+02	ZI=	.38503768+01	THI=	-.25923033+01	OMG=	-.14807257+03	WI=	.14572497+04
XIG=	-.20874395+00	ZIG=	.99200009+00	THTI=	-.15276595+03	OMGI=	-.13596338+03	Q=	.11885000+02
FA=	.11247125+01	FN=	.18103638+01	FX=	.21127421+01	FZ=	-.23092641+00	F=	.21312895+01
MCH=	.90909091-01	MW=	.85511912-01	MT=	-.87687654+00	MQ=	-.57168375+00	DRAG=	.93558867+01
VIN=	.10000000+03	ALT=	.99976961+03	CD=	.00000000	GV=	.87786990+02	DF=	.00000000
ATT=	.25965148+01	AMO=	.44363522+00	COT=	.28545735+00	RBT=	.71152920+00	RRO=	.67499625+00

TIME= .129

I	R	VR	WCS	DB	L*	DS	TORQ	HP	SFB	CL	FN	ALPHA
1	3.332-01	1.001+02	2.104-01	1.839-01	1.316-01	1.974-01	8.716-02	8.821-03	1.610-01	5.300-01	2.634-01	7.72
2	4.166-01	1.001+02	2.103-01	1.842-01	1.316-01	1.984-01	8.362-02	8.843-03	1.610-01	5.297-01	2.648-01	8.33
3	5.000-01	1.002+02	2.102-01	1.846-01	1.317-01	1.994-01	8.006-02	8.868-03	1.610-01	5.294-01	2.662-01	8.93
4	5.834-01	1.003+02	2.100-01	1.850-01	1.318-01	2.005-01	7.651-02	8.896-03	1.610-01	5.290-01	2.676-01	9.53
5	6.668-01	1.004+02	2.098-01	1.856-01	1.319-01	2.015-01	7.294-02	8.926-03	1.611-01	5.285-01	2.691-01	10.13
6	7.502-01	1.005+02	2.096-01	1.862-01	1.320-01	2.026-01	6.937-02	8.960-03	1.612-01	5.280-01	2.705-01	10.73
7	8.336-01	1.006+02	2.094-01	1.868-01	1.322-01	2.037-01	6.579-02	8.997-03	1.613-01	5.275-01	2.720-01	11.32
8	9.170-01	1.007+02	2.092-01	1.875-01	1.323-01	2.048-01	6.220-02	9.036-03	1.614-01	5.268-01	2.735-01	11.92
9	1.000+00	1.008+02	2.089-01	1.883-01	1.325-01	2.059-01	5.859-02	9.078-03	1.616-01	5.262-01	2.750-01	12.51
10	1.084+00	1.009+02	2.086-01	1.892-01	1.327-01	2.071-01	5.498-02	9.123-03	1.618-01	5.254-01	2.765-01	13.10
				1.861+00	1.320+00	2.021+00	7.112-01	8.955-02	1.612+00	-8.580-02	2.699+00	

X=	.12985452+02	Z=	.27148753+00	TH=	.50082239+02	OMSS=	-.14411405+00	W=	.16217282+04
XI=	.99572282+02	ZI=	.41698682+01	THI=	-.37634403+01	OMG=	-.15949568+03	WI=	.13657738+04
XIG=	-.20196215+00	ZIG=	.99160835+00	THTI=	-.91920563+02	OMGI=	-.18251723+03	Q=	.11885000+02
FA=	.13510488+01	FN=	.15909590+01	FX=	.20871628+01	FZ=	.15310466-01	F=	.20872189+01
MCH=	.90909091-01	MW=	.80143608-01	MT=	-.52705003+00	MQ=	-.73473325+00	DRAG=	.80854566+01
VIN=	.10000000+03	ALT=	.99972852+03	CD=	.00000000	GV=	.87602710+02	DF=	.00000000
ATT=	.25824818+01	AMO=	.47929731+00	COT=	.29101687+00	RBT=	.72222788+00	RRO=	.67391598+00

TIME= .139

I	R	VR	WCS	DB	L*	DS	TORQ	HP	SFB	CL	FN	ALPHA
1	3.332-01	1.001+02	2.268-01	1.716-01	1.418-01	1.870-01	9.308-02	8.453-03	1.651-01	5.712-01	2.609-01	8.39
2	4.166-01	1.002+02	2.267-01	1.719-01	1.419-01	1.882-01	8.916-02	8.480-03	1.652-01	5.708-01	2.626-01	9.00
3	5.000-01	1.002+02	2.265-01	1.724-01	1.420-01	1.893-01	8.522-02	8.510-03	1.653-01	5.704-01	2.643-01	9.65
4	5.834-01	1.003+02	2.263-01	1.729-01	1.421-01	1.905-01	8.127-02	8.543-03	1.654-01	5.699-01	2.660-01	10.30
5	6.668-01	1.004+02	2.261-01	1.735-01	1.423-01	1.917-01	7.732-02	8.580-03	1.656-01	5.693-01	2.677-01	10.95
6	7.502-01	1.005+02	2.258-01	1.742-01	1.424-01	1.929-01	7.335-02	8.620-03	1.658-01	5.687-01	2.695-01	11.59
7	8.336-01	1.007+02	2.256-01	1.750-01	1.426-01	1.941-01	6.937-02	8.664-03	1.660-01	5.680-01	2.712-01	12.23
8	9.170-01	1.008+02	2.253-01	1.759-01	1.428-01	1.953-01	6.537-02	8.711-03	1.662-01	5.672-01	2.730-01	12.88
9	1.000+00	1.009+02	2.249-01	1.768-01	1.430-01	1.966-01	6.137-02	8.761-03	1.665-01	5.663-01	2.748-01	13.51
10	1.084+00	1.011+02	2.246-01	1.778-01	1.432-01	1.979-01	5.735-02	8.815-03	1.668-01	5.653-01	2.766-01	14.15
				1.742+00	1.424+00	1.924+00	7.529-01	8.614-02	1.658+00	-1.076-01	2.687+00	

X=	.13980855+02	Z=	.31477723+00	TH=	.47720836+02	OMSS=	-.15638720+00	W=	.17465317+04
XI=	.99508982+02	ZI=	.44484558+01	THI=	-.43552727+01	OMG=	-.17981603+03	WI=	.12570450+04
XIG=	-.19716525+00	ZIG=	.99134430+00	THTI=	-.40765745+02	OMGI=	-.23096243+03	Q=	.11885000+02
FA=	.15064665+01	FN=	.12663675+01	FX=	.20176945+01	FZ=	.31665510+00	F=	.20455857+01
MCH=	.90909091-01	MW=	.73763490-01	MT=	-.23399538+00	MQ=	-.87279788+00	DRAG=	.76943139+01
VIN=	.10000000+03	ALT=	.99968523+03	CD=	.00000000	GV=	.87417759+02	DF=	.00000000
ATT=	.25469010+01	AMO=	.50607833+00	COT=	.29759006+00	RBT=	.71299087+00	RRO=	.67221389+00

TIME= .149

I	R	VR	WCS	DB	L*	DS	TORQ	HP	SFB	CL	FN	ALPHA
1	3.332-01	1.001+02	2.418-01	1.578-01	1.515-01	1.752-01	9.819-02	8.039-03	1.674-01	6.097-01	2.571-01	8.96
2	4.166-01	1.002+02	2.417-01	1.582-01	1.516-01	1.765-01	9.392-02	8.071-03	1.676-01	6.092-01	2.592-01	9.67
3	5.000-01	1.003+02	2.414-01	1.588-01	1.517-01	1.778-01	8.967-02	8.107-03	1.679-01	6.087-01	2.613-01	10.38
4	5.834-01	1.004+02	2.412-01	1.594-01	1.518-01	1.791-01	8.507-02	8.148-03	1.681-01	6.080-01	2.633-01	11.08
5	6.668-01	1.005+02	2.409-01	1.601-01	1.520-01	1.804-01	8.059-02	8.192-03	1.684-01	6.073-01	2.655-01	11.79
6	7.502-01	1.006+02	2.406-01	1.610-01	1.522-01	1.817-01	7.616-02	8.240-03	1.688-01	6.064-01	2.676-01	12.49
7	8.336-01	1.008+02	2.403-01	1.619-01	1.524-01	1.831-01	7.170-02	8.293-03	1.692-01	6.055-01	2.697-01	13.18
8	9.170-01	1.009+02	2.399-01	1.629-01	1.526-01	1.844-01	6.723-02	8.349-03	1.696-01	6.045-01	2.718-01	13.88
9	1.000+00	1.011+02	2.394-01	1.640-01	1.529-01	1.858-01	6.273-02	8.409-03	1.700-01	6.034-01	2.740-01	14.57
10	1.084+00	1.013+02	2.390-01	1.652-01	1.532-01	1.871-01	5.822-02	8.473-03	1.705-01	6.022-01	2.762-01	15.26
				1.609+00	1.527+00	1.811+00	7.831-01	8.232-02	1.688+00	-1.237-01	2.666+00	

X=	.14975642+02	Z=	.36125666+00	TH=	.45138737+02	OMSS=	-.17071673+00	W=	.18605988+04
XI=	.99449138+02	ZI=	.48078197+01	THI=	-.45375637+01	OMG=	-.20383890+03	WI=	.11438962+04
XIG=	-.18909089+00	ZIG=	.99131371+00	THTI=	.76676728+01	OMGI=	-.27698058+03	Q=	.11885000+02
FA=	.18878089+01	FN=	.92878191+00	FX=	.19167360+01	FZ=	.75638808+00	F=	.20601011+01
MCH=	.90909091-01	MW=	.67123827-01	MT=	.88012887-01	MQ=	-.97679951+00	DRAG=	.77443565+01
VIN=	.10000000+03	ALT=	.99963878+03	CD=	.00000000	GV=	.87237089+02	DF=	.00000000
ATT=	.24902557+01	AMO=	.52476258+00	COT=	.30527968+00	RBT=	.71396170+00	RRO=	.66988570+00

TIME= .159

I	R	VR	VCS	DB	LR	DC	TORQ	WP	SFB	CL	FN	ALPHA
1	3.332-01	1.001+02	2.555-01	1.442-01	1.604-01	1.635-01	1.026-01	7.637-03	1.673-01	6.453-01	2.528-01	9.57
2	4.166-01	1.002+02	2.552-01	1.447-01	1.605-01	1.649-01	9.773-02	7.676-03	1.674-01	6.447-01	2.553-01	10.34
3	5.000-01	1.003+02	2.550-01	1.454-01	1.606-01	1.664-01	9.279-02	7.720-03	1.682-01	6.440-01	2.578-01	11.11
4	5.834-01	1.005+02	2.547-01	1.461-01	1.608-01	1.678-01	8.786-02	7.764-03	1.686-01	6.432-01	2.603-01	11.87
5	6.668-01	1.006+02	2.543-01	1.470-01	1.610-01	1.692-01	8.291-02	7.821-03	1.692-01	6.422-01	2.629-01	12.64
6	7.502-01	1.007+02	2.539-01	1.480-01	1.613-01	1.706-01	7.794-02	7.879-03	1.697-01	6.412-01	2.654-01	13.39
7	8.336-01	1.009+02	2.535-01	1.490-01	1.615-01	1.721-01	7.294-02	7.941-03	1.703-01	6.400-01	2.680-01	14.15
8	9.170-01	1.011+02	2.530-01	1.502-01	1.618-01	1.735-01	6.791-02	8.008-03	1.710-01	6.387-01	2.705-01	14.90
9	1.000+00	1.013+02	2.525-01	1.516-01	1.621-01	1.750-01	6.287-02	8.079-03	1.717-01	6.373-01	2.731-01	15.65
10	1.084+00	1.016+02	2.519-01	1.530-01	1.625-01	1.765-01	5.779-02	8.156-03	1.725-01	6.357-01	2.757-01	16.39
				1.479+00	1.613+00	1.700+00	8.033-01	7.868-02	1.696+00	-1.326-01	2.582+00	

T=	.15964849+02	Z=	.41092555+00	TH=	.47615950+02	OMSS=	-.18572190+00	W=	.19648390+04		
XT=	.99392936+02	ZI=	.51263615+01	THT=	-.41845534+01	OMG=	-.23220453+03	WI=	.10451511+04		
XIG=	-.16974193+00	ZIG=	.99130026+00	THIT=	.58448980+02	OMGT=	-.31157173+03	Q=	.11885000+02		
FA=	.21913909+01	FN=	.26625282+00	FX=	.17929306+01	FZ=	.12870096+01	F=	.22074965+01		
MCH=	.90909091-01	MW=	.61329866-01	MT=	.33547418+00	MO=	-.10745153+01	OMAG=	.57985532+01		
VIN=	.10000000+03	ALT=	.49958908+0[illegible]	CD=	.00000000	GV=	.87087098+02	NF=	.00000000		
ATT=	.20199162+01	AHO=	.53489791+00	CDT=	.31387960+00	RBT=	.71512865+00	RHO=	.66587290+00		

TIME= .169

I	R	VR	VCS	DB	LR	DC	TORQ	WP	SFB	CL	FN	ALPHA
1	3.332-01	1.002+02	2.681-01	1.325-01	1.687-01	1.536-01	1.065-01	7.305-03	1.656-01	6.784-01	2.489-01	10.16
2	4.166-01	1.003+02	2.678-01	1.331-01	1.688-01	1.552-01	1.010-01	7.351-03	1.661-01	6.776-01	2.519-01	11.00
3	5.000-01	1.004+02	2.675-01	1.338-01	1.690-01	1.567-01	9.556-02	7.403-03	1.668-01	6.768-01	2.550-01	11.83
4	5.834-01	1.005+02	2.671-01	1.347-01	1.692-01	1.583-01	9.007-02	7.460-03	1.675-01	6.757-01	2.580-01	12.66
5	6.668-01	1.007+02	2.667-01	1.357-01	1.695-01	1.598-01	8.456-02	7.522-03	1.683-01	6.746-01	2.610-01	13.49
6	7.502-01	1.009+02	2.662-01	1.368-01	1.698-01	1.614-01	7.898-02	7.590-03	1.691-01	6.732-01	2.640-01	14.30
7	8.336-01	1.011+02	2.656-01	1.381-01	1.701-01	1.629-01	7.339-02	7.663-03	1.700-01	6.718-01	2.670-01	15.11
8	9.170-01	1.013+02	2.650-01	1.395-01	1.704-01	1.645-01	6.777-02	7.742-03	1.710-01	6.701-01	2.701-01	15.92
9	1.000+00	1.016+02	2.644-01	1.411-01	1.708-01	1.660-01	6.212-02	7.826-03	1.720-01	6.684-01	2.731-01	16.73
10	1.084+00	1.018+02	2.637-01	1.428-01	1.712-01	1.676-01	5.643-02	7.916-03	1.730-01	6.665-01	2.761-01	17.53
				1.358+00	1.698+00	1.606+00	8.163-01	7.574-02	1.689+00	-1.366-01	2.625+00	

T=	.16963511+02	Z=	.46378383+00	TH=	.40444489+02	OMSS=	-.20076231+00	W=	.20607677+04		
XT=	.99360058+02	ZI=	.54457975+01	THT=	-.33070497+01	OMG=	-.26269382+03	WI=	.98726258+03		
XIG=	-.16035289+00	ZIG=	.99126224+00	THIT=	.11181649+03	OMGT=	-.32002537+03	Q=	.11885000+02		
FA=	.25110696+01	FN=	-.37707950+00	FX=	.16561657+01	FZ=	.19161970+01	F=	.25392711+01		
MCH=	.90909091-01	MW=	.57937566-01	MT=	.64182667+00	MO=	-.94397635+00	OMAG=	.69736319+01		
VIN=	.10000000+03	ALT=	.49953522+0[illegible]	CD=	.00000000	GV=	.86662908+02	NF=	.00000000		
ATT=	.23510906+01	AHO=	.54063134+00	CDT=	.32317992+00	RBT=	.71640657+00	RHO=	.66165037+00		

TIME= .179

I	R	VR	VCS	DB	LR	DC	TORQ	WP	SFB	CL	FN	ALPHA
1	3.332-01	1.002+02	2.803-01	1.241-01	1.767-01	1.472-01	1.101-01	7.097-03	1.634-01	7.100-01	2.471-01	10.73
2	4.166-01	1.003+02	2.800-01	1.248-01	1.768-01	1.489-01	1.041-01	7.156-03	1.641-01	7.091-01	2.507-01	11.63
3	5.000-01	1.005+02	2.796-01	1.257-01	1.771-01	1.505-01	9.810-02	7.210-03	1.650-01	7.081-01	2.542-01	12.53
4	5.834-01	1.006+02	2.791-01	1.267-01	1.773-01	1.522-01	9.204-02	7.276-03	1.659-01	7.068-01	2.577-01	13.41
5	6.668-01	1.008+02	2.786-01	1.279-01	1.776-01	1.539-01	8.597-02	7.349-03	1.670-01	7.054-01	2.612-01	14.30
6	7.502-01	1.010+02	2.780-01	1.292-01	1.780-01	1.555-01	7.979-02	7.426-03	1.681-01	7.037-01	2.647-01	15.18
7	8.336-01	1.013+02	2.774-01	1.307-01	1.783-01	1.572-01	7.360-02	7.511-03	1.692-01	7.019-01	2.681-01	16.05
8	9.170-01	1.015+02	2.766-01	1.324-01	1.788-01	1.588-01	6.738-02	7.601-03	1.705-01	7.000-01	2.716-01	16.92
9	1.000+00	1.018+02	2.759-01	1.342-01	1.792-01	1.605-01	6.112-02	7.698-03	1.718-01	6.978-01	2.750-01	17.78
10	1.084+00	1.021+02	2.750-01	1.361-01	1.797-01	1.621-01	5.482-02	7.802-03	1.732-01	6.955-01	2.784-01	18.63
				1.297+00	1.779+00	1.547+00	8.270-01	7.417-02	1.678+00	-1.400-01	2.629+00	

T=	.17956657+02	Z=	.51983134+00	TH=	.38926601+02	OMSS=	-.21592380+00	W=	.21550287+04		
XT=	.99289632+02	ZI=	.57641999+01	THT=	-.19111393+01	OMG=	-.29169939+03	WI=	.99940957+03		
XIG=	-.15443683+00	ZIG=	.99108431+00	THIT=	.16072161+03	OMGT=	-.28242950+03	Q=	.11885000+02		
FA=	.28423732+01	FN=	-.10249991+01	FX=	.15675109+01	FZ=	.25824428+01	F=	.30213732+01		
MCH=	.90909091-01	MW=	.58685350-01	MT=	.92258207+00	MO=	-.82656275+00	OMAG=	.61817587+01		
VIN=	.10000000+03	ALT=	.49948017+0[illegible]	CD=	.00000000	GV=	.86577458+02	NF=	.00000000		
ATT=	.23039648+01	AHO=	.54365639+00	CDT=	.33184235+00	RBT=	.71760671+00	RHO=	.65738705+00		

TIME= .189

I	R	VR	VCS	DB	LR	DC	TORQ	WP	SFB	CL	FN	ALPHA
1	3.332-01	1.002+02	2.931-01	1.206-01	1.847-01	1.458-01	1.140-01	7.056-03	1.624-01	7.420-01	2.489-01	11.29
2	4.166-01	1.004+02	2.928-01	1.215-01	1.849-01	1.476-01	1.075-01	7.116-03	1.633-01	7.410-01	2.528-01	12.24
3	5.000-01	1.005+02	2.923-01	1.224-01	1.852-01	1.494-01	1.009-01	7.183-03	1.643-01	7.397-01	2.568-01	13.19
4	5.834-01	1.007+02	2.918-01	1.236-01	1.855-01	1.512-01	9.436-02	7.257-03	1.654-01	7.382-01	2.607-01	14.14
5	6.668-01	1.009+02	2.911-01	1.249-01	1.858-01	1.530-01	8.773-02	7.338-03	1.666-01	7.365-01	2.646-01	15.07
6	7.502-01	1.012+02	2.904-01	1.264-01	1.862-01	1.547-01	8.106-02	7.426-03	1.679-01	7.345-01	2.685-01	16.00
7	8.336-01	1.014+02	2.897-01	1.281-01	1.867-01	1.565-01	7.434-02	7.521-03	1.693-01	7.324-01	2.723-01	16.93
8	9.170-01	1.017+02	2.888-01	1.300-01	1.872-01	1.583-01	6.758-02	7.623-03	1.708-01	7.300-01	2.761-01	17.85
9	1.000+00	1.020+02	2.879-01	1.320-01	1.877-01	1.600-01	6.078-02	7.732-03	1.723-01	7.275-01	2.799-01	18.76
10	1.084+00	1.024+02	2.869-01	1.342-01	1.883-01	1.619-01	5.394-02	7.849-03	1.739-01	7.248-01	2.837-01	19.66
				1.264+00	1.862+00	1.578+00	8.421-01	7.810-02	1.676+00	-1.461-01	2.664+00	

T=	.18949395+02	Z=	.57906749+00	TH=	.38332114+02	OMSS=	-.22967606+00	W=	.22549206+04		
XT=	.99240257+02	ZI=	.60830009+01	THT=	-.11635390+00	OMG=	-.31433278+03	WI=	.10966956+04		
XIG=	-.15354002+00	ZIG=	.99063845+00	THIT=	.19971988+03	OMGT=	-.14295386+03	Q=	.11885000+02		
FA=	.31845293+01	FN=	-.15473798+01	FX=	.15387287+01	FZ=	.31889071+01	F=	.35405625+01		
MCH=	.90909091-01	MW=	.64354095-01	MT=	.17946781+01	MO=	-.55369795+00	OMAG=	.61530052+01		
VIN=	.10000000+03	ALT=	.49942093+0[illegible]	CD=	.00000000	GV=	.86492404+02	NF=	.00030000		
ATT=	.22986656+01	AHO=	.55976645+00	CDT=	.33065979+00	RBT=	.71849199+00	RHO=	.65400534+00		

TIME= .199

I	R	VR	VCS	DR	LR	DS	TORQ	HR	SFB	CL	FN	ALPHA
1	3.332-01	1.003+02	3.076-01	1.228-01	1.933-01	1.502-01	1.185-01	7.204-03	1.635-01	7.760-01	2.549-01	11.83
2	4.166-01	1.004+02	3.072-01	1.236-01	1.935-01	1.522-01	1.116-01	7.269-03	1.644-01	7.748-01	2.591-01	12.83
3	5.000-01	1.006+02	3.066-01	1.247-01	1.938-01	1.542-01	1.047-01	7.342-03	1.655-01	7.733-01	2.634-01	13.83
4	5.834-01	1.008+02	3.060-01	1.260-01	1.942-01	1.562-01	9.767-02	7.423-03	1.666-01	7.716-01	2.676-01	14.82
5	6.668-01	1.010+02	3.053-01	1.275-01	1.946-01	1.581-01	9.063-02	7.511-03	1.679-01	7.696-01	2.718-01	15.80
6	7.502-01	1.013+02	3.045-01	1.291-01	1.950-01	1.601-01	8.355-02	7.607-03	1.692-01	7.674-01	2.759-01	16.77
7	8.336-01	1.016+02	3.036-01	1.310-01	1.955-01	1.620-01	7.643-02	7.711-03	1.707-01	7.649-01	2.800-01	17.74
8	9.170-01	1.019+02	3.026-01	1.331-01	1.961-01	1.639-01	6.926-02	7.823-03	1.722-01	7.622-01	2.841-01	18.70
9	1.000+00	1.023+02	3.016-01	1.353-01	1.967-01	1.658-01	6.205-02	7.942-03	1.738-01	7.593-01	2.881-01	19.65
10	1.084+00	1.026+02	3.004-01	1.378-01	1.974-01	1.678-01	5.481-02	8.069-03	1.754-01	7.561-01	2.922-01	20.59
				1.291+00	1.950+00	1.591+00	8.691-01	7.590-02	1.689+00	-1.557-01	2.737+00	

Y=	.19941457+02	Z=	.58149060+00	TH=	.38817369+02	OMSS=	-.28171689+00	V=	.23678719+04
YI=	.99190115+02	ZI=	.58015930+01	THI=	.18002081+01	OMG=	-.37664037+02	VI=	.12598803+04
YIG=	-.15872743+00	ZIG=	.98980788+00	THII=	.18552835+03	OMGI=	-.75496830+02	θ=	.11885000+02
FA=	.35322618+01	FN=	-.18239598+01	FX=	.15088739+01	FZ=	.36352972+01	F=	.39753858+01
MCH=	.90909091-01	MW=	.73929776-01	MT=	.19706727+01	MA=	-.22015117+00	DRAG=	.63621780+01
VIN=	.10000000+03	ALT=	.99935851+02	CD=	.00000000	GV=	.86307331+02	DF=	.00000000
ATT=	.23862889+01	AMO=	.56709309+00	COT=	.38221317+00	RBT=	.71891073+00	RHO=	.65248293+00

TIME= .209

I	R	VR	VCS	DR	LR	DS	TORQ	HR	SFB	CL	FN	ALPHA
1	3.332-01	1.003+02	3.243-01	1.305-01	2.025-01	1.607-01	1.240-01	7.528-03	1.660-01	8.128-01	2.647-01	12.36
2	4.166-01	1.004+02	3.238-01	1.314-01	2.028-01	1.629-01	1.168-01	7.597-03	1.668-01	8.115-01	2.691-01	13.39
3	5.000-01	1.006+02	3.232-01	1.326-01	2.031-01	1.651-01	1.096-01	7.674-03	1.678-01	8.098-01	2.734-01	14.43
4	5.834-01	1.008+02	3.225-01	1.340-01	2.035-01	1.673-01	1.024-01	7.759-03	1.688-01	8.078-01	2.778-01	15.45
5	6.668-01	1.011+02	3.216-01	1.356-01	2.040-01	1.695-01	9.507-02	7.852-03	1.700-01	8.056-01	2.821-01	16.47
6	7.502-01	1.014+02	3.207-01	1.374-01	2.045-01	1.716-01	8.774-02	7.954-03	1.712-01	8.031-01	2.864-01	17.48
7	8.336-01	1.017+02	3.197-01	1.394-01	2.051-01	1.738-01	8.036-02	8.065-03	1.725-01	8.003-01	2.907-01	18.48
8	9.170-01	1.020+02	3.186-01	1.415-01	2.057-01	1.760-01	7.294-02	8.184-03	1.739-01	7.973-01	2.949-01	19.47
9	1.000+00	1.024+02	3.174-01	1.440-01	2.064-01	1.782-01	6.549-02	8.311-03	1.754-01	7.940-01	2.991-01	20.45
10	1.084+00	1.028+02	3.161-01	1.467-01	2.072-01	1.803-01	5.800-02	8.447-03	1.769-01	7.905-01	3.033-01	21.42
				1.373+00	2.045+00	1.705+00	9.124-01	7.937-02	1.709+00	-1.657-01	2.881+00	

Y=	.20933095+02	Z=	.70709897+00	TH=	.40345436+02	OMSS=	-.25030738+00	V=	.24976665+04
YI=	.99137186+02	ZI=	.67198380+01	THI=	.34608298+01	OMG=	-.37829357+03	VI=	.14386480+04
YIG=	-.17016297+00	ZIG=	.98852194+00	THII=	.14404586+03	OMGI=	.24323906+02	θ=	.11885000+02
FA=	.38662261+01	FN=	-.18151126+01	FX=	.17715706+01	FZ=	.38867704+01	F=	.42711049+01
MCH=	.90909091-01	MW=	.88819965-01	MT=	.82682322+00	MA=	.74598677-01	DRAG=	.68219885+01
VIN=	.10000000+03	ALT=	.99929790+02	CD=	.00000000	GV=	.86122239+02	DF=	.00000000
ATT=	.24827793+01	AMO=	.59597751+00	COT=	.38861906+00	RBT=	.71889843+00	RHO=	.65319958+00

TIME= .219

I	R	VR	VCS	DR	LR	DS	TORQ	HR	SFB	CL	FN	ALPHA
1	3.332-01	1.003+02	3.430-01	1.427-01	2.123-01	1.762-01	1.305-01	7.975-03	1.680-01	8.518-01	2.765-01	12.87
2	4.166-01	1.005+02	3.425-01	1.437-01	2.125-01	1.786-01	1.231-01	8.046-03	1.687-01	8.503-01	2.809-01	13.94
3	5.000-01	1.007+02	3.418-01	1.450-01	2.130-01	1.811-01	1.158-01	8.125-03	1.694-01	8.484-01	2.854-01	15.00
4	5.834-01	1.009+02	3.410-01	1.464-01	2.134-01	1.835-01	1.084-01	8.213-03	1.702-01	8.463-01	2.898-01	16.06
5	6.668-01	1.012+02	3.401-01	1.481-01	2.140-01	1.860-01	1.010-01	8.310-03	1.711-01	8.438-01	2.942-01	17.10
6	7.502-01	1.015+02	3.391-01	1.500-01	2.145-01	1.885-01	9.349-02	8.417-03	1.721-01	8.410-01	2.985-01	18.14
7	8.336-01	1.018+02	3.379-01	1.522-01	2.152-01	1.910-01	8.599-02	8.532-03	1.732-01	8.380-01	3.029-01	19.17
8	9.170-01	1.022+02	3.367-01	1.545-01	2.159-01	1.935-01	7.848-02	8.656-03	1.743-01	8.347-01	3.072-01	20.19
9	1.000+00	1.026+02	3.353-01	1.571-01	2.167-01	1.960-01	7.087-02	8.789-03	1.755-01	8.311-01	3.116-01	21.19
10	1.084+00	1.030+02	3.339-01	1.599-01	2.176-01	1.985-01	6.325-02	8.931-03	1.768-01	8.272-01	3.159-01	22.19
				1.500+00	2.145+00	1.873+00	9.708-01	8.349-02	1.719+00	-1.698-01	2.963+00	

Y=	.21924182+02	Z=	.77588564+00	TH=	.42670171+02	OMSS=	-.25787418+00	V=	.26431397+04
YI=	.99079611+02	ZI=	.70375890+01	THI=	.45817474+01	OMG=	-.37295339+03	VI=	.15857755+04
YIG=	-.18682801+00	ZIG=	.98679035+00	THII=	.76599361+02	OMGI=	.73230230+02	θ=	.11885000+02
FA=	.41649566+01	FN=	-.15928977+01	FX=	.19827282+01	FZ=	.39981176+01	F=	.44591687+01
MCH=	.90909091-01	MW=	.93053305-01	MT=	.43968033+00	MA=	.24118917+00	DRAG=	.74917769+01
VIN=	.10000000+03	ALT=	.99927412+02	CD=	.00000000	GV=	.85977125+02	DF=	.00000000
ATT=	.25690008+01	AMO=	.63641595+00	COT=	.38528873+00	RBT=	.71865979+00	RHO=	.65557015+00

TIME= .229

I	R	VR	VCS	DR	LR	DS	TORQ	HR	SFB	CL	FN	ALPHA
1	3.332-01	1.003+02	3.633-01	1.575-01	2.223-01	1.946-01	1.376-01	8.468-03	1.677-01	8.915-01	2.885-01	13.39
2	4.166-01	1.005+02	3.627-01	1.586-01	2.226-01	1.974-01	1.302-01	8.539-03	1.681-01	8.899-01	2.929-01	14.49
3	5.000-01	1.007+02	3.619-01	1.599-01	2.231-01	2.002-01	1.227-01	8.620-03	1.686-01	8.879-01	2.974-01	15.58
4	5.834-01	1.009+02	3.611-01	1.614-01	2.236-01	2.029-01	1.152-01	8.710-03	1.691-01	8.856-01	3.019-01	16.66
5	6.668-01	1.012+02	3.600-01	1.632-01	2.241-01	2.058-01	1.077-01	8.810-03	1.698-01	8.829-01	3.063-01	17.73
6	7.502-01	1.015+02	3.589-01	1.652-01	2.248-01	2.086-01	1.002-01	8.920-03	1.705-01	8.799-01	3.108-01	18.79
7	8.336-01	1.019+02	3.576-01	1.675-01	2.255-01	2.114-01	9.260-02	9.039-03	1.712-01	8.766-01	3.152-01	19.84
8	9.170-01	1.023+02	3.563-01	1.700-01	2.264-01	2.143-01	8.499-02	9.168-03	1.720-01	8.730-01	3.197-01	20.88
9	1.000+00	1.027+02	3.548-01	1.727-01	2.272-01	2.172-01	7.734-02	9.306-03	1.729-01	8.691-01	3.241-01	21.91
10	1.084+00	1.032+02	3.532-01	1.757-01	2.282-01	2.202-01	6.965-02	9.454-03	1.738-01	8.649-01	3.286-01	22.93
				1.651+00	2.248+00	2.073+00	1.039+00	8.903-02	1.704+00	-1.615-01	3.085+00	

Y=	.22914665+02	Z=	.84784769+00	TH=	.45812928+02	OMSS=	-.26491864+00	V=	.28001093+04
YI=	.99016944+02	ZI=	.73547185+01	THI=	.49187676+01	OMG=	-.31574675+03	VI=	.16840891+04
YIG=	-.20670212+00	ZIG=	.98471375+00	THII=	.73930904+01	OMGI=	.70899476+02	θ=	.11885000+02
FA=	.44314550+01	FN=	-.12850891+01	FX=	.21956272+01	FZ=	.46581360+01	F=	.46140271+01
MCH=	.90909091-01	MW=	.98420092-01	MT=	.42436338-01	MA=	.25777672+00	DRAG=	.82906635+01
VIN=	.10000000+03	ALT=	.99915215+02	CD=	.00000000	GV=	.85751983+02	DF=	.00000000
ATT=	.26497096+01	AMO=	.68363237+00	COT=	.38607519+00	RBT=	.71887986+00	RHO=	.65847650+00

TIME= 0.234

I	R	VR	WCS	DB	LB	DS	TORQ	HP	SFB	CL	FN	ALPHA
1	3.332-01	1.003+02	3.846-01	1.726-01	2.323-01	2.138-01	1.449-01	8.929-03	1.644-01	9.312-01	2.993-01	13.92
2	4.166-01	1.005+02	3.839-01	1.738-01	2.327-01	2.169-01	1.374-01	9.001-03	1.645-01	9.294-01	3.039-01	15.04
3	5.000-01	1.007+02	3.830-01	1.752-01	2.331-01	2.200-01	1.298-01	9.083-03	1.647-01	9.273-01	3.084-01	16.16
4	5.834-01	1.010+02	3.821-01	1.768-01	2.337-01	2.232-01	1.223-01	9.176-03	1.650-01	9.247-01	3.130-01	17.27
5	6.668-01	1.013+02	3.809-01	1.787-01	2.344-01	2.263-01	1.147-01	9.279-03	1.654-01	9.218-01	3.176-01	18.37
6	7.502-01	1.016+02	3.796-01	1.808-01	2.351-01	2.295-01	1.070-01	9.392-03	1.658-01	9.186-01	3.222-01	19.46
7	8.336-01	1.020+02	3.782-01	1.832-01	2.359-01	2.329-01	9.934-02	9.516-03	1.662-01	9.150-01	3.268-01	20.54
8	9.170-01	1.024+02	3.767-01	1.858-01	2.369-01	2.362-01	9.153-02	9.650-03	1.667-01	9.111-01	3.314-01	21.61
9	1.000+00	1.029+02	3.750-01	1.887-01	2.379-01	2.395-01	8.389-02	9.794-03	1.673-01	9.069-01	3.360-01	22.66
10	1.084+00	1.034+02	3.732-01	1.919-01	2.389-01	2.430-01	7.610-02	9.949-03	1.678-01	9.024-01	3.407-01	23.70
				1.807+00	2.351+00	2.281+00	1.107+00	9.377-02	1.658+00	-1.352-01	3.199+00	

Y=	.23904478+02	Z=	.92297759+00	TH=	.48189098+02	OMSS=	-.27270742+00	V=	.29641580+04
YI=	.98945867+02	ZI=	.76711408+01	THI=	.46879590+01	OMG=	-.31056754+03	WI=	.17403210+04
YIG=	-.22744833+00	ZIG=	.98244020+00	THII=	-.44531135+02	OMGI=	.37712908+02	Q=	.11885000+02
FA=	.45984989+01	FN=	-.99959037+00	FX=	.23873748+01	FZ=	.41684733+01	F=	.48036519+01
MCH=	.90909091-01	MW=	.10212203+00	MT=	-.75560871+00	MO=	.14481470+00	DRAG=	.91250068+01
VIN=	.10000000+03	ALT=	.44907702+07	CD=	.00000000	GV=	.85564803+02	DF=	.00000000
ATT=	.28157791+01	AMO=	.73174776+00	COT=	.34776016+00	RBT=	.71878041+00	RBO=	.66098481+00

TIME= 0.244

I	R	VR	WCS	DB	LB	DS	TORQ	HP	SFB	CL	FN	ALPHA
1	3.332-01	1.003+02	4.064-01	1.864-01	2.427-01	2.318-01	1.521-01	9.304-03	1.587-01	9.705-01	3.088-01	14.46
2	4.166-01	1.005+02	4.056-01	1.877-01	2.426-01	2.352-01	1.444-01	9.378-03	1.586-01	9.685-01	3.135-01	15.63
3	5.000-01	1.008+02	4.046-01	1.891-01	2.432-01	2.388-01	1.367-01	9.453-03	1.586-01	9.662-01	3.182-01	16.78
4	5.834-01	1.011+02	4.035-01	1.905-01	2.438-01	2.423-01	1.289-01	9.550-03	1.587-01	9.634-01	3.230-01	17.92
5	6.668-01	1.014+02	4.022-01	1.929-01	2.445-01	2.459-01	1.212-01	9.667-03	1.588-01	9.602-01	3.278-01	19.06
6	7.502-01	1.017+02	4.008-01	1.952-01	2.454-01	2.496-01	1.134-01	9.785-03	1.589-01	9.567-01	3.326-01	20.18
7	8.336-01	1.021+02	3.992-01	1.977-01	2.463-01	2.533-01	1.055-01	9.914-03	1.591-01	9.528-01	3.374-01	21.29
8	9.170-01	1.026+02	3.975-01	2.005-01	2.474-01	2.571-01	9.767-02	1.005-02	1.594-01	9.486-01	3.423-01	22.38
9	1.000+00	1.031+02	3.956-01	2.036-01	2.485-01	2.610-01	8.975-02	1.021-02	1.597-01	9.440-01	3.472-01	23.47
10	1.084+00	1.036+02	3.936-01	2.070-01	2.498-01	2.649-01	8.180-02	1.037-02	1.600-01	9.391-01	3.522-01	24.54
				1.951+00	2.454+00	2.480+00	1.171+00	9.770-02	1.591+00	-1.065-01	3.303+00	

Y=	.24893558+02	Z=	.10012679+01	TH=	.59710999+02	OMSS=	-.28195352+00	V=	.31319637+04
YI=	.98869156+02	ZI=	.79868187+01	THI=	.49722679+01	OMG=	-.30972662+03	WI=	.17676774+04
YIG=	-.24718910+00	ZIG=	.98011709+00	THII=	-.71902225+02	OMGI=	-.56848152+01	Q=	.11885000+02
FA=	.50068909+01	FN=	-.79412329+00	FX=	.25559087+01	FZ=	.43780066+01	F=	.50694760+01
MCH=	.90909091-01	MW=	.10372731+00	MT=	-.41214477+00	MO=	-.23233192-01	DRAG=	.99195144+01
VIN=	.10000000+03	ALT=	.49899873+07	CD=	.00000000	GV=	.85381578+02	DF=	.00000000
ATT=	.29107376+01	AMO=	.77624435+00	COT=	.35060455+00	RBT=	.71853839+00	RBO=	.66264827+00

TIME= 0.254

I	R	VR	WCS	DB	LB	DS	TORQ	HP	SFB	CL	FN	ALPHA
1	3.332-01	1.004+02	4.283-01	1.980-01	2.520-01	2.477-01	1.588-01	9.573-03	1.520-01	1.009+00	3.170-01	15.03
2	4.166-01	1.006+02	4.274-01	1.993-01	2.525-01	2.515-01	1.509-01	9.650-03	1.518-01	1.007+00	3.220-01	16.24
3	5.000-01	1.008+02	4.264-01	2.009-01	2.531-01	2.554-01	1.430-01	9.739-03	1.516-01	1.005+00	3.270-01	17.43
4	5.834-01	1.011+02	4.251-01	2.028-01	2.539-01	2.594-01	1.350-01	9.840-03	1.515-01	1.002+00	3.320-01	18.62
5	6.668-01	1.015+02	4.236-01	2.049-01	2.547-01	2.635-01	1.270-01	9.953-03	1.514-01	9.980-01	3.371-01	19.79
6	7.502-01	1.019+02	4.220-01	2.074-01	2.557-01	2.676-01	1.190-01	1.008-02	1.514-01	9.942-01	3.422-01	20.95
7	8.336-01	1.023+02	4.202-01	2.101-01	2.568-01	2.718-01	1.109-01	1.022-02	1.514-01	9.899-01	3.474-01	22.10
8	9.170-01	1.028+02	4.183-01	2.132-01	2.579-01	2.761-01	1.028-01	1.036-02	1.515-01	9.852-01	3.526-01	23.23
9	1.000+00	1.033+02	4.162-01	2.165-01	2.592-01	2.804-01	9.459-02	1.053-02	1.516-01	9.802-01	3.579-01	24.34
10	1.084+00	1.039+02	4.139-01	2.201-01	2.606-01	2.849-01	8.636-02	1.070-02	1.517-01	9.749-01	3.632-01	25.44
				2.073+00	2.556+00	2.658+00	1.228+00	1.006-01	1.516+00	-7.019-02	3.398+00	

Y=	.25881839+02	Z=	.10827113+01	TH=	.57827860+02	OMSS=	-.29786592+00	V=	.33013515+04
YI=	.98786436+02	ZI=	.83017527+01	THI=	.33102171+01	OMG=	-.31197903+03	WI=	.17767507+04
YIG=	-.26490754+00	ZIG=	.97787815+00	THII=	-.76967185+02	OMGI=	-.46879618+02	Q=	.11885000+02
FA=	.53939775+01	FN=	-.68620735+00	FX=	.27067730+01	FZ=	.47045918+01	F=	.54275259+01
MCH=	.90909091-01	MW=	.10425473+00	MT=	-.44179164+00	MO=	-.20115672+00	DRAG=	.10633365+02
VIN=	.10000000+03	ALT=	.49891729+07	CD=	.00000000	GV=	.85196301+02	DF=	.00000000
ATT=	.29856488+01	AMO=	.81485975+00	COT=	.35457839+00	RBT=	.71888170+00	RBO=	.66340826+00

TIME= 0.264

I	R	VR	WCS	DB	LB	DS	TORQ	HP	SFB	CL	FN	ALPHA
1	3.332-01	1.004+02	4.503-01	2.071-01	2.617-01	2.612-01	1.651-01	9.739-03	1.455-01	1.048+00	3.245-01	15.62
2	4.166-01	1.006+02	4.493-01	2.085-01	2.623-01	2.655-01	1.569-01	9.820-03	1.452-01	1.045+00	3.297-01	16.88
3	5.000-01	1.009+02	4.481-01	2.102-01	2.630-01	2.699-01	1.486-01	9.914-03	1.449-01	1.042+00	3.350-01	18.12
4	5.834-01	1.012+02	4.466-01	2.123-01	2.639-01	2.743-01	1.404-01	1.002-02	1.446-01	1.039+00	3.404-01	19.35
5	6.668-01	1.016+02	4.450-01	2.147-01	2.649-01	2.788-01	1.320-01	1.014-02	1.444-01	1.035+00	3.459-01	20.57
6	7.502-01	1.020+02	4.431-01	2.173-01	2.660-01	2.834-01	1.237-01	1.027-02	1.442-01	1.031+00	3.514-01	21.77
7	8.336-01	1.025+02	4.411-01	2.203-01	2.672-01	2.881-01	1.153-01	1.042-02	1.441-01	1.026+00	3.569-01	22.96
8	9.170-01	1.030+02	4.389-01	2.236-01	2.686-01	2.929-01	1.068-01	1.058-02	1.440-01	1.021+00	3.626-01	24.13
9	1.000+00	1.036+02	4.365-01	2.272-01	2.701-01	2.977-01	9.832-02	1.076-02	1.440-01	1.016+00	3.683-01	25.28
10	1.084+00	1.042+02	4.339-01	2.312-01	2.717-01	3.027-01	8.974-02	1.094-02	1.439-01	1.010+00	3.740-01	26.42
				2.172+00	2.659+00	2.815+00	1.277+00	1.026-01	1.445+00	-3.566-02	3.489+00	

Y=	.26869766+02	Z=	.11673094+01	TH=	.59511984+02	OMSS=	-.30532391+00	V=	.34709927+04
YI=	.98649413+02	ZI=	.86159541+01	THI=	.25858532+01	OMG=	-.31829446+03	WI=	.17751187+04
YIG=	-.28039394+00	ZIG=	.97561821+00	THII=	-.67039115+02	OMGI=	-.80598891+02	Q=	.11885000+02
FA=	.58385388+01	FN=	-.57169314+00	FX=	.28476221+01	FZ=	.51438795+01	F=	.58770388+01
MCH=	.90909091-01	MW=	.10416396+00	MT=	-.39980457+00	MO=	-.35067087+00	DRAG=	.11258075+02
VIN=	.10000000+03	ALT=	.49803270+07	CD=	.00000000	GV=	.85010952+02	DF=	.00000000
ATT=	.30482569+01	AMO=	.84711949+00	COT=	.35952499+00	RBT=	.71936071+00	RBO=	.66338922+00

TIME= .279

I	R	VR	WSS	DB	LB	DS	TORQ	MB	SFB	CL	FN	ALPHA
1	3.332-01	1.004+02	4.722-01	2.191-01	2.714-01	2.728-01	1.710-01	9.818-03	1.397-01	1.086+00	3.314-01	16.23
2	4.166-01	1.007+02	4.710-01	2.157-01	2.721-01	2.775-01	1.624-01	9.904-03	1.393-01	1.083+00	3.370-01	17.54
3	5.000-01	1.010+02	4.696-01	2.176-01	2.729-01	2.823-01	1.537-01	1.000-02	1.389-01	1.080+00	3.427-01	18.83
4	5.834-01	1.013+02	4.680-01	2.198-01	2.739-01	2.872-01	1.451-01	1.012-02	1.385-01	1.076+00	3.485-01	20.11
5	6.668-01	1.018+02	4.661-01	2.224-01	2.750-01	2.922-01	1.364-01	1.025-02	1.382-01	1.072+00	3.544-01	21.38
6	7.502-01	1.022+02	4.640-01	2.253-01	2.763-01	2.973-01	1.276-01	1.039-02	1.380-01	1.067+00	3.603-01	22.63
7	8.336-01	1.027+02	4.617-01	2.286-01	2.777-01	3.025-01	1.188-01	1.055-02	1.377-01	1.062+00	3.663-01	23.86
8	9.170-01	1.033+02	4.591-01	2.322-01	2.792-01	3.078-01	1.100-01	1.072-02	1.375-01	1.056+00	3.724-01	25.08
9	1.000+00	1.039+02	4.564-01	2.361-01	2.809-01	3.132-01	1.011-01	1.091-02	1.374-01	1.050+00	3.786-01	26.27
10	1.084+00	1.046+02	4.535-01	2.404-01	2.828-01	3.187-01	9.206-02	1.111-02	1.372-01	1.043+00	3.849-01	27.45
				2.252+00	2.767+00	2.952+00	1.318+00	1.038-01	1.387+00	-5.432-03	3.576+00	

Y=	.27855789+02	Z=	.12550281+01	TH=	.55819818+02	OMSS=	-.31905335+00	W=	.36401738+04
XI=	.98605760+02	ZI=	.89294775+01	THI=	.20093229+01	OMG=	-.32736504+03	WI=	.17684304+04
XIG=	-.29395169+00	ZIG=	.97347553+00	THII=	-.49380300+02	OMGI=	-.10591991+03	Q=	.11885000+02
FA=	.63667471+01	FN=	-.[illegible]95950+00	FX=	.29679804+01	FZ=	.56805102+01	F=	.64091421+01
MCH=	.90909091-01	MW=	.10377149+00	MT=	-.28286897+00	MO=	-.48196752+00	DRAG=	.11806237+02
VIN=	.10000000+03	ALT=	.09874497+03	CD=	.00000000	GV=	.84825560+02	DF=	.00000000
ATT=	.31038017+01	AMO=	.27360305+00	COT=	.36523966+00	RBT=	.71993155+00	RRO=	.66276486+00

TIME= .289

I	R	VR	WSS	DB	LB	DS	TORQ	MB	SFB	CL	FN	ALPHA
1	3.332-01	1.005+02	4.940-01	2.197-01	2.809-01	2.829-01	1.764-01	9.830-03	1.346-01	1.123+00	3.380-01	16.85
2	4.166-01	1.008+02	4.926-01	2.214-01	2.817-01	2.881-01	1.674-01	9.921-03	1.342-01	1.120+00	3.440-01	18.21
3	5.000-01	1.011+02	4.910-01	2.234-01	2.827-01	2.934-01	1.583-01	1.003-02	1.337-01	1.116+00	3.502-01	19.56
4	5.834-01	1.015+02	4.891-01	2.259-01	2.838-01	2.987-01	1.492-01	1.015-02	1.333-01	1.112+00	3.564-01	20.90
5	6.668-01	1.019+02	4.870-01	2.287-01	2.851-01	3.042-01	1.401-01	1.029-02	1.329-01	1.107+00	3.627-01	22.21
6	7.502-01	1.024+02	4.846-01	2.319-01	2.865-01	3.098-01	1.309-01	1.045-02	1.325-01	1.102+00	3.692-01	23.51
7	8.336-01	1.030+02	4.820-01	2.354-01	2.881-01	3.156-01	1.217-01	1.062-02	1.322-01	1.096+00	3.757-01	24.79
8	9.170-01	1.036+02	4.791-01	2.394-01	2.899-01	3.214-01	1.124-01	1.081-02	1.319-01	1.090+00	3.823-01	26.05
9	1.000+00	1.043+02	4.760-01	2.437-01	2.919-01	3.274-01	1.030-01	1.101-02	1.317-01	1.083+00	3.890-01	27.29
10	1.084+00	1.050+02	4.727-01	2.484-01	2.940-01	3.335-01	9.350-02	1.123-02	1.314-01	1.076+00	3.958-01	28.51
				2.318+00	2.865+00	3.075+00	1.353+00	1.043-01	1.329+00	2.055-02	3.663+00	

Y=	.2[illegible]1365+02	Z=	.13458875+01	TH=	.56851819+02	OMSS=	-.33373544+00	W=	.38086037+04
XI=	.98503997+02	ZI=	.92423106+01	THI=	.16259077+01	OMG=	-.33834618+03	WI=	.17608816+04
XIG=	-.30616426+00	ZIG=	.97137469+00	THII=	-.29419309+02	OMGI=	-.12158536+03	Q=	.11885000+02
FA=	.69593409+01	FN=	-.45924206+00	FX=	.30855004+01	FZ=	.62969389+01	F=	.70122572+01
MCH=	.90909091-01	MW=	.10232853+00	MT=	-.16886683+00	MO=	-.56735397+00	DRAG=	.12300141+02
VIN=	.10000000+03	ALT=	.49865411+03	CD=	.00000000	GV=	.84640086+02	DF=	.00000000
ATT=	.31561453+01	AMO=	.99521447+00	COT=	.37149793+00	RBT=	.72056194+00	RRO=	.66169813+00

TIME= .299

I	R	VR	WSS	DB	LB	DS	TORQ	MB	SFB	CL	FN	ALPHA
1	3.332-01	1.005+02	5.156-01	2.243-01	2.903-01	2.922-01	1.815-01	9.792-03	1.303-01	1.159+00	3.444-01	17.47
2	4.166-01	1.008+02	5.141-01	2.261-01	2.912-01	2.979-01	1.720-01	9.890-03	1.297-01	1.156+00	3.509-01	18.89
3	5.000-01	1.012+02	5.123-01	2.284-01	2.923-01	3.036-01	1.625-01	1.000-02	1.291-01	1.152+00	3.576-01	20.30
4	5.834-01	1.016+02	5.101-01	2.311-01	2.935-01	3.095-01	1.529-01	1.014-02	1.286-01	1.147+00	3.643-01	21.69
5	6.668-01	1.021+02	5.077-01	2.341-01	2.950-01	3.155-01	1.433-01	1.029-02	1.281-01	1.142+00	3.711-01	23.06
6	7.502-01	1.026+02	5.049-01	2.376-01	2.967-01	3.216-01	1.337-01	1.046-02	1.277-01	1.136+00	3.780-01	24.41
7	8.336-01	1.033+02	5.020-01	2.415-01	2.985-01	3.279-01	1.240-01	1.064-02	1.273-01	1.130+00	3.851-01	25.74
8	9.170-01	1.039+02	4.987-01	2.457-01	3.006-01	3.343-01	1.142-01	1.085-02	1.269-01	1.123+00	3.922-01	27.04
9	1.000+00	1.047+02	4.952-01	2.506-01	3.028-01	3.409-01	1.043-01	1.107-02	1.266-01	1.115+00	3.995-01	28.33
10	1.034+00	1.055+02	4.915-01	2.557-01	3.052-01	3.476-01	9.425-02	1.131-02	1.263-01	1.107+00	4.069-01	29.58
				2.375+00	2.966+00	3.191+00	1.382+00	1.044-01	1.281+00	4.383-02	3.750+00	

Y=	.29825954+02	Z=	.14398720+01	TH=	.57719810+02	OMSS=	-.34900070+00	W=	.33764720+04
XI=	.98408458+02	ZI=	.95344678+01	THI=	.14334435+01	OMG=	-.35045613+03	WI=	.17551056+04
XIG=	-.31761750+00	ZIG=	.[illegible]926710+00	THII=	-.11926804+02	OMGI=	-.13003092+03	Q=	.11885000+02
FA=	.76060317+01	FN=	[illegible]709940+01	FX=	.31988621+01	FZ=	.69757651+01	F=	.76742520+01
MCH=	.90909091-01	MW=	[illegible]298960+00	MT=	-.65589855-01	MO=	-.61694115+00	DRAG=	.12763750+02
VIN=	.10000000+03	ALT=	.44856013+03	CD=	.00000000	GV=	.84454539+02	DF=	.00000000
ATT=	.32074083+01	AMO=	.91288129+00	COT=	.37806937+00	RBT=	.72122867+00	RRO=	.66032393+00

TIME= .309

I	R	VR	WSS	DB	LB	DS	TORQ	MB	SFB	CL	FN	ALPHA
1	3.332-01	1.006+02	5.371-01	2.285-01	2.994-01	3.012-01	1.852-01	9.719-03	1.260-01	1.194+00	3.508-01	18.09
2	4.166-01	1.009+02	5.354-01	2.305-01	3.004-01	3.073-01	1.762-01	9.823-03	1.254-01	1.191+00	3.578-01	19.57
3	5.000-01	1.013+02	5.333-01	2.330-01	3.016-01	3.136-01	1.663-01	9.940-03	1.247-01	1.186+00	3.649-01	21.03
4	5.834-01	1.018+02	5.309-01	2.359-01	3.031-01	3.199-01	1.562-01	1.009-02	1.241-01	1.181+00	3.721-01	22.48
5	6.668-01	1.023+02	5.281-01	2.393-01	3.048-01	3.265-01	1.462-01	1.025-02	1.236-01	1.175+00	3.795-01	23.90
6	7.502-01	1.029+02	5.251-01	2.431-01	3.066-01	3.332-01	1.360-01	1.043-02	1.231-01	1.169+00	3.869-01	25.30
7	8.336-01	1.036+02	5.217-01	2.474-01	3.088-01	3.400-01	1.258-01	1.064-02	1.226-01	1.162+00	3.945-01	26.68
8	9.170-01	1.043+02	5.180-01	2.521-01	3.111-01	3.470-01	1.155-01	1.086-02	1.221-01	1.154+00	4.023-01	28.03
9	1.000+00	1.051+02	5.141-01	2.572-01	3.136-01	3.542-01	1.050-01	1.110-02	1.217-01	1.146+00	4.101-01	29.36
10	1.084+00	1.059+02	5.099-01	2.628-01	3.163-01	3.615-01	9.447-02	1.135-02	1.213-01	1.137+00	4.182-01	30.66
				2.430+00	3.066+00	3.304+00	1.408+00	1.042-01	1.235+00	6.632-02	3.837+00	

Y=	.30809520+02	Z=	.15369745+01	TH=	.58524751+02	OMSS=	-.36475693+00	W=	.41438868+04
XI=	.98304293+02	ZI=	.98659389+01	THI=	.13984377+01	OMG=	-.36302933+03	WI=	.17519463+04
XIG=	-.[illegible]80460+00	ZIG=	.96710839+00	THII=	.22080446+01	OMGI=	-.13219274+03	Q=	.11885000+02
FA=	.32972419+01	FN=	-.11464272+01	FX=	.33119448+01	FZ=	.77011245+01	F=	.83830576+01
MCH=	.90909091-01	MW=	.10280821+00	MT=	.12651216-01	MO=	-.63666122+00	DRAG=	.13217826+02
VIN=	.10000000+03	ALT=	.49846303+03	CD=	.00000000	GV=	.84268916+02	DF=	.00000000
ATT=	.32585180+01	AMO=	.92738073+00	COT=	.38473774+00	RBT=	.72191706+00	RRO=	.65874579+00

TIME= .40

I	R	VR	WSS	DB	LB	DS	TORQ	MR	SFB	CL	FN	ALPHA
1	3.332-01	1.012+02	7.419-01	2.715-01	3.678-01	3.880-01	2.151-01	7.466-03	7.453-02	1.450+00	4.094-01	23.76
2	4.166-01	1.018+02	7.371-01	2.757-01	3.707-01	3.998-01	2.003-01	7.660-03	7.341-02	1.442+00	4.219-01	25.34
3	5.000-01	1.026+02	7.314-01	2.807-01	3.743-01	4.121-01	1.854-01	7.898-03	7.233-02	1.434+00	4.348-01	27.37
4	5.834-01	1.036+02	7.247-01	2.867-01	3.786-01	4.248-01	1.704-01	8.180-03	7.130-02	1.424+00	4.481-01	29.35
5	6.668-01	1.047+02	7.173-01	2.936-01	3.835-01	4.379-01	1.552-01	8.506-03	7.032-02	1.413+00	4.618-01	31.28
6	7.502-01	1.059+02	7.092-01	3.015-01	3.889-01	4.514-01	[illegible]8-01	6.877-03	6.937-02	1.401+00	4.759-01	33.15
7	8.336-01	1.072+02	7.004-01	3.102-01	3.950-01	4.654-01	[illegible]1-01	9.293-03	6.847-02	1.388+00	4.904-01	34.97
8	9.170-01	1.086+02	6.910-01	3.199-01	4.016-01	4.798-01	[illegible]9-01	9.753-03	6.760-02	1.373+00	5.054-01	36.73
9	1.000+00	1.102+02	6.812-01	3.305-01	4.088-01	4.946-01	[illegible]8-02	1.026-02	6.676-02	1.359+00	5.208-01	38.43
10	1.084+00	1.119+02	6.710-01	3.421-01	4.165-01	5.098-01	[illegible]474-02	1.081-02	6.597-02	1.343+00	5.366-01	40.07
				3.013+00	3.886+00	4.464+00	1.465+00	8.870-02	7.001-01	3.097-01	4.705+00	

Y=	.40580671+02	Z=	.26778166+01	TH=	.67505549+02	OMSS=	-.52215635+00	W=	.57492696+04		
XI=	.97057091+02	ZI=	.12936848+02	THI=	.11515245+01	OMG=	-.47971872+03	WI=	.15170343+04		
XIG=	-.44246517+00	ZIG=	.94117000+00	THII=	-.13745414+02	OMGI=	-.12648982+03	Q=	.11885000+02		
FA=	.16666802+02	FN=	-.20665880+01	FX=	.44672630+01	FZ=	.16189398+02	F=	.16794435+02		
MCH=	.90909091-01	MW=	.89019570-01	MT=	-.78898675-01	MO=	-.69991606+00	DRAG=	.17854362+02		
VIN=	.10000000+03	ALT=	.49732219+07	CD=	.00000000	GV=	.82407734+02	DF=	.00000000		
ATT=	.37450352+01	AMO=	.93073632+00	COT=	.44283808+00	RBT=	.72916052+00	RRO=	.63544779+00		

TIME= .50

I	R	VR	WSS	DB	LB	DS	TORQ	MR	SFB	CL	FN	ALPHA
1	3.332-01	1.019+02	8.941-01	2.932-01	4.039-01	4.390-01	2.185-01	3.871-03	4.724-02	1.569+00	4.499-01	26.82
2	4.166-01	1.030+02	8.849-01	3.000-01	4.099-01	4.567-01	1.992-01	4.195-03	4.612-02	1.560+00	4.682-01	29.41
3	5.000-01	1.043+02	8.740-01	3.082-01	4.171-01	4.751-01	1.797-01	4.594-03	4.505-02	1.548+00	4.872-01	31.93
4	5.834-01	1.058+02	8.616-01	3.180-01	4.255-01	4.945-01	1.599-01	5.071-03	4.403-02	1.535+00	5.071-01	34.35
5	6.668-01	1.075+02	8.479-01	3.292-01	4.352-01	5.146-01	1.396-01	5.620-03	4.305-02	1.521+00	5.279-01	36.69
6	7.502-01	1.094+02	8.332-01	3.420-01	4.459-01	5.356-01	1.189-01	6.254-03	4.212-02	1.505+00	5.494-01	38.93
7	8.336-01	1.115+02	8.176-01	3.562-01	4.578-01	5.574-01	9.738-02	6.960-03	4.122-02	1.487+00	5.718-01	41.07
8	9.170-01	1.137+02	8.014-01	3.720-01	4.707-01	5.800-01	7.520-02	7.742-03	4.037-02	1.469+00	5.950-01	43.12
9	1.000+00	1.161+02	7.847-01	3.892-01	4.846-01	6.034-01	5.220-02	8.600-03	3.956-02	1.450+00	6.190-01	45.06
10	1.084+00	1.187+02	7.676-01	4.080-01	4.994-01	6.275-01	2.832-02	9.532-03	3.879-02	1.430+00	6.437-01	46.91
				3.416+00	4.450+00	5.284+00	1.269+00	6.244-02	4.275-01	3.957-01	5.419+00	

Y=	.50210750+02	Z=	.41214455+01	TH=	.72365196+02	OMSS=	-.66539335+00	W=	.69716766+04		
XI=	.95511364+02	ZI=	.15922145+02	THI=	.54170762+00	OMG=	-.59265412+03	WI=	.10646912+04		
XIG=	-.57121680+00	ZIG=	.91328656+00	THII=	-.30544849+02	OMGI=	-.10990771+03	Q=	.11885000+02		
FA=	.26521937+02	FN=	-.28859607+01	FX=	.52844508+01	FZ=	.26149884+02	F=	.26678491+02		
MCH=	.90909091-01	MW=	.62476078-01	MT=	-.17532747+00	MO=	-.64723106+00	DRAG=	.21135229+02		
VIN=	.10000000+03	ALT=	.49587856+07	CD=	.00000000	GV=	.80535585+02	DF=	.00000000		
ATT=	.41052421+01	AMO=	.75426242+00	COT=	.49269232+00	RBT=	.73585037+00	RRO=	.59440865+00		

TIME= .60

I	R	VR	WSS	DB	LB	DS	TORQ	MR	SFB	CL	FN	ALPHA
1	3.332-01	1.025+02	9.940-01	3.036-01	3.765-01	4.390-01	1.870-01	7.568-04	3.797-02	1.443+00	4.458-01	27.35
2	4.166-01	1.040+02	9.803-01	3.128-01	3.878-01	4.616-01	1.680-01	1.208-03	3.690-02	1.446+00	4.691-01	30.46
3	5.000-01	1.058+02	9.643-01	3.240-01	4.017-01	4.863-01	1.478-01	1.767-03	3.583-02	1.450+00	4.943-01	33.49
4	5.834-01	1.078+02	9.464-01	3.372-01	4.182-01	5.129-01	1.273-01	2.432-03	3.476-02	1.453+00	5.216-01	36.41
5	6.668-01	1.100+02	9.269-01	3.525-01	4.706-01	5.687-01	1.203-01	3.193-03	3.268-02	1.569+00	5.751-01	40.34
6	7.502-01	1.125+02	9.062-01	3.699-01	4.867-01	5.923-01	9.501-02	4.075-03	3.176-02	1.551+00	6.033-01	42.82
7	8.336-01	1.153+02	8.846-01	3.893-01	5.044-01	6.211-01	6.860-02	5.062-03	3.090-02	1.531+00	6.327-01	45.16
8	9.170-01	1.183+02	8.674-01	4.107-01	5.235-01	6.510-01	4.107-02	6.154-03	3.008-02	1.511+00	6.633-01	47.37
9	1.000+00	1.214+02	8.400-01	4.342-01	5.440-01	6.819-01	1.219-02	7.350-03	2.930-02	1.489+00	6.949-01	49.44
10	1.084+00	1.248+02	8.175-01	4.597-01	5.657-01	7.139-01	-1.809-02	8.648-03	2.857-02	1.467+00	7.276-01	51.39
				3.694+00	4.679+00	5.725+00	9.501-01	4.065-02	3.287-01	4.168-01	5.828+00	

Y=	.59675587+02	Z=	.58591728+01	TH=	.74391181+02	OMSS=	-.77521423+00	W=	.77976332+04		
XI=	.93765064+02	ZI=	.18818758+02	THI=	.26452997+00	OMG=	-.68370094+03	WI=	.69011933+03		
XIG=	-.56130953+00	ZIG=	.86753719+00	THII=	-.41579787+01	OMGI=	-.78037362+02	Q=	.11885000+02		
FA=	.35600258+02	FN=	-.34982883+01	FX=	.57247871+01	FZ=	.35363702+02	F=	.35824079+02		
MCH=	.90909091-01	MW=	.40496202-01	MT=	-.23866795-01	MO=	-.46463118+00	DRAG=	.22898604+02		
VIN=	.10000000+03	ALT=	.49414083+07	CD=	.00000000	GV=	.78651444+02	DF=	.00000000		
ATT=	.44978852+01	AMO=	.51971236+00	COT=	.52262583+00	RBT=	.74658798+00	RRO=	.54701549+00		

TIME= .70

I	R	VR	WSS	DB	LB	DS	TORQ	MR	SFB	CL	FN	ALPHA
1	3.332-01	1.031+02	1.056+00	3.101-01	3.845-01	4.533-01	1.822-01	-1.506-03	3.245-02	1.459+00	4.588-01	28.71
2	4.166-01	1.048+02	1.039+00	3.211-01	3.982-01	4.794-01	1.601-01	-9.507-04	3.140-02	1.462+00	4.854-01	32.08
3	5.000-01	1.069+02	1.019+00	3.346-01	4.149-01	5.077-01	1.376-01	-2.642-04	3.037-02	1.466+00	5.144-01	35.34
4	5.834-01	1.093+02	9.966-01	3.506-01	4.347-01	5.386-01	1.144-01	5.533-04	2.934-02	1.469+00	5.460-01	38.47
5	6.668-01	1.120+02	9.727-01	3.690-01	4.575-01	5.720-01	5.018-02	1.501-03	2.831-02	1.473+00	5.801-01	41.46
6	7.502-01	1.149+02	9.476-01	3.899-01	5.141-01	6.302-01	7.594-02	2.569-03	2.645-02	1.571+00	6.399-01	45.24
7	8.336-01	1.182+02	9.217-01	4.132-01	5.364-01	6.643-01	4.589-02	3.778-03	2.562-02	1.550+00	6.746-01	47.69
8	9.170-01	1.216+02	8.954-01	4.390-01	5.605-01	6.997-01	1.424-02	5.113-03	2.483-02	1.529+00	7.108-01	49.99
9	1.000+00	1.253+02	8.690-01	4.672-01	5.862-01	7.365-01	-1.913-02	6.573-03	2.409-02	1.506+00	7.482-01	52.13
10	1.084+00	1.292+02	8.428-01	4.979-01	6.134-01	7.744-01	-5.435-02	8.156-03	2.339-02	1.482+00	7.869-01	54.12
				3.893+00	4.900+00	6.056+00	7.470-01	2.552-02	2.762-01	4.228-01	6.145+00	

Y=	.68960076+02	Z=	.78824039+01	TH=	.75556497+02	OMSS=	-.85011350+00	W=	.83239879+04		
XI=	.91910717+02	ZI=	.21632005+02	THI=	.14277635+00	OMG=	-.74514993+03	WI=	.43227874+03		
XIG=	-.58955729+00	ZIG=	.86162983+00	THII=	-.72405067+00	OMGI=	-.53794759+02	Q=	.11885000+02		
FA=	.42583439+02	FN=	-.47141569+01	FX=	.63567254+01	FZ=	.42513369+02	F=	.42843572+02		
MCH=	.90909091-01	MW=	.25366117-01	MT=	-.13170466-02	MO=	-.32338737+00	DRAG=	.24224755+02		
VIN=	.10000000+03	ALT=	.49211760+07	CD=	.00000000	GV=	.76755963+02	DF=	.00000000		
ATT=	.47330343+01	AMO=	.35326726+00	COT=	.54591687+00	RBT=	.75070778+00	RRO=	.41254026+00		

NOT REPRODUCIBLE

TIME= .809

I	P	VR	MSS	DB	LR	DS	TORQ	MP	SFB	CL	FN	ALPHA
1	3.332-01	1.035+02	1.094+00	3.142-01	3.896-01	4.625-01	1.780-01	-3.018-03	2.936-02	1.468+00	4.673-01	29.60
2	4.166-01	1.054+02	1.074+00	3.266-01	4.050-01	4.908-01	1.588-01	-2.386-03	2.830-02	1.471+00	4.962-01	33.14
3	5.000-01	1.077+02	1.051+00	3.417-01	4.238-01	5.219-01	1.383-01	-1.605-03	2.733-02	1.474+00	5.279-01	36.58
4	5.834-01	1.103+02	1.026+00	3.596-01	4.460-01	5.587-01	1.052-01	-6.761-04	2.632-02	1.478+00	5.624-01	39.79
5	6.668-01	1.133+02	9.991-01	3.803-01	4.716-01	5.926-01	7.896-02	4.002-04	2.533-02	1.487+00	5.998-01	42.89
6	7.502-01	1.166+02	9.709-01	4.037-01	5.005-01	6.319-01	5.119-02	1.622-03	2.434-02	1.485+00	6.401-01	45.82
7	8.336-01	1.202+02	9.421-01	4.299-01	5.581-01	6.932-01	2.982-02	2.982-03	2.272-02	1.559+00	7.028-01	49.78
8	9.170-01	1.240+02	9.131-01	4.588-01	5.858-01	7.326-01	-5.160-03	4.494-03	2.156-02	1.537+00	7.429-01	51.63
9	1.000+00	1.281+02	8.841-01	4.905-01	6.152-01	7.778-01	-4.178-02	6.145-03	2.125-02	1.514+00	7.845-01	53.80
10	1.084+00	1.323+02	8.556-01	5.249-01	6.463-01	8.155-01	-8.057-02	7.933-03	2.058-02	1.489+00	8.274-01	55.81
				4.030+00	5.087+00	6.270+00	6.000-01	1.589-02	2.475-01	4.243-01	6.351+00	

XI=	.77055339+02	ZI=	.10187818+02	THI=	.76239518+02	OMEGI=	-.90011991+00	MI=	.86526732+00
YI=	.8998725E+02	ZII=	.2436296E+01	THII=	.8498648?+01	OMGI=	-.78662770+03	MII=	.26985528+03
XIG=	-.60525877+00	ZIG=	.81635096+00	THIII=	.12850150+00	OMGII=	-.3512815E+02	Q=	.11885000+02
FA=	.47597A20+02	FN=	-.52011787+01	FX=	.62698966+01	FY=	.4746886E+02	F=	.47881151+02
MCH=	.90909091-01	MW=	.15811636-01	MT=	.71463879-03	MO=	-.21350773+00	DRAG=	.25079533+02
VIN=	.10000000+03	ALT=	.4998171E+03	CD=	.00000000	GV=	.7A851022+02	DF=	.00000000
ATT=	.4888330?+01	AMO=	.23190588+00	CDT=	.56983369+00	RBT=	.75312096+00	RRO=	.38649803+00

TIME= .909

I	P	VR	MSS	DB	LR	DS	TORQ	MP	SFB	CL	FN	ALPHA
1	3.332-01	1.037+02	1.117+00	3.169-01	3.929-01	4.689-01	1.751-01	-3.995-03	2.758-02	1.473+00	4.728-01	30.18
2	4.166-01	1.058+02	1.096+00	3.302-01	4.094-01	4.983-01	1.505-01	-3.309-03	2.658-02	1.476+00	5.033-01	33.62
3	5.000-01	1.083+02	1.071+00	3.465-01	4.296-01	5.312-01	1.253-01	-2.462-03	2.558-02	1.479+00	5.368-01	37.32
4	5.834-01	1.111+02	1.044+00	3.657-01	4.535-01	5.670-01	9.897-02	-1.458-03	2.459-02	1.483+00	5.733-01	40.65
5	6.668-01	1.143+02	1.014+00	3.880-01	4.811-01	6.059-01	7.127-02	-2.887-04	2.361-02	1.487+00	6.129-01	43.81
6	7.502-01	1.178+02	9.843-01	4.131-01	5.123-01	6.480-01	4.191-02	1.035-03	2.264-02	1.490+00	6.558-01	46.79
7	8.336-01	1.216+02	9.535-01	4.413-01	5.726-01	7.127-01	1.795-02	2.507-03	2.108-02	1.563+00	7.216-01	50.29
8	9.170-01	1.256+02	9.227-01	4.724-01	6.028-01	7.534-01	-1.868-02	4.191-03	2.033-02	1.541+00	7.645-01	52.67
9	1.000+00	1.299+02	8.921-01	5.065-01	6.348-01	7.980-01	-5.767-02	5.925-03	1.963-02	1.517+00	8.089-01	54.86
10	1.084+00	1.345+02	8.621-01	5.435-01	6.685-01	8.430-01	-9.886-02	7.855-03	1.898-02	1.492+00	8.547-01	56.87
				4.178+00	5.158+00	6.427+00	5.057-01	9.955-03	2.306-01	4.248-01	6.505+00	

XI=	.86956049+02	ZI=	.12752297+02	THI=	.76688288+02	OMEGI=	-.93333011+00	MI=	.88575477+00
YI=	.8802?096+02	ZII=	.27013463+02	THII=	.58927852-01	OMGI=	-.81425715+03	MII=	.16879661+03
XIG=	-.61884392+00	ZIG=	.81165752+00	THIII=	-.70519891+00	OMGII=	-.23470295+02	Q=	.11885000+02
FA=	.51790038+02	FN=	-.55208125+01	FX=	.60966231+01	FY=	.5098A400+02	F=	.51387884+02
MCH=	.90909091-01	MW=	.20088738-02	MT=	-.17518817-02	MO=	-.14197027+00	DRAG=	.25706873+02
VIN=	.10000000+03	ALT=	.4972477E+03	CD=	.00000000	GV=	.7297?241+02	DF=	.00000000
ATT=	.5008?869+01	AMO=	.15336837+00	CDT=	.57898137+00	RBT=	.75466888+00	RRO=	.30325738+00

TIME= 1.009

I	P	VR	MSS	DB	LR	DS	TORQ	MP	SFB	CL	FN	ALPHA
1	3.332-01	1.039+02	1.132+00	3.186-01	3.951-01	4.722-01	1.[illegible]-01	-4.622-03	2.651-02	1.476+00	4.764-01	30.56
2	4.166-01	1.061+02	1.109+00	3.326-01	4.124-01	5.037-01	1.[illegible]-01	-3.899-03	2.552-02	1.479+00	5.080-01	34.27
3	5.000-01	1.086+02	1.083+00	3.496-01	4.335-01	5.377-01	1.214-01	-3.007-03	2.453-02	1.482+00	5.426-01	37.82
4	5.834-01	1.116+02	1.056+00	3.698-01	4.585-01	5.788-01	9.665-02	-1.986-03	2.355-02	1.486+00	5.805-01	41.21
5	6.668-01	1.149+02	1.026+00	3.931-01	4.874-01	6.249-01	6.601-02	-7.197-04	2.258-02	1.490+00	6.217-01	44.41
6	7.502-01	1.186+02	9.921-01	4.198-01	5.201-01	6.586-01	3.589-02	6.738-04	2.162-02	1.493+00	6.662-01	47.42
7	8.336-01	1.225+02	9.601-01	4.489-01	5.822-01	7.250-01	1.017-02	2.221-03	2.009-02	1.566+00	7.341-01	50.98
8	9.170-01	1.267+02	9.281-01	4.815-01	6.141-01	7.689-01	-2.789-02	3.938-03	1.935-02	1.543+00	7.787-01	53.33
9	1.000+00	1.312+02	8.965-01	5.172-01	6.478-01	8.147-01	-6.878-02	5.812-03	1.866-02	1.519+00	8.250-01	55.53
10	1.088+00	1.359+02	8.656-01	5.560-01	6.834-01	8.613-01	-1.113-01	7.839-03	1.802-02	1.494+00	8.727-01	57.55
				4.187+00	5.235+00	6.[illegible]	4.820-01	6.291-03	2.204-01	4.243-01	6.606+00	

XI=	.95659727+02	ZI=	.15582?00+02	THI=	.76893057+02	OMEGI=	-.95518768+00	MI=	.89863890+00
YI=	.8603978?+02	ZII=	.2958598A+02	THII=	.74040926-01	OMGI=	-.83247225+03	MII=	.10662296+03
XIG=	-.61758269+00	ZIG=	.78786688+00	THIII=	-.15786401+00	OMGII=	-.15335550+02	Q=	.11885000+02
FA=	.53856776+02	FN=	-.57819879+01	FX=	.65300019+01	FY=	.5336628?+02	F=	.53768270+02
MCH=	.90909091-01	MW=	.62566751-02	MT=	-.99383787-03	MO=	-.93130361-01	DRAG=	.26120001+02
VIN=	.10000000+03	ALT=	.4998171E+03	CD=	.00000000	GV=	.71023750+02	DF=	.00000000
ATT=	.5081?832+01	AMO=	.10019698+00	CDT=	.58799839+00	RBT=	.75566738+00	RRO=	.22671339+00

TIME= 1.109

I	P	VR	MSS	DB	LR	DS	TORQ	MP	SFB	CL	FN	ALPHA
1	3.332-01	1.040+02	1.141+00	3.197-01	3.965-01	4.747-01	1.719-01	-5.025-03	2.585-02	1.478+00	4.788-01	30.80
2	4.166-01	1.062+02	1.117+00	3.341-01	4.143-01	5.063-01	1.467-01	-4.277-03	2.486-02	1.481+00	5.110-01	34.56
3	5.000-01	1.088+02	1.090+00	3.517-01	4.361-01	5.412-01	1.196-01	-3.354-03	2.388-02	1.484+00	5.465-01	38.15
4	5.834-01	1.119+02	1.060+00	3.725-01	4.618-01	5.793-01	9.190-02	-2.258-03	2.291-02	1.488+00	5.852-01	41.57
5	6.668-01	1.153+02	1.029+00	3.968-01	4.916-01	6.207-01	6.757-02	-9.304-04	2.194-02	1.491+00	6.274-01	44.79
6	7.502-01	1.191+02	9.968-01	4.246-01	5.253-01	6.655-01	3.131-02	4.474-04	2.099-02	1.495+00	6.730-01	47.83
7	8.336-01	1.231+02	9.640-01	4.540-01	5.885-01	7.339-01	5.021-03	2.046-03	1.948-02	1.567+00	7.422-01	51.35
8	9.170-01	1.274+02	9.313-01	4.876-01	6.215-01	7.797-01	-3.382-02	3.818-03	1.875-02	1.544+00	7.880-01	53.75
9	1.000+00	1.320+02	8.990-01	5.243-01	6.568-01	8.260-01	-7.539-02	5.751-03	1.807-02	1.520+00	8.355-01	55.96
10	1.088+00	1.368+02	8.675-01	5.643-01	6.937-01	8.732-01	-1.195-01	7.842-03	1.744-02	1.494+00	8.846-01	57.98
				4.228+00	5.295+00	6.598+00	3.987-01	4.000-03	2.142-01	4.241-01	6.672+00	

XI=	.10816382+03	ZI=	.18666472+02	THI=	.77089393+02	OMEGI=	-.96981339+00	MI=	.90[illegible]+00
YI=	.8405359?+02	ZII=	.3208?370+02	THII=	.21890985-01	OMGI=	-.8883[illegible]+03	MII=	.67788693+02
XIG=	-.61585650+00	ZIG=	.76993357+00	THIII=	-.98772208-01	OMGII=	-.99505688+01	Q=	.11885000+02
FA=	.55027118+02	FN=	-.58883253+01	FX=	.65975356+01	FY=	.5898615?+02	F=	.55340883+02
MCH=	.90909091-01	MW=	.79779805-02	MT=	-.56695285-03	MO=	-.60895875-01	DRAG=	.26352100+02
VIN=	.10000000+03	ALT=	.4983330?+03	CD=	.00000000	GV=	.69170099+02	DF=	.00000000
ATT=	.5173523?+01	AMO=	.68956535-01	CDT=	.58828459+00	RBT=	.75630083+00	RRO=	.16251012+00

TIME= 1.209

I	R	VR	MS	DB	LR	DS	TORQ	MR	SFB	CL	FN	ALPHA
1	3.332-01	1.041+02	1.147+00	3.209-01	3.974-01	6.763-01	1.711-01	-5.283-03	2.583-02	1.479+00	8.803-01	30.96
2	8.166-01	1.064+02	1.122+00	3.351-01	8.155-01	5.084-01	1.450-01	-8.519-03	2.445-02	1.487+00	5.130-01	34.74
3	5.000-01	1.090+02	1.095+00	3.510-01	8.377-01	5.437-01	1.182-01	-3.577-03	2.347-02	1.486+00	5.489-01	38.76
4	5.834-01	1.121+02	1.065+00	3.742-01	8.680-01	5.824-01	9.008-02	-2.458-03	2.250-02	1.489+00	5.883-01	41.80
5	6.668-01	1.156+02	1.033+00	3.986-01	8.983-01	6.245-01	6.037-02	-1.163-03	2.155-02	1.493+00	6.311-01	45.04
6	7.502-01	1.194+02	9.997-01	8.263-01	5.286-01	6.701-01	2.858-02	3.088-04	2.060-02	1.496+00	6.775-01	48.09
7	8.336-01	1.235+02	9.668-01	8.573-01	5.926-01	7.386-01	1.650-03	1.936-03	1.910-02	1.567+00	7.475-01	51.62
8	9.170-01	1.279+02	9.333-01	8.915-01	6.263-01	7.804-01	-3.790-02	3.745-03	1.837-02	1.585+00	7.941-01	54.02
9	1.000+00	1.326+02	9.005-01	5.290-01	6.620-01	8.319-01	-8.005-02	5.717-03	1.770-02	1.520+00	8.424-01	56.23
10	1.084+00	1.374+02	8.686-01	5.697-01	6.995-01	8.809-01	-1.209-01	7.850-03	1.707-02	1.455+00	8.922-01	58.27
				8.255+00	5.318+00	6.681+00	3.721-01	2.553-03	2.102-01	8.239-01	6.715+00	

X=	.11287017+03	Z=	.21997135+02	THI=	.77148141+02
XI=	.82076815+02	ZI=	.38508776+02	THI=	.13606359-01
XIG=	-.61230811+00	ZIG=	.74280071+00	THII=	-.61958977-01
FA=	.56055274+02	FN=	-.59768327+01	FX=	.66813307+01
MCH=	.90909091-01	MW=	.25385354-09	MT=	-.35562156-03
VIN=	.10000000+03	ALT=	.47800287+03	CD=	.00000000
ATT=	.51656381+01	AMO=	.41905172-01	COT=	.59177233+00
OMSS=	-.97861844+00	W=	.91200647+04		
OMG=	-.85272161+03	WI=	.43260657+02		
OMGI=	-.64234897+01	Q=	.11845000+02		
FZ=	.55980433+02	F=	.56373078+02		
MG=	-.39079954-01	DRAG=	.26565322+02		
GV=	.67196128+03	NF=	.00000000		
RBT=	.75670956+00	RMO=	.11262285+00		

TIME= 1.309

I	R	VR	MS	DB	LR	DS	TORQ	MR	SFB	CL	FN	ALPHA
1	3.332-01	1.042+02	1.150+00	3.209-01	3.979-01	6.773-01	1.705-01	-5.449-03	2.517-02	1.480+00	8.812-01	31.06
2	8.166-01	1.066+02	1.126+00	3.357-01	8.163-01	5.097-01	1.443-01	-8.674-03	2.419-02	1.483+00	5.182-01	34.86
3	5.000-01	1.092+02	1.098+00	3.539-01	8.388-01	5.458-01	1.173-01	-3.719-03	2.321-02	1.486+00	5.585-01	38.89
4	5.834-01	1.123+02	1.067+00	3.759-01	8.659-01	5.885-01	8.940-02	-2.585-03	2.225-02	1.490+00	5.983-01	41.94
5	6.668-01	1.158+02	1.035+00	4.000-01	8.961-01	6.270-01	5.847-02	-1.273-03	2.129-02	1.493+00	6.395-01	45.20
6	7.502-01	1.196+02	1.002+00	8.281-01	5.308-01	6.730-01	2.681-02	2.142-04	2.035-02	1.497+00	6.803-01	48.25
7	8.336-01	1.238+02	9.679-01	8.594-01	5.953-01	7.420-01	-5.373-04	1.867-03	1.886-02	1.568+00	7.509-01	51.79
8	9.170-01	1.282+02	9.345-01	8.940-01	6.298-01	7.884-01	-8.088-02	3.699-03	1.814-02	1.585+00	7.980-01	54.20
9	1.000+00	1.329+02	9.015-01	5.320-01	6.656-01	8.364-01	-8.307-02	5.697-03	1.746-02	1.521+00	8.468-01	56.41
10	1.084+00	1.378+02	8.693-01	5.732-01	7.036-01	8.860-01	-1.284-01	7.857-03	1.684-02	1.495+00	8.972-01	58.43
				8.273+00	5.339+00	6.670+00	3.582-01	1.637-03	2.078-01	8.737-01	6.743+00	

X=	.12057959+03	Z=	.25566271+02	THI=	.77210752+02
XI=	.80116193+02	ZI=	.36863195+02	THI=	.86952127-02
XIG=	-.60599077+00	ZIG=	.72141390+00	THII=	-.39348536-01
FA=	.56722766+02	FN=	-.60366327+01	FX=	.66695952+01
MCH=	.90909091-01	MW=	.16234255-09	MT=	-.22586054-03
VIN=	.10000000+03	ALT=	.47443373+03	CD=	.00000000
ATT=	.51870344+01	AMO=	.26950791-01	COT=	.59194514+00
OMSS=	-.98458859+00	W=	.91532941+04		
OMG=	-.85697147+03	WI=	.27665739+02		
OMGI=	-.41327738+01	Q=	.11845000+02		
FZ=	.56651828+02	F=	.57043090+02		
MG=	-.25156540-01	DRAG=	.26678382+02		
GV=	.65291818+03	NF=	.00000000		
RBT=	.75647158+00	RMO=	.76055286-01		

TIME= 1.409

I	R	VR	MS	DB	LR	DS	TORQ	MR	SFB	CL	FN	ALPHA
1	3.332-01	1.042+02	1.153+00	3.212-01	3.983-01	6.779-01	1.703-01	-5.556-03	2.497-02	1.481+00	8.818-01	31.11
2	8.166-01	1.065+02	1.128+00	3.361-01	8.168-01	5.108-01	1.440-01	-8.775-03	2.399-02	1.484+00	5.189-01	34.92
3	5.000-01	1.092+02	1.100+00	3.549-01	8.398-01	5.469-01	1.168-01	-3.814-03	2.302-02	1.487+00	5.594-01	38.96
4	5.834-01	1.124+02	1.069+00	3.759-01	8.661-01	5.856-01	8.931-02	-2.671-03	2.206-02	1.490+00	5.994-01	42.02
5	6.668-01	1.159+02	1.036+00	8.008-01	8.970-01	6.293-01	5.813-02	-1.350-03	2.111-02	1.494+00	6.398-01	45.28
6	7.502-01	1.197+02	1.003+00	8.290-01	5.320-01	6.796-01	2.591-02	1.475-04	2.017-02	1.497+00	6.819-01	48.34
7	8.336-01	1.239+02	9.691-01	8.605-01	5.711-01	7.283-01	-8.652-03	1.818-03	1.924-02	1.501+00	7.325-01	51.70
8	9.170-01	1.284+02	9.359-01	8.958-01	6.311-01	7.905-01	-4.180-02	3.656-03	1.797-02	1.585+00	8.001-01	54.19
9	1.000+00	1.331+02	9.023-01	5.336-01	6.675-01	8.388-01	-8.461-02	5.667-03	1.730-02	1.521+00	8.492-01	56.50
10	1.084+00	1.380+02	8.700-01	5.751-01	7.058-01	8.887-01	-1.302-01	7.841-03	1.668-02	1.495+00	8.999-01	58.52
				8.242+00	5.325+00	6.665+00	3.381-01	9.581-04	2.065-01	8.738-01	6.738+00	

X=	.12849833+03	Z=	.24367615+02	THI=	.77759755+02
XI=	.78184551+02	ZI=	.39153141+02	THI=	.68533399-02
XIG=	-.59638597+00	ZIG=	.70173827+00	THII=	-.25690588+00
FA=	.57058035+02	FN=	-.60670377+01	FX=	.66658222+01
MCH=	.90909091-01	MW=	.97485927-09	MT=	-.14746398-02
VIN=	.10000000+03	ALT=	.47063239+03	CD=	.00000000
ATT=	.51824759+01	AMO=	.13524268-01	COT=	.59338359+00
OMSS=	-.98756760+00	W=	.91739970+04		
OMG=	-.15993275+03	WI=	.16613184+02		
OMGI=	-.89970759+01	Q=	.11845000+02		
FZ=	.55991731+02	F=	.57279684+02		
MG=	-.11 134803-01	DRAG=	.26661689+02		
GV=	.63399277+03	NF=	.00000000		
RBT=	.75387605+00	RMO=	.80000273-01		

TIME= 1.509

I	R	VR	MS	DB	LR	DS	TORQ	MR	SFB	CL	FN	ALPHA
1	3.332-01	1.042+02	1.154+00	3.213-01	3.984-01	6.781-01	1.700-01	-5.607-03	2.499-02	1.480+00	8.820-01	31.14
2	8.166-01	1.065+02	1.129+00	3.363-01	8.170-01	5.108-01	1.437-01	-8.824-03	2.401-02	1.483+00	5.153-01	34.96
3	5.000-01	1.092+02	1.101+00	3.546-01	8.397-01	5.468-01	1.164-01	-3.857-03	2.304-02	1.487+00	5.519-01	38.61
4	5.834-01	1.124+02	1.070+00	3.763-01	8.666-01	5.862-01	8.785-02	-2.710-03	2.207-02	1.490+00	5.920-01	42.07
5	6.668-01	1.159+02	1.037+00	4.013-01	8.976-01	6.295-01	5.758-02	-1.387-03	2.112-02	1.494+00	6.356-01	45.33
6	7.502-01	1.198+02	1.003+00	8.296-01	5.327-01	6.755-01	2.525-02	1.216-04	2.018-02	1.497+00	6.828-01	48.40
7	8.336-01	1.240+02	9.695-01	8.613-01	5.720-01	7.254-01	-9.441-03	1.800-03	1.924-02	1.501+00	7.336-01	51.26
8	9.170-01	1.285+02	9.358-01	8.963-01	6.329-01	7.919-01	-4.272-02	3.686-03	1.797-02	1.586+00	8.016-01	54.35
9	1.000+00	1.332+02	9.025-01	5.346-01	6.689-01	8.404-01	-8.5F -02	5 666-03	1.730-02	1.521+00	8.508-01	56.56
10	1.084+00	1.382+02	8.702-01	5.763-01	7.074-01	8.904-01	-1.3. 01	7.850-03	1.667-02	1.495+00	9.016-01	58.59
				8.288+00	5.332+00	6.674+00	3.315-01	7.027-04	2.066-01	8.747-01	6.747+00	

X=	.13621782+03	Z=	.33348780+02	THI=	.77252515+02
XI=	.76283857+02	ZI=	.41379729+02	THI=	.19605533-01
XIG=	-.58678862+00	ZIG=	.68194747+00	THII=	.37857279+01
FA=	.57308709+02	FN=	-.61210057+01	FX=	.66748165+01
MCH=	.90909091-01	MW=	.7716A282-09	MT=	-.21730079-01
VIN=	.10000000+03	ALT=	.46660522+03	CD=	.00000000
ATT=	.51900468+01	AMO=	.8039321A-02	COT=	.59817817+00
OMSS=	-.98972877+00	W=	.91849872+04		
OMG=	-.86133818+03	WI=	.13150696+02		
OMGI=	-.86299060+00	Q=	.11885000+02		
FZ=	.57242890+02	F=	.57630688+02		
MG=	-.52582190-02	DRAG=	.26697665+02		
GV=	.61522688+03	NF=	.00000000		
RBT=	.75698692+00	RMO=	.24254408-01		

TIME= 1.600

I	P	VR	WS	DB	LR	DS	TORQ	MR	SFB	CL	FN	ALPHA
1	3.732-01	1.042+02	1.155+00	3.214-01	3.986-01	4.784-01	1.700-01	-5.655-03	2.483-02	1.481+00	4.823-01	31.16
2	4.166-01	1.065+02	1.130+00	3.365-01	4.177-01	5.112-01	1.876-01	-4.869-03	2.785-02	1.484+00	5.156-01	34.99
3	5.000-01	1.093+02	1.101+00	3.548-01	4.404-01	5.472-01	1.163-01	-3.900-03	2.288-02	1.487+00	5.523-01	38.64
4	5.838-01	1.124+02	1.070+00	3.765-01	4.669-01	5.867-01	8.765-02	-2.749-03	2.192-02	1.491+00	5.925-01	42.10
5	6.668-01	1.160+02	1.038+00	4.016-01	4.980-01	6.297-01	5.732-02	-1.418-03	2.097-02	1.494+00	6.362-01	45.37
6	7.502-01	1.199+02	1.006+00	4.300-01	5.337-01	6.762-01	2.693-02	9.007-05	2.003-02	1.498+00	6.835-01	48.43
7	8.336-01	1.241+02	9.701-01	4.617-01	5.725-01	7.262-01	-9.831-03	1.777-03	1.911-02	1.501+00	7.344-01	51.30
8	9.170-01	1.285+02	9.362-01	4.968-01	6.329-01	7.927-01	-4.322-02	3.624-03	1.789-02	1.546+00	8.023-01	54.38
9	1.000+00	1.333+02	9.030-01	5.352-01	6.696-01	8.413-01	-8.627-02	5.699-03	1.717-02	1.521+00	8.517-01	56.59
10	1.088+00	1.382+02	8.705-01	5.770-01	7.082-01	8.913-01	-1.521-01	7.839-03	1.655-02	1.495+00	9.027-01	58.62
				6.292+00	5.337+00	6.691+00	3.292-01	1.821-04	2.052-01	9.237-01	6.753+00	

X=	.1437518E+03	Z=	.3768137E+02	TH=	.7729836E+02	OMEGX=	-.9908286E+00	W=	.9193676E+00
XI=	.7481195E+02	ZI=	.8358278E+01	THI=	.1160402E-02	OMG=	-.8621587E+01	WI=	.6471249E+01
XIG=	-.5767553E+00	ZIG=	.6627592E+00	THII=	-.7988659E+00	OMGI=	-.8117421E+00	Q=	.1188500E+02
FA=	.5782859E+02	FN=	-.6099173E+01	FX=	.6681152E+01	FZ=	.5736380E+02	F=	.5775157E+02
MCH=	.9090909E-01	MW=	.3797426E-01	MT=	-.9289390E-02	MOZ=	-.4997568E-02	DRAG=	.2672861E+02
VIN=	.1000000E+03	ALT=	.9623546E+01	CD=	.0000000	GV=	.5966583E+02	DF=	.0000000
ATT=	.5198413E+01	AMO=	.5285374E-01	CDT=	.5945816E+00	RBT=	.7570247E+00	RMO=	.1610255E-01

TIME= 1.700

I	P	VR	WS	DB	LR	DS	TORQ	MR	SFB	CL	FN	ALPHA
1	3.732-01	1.042+02	1.155+00	3.215-01	3.987-01	4.786-01	1.699-01	-5.679-03	2.481-02	1.481+00	4.824-01	31.18
2	4.166-01	1.065+02	1.130+00	3.365-01	4.173-01	5.113-01	1.875-01	-4.892-03	2.783-02	1.484+00	5.158-01	35.00
3	5.000-01	1.093+02	1.102+00	3.549-01	4.401-01	5.474-01	1.161-01	-3.921-03	2.286-02	1.487+00	5.525-01	38.66
4	5.838-01	1.124+02	1.071+00	3.767-01	4.671-01	5.870-01	8.750-02	-2.768-03	2.190-02	1.491+00	5.927-01	42.12
5	6.668-01	1.160+02	1.038+00	4.018-01	4.982-01	6.300-01	5.719-02	-1.435-03	2.095-02	1.494+00	6.365-01	45.39
6	7.502-01	1.199+02	1.006+00	4.302-01	5.335-01	6.765-01	2.471-02	7.539-05	2.001-02	1.498+00	6.838-01	48.45
7	8.336-01	1.241+02	9.703-01	4.620-01	5.729-01	7.266-01	-1.010-02	1.761-03	1.909-02	1.501+00	7.348-01	51.32
8	9.170-01	1.286+02	9.364-01	4.971-01	6.333-01	7.933-01	-4.358-02	3.615-03	1.782-02	1.546+00	8.028-01	54.40
9	1.000+00	1.333+02	9.031-01	5.356-01	6.701-01	8.419-01	-8.665-02	5.683-03	1.715-02	1.521+00	8.523-01	56.62
10	1.088+00	1.383+02	8.707-01	5.774-01	7.087-01	8.921-01	-1.326-01	7.836-03	1.653-02	1.495+00	9.033-01	58.64
				6.298+00	5.340+00	6.685+00	3.260-01	2.436-04	2.050-01	9.237-01	6.757+00	

X=	.1511007E+03	Z=	.4210119E+02	TH=	.7729871E+02	OMEGX=	-.9915808E+00	W=	.9198508E+00
XI=	.7257377E+02	ZI=	.8566854E+01	THI=	.9388567E-03	OMG=	-.8627556E+01	WI=	.3945001E+01
XIG=	-.5669655E+00	ZIG=	.6942975E+00	THII=	.7287830E-01	OMGI=	-.5289512E+00	Q=	.1188500E+02
FA=	.5751405E+02	FN=	-.6110349E+01	FX=	.6686682E+01	FZ=	.5745073E+02	F=	.5783772E+02
MCH=	.9090909E-01	MW=	.2719426E-01	MT=	.1887218E-03	MOZ=	-.3197178E-02	DRAG=	.2673857E+02
VIN=	.1000000E+03	ALT=	.9578988E+01	CD=	.0000000	GV=	.5783251E+02	DF=	.0000000
ATT=	.5197159E+01	AMO=	.3397120E-02	CDT=	.5948718E+00	RBT=	.7570672E+00	RMO=	.1042193E-01

TIME= 1.800

I	P	VR	WS	DB	LR	DS	TORQ	MR	SFB	CL	FN	ALPHA
1	3.732-01	1.042+02	1.156+00	3.215-01	3.987-01	4.786-01	1.698-01	-5.698-03	2.479-02	1.481+00	4.825-01	31.18
2	4.166-01	1.065+02	1.131+00	3.366-01	4.174-01	5.114-01	1.874-01	-4.906-03	2.781-02	1.484+00	5.159-01	35.01
3	5.000-01	1.093+02	1.102+00	3.550-01	4.402-01	5.476-01	1.161-01	-3.934-03	2.284-02	1.487+00	5.526-01	38.67
4	5.838-01	1.125+02	1.071+00	3.768-01	4.672-01	5.871-01	8.740-02	-2.780-03	2.188-02	1.491+00	5.929-01	42.13
5	6.668-01	1.160+02	1.038+00	4.019-01	4.983-01	6.302-01	5.709-02	-1.446-03	2.093-02	1.494+00	6.367-01	45.40
6	7.502-01	1.199+02	1.005+00	4.304-01	5.336-01	6.769-01	2.456-02	6.669-05	1.999-02	1.498+00	6.841-01	48.47
7	8.336-01	1.241+02	9.705-01	4.622-01	5.731-01	7.269-01	-1.024-02	1.754-03	1.907-02	1.501+00	7.351-01	51.33
8	9.170-01	1.286+02	9.366-01	4.973-01	6.335-01	7.936-01	-4.375-02	3.609-03	1.780-02	1.546+00	8.031-01	54.42
9	1.000+00	1.334+02	9.032-01	5.359-01	6.704-01	8.423-01	-8.690-02	5.680-03	1.713-02	1.521+00	8.526-01	56.63
10	1.088+00	1.383+02	8.707-01	5.777-01	7.091-01	8.925-01	-1.329-01	7.835-03	1.651-02	1.495+00	9.037-01	58.66
				6.295+00	5.342+00	6.687+00	3.245-01	1.435-04	2.048-01	9.237-01	6.759+00	

X=	.1582675E+03	Z=	.4676978E+02	TH=	.7730365E+02	OMEGX=	-.9920677E+00	W=	.9201868E+00
XI=	.7077108E+02	ZI=	.8768365E+01	THI=	.6819076E-03	OMG=	-.8631962E+01	WI=	.2832958E+01
XIG=	-.5586628E+00	ZIG=	.6768962E+00	THII=	-.6980738E-02	OMGI=	.3351080E+00	Q=	.1188500E+02
FA=	.5756861E+02	FN=	-.6115235E+01	FX=	.6686955E+01	FZ=	.5750501E+02	F=	.5789249E+02
MCH=	.9090909E-01	MW=	.1926598E-01	MT=	-.1467381E-04	MOZ=	-.2088997E-02	DRAG=	.2674782E+02
VIN=	.1000000E+03	ALT=	.9532717E+01	CD=	.0000000	GV=	.5602563E+02	DF=	.0000000
ATT=	.5139920E+01	AMO=	.2186083E-02	CDT=	.5950545E+00	RBT=	.7570837E+00	RMO=	.6736623E-02

TIME= 1.909

I	P	VR	WS	DB	LR	DS	TORQ	MR	SFB	CL	FN	ALPHA
1	3.732-01	1.042+02	1.156+00	3.216-01	3.987-01	4.787-01	1.698-01	-5.704-03	2.477-02	1.481+00	4.826-01	31.19
2	4.166-01	1.065+02	1.131+00	3.366-01	4.174-01	5.115-01	1.874-01	-4.915-03	2.780-02	1.484+00	5.159-01	35.02
3	5.000-01	1.093+02	1.102+00	3.551-01	4.403-01	5.476-01	1.160-01	-3.942-03	2.283-02	1.487+00	5.527-01	38.67
4	5.838-01	1.125+02	1.071+00	3.768-01	4.673-01	5.872-01	8.734-02	-2.788-03	2.187-02	1.491+00	5.930-01	42.14
5	6.668-01	1.160+02	1.039+00	4.020-01	4.984-01	6.303-01	5.698-02	-1.452-03	2.092-02	1.494+00	6.368-01	45.41
6	7.502-01	1.199+02	1.006+00	4.304-01	5.338-01	6.769-01	2.447-02	6.116-05	1.998-02	1.498+00	6.842-01	48.47
7	8.336-01	1.241+02	9.706-01	4.623-01	5.732-01	7.271-01	-1.039-02	1.750-03	1.906-02	1.501+00	7.352-01	51.34
8	9.170-01	1.286+02	9.366-01	4.975-01	6.337-01	7.938-01	-4.389-02	3.606-03	1.779-02	1.546+00	8.033-01	54.43
9	1.000+00	1.334+02	9.033-01	5.360-01	6.706-01	8.425-01	-8.706-02	5.678-03	1.712-02	1.521+00	8.529-01	56.64
10	1.088+00	1.383+02	8.708-01	5.779-01	7.093-01	8.928-01	-1.330-01	7.835-03	1.650-02	1.495+00	9.040-01	58.67
				6.296+00	5.345+00	6.688+00	3.236-01	8.958-05	2.046-01	9.237-01	6.761+00	

X=	.1652560E+03	Z=	.5162698E+02	TH=	.7730671E+02	OMEGX=	-.9923772E+00	W=	.9203328E+00
XI=	.6900550E+02	ZI=	.8967608E+01	THI=	.8352072E-03	OMG=	-.8638545E+01	WI=	.1516815E+01
XIG=	-.5629387E+00	ZIG=	.6093994E+00	THII=	-.1574786E-02	OMGI=	-.2157155E+00	Q=	.1188500E+02
FA=	.5760373E+02	FN=	-.6118485E+01	FX=	.6688833E+01	FZ=	.5754073E+02	F=	.5792776E+02
MCH=	.9090909E-01	MW=	.8900675E-02	MT=	-.9039273E-05	MOZ=	-.1318857E-02	DRAG=	.2675373E+02
VIN=	.1000000E+03	ALT=	.9483630E+01	CD=	.0000000	GV=	.5625042E+02	DF=	.0000000
ATT=	.5200081E+01	AMO=	.1405604E-02	CDT=	.5951717E+00	RBT=	.7570973E+00	RMO=	.4334029E-02

TIME= 2.009

I	R	VR	WCS	DB	LR	DS	TORQ	HP	SFB	CL	FN	ALPHA
1	3.332-01	1.042+02	1.156+00	3.216-01	3.987-01	4.787-01	1.698-01	-5.709-03	2.477-02	1.481+00	4.826-01	31.19
2	4.166-01	1.065+02	1.131+00	3.366-01	4.174-01	5.115-01	1.437-01	-4.920-03	2.379-02	1.484+00	5.160-01	35.02
3	5.000-01	1.093+02	1.102+00	3.551-01	4.403-01	5.477-01	1.160-01	-3.947-03	2.282-02	1.487+00	5.528-01	38.68
4	5.834-01	1.125+02	1.071+00	3.769-01	4.673-01	5.873-01	8.730-02	-2.792-03	2.186-02	1.491+00	5.930-01	42.14
5	6.668-01	1.160+02	1.038+00	4.020-01	4.985-01	6.304-01	5.649-02	-1.446-03	2.091-02	1.494+00	6.369-01	45.41
6	7.502-01	1.199+02	1.005+00	4.305-01	5.338-01	6.770-01	2.441-02	5.790-05	1.997-02	1.498+00	6.903-01	48.48
7	8.336-01	1.241+02	9.706-01	4.624-01	5.733-01	7.272-01	-1.046-02	1.747-03	1.905-02	1.501+00	7.353-01	51.35
8	9.170-01	1.286+02	9.361-01	4.976-01	6.138-01	7.939-01	-4.397-02	3.605-03	1.778-02	1.546+00	8.035-01	54.43
9	1.000+00	1.334+02	9.033-01	5.361-01	6.707-01	8.497-01	-8.716-02	5.637-03	1.711-02	1.521+00	8.536-01	56.65
10	1.084+00	1.384+02	8.708-01	5.780-01	7.094-01	8.930-01	-1.332-01	7.835-03	1.649-02	1.495+00	9.041-01	58.67
				4.297+00	5.343+00	6.689+00	3.230-01	5.639-05	2.046-01	4.237-01	6.761+00	

X=	.17206980+03	Z=	.56701659+02	TH=	.77308709+02	OMSS=	-.99257042+00	W=	.92044812+04
XI=	.67278211+02	ZI=	.51609905+02	THI=	.29565193-03	OMG=	-.86361994+03	WI=	.95568867+00
XIG=	-.53088206+00	ZIG=	.59300803+00	THII=	-.12155164-02	OMGI=	-.13856002+00	Q=	.11085000+02
FA=	.57626282+02	FN=	-.61205323+01	FX=	.66893814+01	FZ=	.57563921+02	F=	.57950403+02
MCH=	.90909091-01	MW=	.56079811-04	MT=	-.59770639-05	MQ=	-.84393840-03	DRAG=	.26757526+02
VIK=	.10000000+03	ALT=	.44329834+03	CD=	.00000000	GV=	.52507764+02	DF=	.00000000
ATT=	.52097703+01	AMO=	.90366789-03	CDT=	.59524677+00	RBT=	.75710634+00	RHO=	.27979930-02

TIME= 3.009

I	R	VR	WCS	DB	LR	DS	TORQ	HP	SFB	CL	FN	ALPHA
1	3.332-01	1.042+02	1.156+00	3.216-01	3.986-01	4.788-01	1.657-01	-5.721-03	2.474-02	1.481+00	4.927-01	31.20
2	4.166-01	1.065+02	1.131+00	3.367-01	4.175-01	5.117-01	1.433-01	-4.931-03	2.376-02	1.484+00	5..61-01	35.03
3	5.000-01	1.093+02	1.103+00	3.552-01	4.404-01	5.479-01	1.159-01	-3.957-03	2.279-02	1.487+00	5.529-01	38.69
4	5.834-01	1.125+02	1.071+00	3.770-01	4.675-01	5.875-01	8.719-02	-2.800-03	2.184-02	1.491+00	5.932-01	42.16
5	6.668-01	1.160+02	1.039+00	4.021-01	4.987-01	6.306-01	5.675-02	-1.463-03	2.089-02	1.494+00	6.371-01	45.43
6	7.502-01	1.199+02	1.005+00	4.307-01	5.340-01	6.773-01	2.424-02	5.336-05	1.995-02	1.498+00	6.846-01	48.50
7	8.336-01	1.242+02	9.707-01	4.626-01	5.736-01	7.275-01	-1.067-02	1.745-03	1.902-02	1.502+00	7.357-01	51.36
8	9.170-01	1.287+02	9.367-01	4.978-01	6.341-01	7.943-01	-4.473-02	3.604-03	1.776-02	1.546+00	8.038-01	54.45
9	1.000+00	1.334+02	9.033-01	5.364-01	6.710-01	8.471-01	-8.745-02	5.639-03	1.709-02	1.521+00	8.534-01	56.66
10	1.084+00	1.384+02	8.708-01	5.784-01	7.098-01	8.934-01	-1.335-01	7.840-03	1.647-02	1.495+00	9.046-01	58.69
				4.298+00	5.345+00	6.692+00	3.217-01	9.620-06	2.043-01	4.237-01	6.764+00	

X=	.23148251+03	Z=	.11708945+03	TH=	.77315068+02	OMSS=	-.99313466+00	W=	.92068546+04
XI=	.52226884+02	ZI=	.68500854+02	THI=	-.57081119-03	OMG=	-.86408929+03	WI=	.12816067+00
XIG=	-.40586304+00	ZIG=	.46791948+00	THII=	.17781699-01	OMGI=	.73542612-01	Q=	.11885000+02
FA=	.57690466+02	FN=	-.61257011+01	FX=	.66920434+01	FZ=	.57627516+02	F=	.58014774+02
MCH=	.90909091-01	MW=	.75204682-05	MT=	.99770949-04	MQ=	.44795163-03	DRAG=	.26768175+02
VIN=	.10000000+03	ALT=	.38291055+03	CD=	.00000000	GV=	.37322865+02	DF=	.00000000
ATT=	.52027658+01	AMO=	-.54337084-03	CDT=	.59545392+00	RBT=	.75712879+00	RHO=	-.16914729-02